Astroparticle physics

Lectures at the PhD School of the University of Padua, 2017

Alessandro De Angelis

ASTROPARTICLE PHYSICS

by Alessandro De Angelis

Lectures for the PhD courses in Astronomy and Physics

Padova, 2017

Preface

One of the new frontiers of fundamental physics is the field called astroparticle physics, joining astrophysics and elementary particle physics. In particular the gamma-ray sky at high-energy (above the MeV) unveils the nature of fundamental astrophysical phenomena, and opens a window on new physics, possibly including the nature of dark matter.

This book collects the slides and some extra material presented in the course on astroparticle physics held for the PhD in Astronomy and for the PhD in Physics at the University of Padova in the Academical Year 2016/17. This course introduces such an interdisciplinary subject, providing students with the tools needed to understand current problems, read a modern article in the field, and analyze the data from the leading high-energy telescope Fermi/LAT - which are, as usual for NASA, public. Some basics links related to neutrino astrophysics and to the recent field of astrophysics with gravitational waves are also provided.

Students attending this course are expected to know already the basics of quantum mechanics and of special relativity; they should also know about basic physics processes and the expansion of the Universe. At the end of this course, the successful students are able to:

1. Understand the basic physical processes involving high-energy particles and originating the emission of high-energy messengers - in particular, photons from astrophysical accelerators in high-density regions and from Dark Matter.
2. Know the methods and observing techniques to study high-energy emissions.
3. Describe the sky as seen with high-energy detectors.
4. Identify the kinds of astrophysical sources visible at high energies and relate them to relevant emission processes.
5. Have insight into current research in gamma and multimessenger astroparticle physics.
6. Read a scientific article related to gamma and multimessenger astroparticle physics.
7. Analyze the data from the Fermi/LAT gamma-ray satellite; extract a spectral energy distribution and a light curve for a generic source.

The lectures follow the textbook by De Angelis and Pimenta, “Introduction to particle and astroparticle physics”, Springer 2015; some material has been updated, and this update is reflected in the slides presented in this book.

I thank Claudia Lazzaro and Francesco Longo, who wrote, respectively, the chapter on gravitational waves and the chapter on the analysis of Fermi-LAT data. M. Pimenta, S. Andringa, S. Ansoldi, U. Barres, D. Cannone, R. Conceiçao, R. Shellard, F. Simonetto, B. Tomé helped in the solution of the exercises. And mostly I thank the students, who motivated and inspired the course.

Alessandro De Angelis

Padova, May 2, 2017

Table of Contents

(*) = Mandatory for physicists only.

Multimessenger astroparticle physics

Alessandro De Angelis, INFN/INAF Padova and LIP/IST Lisboa

Lecture 1
Introduction to the course. High-energy phenomena in the Universe.
Production of cosmic rays: nuclei, photons, neutrinos.

About this course

- https://www.dropbox.com/s/6x77ukpur4yzytj/hea_deangelis_syllabus5.htm?dl=0

8 theory lectures + 2 "hands-on",
Tue 3pm; Wed 10am; Thu 3pm

What you will learn:

- Understand the basic physical processes originating the emission of high-energy particles from astrophysical sources
  - In particular: photons from accelerators in high-density regions and from Dark Matter
- Know the methods and observing techniques to study high-energy emissions.
- Describe the sky as seen with high-energy detectors.
- Identify the kinds of astrophysical sources visible at high energies and relate them to relevant emission processes.
- Have insight into current research in gamma and multimessenger astroparticle physics.
- Read a scientific article related to gamma and multimessenger astroparticle physics.
- Analyze the data from the Fermi LAT gamma-ray satellite; extract a spectral energy distribution and a light curve for a generic source.
- You can be evaluated on a final short seminar on an article or a research topic selected according to your interest.

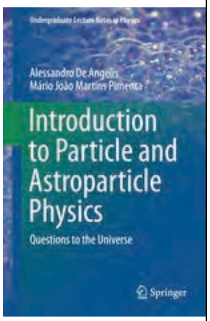

	Subject	Course material	Exercises	Notes
1) March 28, 2017 (2h) Starting at 15h, Room 207	Introduction; high-energy phenomena in the Universe. The budget of energy and matter in the Universe: Dark Matter.	1.4, 3.1, 8.1.4, 8.3.3, 8.4, 7.6 (from the textbook) Slides	1.6, 1.7, 8.11, 8.12, 8.13	
2) March 29 (3h) Starting at 10h, Room 315	Detection of charged particles, neutrinos, gravitational waves			Mandatory for physicists only
3-4) March 30 (2h) Starting at 15h, Room 315 & April 4 (2h) Starting at 15h, Room 315	How to detect high-energy photons.	4.1, 4.2.2, 4.2.3, 4.2.5, 4.3.2, 4.5 excluding 4.5.5 (from the textbook) Slides	4.2, 4.4, 4.5, 4.6, 4.7, 4.8, 4.9, 4.12, 4.14, 10.4, 10.5, 10.8	
5-6) April 5 (2h) Starting at 10h, Room 315 & April 6 (2h) Starting at 15h, Room 315	How high-energy photons are produced and how they propagate. Acceleration sites. Dark matter and high-energy astrophysics. Multimessenger high-energy astrophysics.	10.1.2, 10.2, 10.3 excluding 10.3.6, 10.4.1, 10.4.2, 10.4.3, 10.5.1, 10.5.2, 10.5.3 (from the textbook) Slides	10.3, 2.5, 10.12, 10.6, 10.14, 10.15, 10.13	
7) April 12 (3h) Starting at 10h, Room 315	Results from the detection of charged particles, neutrinos, gravitational waves			Mandatory for physicists only
8) April 13 (2h) Starting at 15h, Room 315	A look to the future.	10.5.4, 10.5.5 (from the textbook); original part on future detectors. Slides	No exercises ☺	
9-10) April 18, h 15 (3h) & April 19, h 10 (3h) Aula Informatica Polo Didattico [Longo – Menguzzato]	Tutorial: analysis of real Fermi data. Students will learn how to access and analyze public data from the space-borne Fermi Large Area Telescope. They will extract the spectrum and light-curve from a real gamma-ray source, and discuss its properties in terms of the concepts learnt in the theoretical sessions.	Slides		

About your lecturers

Alessandro De Angelis is a high-energy (astro)physicist. Professor in Udine and Lisbon, he is Director of Research at INFN Padova and PI of the e-ASTROGAM mission; he works for the MAGIC and CTA Collaborations. His main research interest is fundamental physics, especially astrophysics and elementary particle physics at accelerators. After graduating in Padova, Alessandro was employed at CERN in the 1990s, and he later was among the founders of the NASA Fermi gamma-ray telescope. He lectured electromagnetism and astroparticle physics in Italy and Portugal; has been visiting Professor at the ICRR Tokyo, MPI Munich, and Paris VI.

Office phone: 049 967.7364; email alessandro.deangelis@pd.infn.it

Francesco Longo is a gamma-ray astrophysicist, staff at the University of Trieste and leader of the local Fermi/MAGIC/CTA group. He convenes the working group on Transients in MAGIC, and is involved in R&D of e-ASTROGAM. His main research topics are GRBs and fast transients. Graduated inTrieste, he made his PhD in Ferrara with Pierluigi Fortini in 2002. After this he worked at the University of Trieste with Guido Barbiellini and was involved in the development of the gamma-ray satellites AGILE and Fermi, particularly in their MonteCarlo simulations. Later he coordinated the Fermi working group on "Solar Flares. Currently he is teaching Particle Astrophysics at the University of Trieste. He was Visiting professor at the University of Ljubljana.

Office phone: 0403756222; email francesco.longo@ts.infn.it

Messengers from the Universe - I

- Coulomb 1785: electroscopes can spontaneously discharge by the action of the air and not by defective insulation
- 1879: Crookes measures that the speed of discharge of an electroscope decreased when pressure was reduced (=> direct agent is the ionized air)
- Curie 1900: the discharge rate of an electroscope can be used to gauge the level of radioactivity
- Beginning of the XX century: is the radioactivity discharging electroscopes due to radioisotopes in the soil, or to radiation coming from the Cosmos?

Messengers from the Universe - II

- 1911/12: Domenico Pacini and Victor Hess perform two complementary experiments: Pacini discovers that ionizin gardiation decreases underwater, and Hess that it increases at high altitudes
  - 20% of the natural radiation at ground is due to cosmic radiation!!! Can we use this cosmic radiation for science?

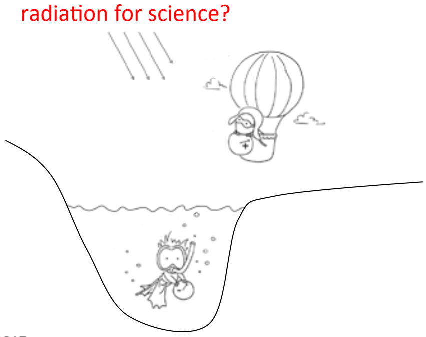

I RC secondari

- Interazione dei RC coi nuclei dell'atmosfera → sciami di particelle secondarie → **RC secondari** .
- L'atmosfera funge da *convertitore*
- La radiazione primaria può essere direttamente studiata solo fuori dall'atmosfera terrestre (sonde)
- La radiazione al suolo può essere studiata con rivelatore di sciami
- Esperimenti *underground* per la componente penetrante (muoni e neutrini)

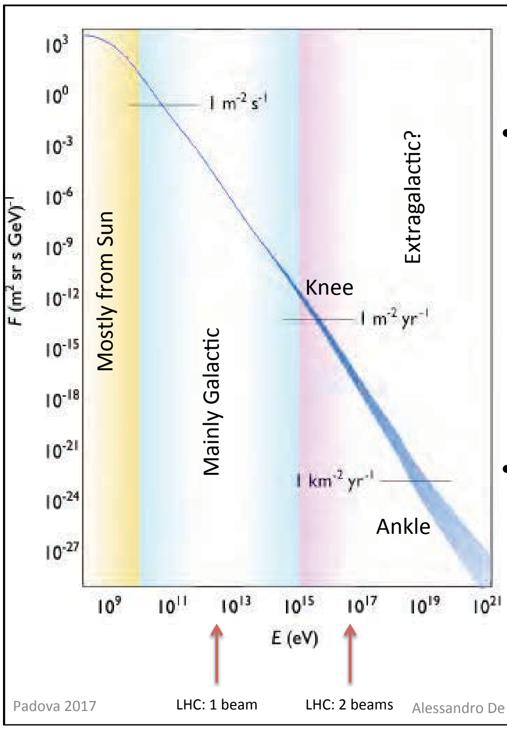

Cosmic Rays ("astroparticles")

- Once per second per cm^2 a high-energy particle from the sky hits the Earth
  - Mostly (~89%) protons
  - He (~9%) nuclei and heavier (~1%);
  - Electrons are ~1%

$$\boxed{\frac{dN}{dE} \simeq 1.8 \times 10^4 \left(\frac{E}{\mathrm{GeV}}\right)^{-2.7} \frac{\mathrm{particles}}{\mathrm{m^2\,s\,sr\,GeV}}}$$

- The flux falls as ~E$^{-2.7}$ as energy increases
  - 10^{21} eV once per second on Earth
    - The highest energies in (astro)physics
    - More than 100 times higher than the LHC c.m. energies

4

The measurement of the energy spectrum of cosmic rays above 3 10^{17} eV

To characterize the spectral features, data are described with a power law below the ankle

$$J(E) \propto E^{-\gamma_1}$$

and a power law with smooth suppression above

$$J(E; E > E_a) \propto E^{-\gamma_2}\left[1+\exp\left(\frac{\log_{10}E-\log_{10}E_{1/2}}{\log_{10}W_c}\right)\right]^{-1}$$

γ_1, γ_2 are the spectral indices below/above the ankle at E_a.
$E_{1/2}$ is the energy at which the flux has dropped to half of its peak value before the suppression, the steepness of which is described with $\log_{10}W_c$.

Combined energy spectrum of UHECRs as measured at the Pierre Auger Observatory. A. Schulz @ ICRC2013

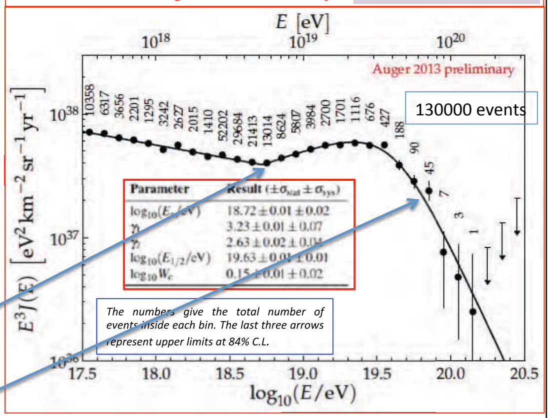

A. The **ankle** has been clearly seen

B. The **suppression** in the flux of UHECRs has been firmly established with (>20 σ)

Possible UHECR Sources: 2 scenarios

Bottom-Up Acceleration
(Astrophysical Acceleration Mechanisms)

UHECR's are accelerated in extended objects or catastrophic events (supernova remnants, rotating neutron stars, AGNs, radio galaxies)

Experimental evidence:
- ✓ anisotropy in arrival directions
- ✓ Photons < ≈1%

Top–Down Decay
(Physics Beyond the Standard Model)

Decay of topological defects
Monopoles Relics
Supersymmetric particles
Strongly interacting neutrinos
Decay of massive new long lived particles
Etc.

Now disfavored from the measurement of the **photon flux** with the PAO

Experimental evidence:
- ✓ isotropy in arrival directions
- ✓ Photons > ≈10%

Bottom-up models

Where do they come from?

r_L must be smaller than the dimension of the source L to remain confined.

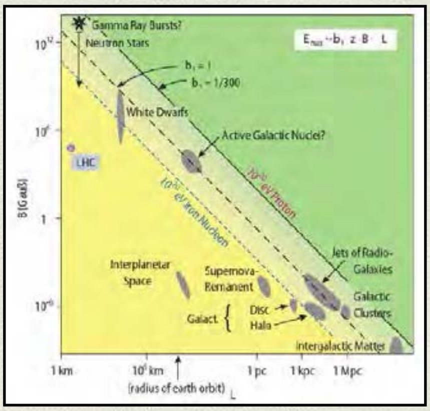

$$r_L = \frac{E_{15}}{ZB_{\mu G}}[\mathrm{pc}]$$

$$\boxed{E_{max} \simeq ZeBL\beta}$$

Finally, one should consider also energy losses at the source

---

$E \propto BR$

Whatever is the acceleration mechanism…

Large Hadron Collider

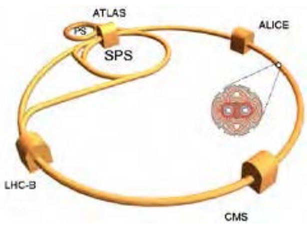

R ~ 10 km, B ~ 10 T
⇒ E ~ 10 TeV

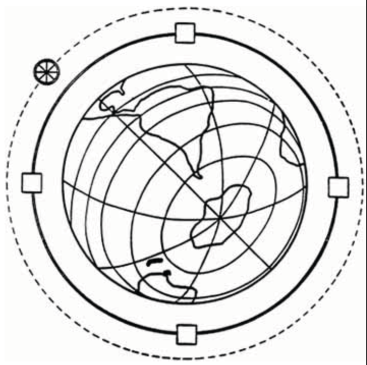

Tycho SuperNova Remnant

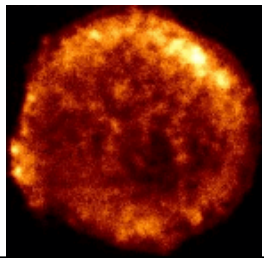

R ~ 10^{15}km, B ~ 10^{-10}T
⇒ E ~ 1000 TeV

The maximum energy possible on Earth is ~ 5000 TeV

A. De Angelis

12

Propagation of charged CR in the Universe

- Gyroradius
  B in the Galaxy: a few μG; outside the Galaxy: 1nG > B > 1 fG

$$\frac{r}{1\ \mathrm{pc}} \cong \frac{\dfrac{E}{1\ \mathrm{PeV}}}{\dfrac{B}{1\ \mu G}}$$

- If you want to look at the GC (d ~ 8 kpc) you need E > 2 10^{19} eV
  - But only 1 particle / km^2 / year
  - *And no galactic emitters expected at this energy*
- But in principle one could look outside the galaxy, were B is smaller and there are SMBHs…
  - *No: the resonant interaction with the CMB (GZK effect) provides a cutoff at E ~ 10^{19} eV*
- Conclusion: extremely difficult to use charged CR for astrophysics

13

Correlations with known sources are not statistically significant

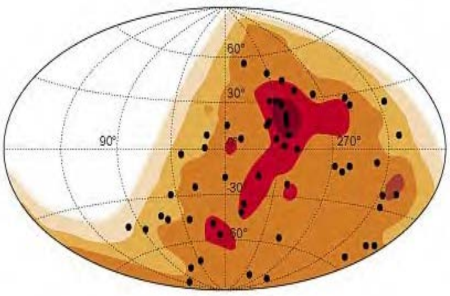

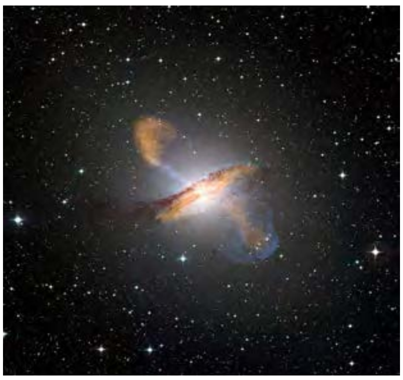

Neutral messengers must be used for astronomy & astrophysics

- Neutrinos: very difficult to detect due to the small interaction cross section (despite a km^3 detector in Antarctica, the only cosmic sources localized up to now are SN1987A, the Sun, and the Earth)
  - But: ~8 neutrinos per year from astrophysical sources identified by IceCube!
- Gravitational waves: just started
- Photons: they have a long tradition in astronomy since millennia… And they are the "starry messangers" by default since 1610 at latest…


SIDEREVS
NVNCIVS
MAGNA, LONGEQVE ADMIRABILIA Spectacula pandens, suspiciendaque proponens vnicuique, præsertim verò
PHILOSOPHIS, atq ASTRONOMIS, quæ à
GALILEO GALILEO
PATRITIO FLORENTINO
Patauini Gymnasij Publico Mathematico
PERSPICILLI
QVATVOR PLANETIS
MEDICEA SIDERA
NVNCVPANDOS DECREVIT.
VENETIIS, Apud Thomam Baglionum. M DC X.

The observed photon spectrum extends over 30 decades (measurements up to 1 TeV)

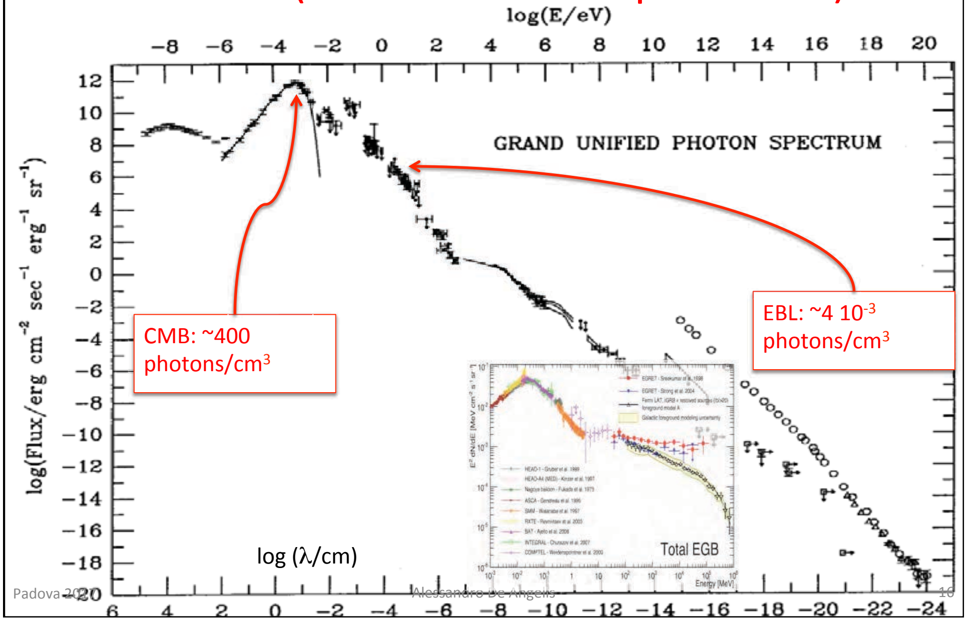

And also to high energies (above the thermal regions)

- LE or MeV : 0.1 (0.03) -100 (30) MeV
- HE or GeV : 0.1 (0.03) -100 (30) GeV
- VHE or TeV : 0.1 (0.03) - 100 (30) TeV
- UHE or PeV : 0.1 (0.03) -100 (30) PeV

- LE,HE domain of space-based astronomy
- VHE+ domain of ground-based astronomy

- When no ambiguity, we call “HE” all the HE and VHE+

3k HE and >200 VHE photon emitters

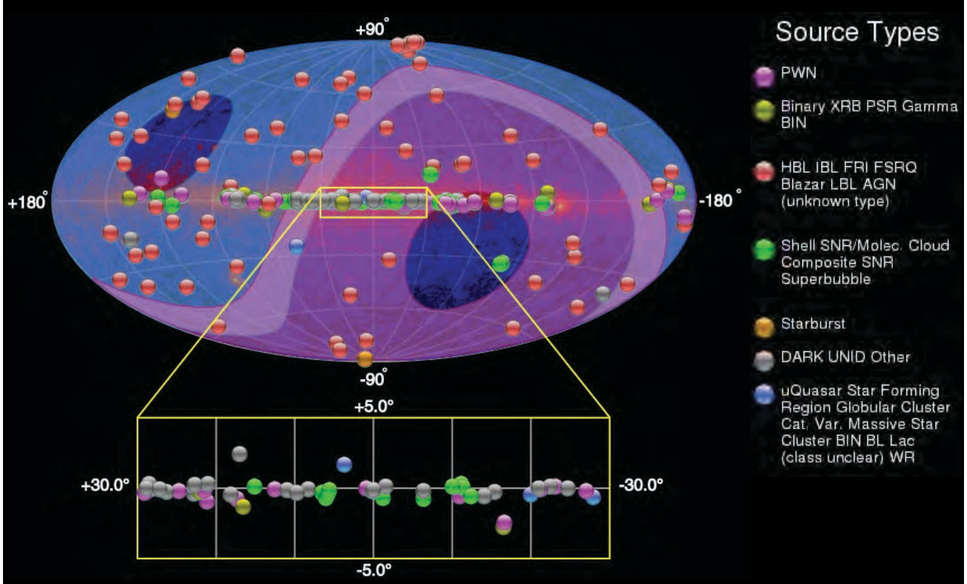

How can (V)HE photons be produced?

1. Interaction of accelerated charged particles with radiation and matter fields
   - The particle is accelerated via the Fermi 1st order mechanism (collective shocks with a preferred direction)
   - It undergoes purely leptonic mechanisms (electrons), or hadronic collisions (protons) with subsequent π^0 decays
2. Top-down mechanisms
   - The decay or the annihilation of a heavy particle produce unavoidably photons, either direcly or in a q-qbar chain
   - Are there reservoirs of “TeV” particles around? Unlikely unless there are new particles…

(1) Interaction of accelerated charged particles with radiation and matter fields

- Gamma-ray production and absorption processes: several but well studied
- These phenomena generally proceed under extreme physical conditions in environments characterized by
  - huge gravitational, magnetic and electric fields,
  - very dense background radiation,
  - relativistic bulk motions (black-hole jets and pulsar winds)
  - shock waves, highly excited (turbulent) media, etc.
- They are related to, and their understanding requires knowledge of,
  - nuclear and particle physics,
  - quantum and classical electrodynamics,
  - special and general relativity,
  - plasma physics, (magneto) hydrodynamics, etc.
  - astronomy & astrophysics

Leptonic and hadronic production of gamma rays

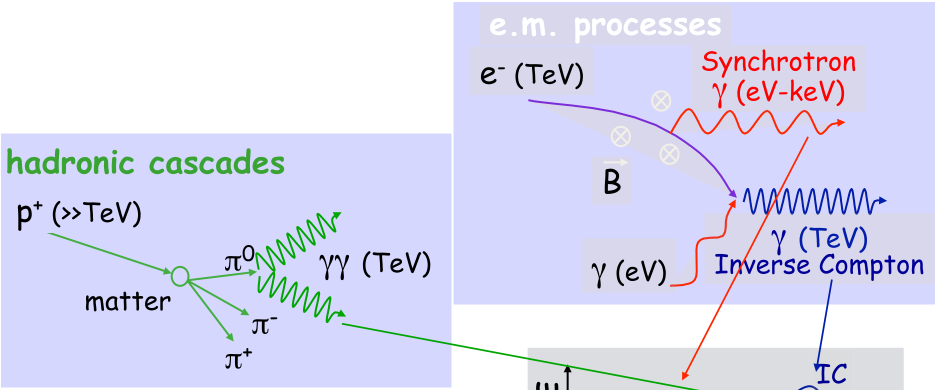

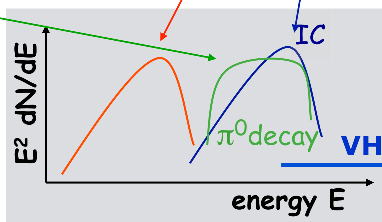

In the VHE region,
$dN/dE \sim E^{-\Gamma}$ (Γ: spectral index)

To distinguish between hadron/leptonic origin study Spectral Energy Distribution (SED): (differential flux) · E^2

The hadronic mechanism is at work also for neutrinos…

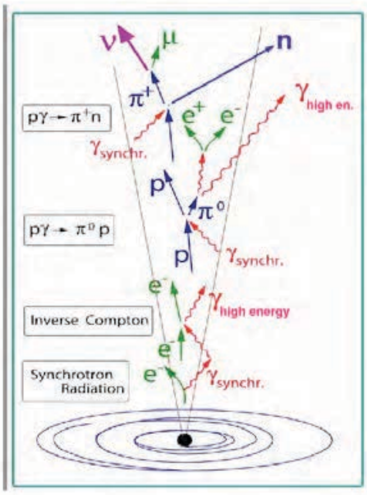

In a hadronic process (isospin symmetry)

- $N(\pi+) \sim N(\pi-) \sim N(\pi^0)$ Same energies!

Proton colliding with nucleus in molecular cloud or photon in field

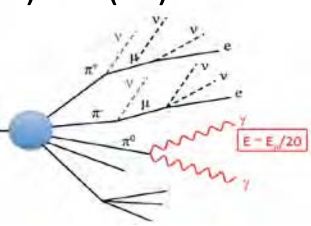

$\pi+ \rightarrow \mu+ \nu$

$\pi- \rightarrow \mu+ \nu$

$\pi^0 \rightarrow \gamma\gamma$

A “typical” (V)HE γ source: Crab Nebula

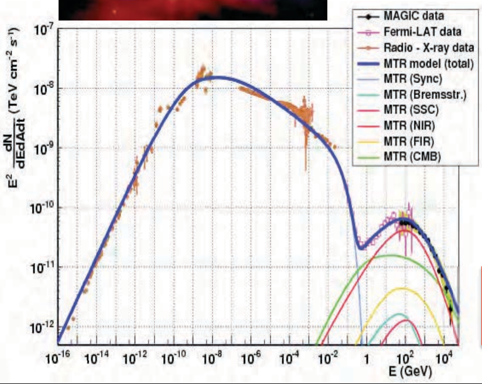

- The Crab Nebula is a nearby (~2 kpc away) PWN and the first source detected in VHE gamma-rays [Weekes 1989].
- It is the brightest steady VHE gamma-ray source, therefore it has become the so-called “standard candle” in VHE astronomy.
  - Recent observation of flares in the GeV range have however shown that occasionally the Crab flux can vary.

$$\frac{dN_\gamma}{dE} \simeq 3.23 \times 10^{-11} \left(\frac{E}{\mathrm{TeV}}\right)^{-2.47-0.24\left(\frac{E}{\mathrm{TeV}}\right)} \mathrm{TeV}^{-1}\mathrm{s}^{-1}\mathrm{m}^{-2}$$

γ-ray detection: signal vs. background

- Is Crab Nebula easy to detect?
- Suppose to have a 100 x 100 m^2 detector with a resolution of 1 square degree:

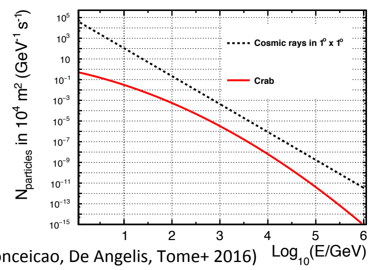

Conceicao, De Angelis, Tome+ 2016)

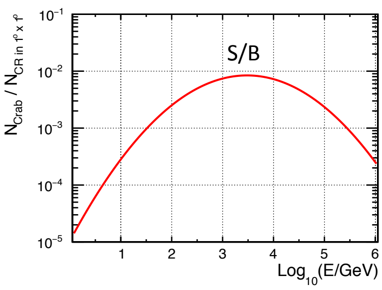

Conclusion: you need large effective area, good angular resolution, proton rejection

Summary of Lecture 1

- A huge flux of particles comes from space, reaching energies that we are not able to produce at accelerators
  - Most are charged, and they can hardly be used for astronomy
  - Fortunately, a fraction of them are neutral: gamma-rays, neutrinos, gravitational waves
- Astronomy with gamma rays has given many important results in the recent years:
  - More than 200 VHE sources discovered and studied
  - Main mechanisms of emission understood

  and it might discover emissions from decay/annihilation of new particles beyond the Standard Model
- Recently we have established that we can make astrophysics with neutrinos, but we shall need huge detectors or new concepts:
  - ~10 astrophysical neutrinos/year/km3 of traditional detector
  - ~1 GW signal/year with 2 ~4km interpherometers.

Exercises

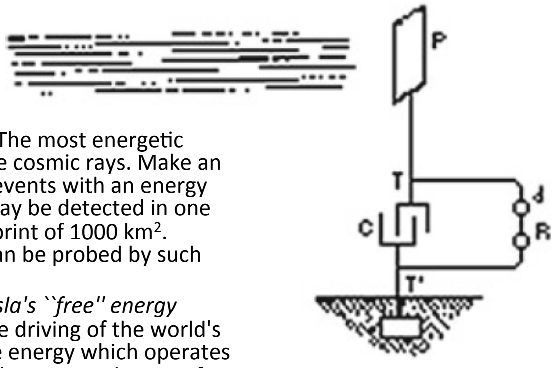

1. *Cosmic ray fluxes and wavelength.* The most energetic particles ever observed at Earth are cosmic rays. Make an estimation of the number of such events with an energy between 3 10^{18} and 10^{19} eV that may be detected in one year by an experiment with a footprint of 1000 km^2. Evaluate the structure scale that can be probed by such particles.
2. *Energy from cosmic rays: Nikola Tesla's ``free'' energy generator.* ``This new power for the driving of the world's machinery will be derived from the energy which operates the universe, the cosmic energy, whose central source for the earth is the sun and which is everywhere present in unlimited quantities.'' Immediately after the discovery of of natural radioactivity, in 1901, Nikola Tesla patented an engine using the energy involved (and expressed a conjecture about the origin of such radioactivity). On the right we show a drawing (made by Tesla himself) of Tesla's first radiant energy receiver. If an antenna (the higher the better: why?) is wired to one side of a capacitor (the other going to ground,) the potential difference will charge the capacitor. Suppose you can intercept all high-energy cosmic radiation (assume 1 particle per square centimeter per second with an average energy of 3 GeV); what is the power you could collect with a 1 m^2 antenna, and how does it compare with solar energy?

Multimessenger astroparticle physics

Alessandro De Angelis, INFN/INAF Padova and LIP/IST Lisboa

Lecture 2
The Fermi mechanism. Charged cosmic rays and their detection.
(mandatory for physicists only)
.

Thermal radiation: Black Body Spectrum

Cosmic Microwave Background:
2.7 K

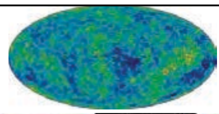

A Galactic gas cloud
called Rho Ophiuchi:
60 K

Dim star near the
center of the Orion Nebula:
600 K

the Sun:
6000 K

Cluster of very bright stars, Omega Centauri,
as observed from the space:
60,000 K

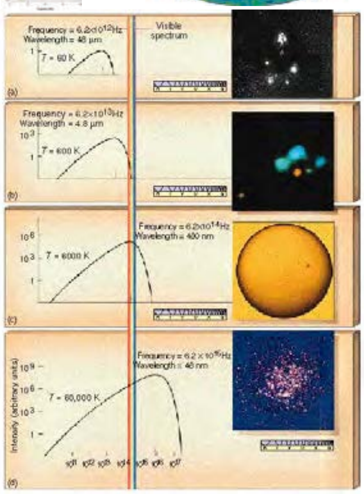

Accretion Disks can reach
temperatures >> 10^5 K

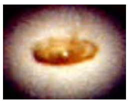

But this is still
~1 keV, in the
X-Ray band!

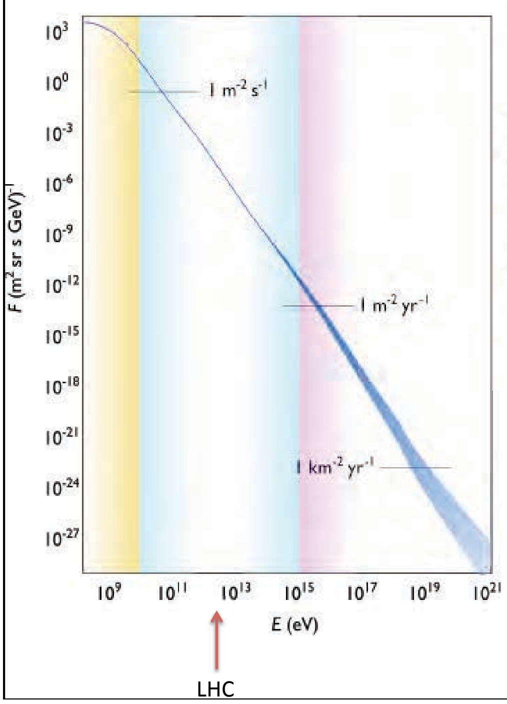

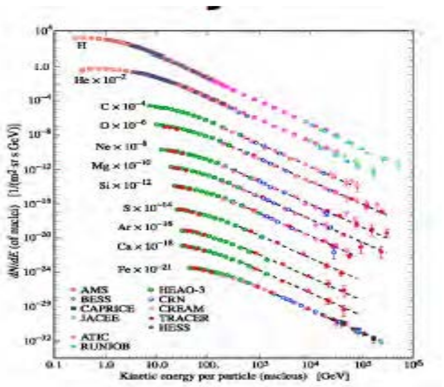

...and heavier than Fe (wow!!!)

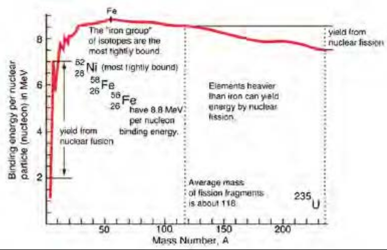

How to generate energies much higher than thermal?

A. De Angelis

Acceleration Mechanisms

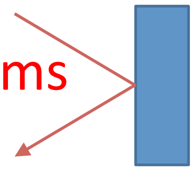

- Fermi Mechanism
  - energetic charged particles can gain energy by scattering off local magnetic turbulence (Fermi 1949)
    - Assume particle scatters off much more massive object moving with speed **u**. Then in the cm frame (~ frame of massive object) its energy and momentum before the scatter are

$$E' = \gamma_u (E + up\cos\theta)$$
$$p'_x = \gamma_u \left(p\cos\theta + uE/c^2\right)$$

    - The particle scatters elastically: its energy is conserved and its *x*-momentum reversed. In original (lab) frame

$$E_2 = \gamma_u (E' + up'_x) = \gamma_u^2 E\left(1 + \frac{2uv}{c^2}\cos\theta + \frac{u^2}{c^2}\right)$$

Acceleration Mechanisms

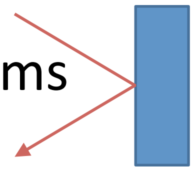

- Fermi (2nd order) Mechanism
  - energetic charged particles can gain energy by scattering off local magnetic turbulence (Fermi 1949)
    - We need to average over angle. Head-on collisions are slightly likely than overtaking collisions, so middle term doesn't just go away. In relativistic limit we find

$$\left\langle \frac{\Delta E}{E} \right\rangle = \frac{8}{3}\left(\frac{u}{c}\right)^2$$

    - Hence this process is known as **second-order Fermi acceleration**.
  - The good news
    - this produces a power law energy spectrum: $N(E) \propto E^{-x}$ where $x = 1 + 1/\alpha\tau$, α is the rate of energy increase and τ is the residence time of the particle
  - The bad news
    - since $u \ll c$, it's slow and inefficient

Can we go to 1st order?

Simple model

A particle of velocity v collides perpendicularly with a shock front u_1. Behind the shock the gas recedes at a speed u_2 so in the lab frame the gas has a recesing speed of $u_1 - u_2$. As the particle is reflected back it gains the kinetic energy of the shocked gas. The kinetic energy gain is:

$$\Delta E = \frac{1}{2}m(v + (u_1 - u_2))^2 - \frac{1}{2}mv^2$$
$$= \frac{1}{2}m(2v(u_1 - u_2) + (u_1 - u_2)^2)$$

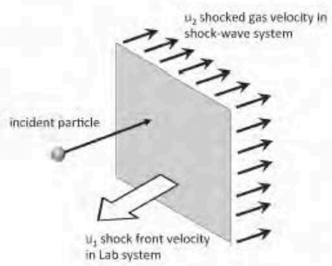

Assuming $v \gg u_1, u_2, u_1 > u_2$ then:

$$\frac{\Delta E}{E} \approx \frac{2(u_1 - u_2)}{v}$$

Acceleration Mechanisms

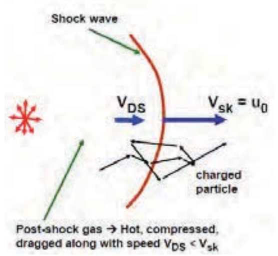

- First-order Fermi Mechanism (Diffusive Shock Acceleration)
  - $O(u/c)$ term gets lost in integral over angles in the 2nd oreder mechanism —we could retrieve this if we could arrange to have mostly head-on scatters
  - Consider shock wave as sketched above
    - high-energy particles will scatter so that their distribution is isotropic in the rest frame of the gas
    - There is a preferred direction in the expansion

    => crossing shock **in either direction** produces head-on collision on average

8

Acceleration Mechanisms

- DSA, continued
  - therefore average energy gain per crossing is

$$\left\langle \frac{\Delta E}{E} \right\rangle = \frac{V}{c} \int_0^{\frac{\pi}{2}} 2\cos^2\theta \sin\theta \, \mathrm{d}\theta = \frac{2}{3}\frac{V}{c}$$

9

Acceleration Mechanisms

- DSA spectrum
  - if average energy of particle after one collision is $E_1 = fE_0$, and if P is probability that particle remains in acceleration region, then after k collisions there are $N_k = N_0 P^k$ particles with average energy $E_k = f^k E_0$.
  - Hence $\frac{\ln(N/N_0)}{\ln(E/E_0)} = \frac{\ln P}{\ln f}$, or $\frac{N}{N_0} = \left(\frac{E}{E_0}\right)^{\ln P/\ln f}$
  - This is the number of particles with $E \geq E_k$ (since some of these particles will go on to further collisions), so differential spectrum is $N(E)\,\mathrm{d}E \propto E^{(\ln P/\ln f)-1}\,\mathrm{d}E$
  - "universal" power law, independent of details of shock

10

Zwicky conjectures (1933)

1. Heavy enough stars collapse at the end of their lives into super-novae
2. Implosions produce explosions of cosmic rays
3. They leave behind neutron stars

(Zwicky in1930)

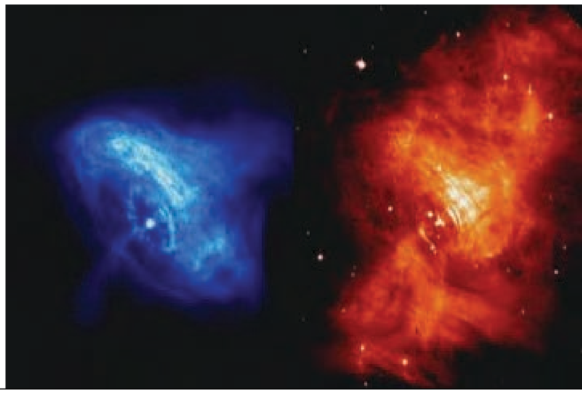

Tycho's Supernova (SN 1572)

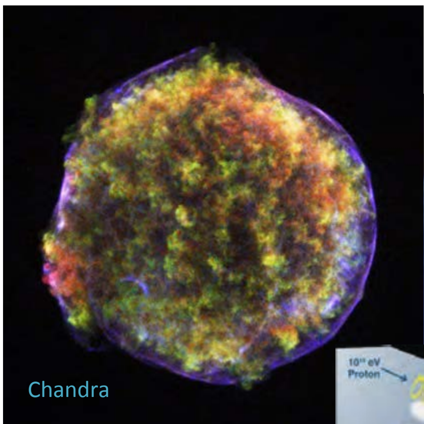

Shock front seen in high-energy electrons
"Stripes" may signal presence of high-energy protons

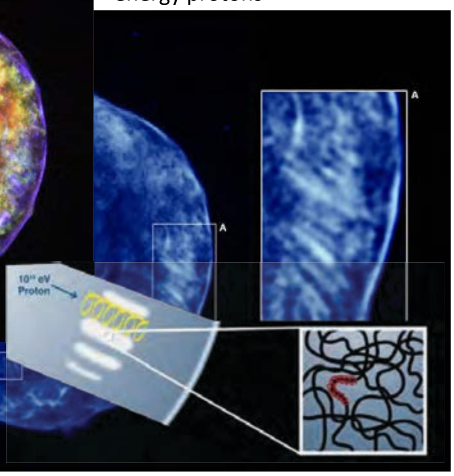

Radio Galaxies

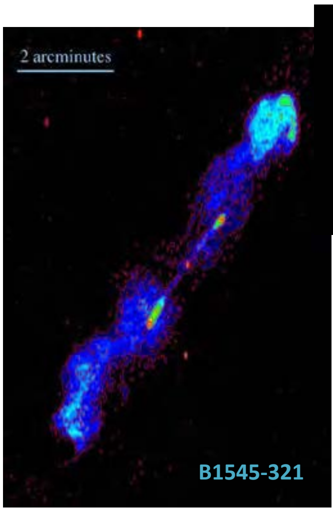

13 cm wavelength ATCA image by L. Saripalli, R. Subrahmanyan and Udaya Shankar

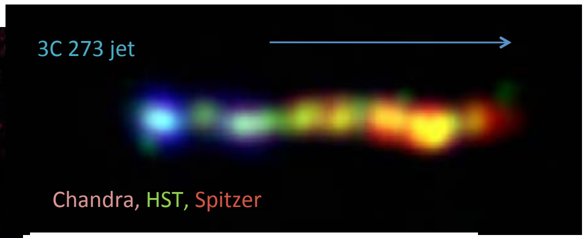

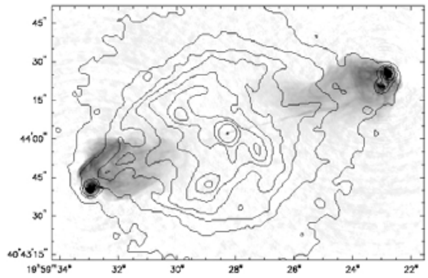

Cygnus A in X-ray (Chandra) and radio (VLA)

Leaky box (qualitative)

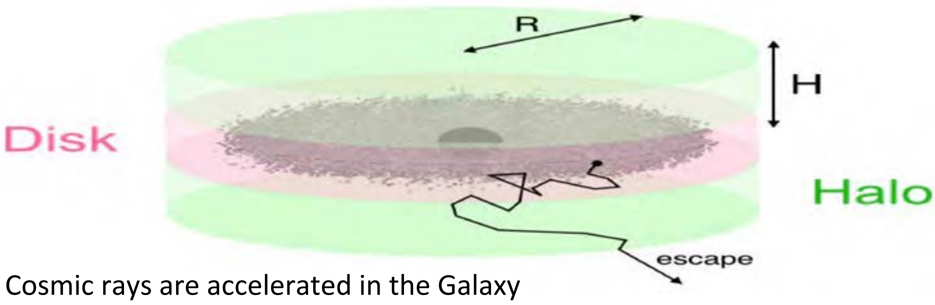

- Cosmic rays are accelerated in the Galaxy
- They are trapped by B if
  r (pc) = E (PeV) / Z B (μG) << H
- → They can escape, and escaping probability increases with energy and decreases with Z

BTW, also acceleration is more effective with Z…

=> Several knees. Importance of rigidity (p/eZ)

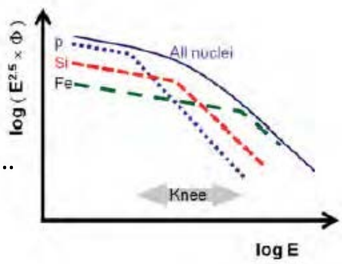

Chemical composition of Galactic CR

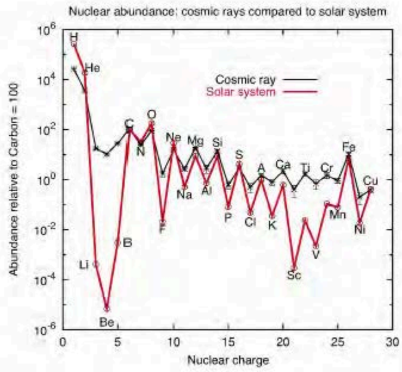

- The chemical composition of cosmic rays is similar to the abundances of the elements in the Sun indicating an **stellar origin of cosmic rays.**
- However there are some differences: Li, Be, B are secondary nuclei produced in the spallation of heavier elements (C and O). Also Mn, V, and Sc come from the fragmentation of Fe. These are usually referred as **secondary cosmic rays.**
- The see-saw effect is due to the fact that nuclei with odd Z and/or A have weaker bounds and are less frequent products of thermonuclear reactions.

By measuring the primary-to-secondary ratio we can infer the propagation and diffusion processes of CR

Metodi di misura dei raggi cosmici

Misure dirette, E<10^{14} ev
Misure indirette, E>10^{14} ev

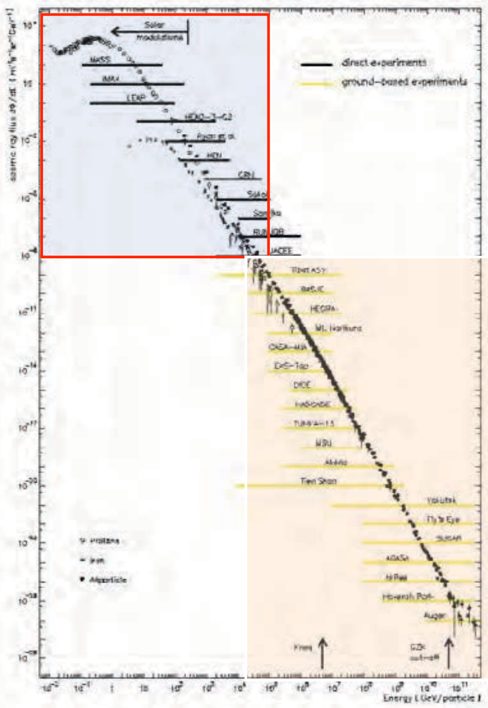

RC secondari

Lo spessore di atmosfera equivale a 10 m di acqua

1. Flusso sulla sommità (H=0 gcm^{-2}):
   10000 $m^{-2}\ s^{-1} sr^{-1}$
   p (90%), He (9%), A (1%)

2. Flusso a livello del mare (H=1000 gcm^{-2}):
   200 $m^{-2}\ s^{-1} sr^{-1}$
   Muoni, neutrini, e+e-, γ

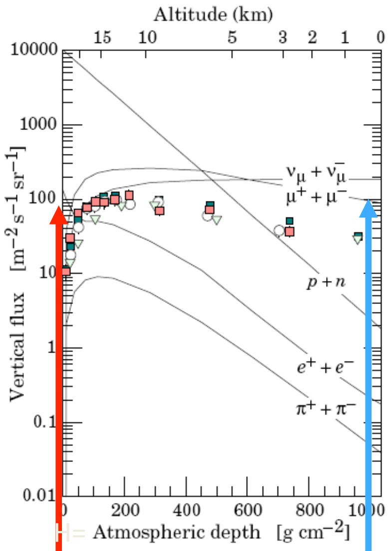

3. Underground: muoni e neutrini

Il flusso decresce in modo esponenziale con la profondità.

Per h>13 km w.e. sopravvivono solo le particelle indotte da neutrini.

Nascita di esperimenti underground a basso fondo

Ai LNGS il flusso è ridotto di un fattore 10^6 rispetto a quello al livello del mare.

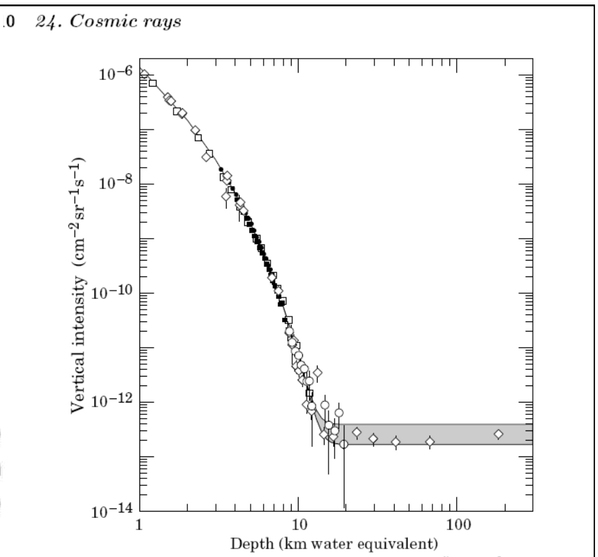

Figure 24.5: Vertical muon intensity vs depth (1 km.w.e. = 10^5 g cm^{-2} of standard rock). The experimental data are from: ◊: the compilations of Crouch [45], □: Baksan [46], ○: LVD [47], •: MACRO [48], ■: Frejus [49]. The shaded area at large depths represents neutrino-induced muons of energy above 2 GeV. The upper line is for horizontal neutrino-induced muons, the lower one for vertically upward muons.

http://pdg.lbl.gov/2016/reviews/cosmicrayrpp.pdf

Cosmic rays arrive on Earth with very different energies

THE SPECTRUM

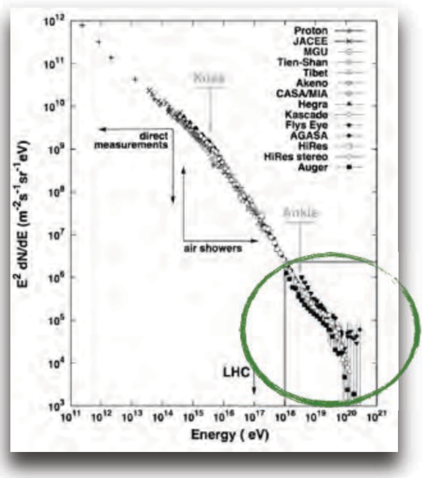

ULTRA-HIGH ENERGY COSMIC RAYS

- Extremely low flux
- Flattening of the spectrum at the ankle
- Suppression of the flux

Why is UHECR study interesting?

They are the most energetic particles in the universe!

Direct measurement of Cosmic Rays

20

Identificazione di particelle

Identificazione di particelle= massa, carica, energia/impulso
Spettrometro: strumento per la misura della rigidità
in campo magnetico. B è noto, Z e p possono essere misurati

La risoluzione nella misura dell'impulso è dipende dalla precisione nella misura della traccia e dallo scattering multiplo della traccia all'interno del magnete.

Un sistema di tempo di volo (ToF) (ad esempio A,C sono 2 contatori a scintillazione o contatori proporzionali) fornisce la misura di dE/dx (ossia Z^2), tempo, posizione e trigger. La misura del ToF tra due posizioni note fornisce la velocità della particella. Da r_L si ottiene la massa della particella.

Talvolta, un rivelatore distruttivo (calorimetro) può essere usato per avere una misura indipendente dell'energia totale della particella.

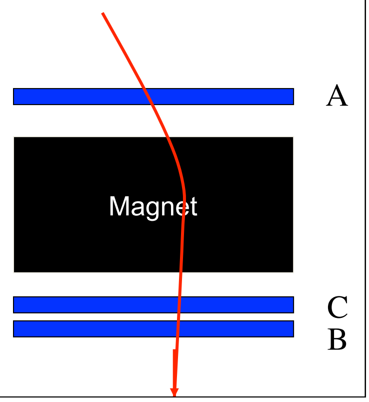

Esperimenti nello spazio

Sviluppi recenti: esperimenti nello spazio (PAMELA, AMS, altri) finalizzati alla misura diretta di RC e della **ricerca di antimateria**.
Spettrometri: misurano la carica dei RC → RC, antinuclei.
Occorre però un campo magnetico → magnete nello spazio, superconduttori, criogenia → pesanti, costosi!
Identificazione di particelle: occorre una ottima discriminazione di particelle per separare elettroni da antiprotoni. Occorrono diversi strumenti a seconda dell'energia della particella:

- **Low energy:** TOF, Cherenkov
- **High energy:** RICH, TRD, calorimetri elettromagnetici

Tipicamente: 1 antiprotone su $10^{5\div6}$.

22

Ricerca di antinuclei nei RC: il mistero della mancanza di antimateria nell'Universo

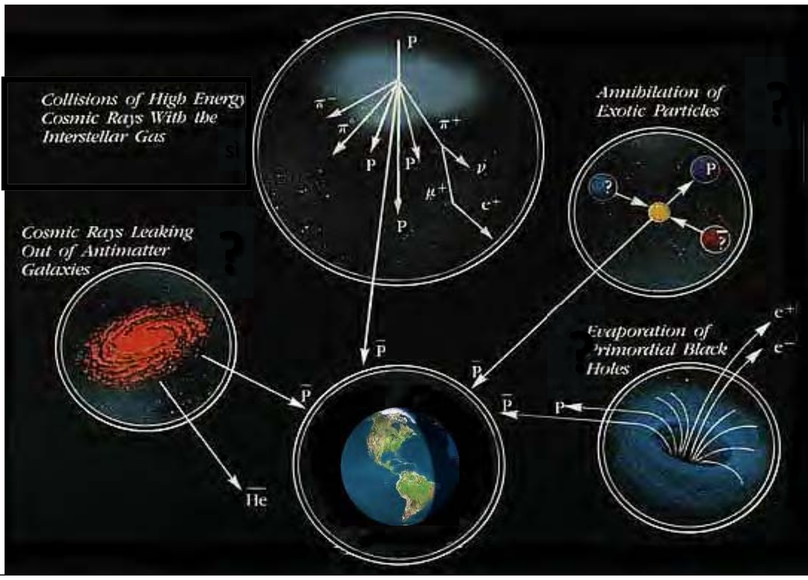

PAMELA

Lanciato 15/6/2006 da Baikonur Cosmodrome-Kazakhstan

http://wizard.roma2.infn.it/pamela/

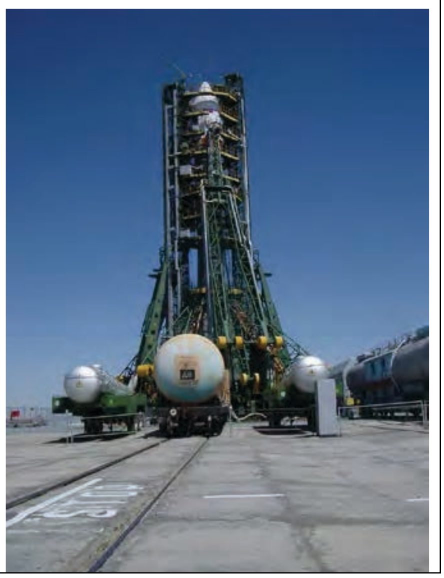

PAMELA

- Obiettivi dell'esperimento:
  - Misurare lo spettro di antiprotoni, positroni e (anti)nuclei in un ampio intervallo di energie;
  - Ricerca di antimateria "primordiale"
  - Studio del flusso dei RC primari
- PAMELA è capace di misurare rigidità magnetiche (=impulso/carica) sino a **700 GV/c**.

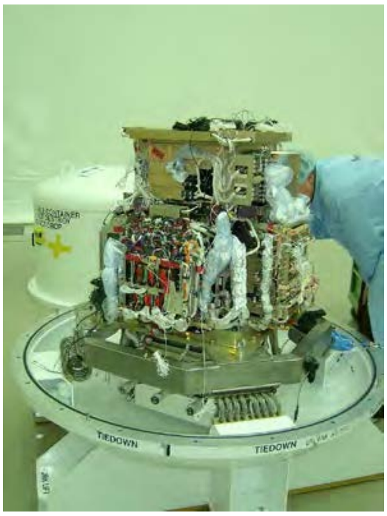

25

PAMELA

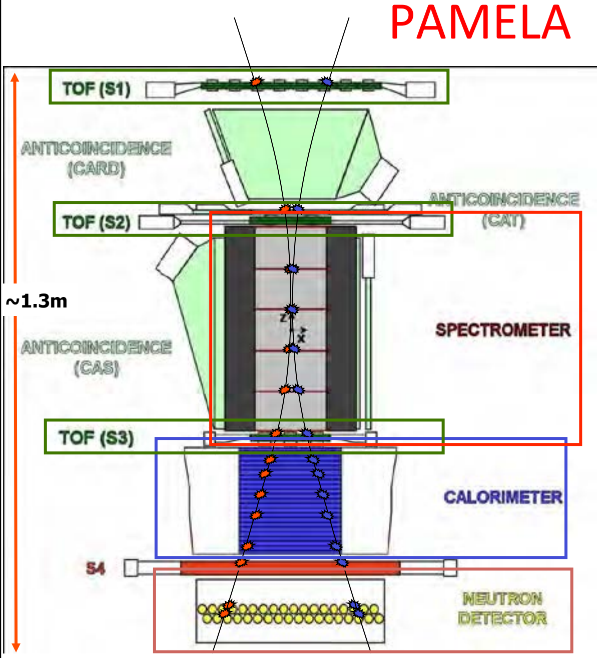

- Identificazione di particelle usando:
  - TOF
  - Calorimetro Em
  - Rivelatore di neutroni (basato sulla cattura da parte di ^{3}He n)→ aiuta a discriminare cascate elettromagnetiche da quelle adroniche
  - Misura della rigidità tramite spettrometro, costituito da un magnete permanente ed un sistema tracciante al silicio

Integrazione e posizionamento nel satellite

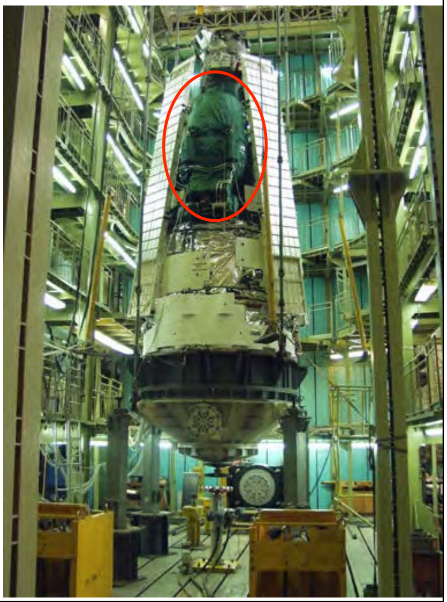

Lo Spettrometro Magnetico

Per avere un idea del grado di complessità di tali esperimenti, guardiamo con qualche dettaglio lo spettrometro magnetico:

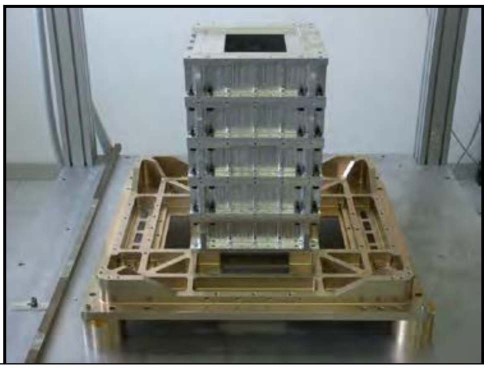

- **Magnete Permanente**
  - 5 blocchi di Nb-B-Fe
  - 0.48 T al centro della cavità
  - "Torre" Magnetica = (13.2 x 16.2 cm^2) x 44.5 cm high $\Rightarrow$ accettanza: 20.5 cm^2 sr

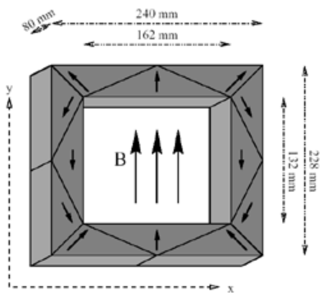

Alpha Magnetic Spectrometer Experiment

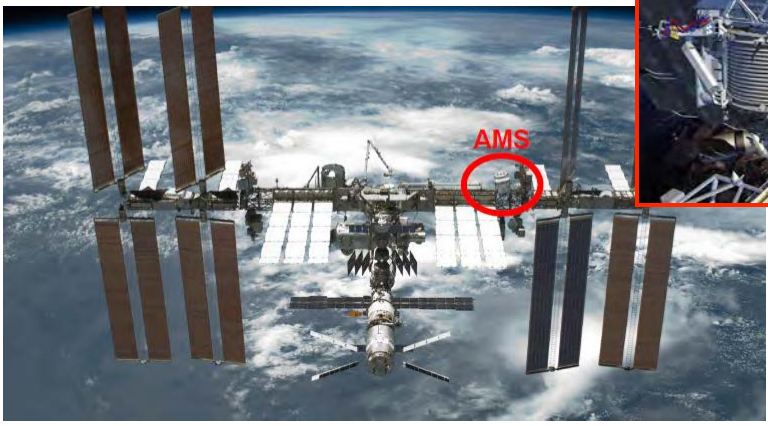

- ISS : 108 m x 80m, 420 t
- orbit height 400km

Inclination = 51.57°
15.62 revolutions/day

AMS Transfer to the Shuttle, 26 March 2011

30


AMS is grappled by the Shuttle
Remote Manipulator System (SRMS)
May 19, 2011

33

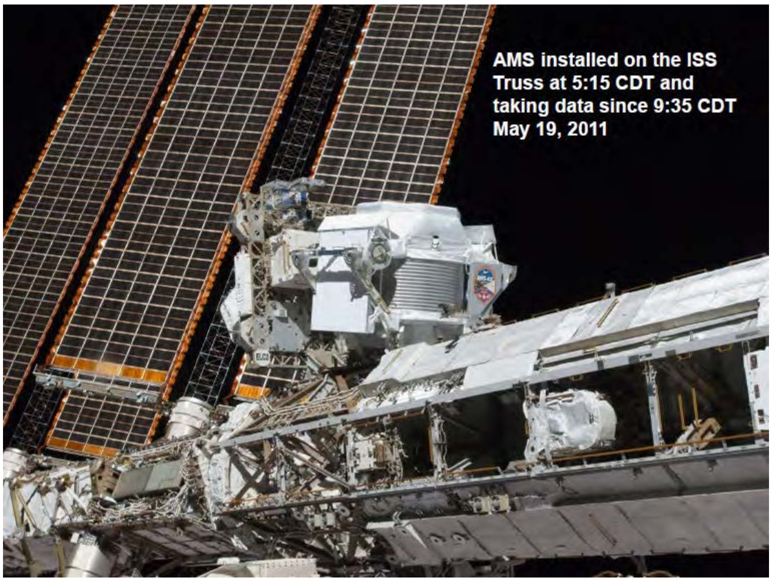
AMS installed on the ISS
Truss at 5:15 CDT and
taking data since 9:35 CDT
May 19, 2011

34

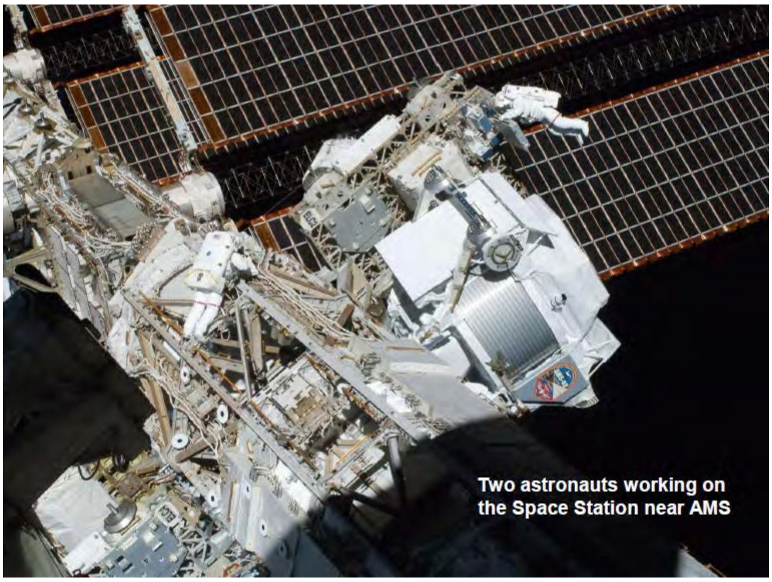

35

Cosmic ray studies with AMS

Goals:

- **Searches for primordial antimatter:**
  - Light anti-nuclei: $\overline{D}$, $\overline{He}$, ...
  - $\overline{p}$ / p ratio
- **Dark Matter searches:**
  - e^+, $e^\pm$, $\overline{p}$, ...
  - simultaneous observation of several signal channels.
- **Searches for new forms of matter:**
  - strangelets, ...
- **Measuring CR spectra – refining propagation models;**
- **Identification of local sources of high energy CR (~TeV):**
  - SNR, Pulsars, PBH, ...
- **Study effects of solar modulation on CR spectra over 11 year solar cycle**
- ...

36

A TeV Detector in Space: AMS-02 on the Space Station.

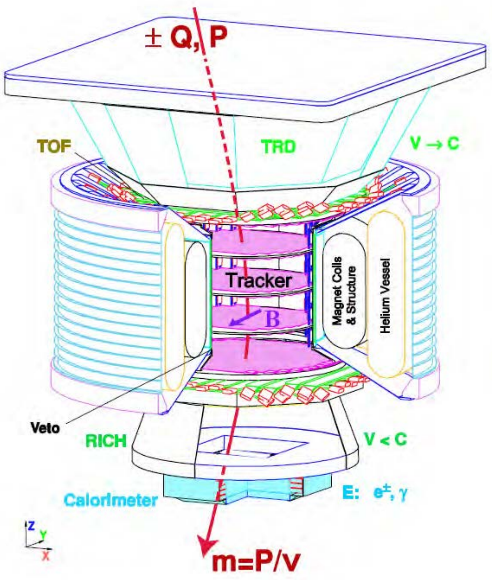

The value of |Q| is measured independently in Tracker, RICH and TOF.

The signed charge, ±Q, and the momentum of the particle, P, aremeasured by the 8 layers of doubled-sided silicon tracker in the magnet.

The velocity, β = v/*c*, is measured by the TOF, TRD and RICH.

The energy of electromagnetic particles is measured by the calorimeter.

AMS features

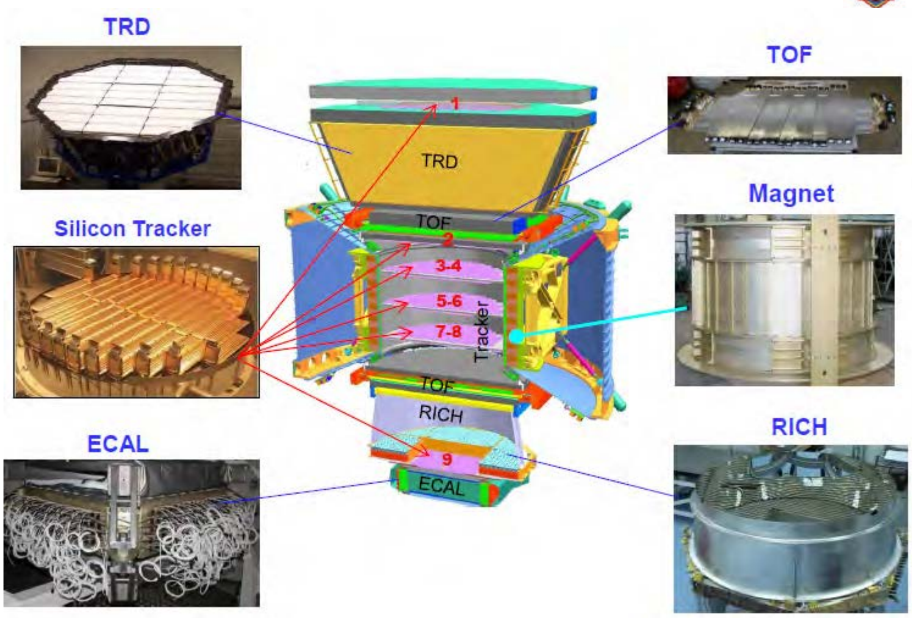

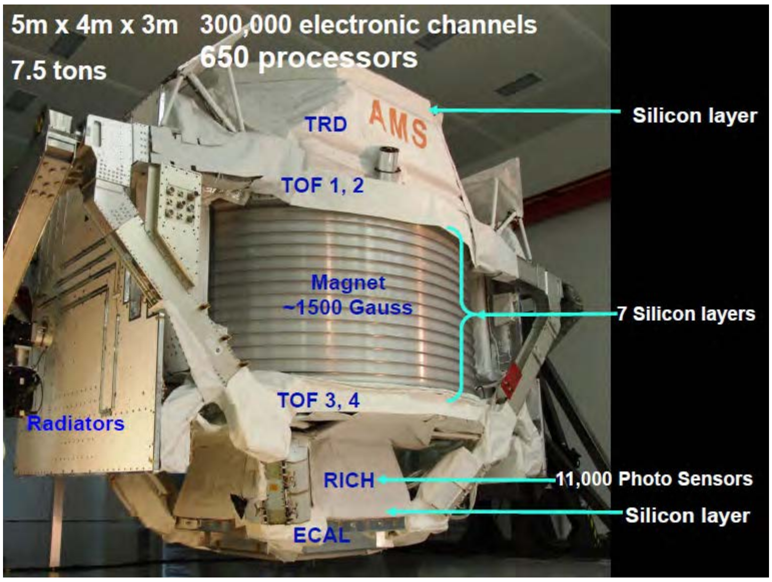

39

The BESS experiment

Balloon-borne Experiment with Superconducting Spectrometer

- Joint project of Japanese and USA Institutions to search for antimatter in the cosmic radiation
- **http://bess.kek.jp/**
- Last flight: 8 days from McMurdo (Antarctica) in Dec 2004

- Top and bottom Tof scintillators that also measure the particle energy loss
- Aerogel Cherenkov counter mounted under the top ToF
- 2 inner drift chambers (IDC) inside the magnetic field space
- Central tracking device in magnetic field region made of JET type drift chambers

BESS-TeV Spectrometer

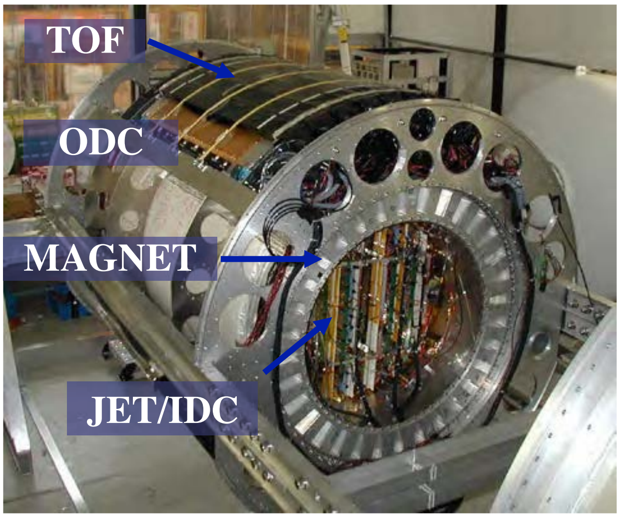

Electrons

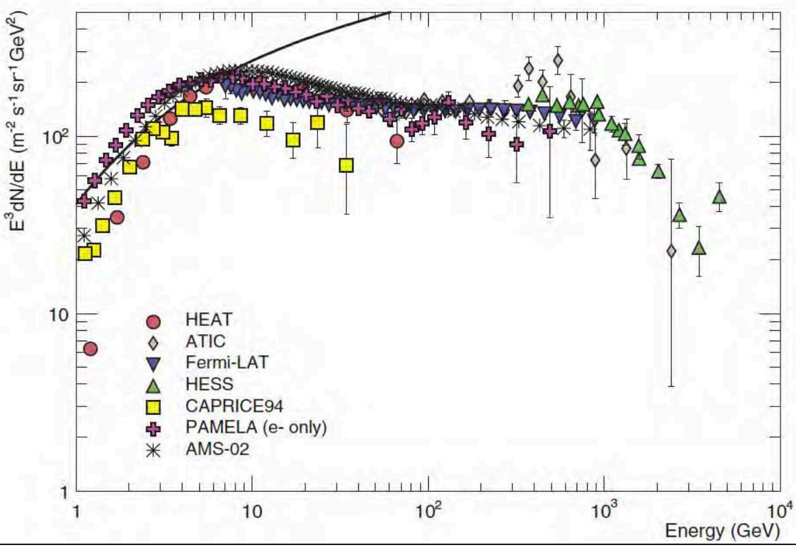

Electron to positron ratio

- As antimatter is rare in the Universe today, all antimatter we observe are by-product of particle interactions such as Cosmic Rays interacting with the interstellar gas.
- The PAMELA and AMS-02 satellite experiments measured the positron to electron ratio to increase above 10 GeV instead of the expected decrease at higher energy.

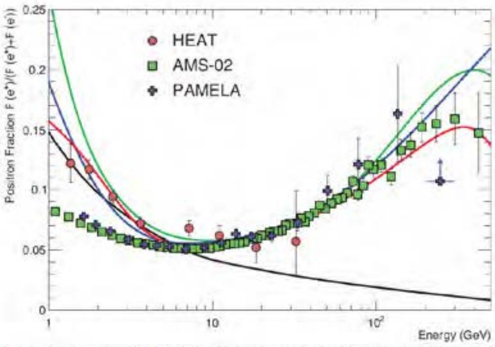

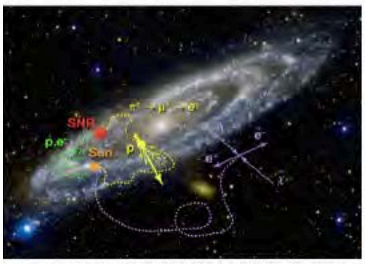

Image: GALEX, JPL-Caltech, NASA; Drawing: APS/Alan Stonebraker.

This excess might hint to to contributions from individual nearby sources (supernova remnants or pulsars) emerging above a background suppressed at high energy by synchrotron losses

Indirect measurements of Cosmic Rays: Extensive Air Showers

44

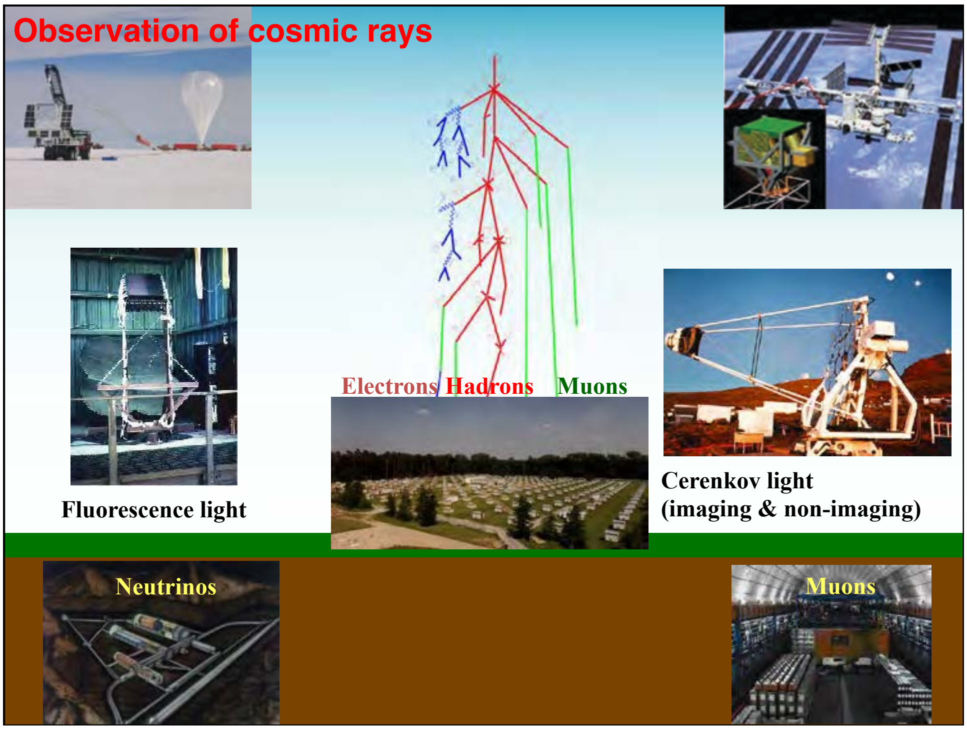

Higher energies: Extended Air Showers

- L'interazione di un primario in Atmosfera origina uno sciame di particelle con 3 componenti:
  - Elettromagnetica (EM)
  - Muoni
  - adroni

- **Le Energie dei RC molto maggiori delle E raggiungibili con acceleratori. E' possibile esplorare interazioni adroniche in regioni cinematiche non ancora studiate.**
- **Tevatron: protoni e antiprotoni collidono frontalmente con energia nel CdM ~2 TeV**
- **LHC: protoni protoni "head-on" ~14 TeV**

46

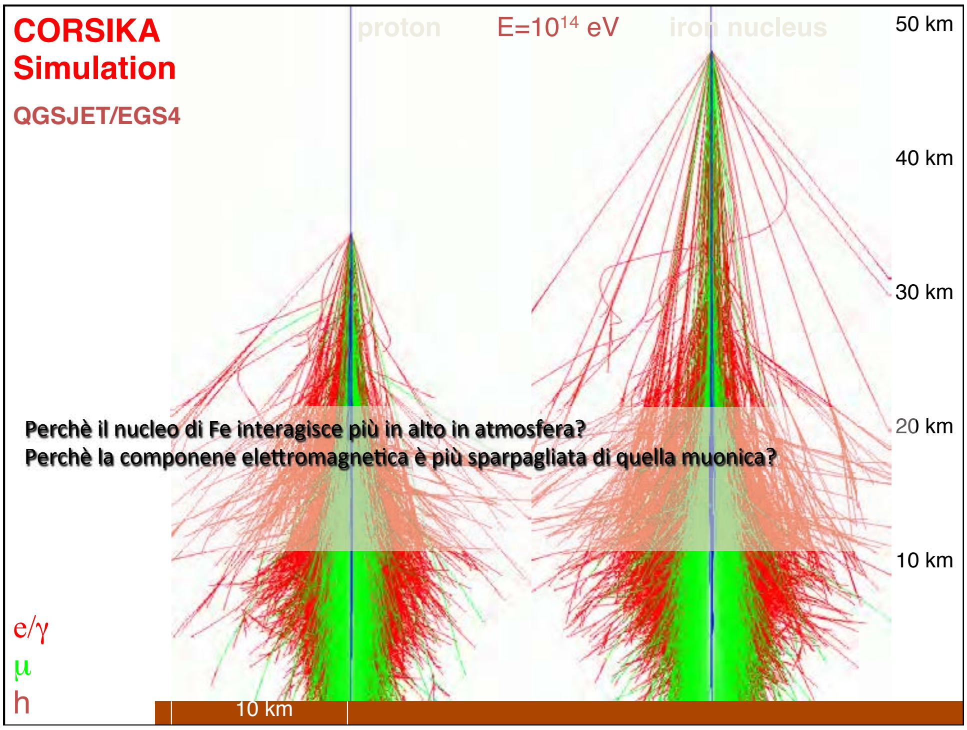

Come rivelare I RC di alta energia?

Per rivelare I raggi cosmici di energia elevata, occorre:

Una grande area di raccolta, S

Una grande accettanza in angolo solido, Ω

Un grande tempo di esposizione T

La grandezza "exposure" SΩT = m²-steradian-days determina il numero di eventi di alta energia rivelabili.

Il flusso di primari con energia $E_o > 10^{19}$ eV è circa:
0.5 particelle per km²-sr-*year*

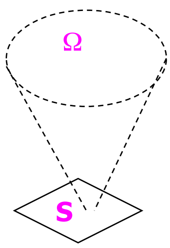

48

Le componenti dello sciame

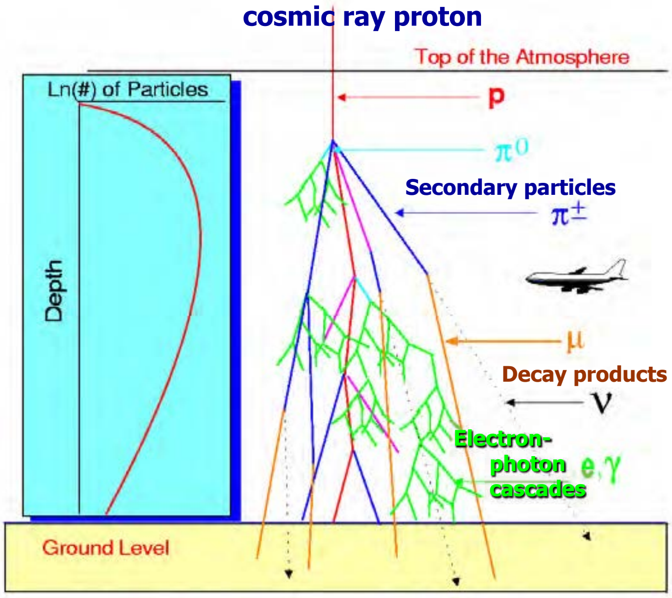

Caratteristiche generali dello sciame

- Gli adroni vengono esponenzialmente attenuati
- Lo sciame EM si sviluppa esponenzialmente sino ad un massimo, la cui profondità aumenta con E_0 (E primario)
- Sulla superficie terrestre (ed underground), prevalentemente muoni

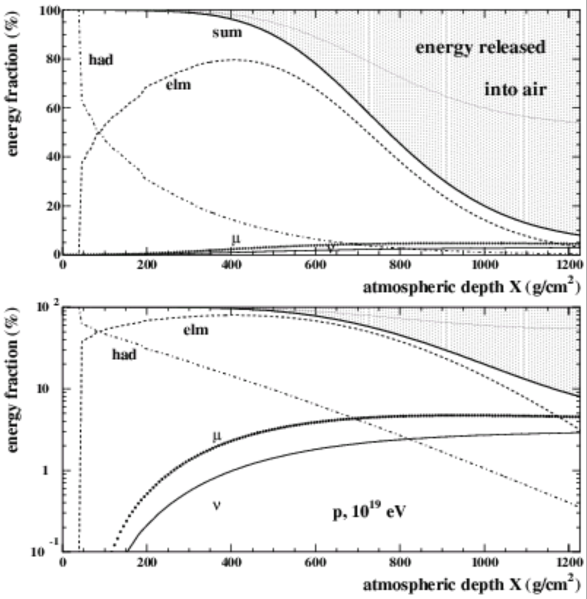

Caratteristiche generali dello sciame

- Un altro modo di vedere le cose:

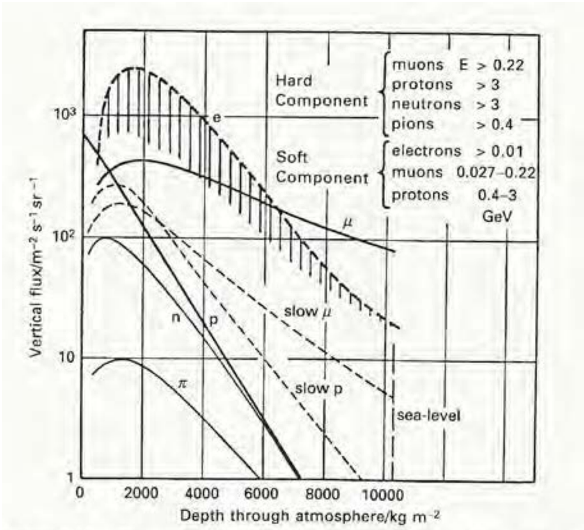

Figure 5.12. The vertical fluxes of different components of cosmic rays i[n the] atmosphere. (From A. M. Hillas (1972). *Cosmic rays*, page 50, Oxford: P[...]

EAS detectors

- Apparati sperimentali (Extensive Air Shower Arrays, EAS) che misurano sciami estesi sono in genere situati in alta quota.
- Misurano lo sciame "campionandolo" su una vasta superficie

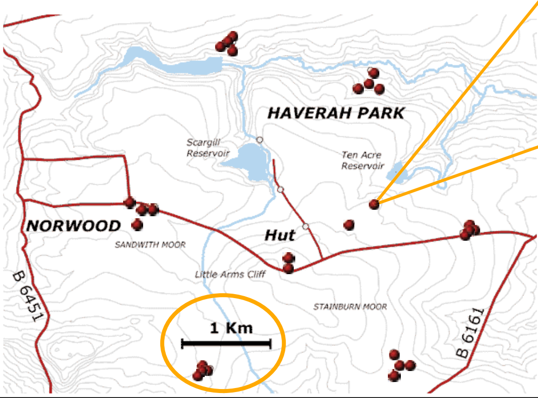

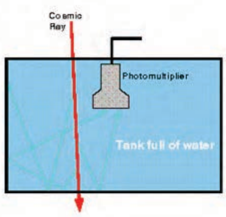

- Il rivelatore di sciami KASKADE (Karlsruhe) in Germania
- Ciascuna casetta contiene un rivelatore
- Distanza media: 13 m. L'edificio centrale contiene l'elettronica necessaria per l'esperimento
- Ottimizzato per lo studio dei RC nella regione del ginocchio. Non necessita di essere molto grande.

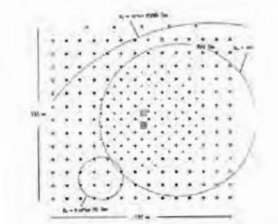

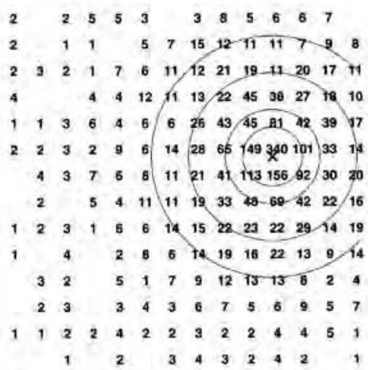

Fig. 8.13. Map of an air shower in a 196 detector array on a 15 m grid. The densities from (8.18) fluctuate with a Gaussian distribution with $\sigma = \sqrt{\rho}$. Because of that some detectors do not trigger.

Distribuzione laterale (un esempio)

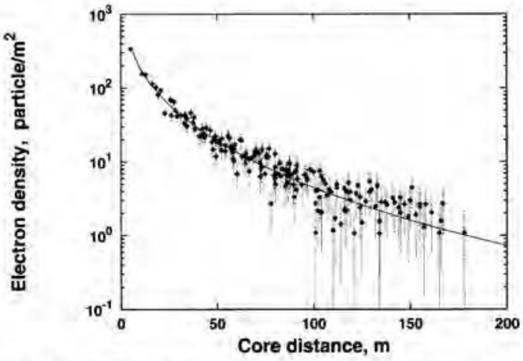

Fig. 8.15. The density distribution for the shower mapped in Fig. 8.13. The line shows the average charged particle lateral distribution.

55

LA FISICA DELLO SCIAME ESTESO

- La distanza media tra i contatori determina la *energia minima* dello sciame rivelabile.
- Il numero dei contatori, la *precisione* della misura
- L'area totale coperta, determina la *massima energia* misurabile.
- Ciascun contatore (*casetta*) misura in modo proporzionale la perdita di energia delle particelle che lo attraversa; da qui, si risale al numero di particelle incidenti
- Dalle misure della densità di particelle in ciascuna casetta dell'array, si risale alla distribuzione laterale *D(r)*.
- Dalla misura di *D(r)* si risale all'energia del primario, *e dalla frequenza del numero di conteggi* si risale al flusso.
- La direzione dello sciame può essere determinata dalla *misura dei tempi di ritardo temporale* nell'arrivo dello sciame su diverse casette (le particelle dello sciame sono $\perp$ al suo asse)

56

Il principio della rivelazione degli sciami con EAS
e determinazione della direzione del primario

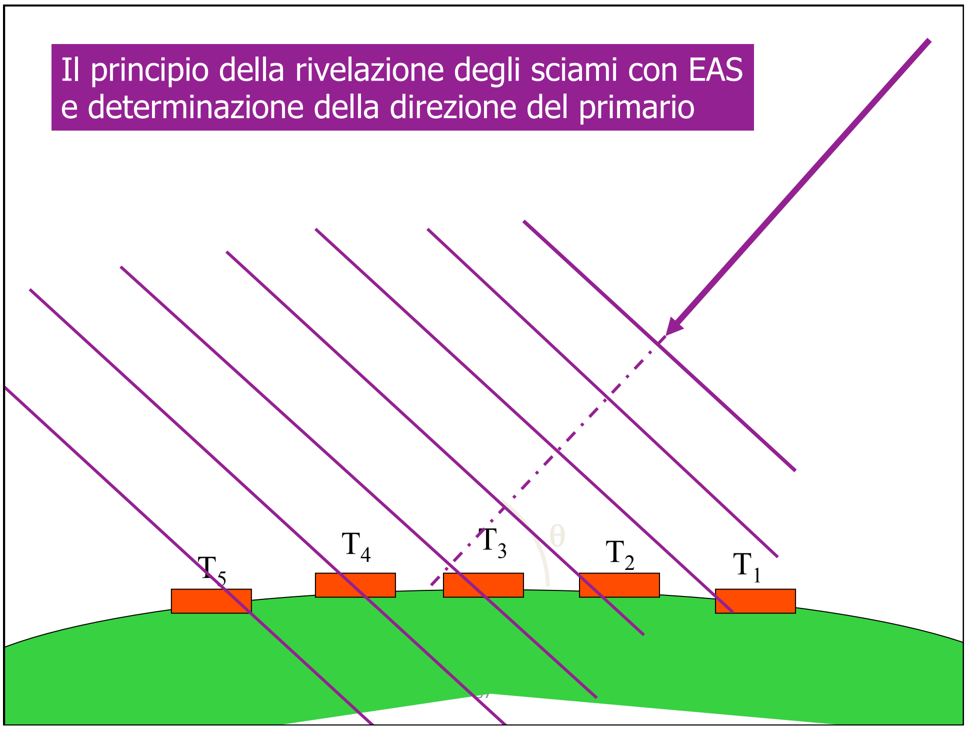

I dati sperimentali

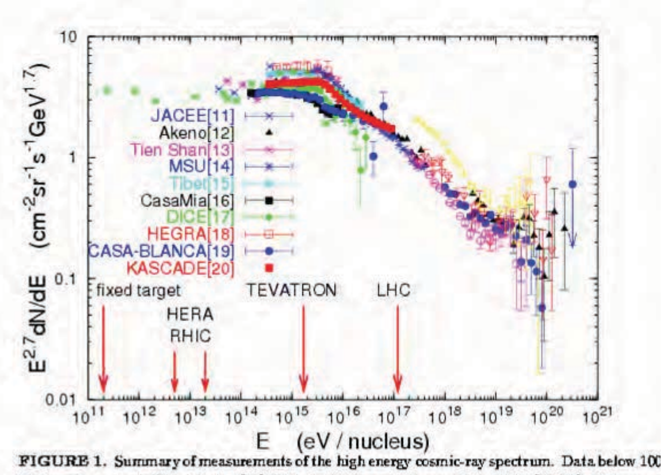

FIGURE 1. Summary of measurements of the high energy cosmic-ray spectrum. Data below 100 TeV are from a satellite detector [10]. Data in the knee region are from Refs. [11–20]. References for data above 10^{17} eV are given in Fig. 4.

Composizione chimica dei RC nella regione degli EAS

- Il modello del ***leaky box*** prevede un arricchimento di elementi pesanti nei RC sino al ginocchio.
- Gli EAS possono misurare <A> con difficoltà.
- Le misure possono essere poi confrontate con *modelli estremi* (solo p o Fe) via MC

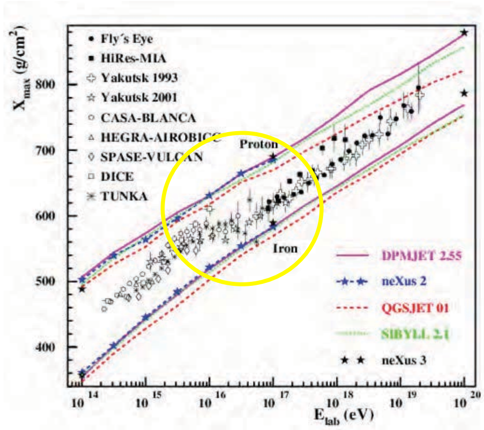

59

Altri metodi di Rivelazione

Le particelle cariche dello sciame EM che giungono al suolo possono essere rivelate da **rivelatori di sciami estesi** (§5.3)

Gli sciami di particelle producono anche **luce nell'atmosfera per effetto Cherenkov** (gli elettroni con E>20÷30 MeV).

La luce Cerenkov può venire rivelata (**telescopi Cherenkov**) nelle notti senza luna da appositi rivelatori al suolo.

Gli sciami EM inducono anche **l'eccitazione dell'azoto atmosferico**, che riemette irraggiando luce. Questa fluore-scenza può essere rivelata al suolo (**Rivelatori fluorescenza**).

La componente di muoni può essere rivelata da rivelatori "**underground**".

60

Rivelatori di sciami di altissima energia

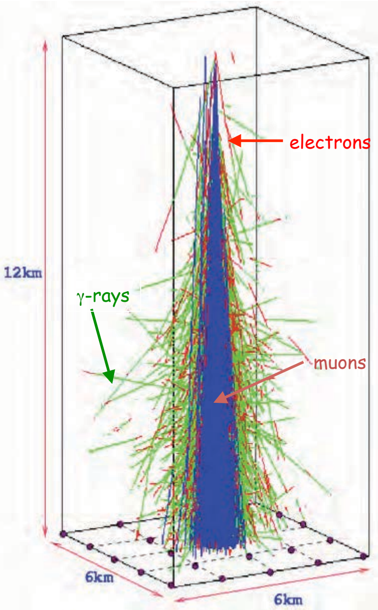

- Rivelatori di radiazione Cherenkov e fluorescenza in atmosfera (HiRes)
- Rivelatori al suolo (array) di vario genere (AGASA)
- Miste (AUGER)

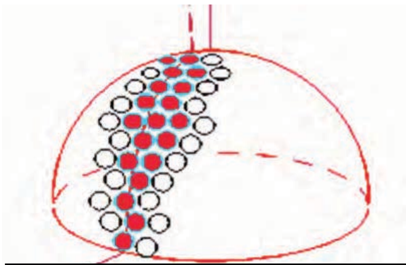

61

[redacted]

Il rivelatore Fly's Eye (USA)

Utah, 160 km da Slat Lake City

Specchi con fotomoltiplicatori rivelano la fluorescenza (visibile e UV) di N_2 indotta dalla cascata

Si può quindi studiare lo sviluppo dello sciame e risalire alla energia del primario

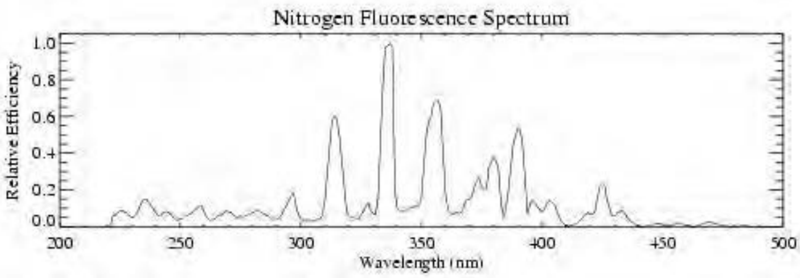

Il rivelatore Fly's Eye - 2

- 67 specchi con PM osservano la volta celeste
- È possibile ricostruire il profilo della cascata

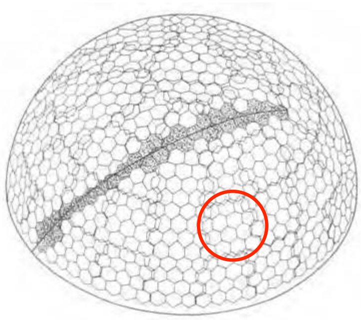

Si misura così energia (sviluppo shower) e direzione del primario

FE2: visione stereoscopica

63

Fly's eye→HiRes

- *Stereo* Hires: due insiemi di rivelatori per ricostruire in 3D lo sviluppo dello sciame
  - Migliore risoluzione angolare, studio correlazioni a piccoli angoli
  - Migliore comprensione della composizione chimica dei primari

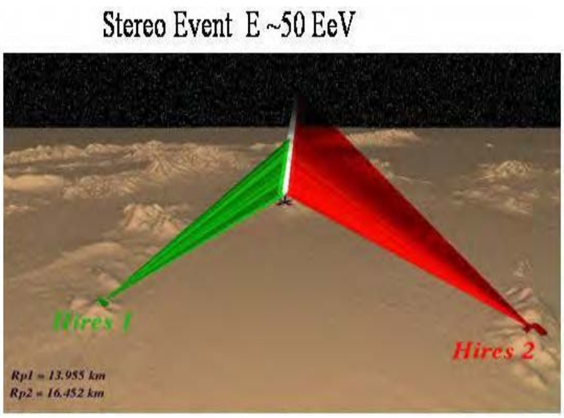

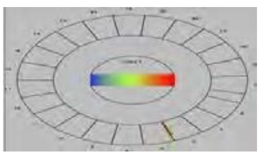

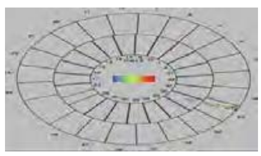

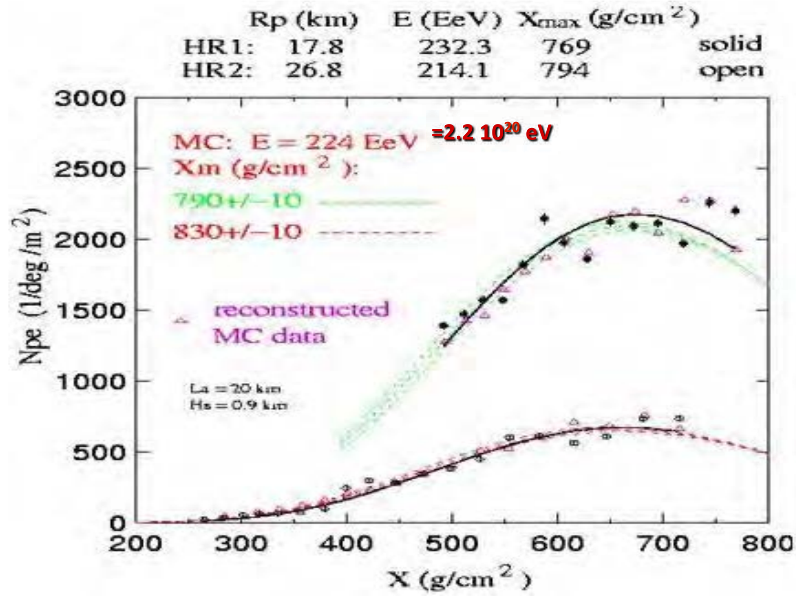

65

Agasa (Giappone)

- 100 km^2, 111 rivelatori a scintillazione, 27 per muoni, separazione ~1 km – $5 \cdot 10^{16}$ m^{2}s sr per E>10^{19} eV, θ < 45°

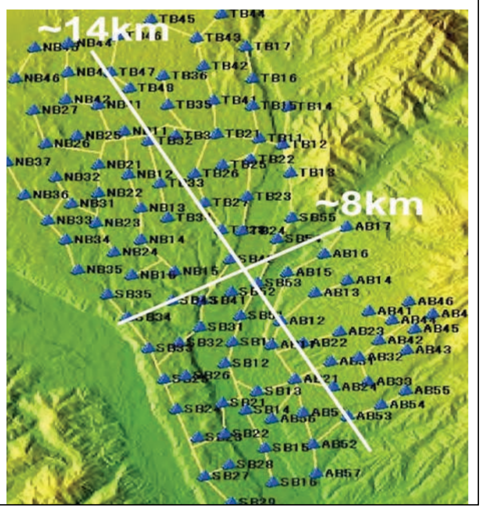

Volume di confinamento dei RC di origine extragalattico: il Cut-off di Greisen (GZK)

- L' universo è permeato dalla Radiazione Cosmica di Fondo a ~3 K (CMBR) → 160.2 GHz
- CMBR: fotoni di energia

Eγ ^{CMBR} = hν = 2π×6·10^{-22} MeV·s × 160.2 ·10^{9}Hz= 6**· 10^{-4} eV**

- La densità dei fotoni di fondo è ~400/cm^{3}
- Il fondo di radiazione pone un limite sulla distanza massima da cui i RC possono provenire.

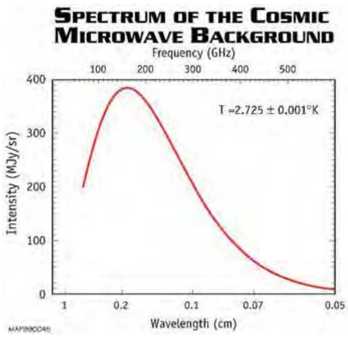

$G_{reisen}Z_{atsepin}K_{uzmin}$ cutoff

Soglia per reazioni di fotoproduzione

- **Fotoproduzione**: Protoni di alta energia possono interagire con fotoni, producendo un pione:

$$\boxed{\begin{array}{l} \gamma^{CMBR}+p \rightarrow \Delta^{*}(1236) \quad \rightarrow n+\pi^{+} \\ \qquad\qquad\qquad\qquad\quad \rightarrow p+\pi^{0} \end{array}}$$

- È necessario essere sopra la soglia di fotoproduzione nel sistema del CM: $E_0^{FP} \approx 300$ MeV
- Il processo ha una sezione d'urto in risonanza

$$\sigma_0^{P} \approx 250\ \mu b$$

Sezione d'urto per la Δ

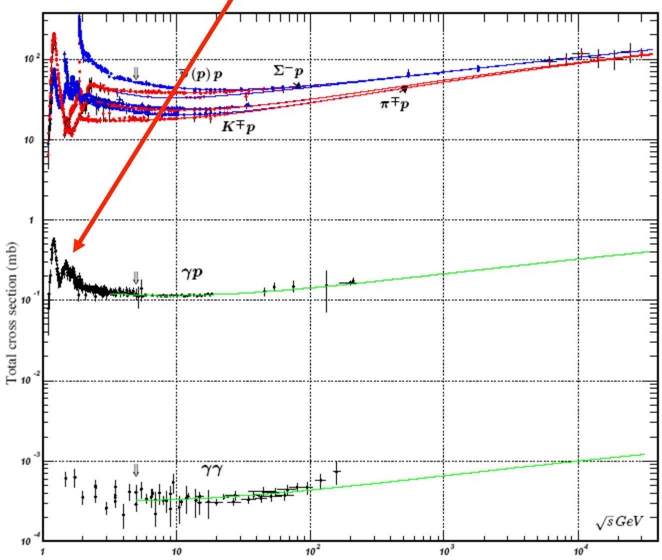

Soglia per la fotoproduzione (FP)

- Vogliamo determinare il valore di γ tale che si abbia un valore E_o^{PF} > 300 MeV
- La trasformazione di Lorentz tra i due SdR:

$$\left[x_0 = \gamma(x_0' + \frac{V}{c} x_1')\right]$$

$$E_0^{FP} = \gamma(E_\gamma^{CMBR} + \frac{v_p}{c} E_\gamma^{CMBR}) =$$
$$= \gamma E_\gamma^{CMBR}(1 + v_p / c) \approx 2\gamma E_\gamma^{CMBR}$$

E^{FP}_0 = Soglia fotoproduzione (~300 MeV)
E_γ^{CMBR}=Energia fotone =hν
γ = boost Lorentz del protone

- Dalla relazione, si ricava il valore di γ necessario per la fotoproduzione nel sistema di riferimento del laborarorio

$$\gamma = \frac{E_0^{FP}}{2E_\gamma^{CMBR}} \approx \frac{300MeV}{2\cdot 4.7\cdot 10^{-4}eV} \approx 3\cdot 10^{11}$$

- L'energia di soglia per i protoni per produrre π è quindi

$$E_0^{GZK} = \gamma(m_p c^2) \approx 3\cdot 10^{20}eV$$

Se l'energia del protone supera E_0^{GZK}, si innesca la FP.
In ogni processo, il p perde circa 1/10 della sua energia
Nota la densità numerica della CMBR (n_γ=400 cm^{-3}), si stima il cammino libero medio del p:

$$\lambda = (\sigma_{\gamma p} n_\gamma)^{-1} = 10^{25}cm = 3Mpc$$

Si può dunque stimare che i p NON possano giungere da distanze superiori a 10×3 Mpc = 30 Mp
Figura: Risultato di calcoli dettagliati.

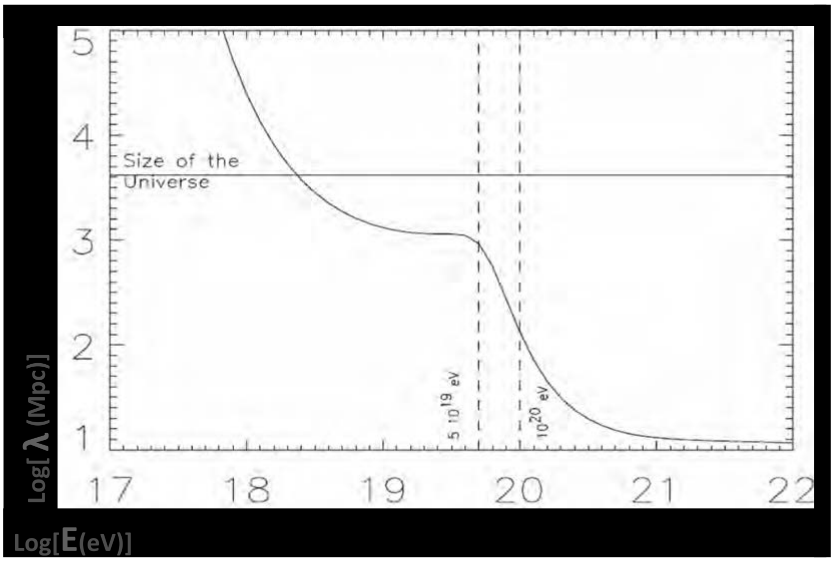

$$p + \gamma_{CMB} \rightarrow p + \pi^0$$
$$\rightarrow n + \pi^+$$
$$\rightarrow p + e^+ + e^-$$

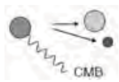

$$A + \gamma_{CMB} \rightarrow (A-1) + n$$
$$\rightarrow (A-2) + 2n$$
$$\rightarrow A + e^+ + e^-$$

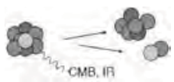

Particle energy rapidly degraded:
cut-off of the flux

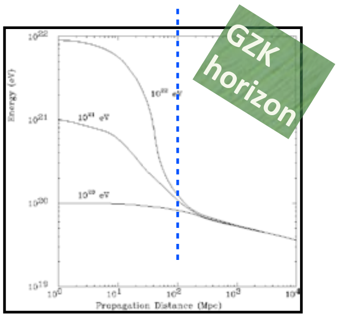

UHECR sources must be "nearby"

Is the observed cut-off due to propagation effects or to a limit on the maximum energy reachable by astrophysical accelerators?

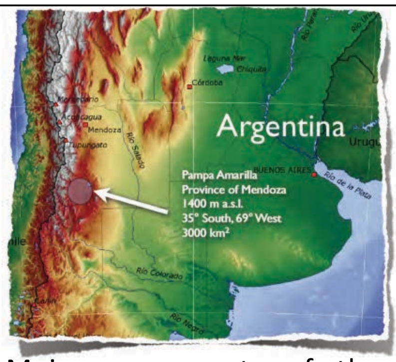

Large detectors are needed!

Located in the southern hemisphere, it is the **world's largest experiment of UHECRs** with its extension of **3000 km^2**

Powerful **hybrid detection** technique

Main components of the observatory:

- **Surface detector (SD)**: array of 1600 water-Cherenkov tanks, spaced by 1.6 km

- **Fluorescence detector (FD)**: 24 telescopes in 4 buildings

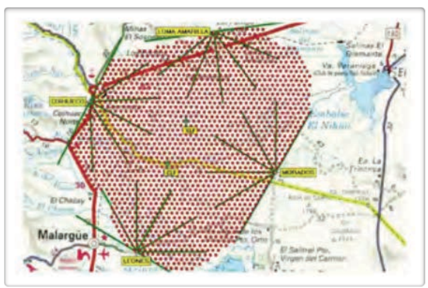

74

AUGER: Un rivelatore ibrido

Rivelatore di sciami: 1600 taniche cilindriche (ciascuna di 10 m^2 ed alte 1.5 m) riempite di acqua, per rivelare gli sciami al suolo tramite la luce Cerenkov emessa dagli elettroni nell'acqua

Il rivelatore di sciami misura la distribuzione laterale e temporale dello sciame

Distanza tra taniche: 1.5 km

Area di forma esagonale, di 60×60 km2

Rivelatori di fluorescenza: 6 telescopi con ciascuno 4 "occhi" per determinare il profilo longitudinale dello sciame e l'altezza del suo massimo.

75

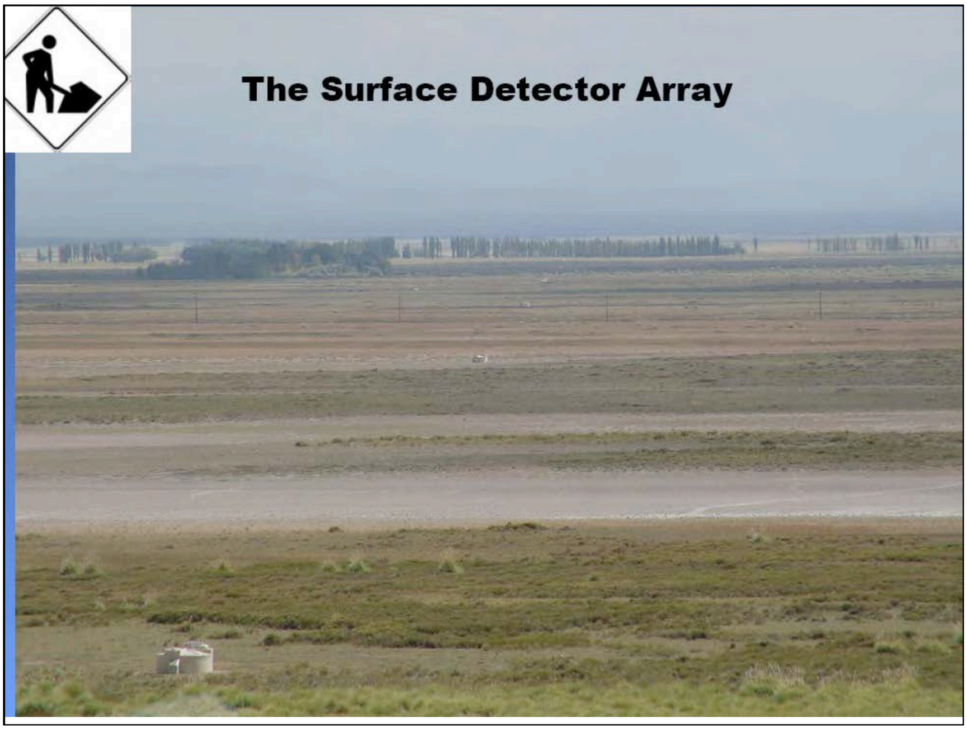

Uno dei rivelatori Čerenkov di AUGER

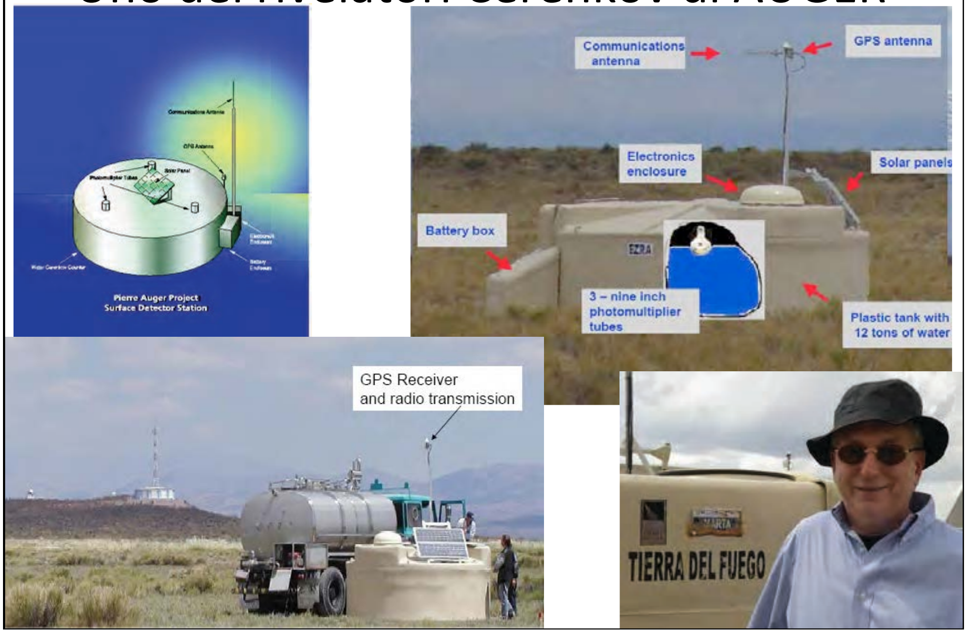

Rivelatori di Fluorescenza

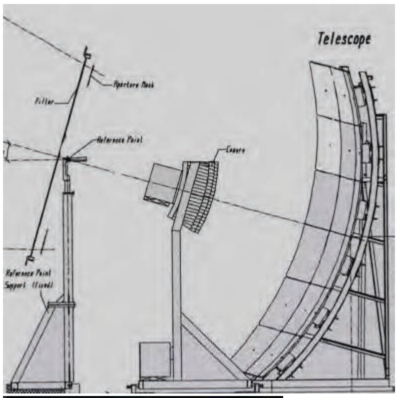

2 FD Telescopes

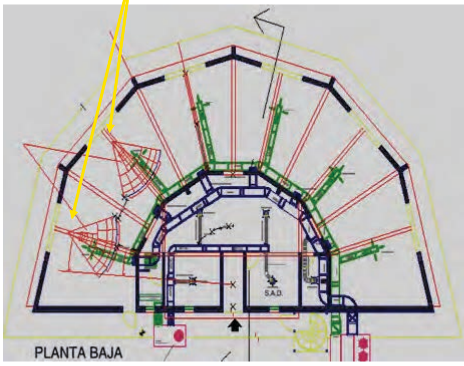

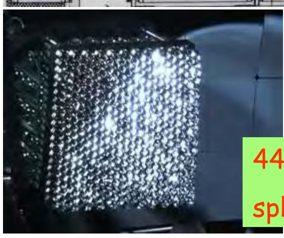

440 photomultipliers upon a spherical cup of 1.741 m ray

Rivelatori di fluorescenza: il profilo longitudinale dello sciame

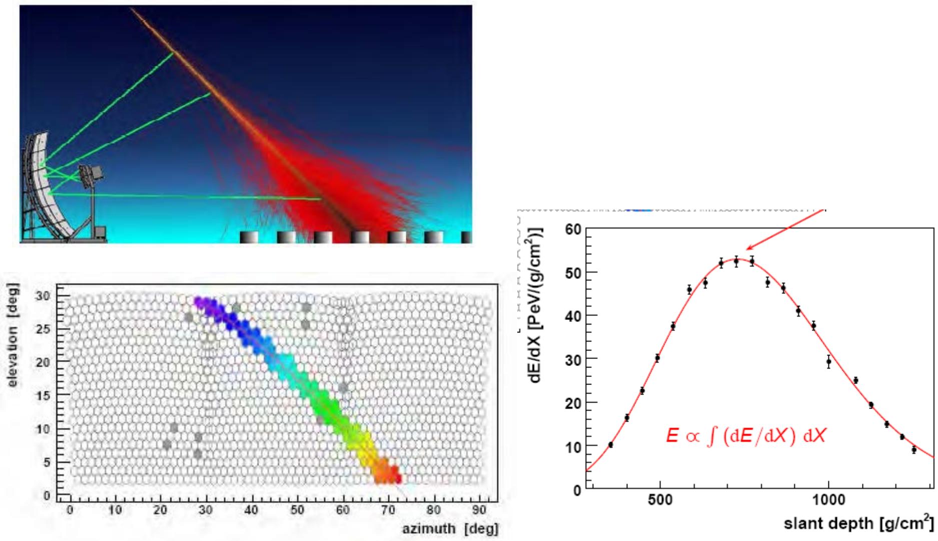

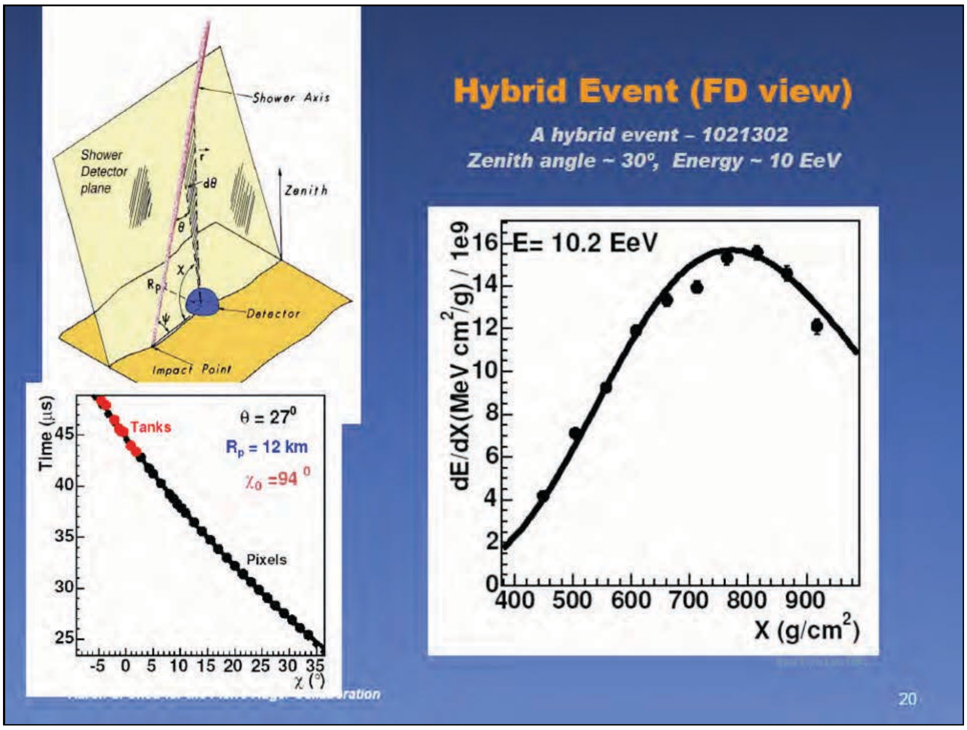

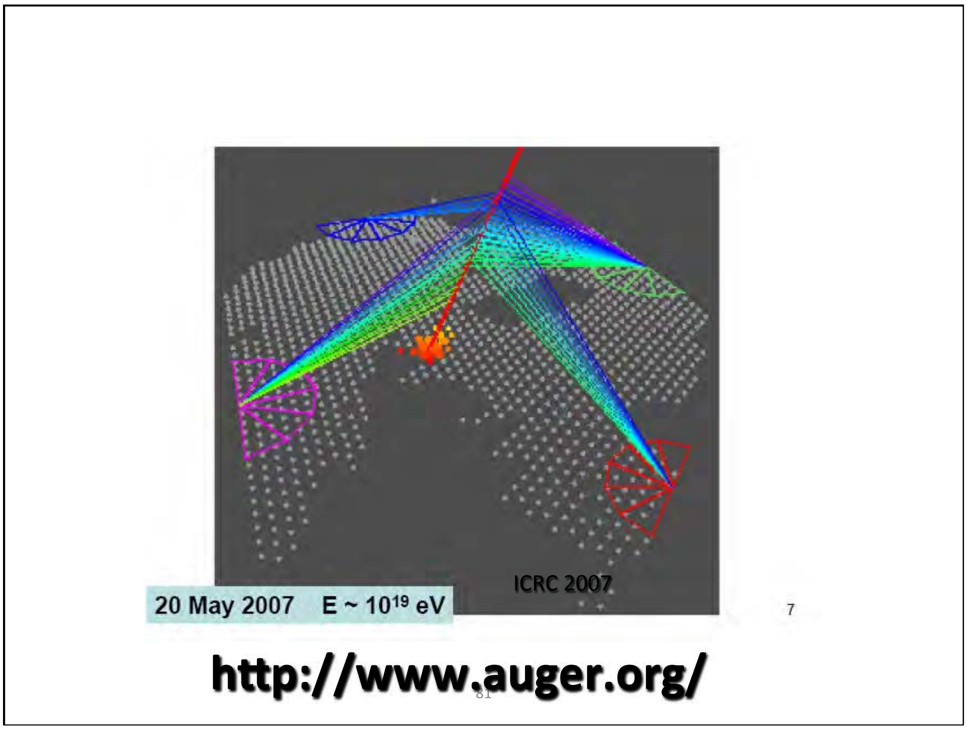
ICRC 2007
20 May 2007 E ~ 10^19 eV
7
http://www.auger.org/

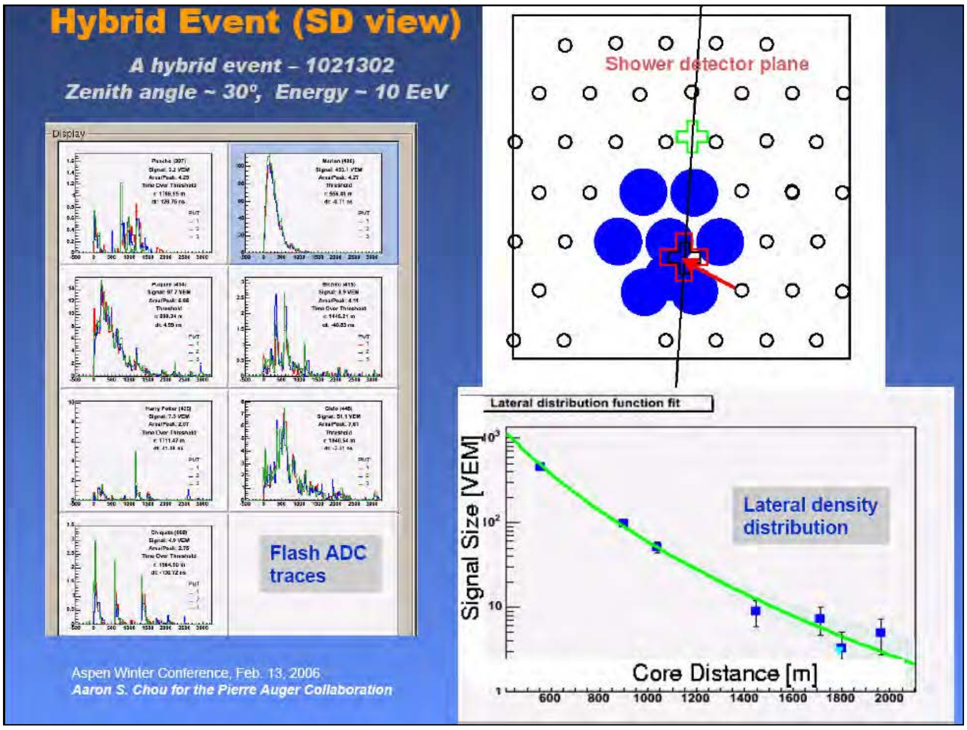
Hybrid Event (SD view)
A hybrid event – 1021302
Zenith angle ~ 30°, Energy ~ 10 EeV
Display
Flash ADC traces
Aspen Winter Conference, Feb. 13, 2006
Aaron S. Chou for the Pierre Auger Collaboration
Shower detector plane
Lateral distribution function fit
Signal Size [VEM]
Lateral density distribution
Core Distance [m]

- L'energia del RC viene misurata con entrambe le tecniche sperimentali
- Vi è correlazione tra le due misure

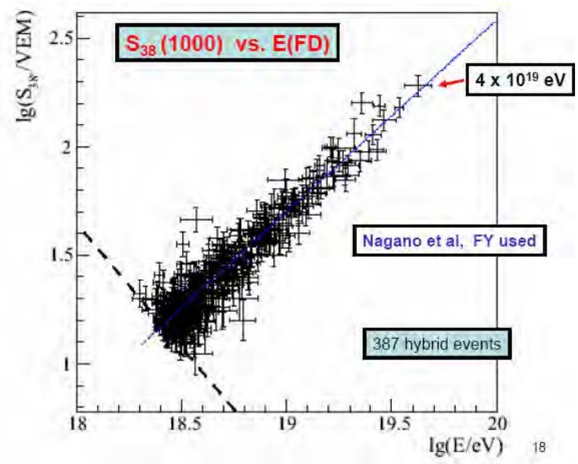

ICRC 2007

83

Correlation of the Highest-Energy Cosmic Rays with Nearby Extragalactic Objects

The Pierre Auger Collaboration*

www.sciencemag.org on November 9, 2007

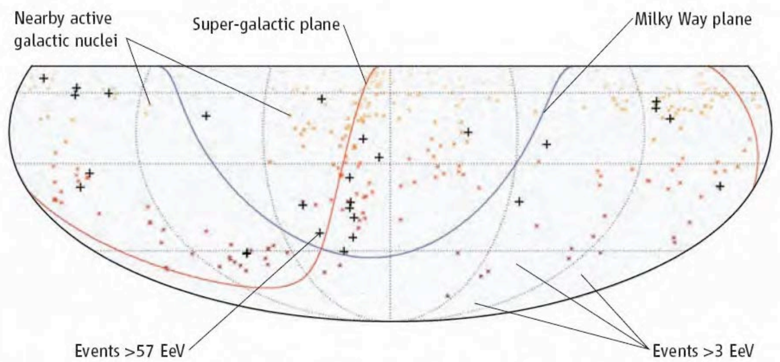

Sky map (2) showing cosmic rays detected by the Pierre Auger Observatory. Low-energy cosmic rays appear to originate from evenly distributed sources (blue dots), but the origins of the highest-energy events (crosses) correlate with the distribution of local matter as represented by nearby active galactic nuclei (red stars). Thus, active galactic nuclei are a likely source of these rare high-energy cosmic rays.

BREAKING NEWS 2009: AUGER trova una correlazione molto meno accentuata tra provenienza dei UHERC AGM

- I dati di Auger sono in accordo con il cut-off GZK: la diminuzione del flusso di RC sopra 6×10^{19} eV è dovuta all'interazione dei p con la radiazione cosmica di fondo
- La distribuzione di arrivo dei RC più energetici e' solo marginalmente correlata con la distribuzione degli AGN sino a 100 Mpc.

UHECR differential energy spectrum

measured with unprecedented precision

Suppression of the flux observed with a significance > 20σ

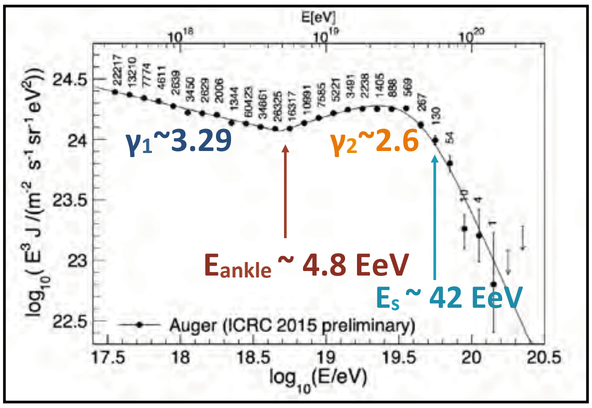

The observation of the suppression might not tell us anything on the accelerated particles.. Mass composition measurements might do!

UHECR study is an experimental challenge

Extremely low fluxes..

A direct detection can not be performed

We need **very large surface detection areas**

and we can measure the secondary fluxes of particles!

Extensive air showers

NB: not only particles, also radiation, e.g. fluorescence light.
So, particle detectors and/or light detectors

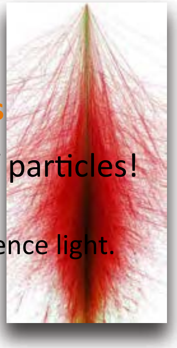

and extremely high energies

Monte-Carlo simulations of EAS rely on models for the hadronic interactions, which are an extrapolation of LHC results to much higher energies and different kinematic regions

Extensive air showers (EAS)

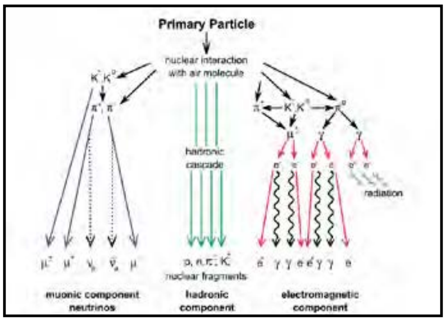

$$X = \int_z^\infty \rho(z')dz'$$

Important quantities:
- Depth at which the maximum shower size is reached: X_{max}
- Elongation rate $dX_{max}/d\log E$
- Shower-to-shower fluctuations $\sigma(X_{max})$

They carry information on the UHECR chemical composition

Iron induced showers compared to **proton** ones:
- more secondaries and more muons at ground
- smaller shower to shower fluctuations
- develop early in the atmosphere (smaller X_{max})

The hadronic interaction models used for simulating EAS are the largest source of uncertainty for the mass composition analysis.

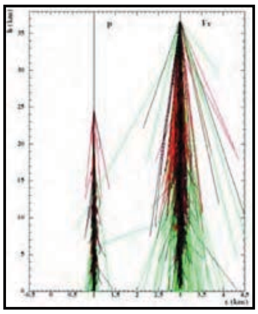

44

Mass composition measured by the FD

The Pierre Auger Collaboration, PRD 90 (2014) 122005

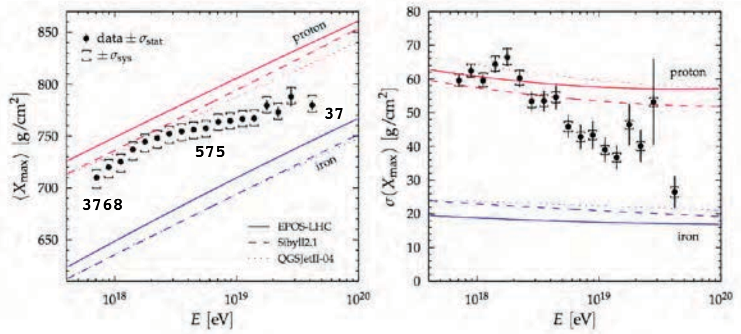

✓ Data comparison with models shows a composition mainly light up to about $3 \cdot 10^{18}$ eV, then trend towards heavier elements is observed.

✓ Direct calorimetric measurement of the mass, but good statistics only up to $3 \cdot 10^{19}$ eV.

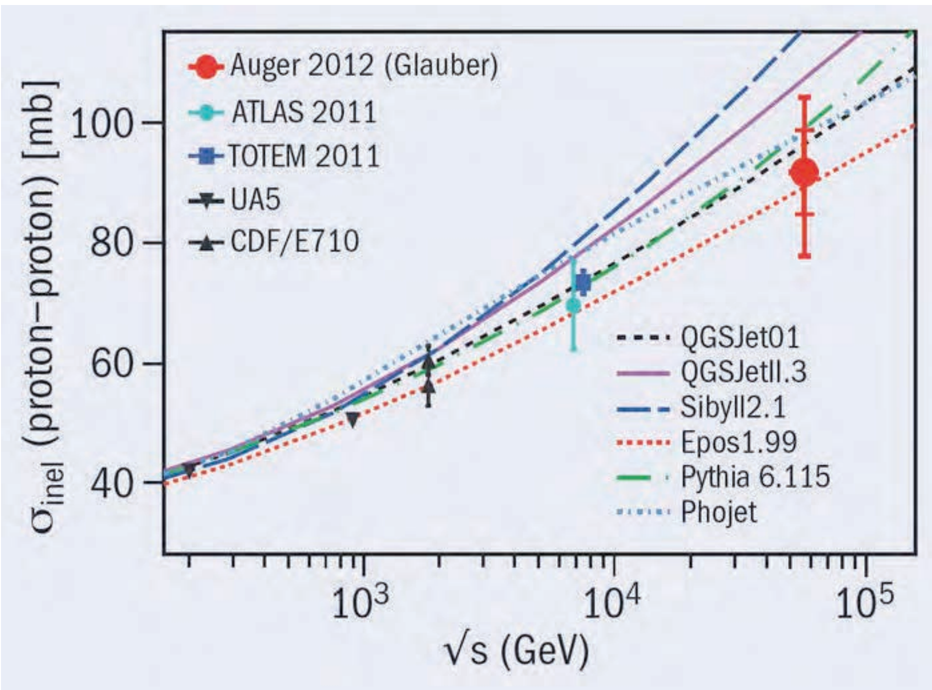

Multimessenger astroparticle physics

Alessandro De Angelis, INFN/INAF Padova and LIP/IST Lisboa

Lecture 3
The budget of energy and matter in the Universe; dark matter.

How can (V)HE photons be produced?

1. Interaction of accelerated charged particles with radiation and matter fields
   – The particle is accelerated via the Fermi 1^{st} order mechanism (collective shocks with a preferred direction)
   – It undergoes purely leptonic mechanisms (electrons), or hadronic collisions (protons) with subsequent π^0 decays
2. Top-down mechanisms
   – The decay or the annihilation of a heavy particle produce unavoidably photons, either direcly or in a q-qbar chain
   – Are there reservoirs of "TeV" particles around? Unlikely unless there are new particles…

(2) Top-down: are there new (heavy) particles which can produce HE photons?

- Rotation curves of spiral galaxies

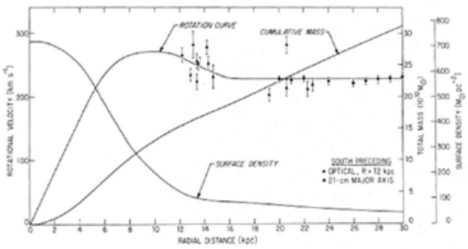

  - flat at large radii: if light traced mass we would expect them to be Keplerian at large radii, $v \propto r^{-1/2}$, because the light is concentrated in the central bulge
    - and disc light falls off exponentially
    - Zwicky had already noted in 1933 that the velocities of galaxies in the Coma cluster were too high to be consistent with a bound system
    - Observed for many galaxies, including the Milky Way

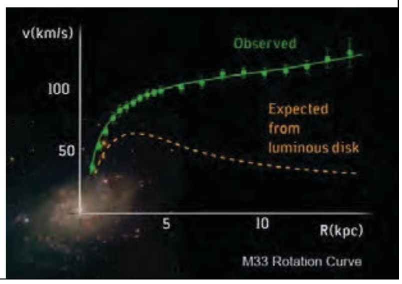

A way out

To assume that in and around the Galaxies there is

Dark Matter

subject to gravitational interaction but no electromagnetic interaction

$$M(r) \propto r \Rightarrow v_{rot} = \sqrt{\frac{GM(r)}{r}} = const.$$

- Must be "cold", i.e., non-relativistic (it is trapped by the gravitational field)
- The hypothsis is not odd: remember that the existence of Neptune was suggested on the basis of the irregular motions of Uranus
- How much DM do we need? results to be 5 times more than luminous matter (astrophysics, evolution of the Universe)

The Hubble constant and the energy density of the Universe determine the fate of the Universe

Velocity of recession

$$v = HR$$

Escape velocity

$$v_{esc} = \sqrt{\frac{2GM}{R}} = \sqrt{\frac{2G}{R}\cdot\frac{4}{3}\pi R^3\cdot\rho} = R\sqrt{\frac{8\pi G}{3}\cdot\rho}$$

Universe will recollapse if

$$v < v_{esc} \Rightarrow H < \sqrt{\frac{8\pi G}{3}\rho}$$

i.e., if

$$\rho > \rho_{crit} = \frac{3H^2}{8\pi G}$$

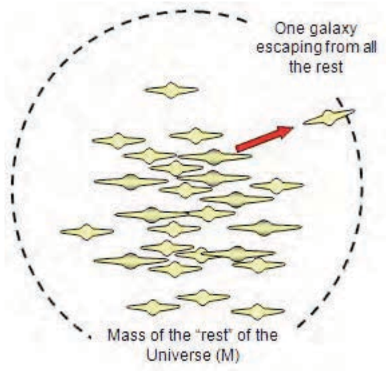

- Take H = 70 km s^{-1} Mpc^{-1} then:
  Critical density = $3H^2/8\pi G \sim 9.22\times10^{-27}$ kg m^{-3}
  The mass of a proton is ~ 1.66×10^{-27} kg => ~6 protons per cubic meter in average

Travel into the future

- Define a "normalized density" $\Omega = \rho/\rho_{crit}$
- $\Omega < 1$: the Universe will expand forever
- $\Omega > 1$: the Universe will eventually recollapse due to the action of Gravity

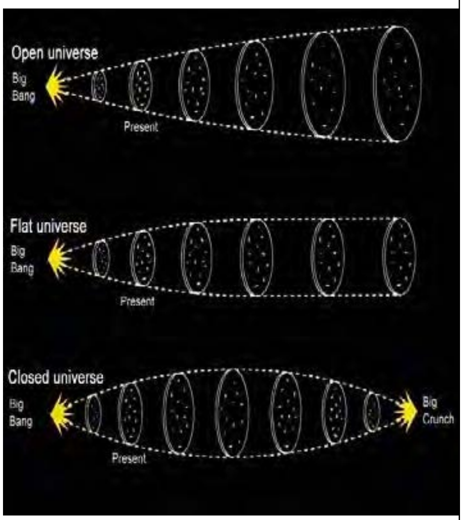

What is the matter density of the Universe?

- A simple technique to measure is just to count galaxies!

Look into a dark spot with the HST for a long time, extrapolate to the full space, add some dust and some black holes…

$\Omega_B \sim \Omega_M \sim 0.05 << 1$

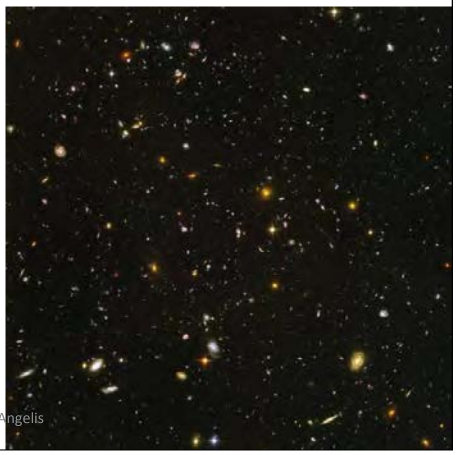

- You can also use some cosmological models to confirm & increase the accuracy
- And how much Dark Matter? From the motions in the Galaxies, and astrophysics

$\Omega_{CDM} \sim 0.26$

The ΛCDM model

$$H^2 - \frac{8}{3}\pi G\rho = -\frac{k}{R^2}$$

- The key CDM parameters are:

H_0 = (67.3 ± 1.2) km/s Mpc^{-1}

Ω_M, the matter density ~ Ω_B = 0.050 ± 0.002

Ω_{CDM}, the DM density = 0.265 ± 0.011

… (radiation, anisotropies)

We are convinced that k = 0

$\Omega_M + \Omega_{CDM} + \Omega_r + \Omega_\Lambda = 1$

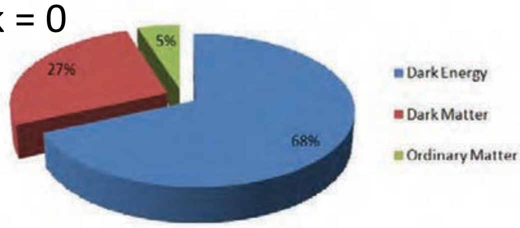

But the density of DM is much larger nearby

- 1.5 proton masses (~1.5 GeV) per cubic meter of dark matter in the Universe, so what?
- Well, there is a lot more near us…
- From the study of the rotation curve of the Milky Way, close to the solar system the density is 10^5 times larger than average: 4 10^5 proton masses/m^3
- The Earth moves in such a sea of dark matter. What is it?

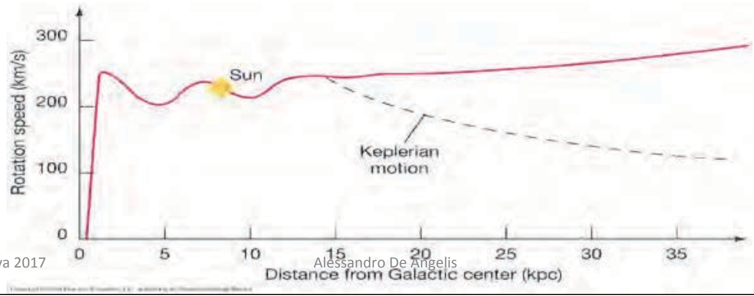

What we know about Dark Matter

- Impossible to avoid if you believe that gravity is universal
  - Electrically neutral (dark, not observed in direct searches)
  - Non-baryonic (BBN, astrophysics)
  - Cold (astrophysics, structure formation)
  - "Weakly" interacting (bullet cluster, non-observation in direct searches)
  - If "weak"~ Weak at production => (very small m) or m > 45 GeV (LEP) – Both ranges have important consequences in observational astrophysics
  - Ω_{CDM} = 0.265 ± 0.011 (WMAP, Planck) ~ 5 Ω_B
- No Standard Model candidate
  - neutrinos are too light, and they are "hot" (relativistic at decoupling)
    - hot dark matter does not reproduce observed large-scale structure

➔ Physics beyond the standard model

- WIMPs are particularly good candidates
  - well-motivated from particle physics [SUSY]
  - thermal production "automatically" leads to the right relic abundance

WIMPs

- WIMPs must have been in thermal equilibrium in the early Universe, when the temperature T exceeded by far the mass of the particle, $k_BT >> m_\chi$.
- The equilibrium abundance was maintained by annihilation of the WIMP with its anti-WIMP χbar into lighter particles (χ χbar → f fbar) and vice versa (f fbar → χ χbar). If the WIMP is a gauge boson as the photon, or a Majorana particle, χ = χbar.
- When at a given time t* the Universe cooled to a temperature such that $k_BT << m_\chi$, the interaction length becomes larger than the radius of the Universe (or the rate Γ for the annihilation falls below the Universe expansion rate): decoupling

$$\lambda = 1/H \Rightarrow H(t^*) = \Gamma = \langle \sigma_\chi v \rangle n_\chi \quad [\mathrm{cm}^2][\mathrm{cm/s}][\mathrm{cm}^{-3}]$$

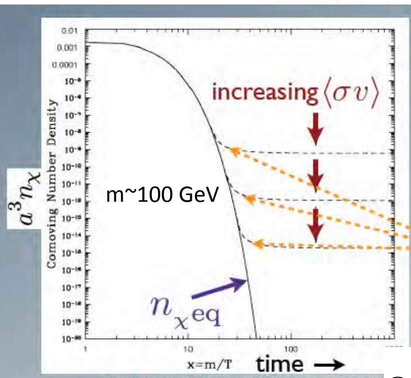

$$\frac{dn_\chi}{dt} + 3Hn_\chi = -\langle \sigma v \rangle \left(n_\chi^2 - n_{\chi\,\mathrm{eq}}^2 \right)$$

$\langle \sigma v \rangle$: $\chi\chi \to$ SM SM (thermal average)

"Freeze-out" when annihilation rate falls behind expansion rate ($\to a^3 n_\chi \sim$ const.)

Fig.: Jungman, Kamionkowski & Griest, Ph

$$\Omega_\chi \approx \frac{3\times10^{-27}\ \mathrm{cm}^3/\mathrm{s}}{<\sigma v>} \approx 0.1\ ;\ k_BT \sim \frac{m_\chi c^2}{20} \Rightarrow v \sim \frac{c}{4}$$

$$\Omega_\chi \approx \frac{3\times10^{-27}\ \mathrm{cm}^3/\mathrm{s}}{<\sigma v>} \approx 0.1 \Rightarrow \boxed{<\sigma v> \sim 3\times10^{-26}\ \mathrm{cm}^3/\mathrm{s}}$$

The WIMP "miracle"

- For electroweak interactions (see μμ production in ee collisions),

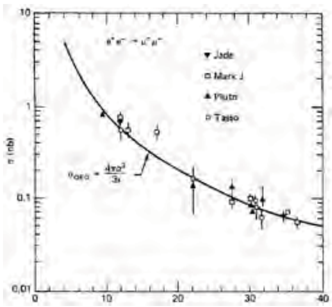

$$\sigma_W v \sim \frac{86.8\ \mathrm{nb}}{(E/\mathrm{GeV})^2}\frac{c}{4} \sim \frac{86.8\ \mathrm{x}\ 10^{-33}\ \mathrm{cm}^2}{(E/\mathrm{GeV})^2} 3\ \mathrm{x}\ 10^9\ \frac{\mathrm{cm}}{\mathrm{s}} \sim \frac{3\ \mathrm{x}\ 10^{-26}\ \mathrm{cm}^3/\mathrm{s}}{(E/100\ \mathrm{GeV})^2}$$

=> Weak coupling gives for free the right density at m_χ~100 GeV

In general at any time in a matter-dominated Universe (another miracle, Scherrer & Turner 1986)

Ω_χ approximately proportional to m_χ^2/M^2 for $\Omega_\chi < 1$

12

Beyond the Minimal SM of Particle Physics

- The SM of PP has been incredibly successful. It looks however an ad-hoc model, and the SU(3)⊗ SU(2)⊗ U(1) looks like a low-energy symmetry which is part of a bigger picture.
  - The SM looks a bit too complicated to be thought as the fundamental theory:
    - There are many particles, suggesting some higher symmetries (between families, between quarks and leptons, between fermions and bosons) grouping them in supermultiplets
      - Compositeness?
    - There are many free parameters
  - It does not describe gravity, which is the interaction driving the evolution of the Universe at large scale
  - It does not include dark matter
  - Interactions don't unify at high energy
  - The fundamental constants have values consistent with conditions for life as we know; this requires a fine tuning.
- Is there any physics beyond the SM we would need anyway and can provide "for free" DM candidates?

SUSY and the neutralino

- The most popular among non-minimal GUTs in particle physics is SUperSYmmetry.
- SUSY involves a symmetry between fermions and bosons: a SUSY transformation changes a boson into a fermion and vice-versa (each fermion has a superpartner which is a boson and vice-versa)
- To each particle a quantum number can be associated (R=1 for "our" particles and R=-1 for their partners). If SUSY is not violated or if it is mildly violated, R-parity is conserved, and the LSP is stable
- SUSY provides "for free" unification of forces at a scale elow the Planck scale, provided

  25 GeV < m_{LSP} < 25 TeV (90% C.L.)
- The LSP is likely one of the neutralinos χ (a Majorana fermion!)
  - Warning: there are many "SUSYs"

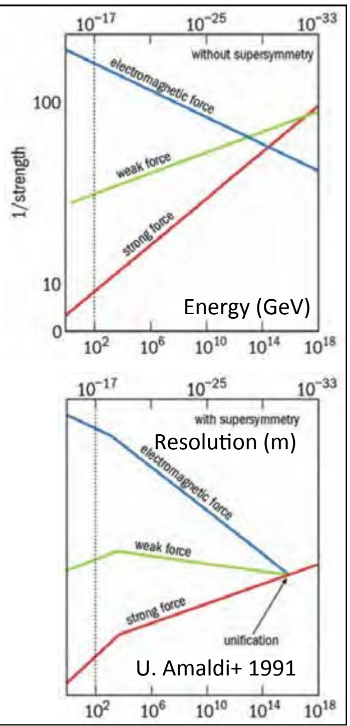

How do WIMPs produce photons?

- The energy "blob" from χχ annihilation might decay:
  - Directly into 2γ, or into Zγ if kinematically allowed. Clear experimental signature (photon line), but not very likely (requires one loop). In SUSY, the BR depends on what is the lightest neutralino composition.
  - Into a generic f-fbar pair, then generating a hadronic cascade with π^0 decaying into photons in the final state. Remind that flavors are left-handed and anti-flavors are right-handed with amplitude $[1+|p|/(E+m_f)]/2 \sim v/c$, and in this case for an s-wave you need to "force" one of the decay products to have the "wrong" elicity.

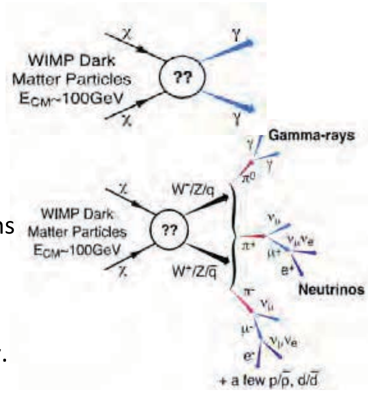

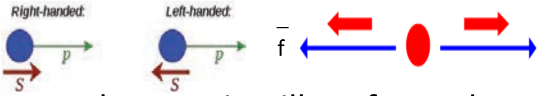

$$M_{fi} \propto \frac{1}{2}\left(1-\frac{|p|}{E+m_f}\right) = \frac{m_f}{2m_\chi + m_f}$$

=> The χχ pair will prefer to decay into the heaviest available pair – i.e., if 20 GeV < m_χ < 80 GeV, into b-bbar

WIMPs produce antimatter, too…

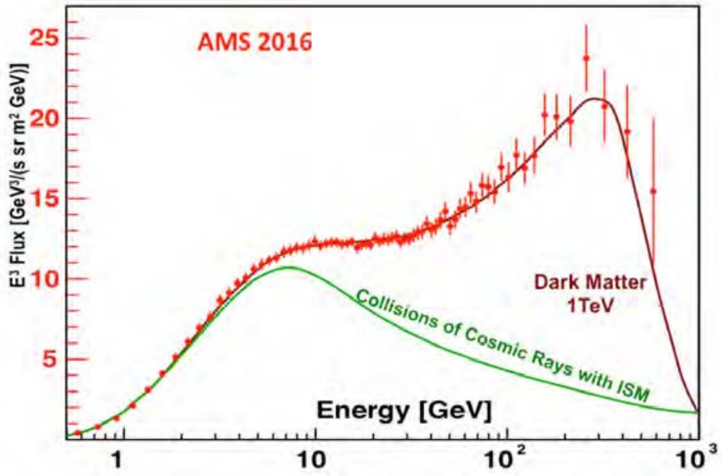

WISPs and other DM candidates

- WIMPs in the form of SUSY LSP are not the only possible "cold" DM candidates theoretically motivated:
  - WISPs, or weakly interacting slim particles.
    - Axions. Hypothetical light pseudoscalar postulated to explain the strong CP problem (CP should not be a symmetry of the QCD Lagrangian; however, CP appears to be conserved in QCD). A SSB at a very-high-energy scale, giving rise to an associated boson called the axion, might explain it. Being pseudoscalar (like the π^0), the axion can decay into two photons.

$$g_{a\gamma\gamma} \approx \frac{1}{M} ; \frac{m_a}{1 \text{ eV}} \sim \frac{1}{\text{M}/(6 \text{ x } 10^6 \text{ GeV})}$$

    Some other consequences for cosmological photon propagation (see later in these lectures).
    - ALPs. An extension of axions, relaxing the above relation between mass and coupling.
    - Sterile Neutrinos. A neutrino which does not interact via weak interactions. Constraints form cosmology make it unlikely that they can be the main component of DM; sterile neutrinos with masses of ~ keV and above could be, with some difficulty, accommodated in the present theories.
    - Matter in parallel branes; Shadow or Mirror matter. Some theories postulate the presence of matter in parallel branes, interacting with our world only via gravity or a super-weak interaction. In theories popular in the 1960s, a "mirror matter" was postulated to form astronomical mirror objects; the cosmology in the mirror sector could be different from ours, possibly explaining the formation of dark halos. This mirror-matter cosmology has been claimed to explain a wide range of phenomena.
  - Other possible candidates:
    - Superheavy Particles. Particles above the GZK cutoff (WIMPzillas) and other gravitational monsters could have been produced in the early Universe; their presence could result in excess of CR at UHE.
- And don't forget modifications of the theory of gravitation…

Summary of Lecture 3

- If our understanding of gravity is correct, unknown ``dark'' particles populate the Universe with a density 5 times larger than ordinary matter. Their presence should manifest itself in a flux of cosmic gamma-rays (and an excess of neutrinos and anti-matter), or in any case affect the flux of cosmic gamma-rays.

Exercises

1. *Virialized systems.* A cluster of galaxies, called Abell 2715 (at a redshift z ~ 0.114), contains about 200 galaxies, each the mass of the Milky Way. The average distance of the galaxies from the center of the cluster is 1 Mpc. If Abell 2715 is a virialized system, what is the approximate average velocity of the galaxies with respect to the center? The Milky Way has a mass of about 2 10^{42} kg.
2. *M/L.* At r = 10^5 light-years from the center of a galaxy the measurement yields v_{meas} = 225 km/s while the expected velocity calculated from the luminous mass is of v_{calc} = 15 km/s. Calculate the visible and the true galaxy mass, and the ratio M/L between the total and the luminous masses. How high is the average dark matter mass density?
3. *The WIMP annihilation prefers the production of heavy fermions.* Demonstrate that, in the reaction χχ ➔ f fbar,

$$\frac{1}{2}\left(1-\frac{|p|}{E+m_f}\right)=\frac{m_f}{2m_\chi+m_f}$$

and use the above relation to compute, for a WIMP of mass of 30 GeV, the ratios of the branching fractions into τ+τ- and into b-bbar

Multimessenger astroparticle physics

Alessandro De Angelis, INFN/INAF Padova and LIP/IST Lisboa

Lectures 4-5

How to detect high-energy photons (and, shortly, other kinds of cosmic rays).

Detecting particles

- Particle detectors measure physical quantities related to the outcome of a collision; they should ideally identify all the outcoming (and the incoming, if unknown) particles, and measure their kinematical characteristics (momentum, energy, velocity).
- In order to detect a particle, one must make use of its interaction with a sensitive material. The interaction should possibly not destroy the particle one wants to detect; however, for some particles this is the only way to obtain information about them.
- In order to study the properties of detectors, we shall first need to review the characteristics of the interaction of particles with matter.

Some reminders of particle physics…

Cross-section = σ (normally given per particle, or per atom, in a reaction)

Frequently used unit: 1 barn = 10^{-24} cm^2 (surface of a large atom; π (0.5 fm)^2 ~ few mb)

Attenuation length or "mean free path" $\lambda = 1/n\sigma$, where n is the number density of atoms

- Attenuation of a beam $I = I_0 \exp(-x/\lambda)$
- For materials, we often use the attenuation coefficient, μ, which is the cross section per mass (cm^2/g) (this is what you usually find in the PDG)
- Then attenuation length $\lambda = 1/n\sigma = 1/\mu\rho$, where ρ is density of the material

PARTICLE INTERACTIONS WITH MATTER

Interactions of photons with matter above the keV

- Photoelectric absorption
  - Photon is absorbed by atom
  - Electron is excited or ejected
- Compton scattering
  - Photon scatters off an electron
- Pair production
  - Photon interacts in electric field of nucleus and produces an $e^+ e^-$ pair

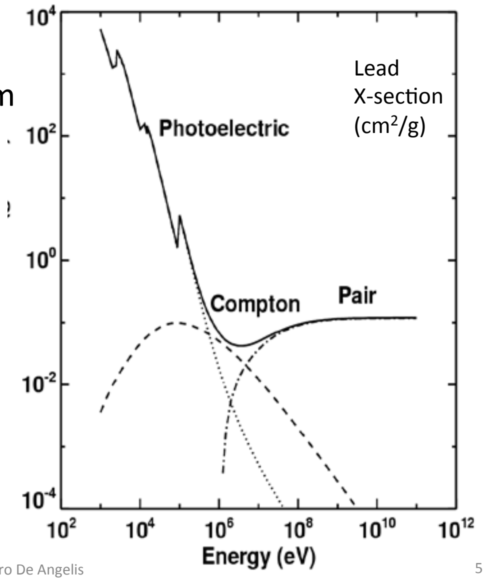

Photoelectric absorption

- Photons interact with matter by photoabsorption which causes excitation or ionization of atoms. Photons are absorbed.
- No simple analytic formula (guess why). "Edges" occur at the characteristic electronic transition energies. When in emission, elements produce characteristic lines at these energies

$$\sigma \propto \frac{Z^{\nu}}{E^3}$$

with v = 4-5

- High-Z detectors are more efficient
- Above the highest edge, the cross-section scales roughly as E^{-3}. This means that photo-absorption rapidly becomes inefficient at high energies.

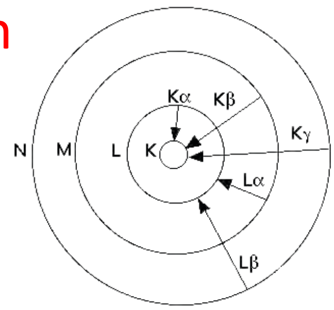

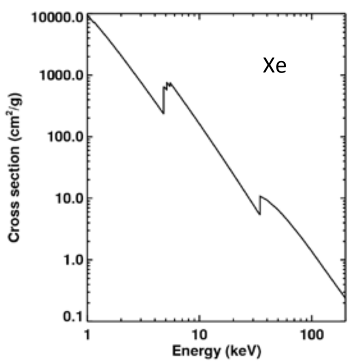

Compton scattering

- Is the scattering of a photon by an electron
- If the electron is initially free and at rest, after the collision, the photon is scattered at an angle θ and comes out with a reduced energy E' < E

$$E' = \frac{E}{1 + \frac{E}{m_e c^2}(1 - \cos\theta)}$$

The electron acquires an energy E' – E

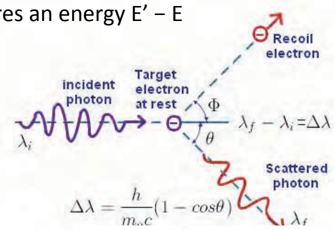

- Cross-section below $m_e c^2$ $\sigma_T \simeq \frac{8\pi\alpha^2}{3(m_e c^2)^2}(\hbar c)^2$ ~ 665 mb

  well above $m_e c^2$ $\sigma_{KN} \sim \sigma_T \frac{3}{8}\frac{m_e c^2}{E}\left[\ln\left(\frac{2E}{m_e c^2}\right) + \frac{1}{2}\right]$

- The scattering electron could also be moving: in this case, we might have E' > E ("inverse" Compton)

Pair Production: γ ➔e+e-

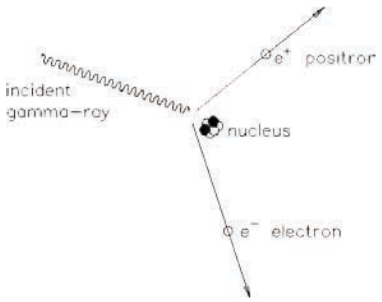

Nucleus is needed to conserve momentum and energy

$$\sigma_{Pair} \sim \frac{7}{9}\frac{1}{n_a X_0} \Rightarrow \lambda_{Pair} \sim \frac{9}{7} X_0$$

$$X_0 \sim \frac{716.4A}{Z(Z+1)\ln(287/\sqrt{Z})} \text{g cm}^{-2}$$

Active above 1MeV, it dominates from a few MeV to some 10^{20} eV

Cross section constant in this regime till 10 PeV, usually expressed in terms of the radiation length X_0- characteristic of the material

Above 10^{20} eV, the main interactions of the photon are strong interactions!

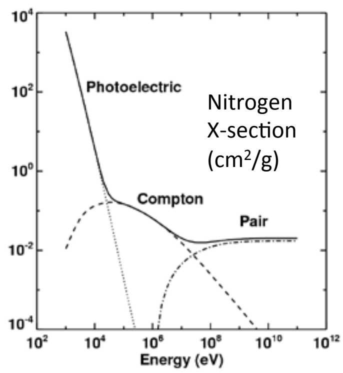

Pair Production - II

λ = (9/7) Xo for Eγ >> $2m_e$

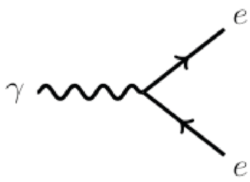

Energy spectrum ~ flat

Angular opening ~m_e/E

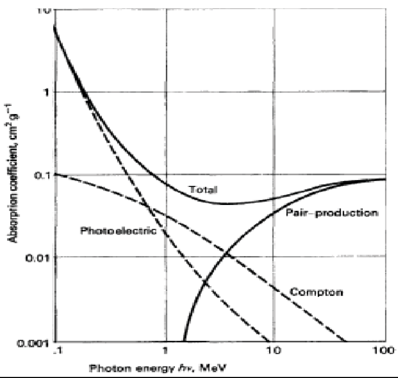

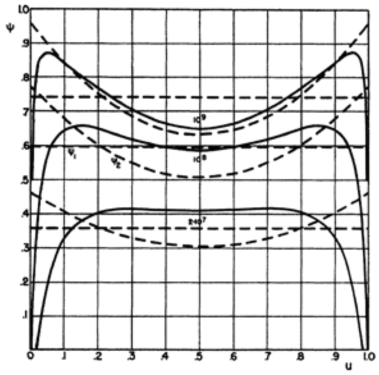

Charged particles: "Collision" energy loss

This is one of the most important sources of energy loss by charged particles. The average value of the specific (i.e., calculated per unit length) energy loss due to ionization and excitation whenever a particle goes through a homogeneous material of density ρ are described by the so-called Bethe formula[1]. This has an accuracy of a few % in the region $0.1 < \beta\gamma < 1000$ for materials with intermediate atomic number.

$$-\frac{dE}{dx} \simeq \rho D \left(\frac{Z}{A}\right) \frac{(z_p)^2}{\beta^2} \left[\frac{1}{2} \ln \left(\frac{2m_e c^2 \beta^2 \gamma^2}{I}\right) - \beta^2 - \frac{\delta(\beta,\rho)}{2},\right] \quad (4.1)$$

where

- ρ is the material density, in g/cm^3;
- Z and A are the atomic and mass number of the material, respectively;
- z_p is the charge of the incoming particle, in units of the electron charge;
- $D \simeq 0.307$ MeV cm^2/g;
- $m_e c^2$ is the energy corresponding to the electron mass;
- I is the mean excitation energy in the material; it can be approximated as $I \simeq 16\text{eV} \times Z^{0.9}$ for $Z > 1$;

$$-\frac{dE}{dx} \simeq \rho D \left(\frac{Z}{A}\right) \frac{(z_p)^2}{\beta^2} \left[\frac{1}{2} \ln\left(\frac{2m_e c^2 \beta^2 \gamma^2}{I}\right) - \beta^2 - \frac{\delta(\beta, p)}{2},\right]$$

The energy loss by ionization (Figure 4.1) is thus in first approximation:

- independent of the mass of the particle;
- typically small for high energy particles (about 2 MeV/cm in water; one can roughly assume a proportionality to the density of the material);
- proportional to $1/\beta^2$ for $\beta\gamma \lesssim 3$ (the minimum of ionization: minimum ionizing particle, or mip);
- basically constant for $\beta > 0.96$ (logarithmic increase after the minimum);
- proportional to Z/A (Z/A being about equal to 0.5 for all elements but Hydrogen and the heaviest nuclei).

In practical cases, most relativistic particles (e.g., cosmic-ray muons) have mean energy loss rates close to the minimum; they can be considered within less than a factor of two as minimum-ionizing particles. The radiation from a mip is well approximated as

$$\frac{1}{\rho}\frac{dE}{dx} \simeq 3.5 \left(\frac{Z}{A}\right) \text{MeV cm}^2/\text{g}\,.$$

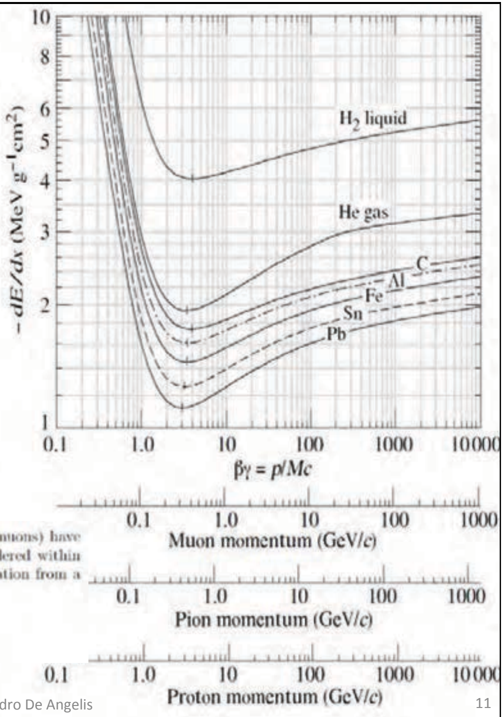

Multiple scattering

When a charged particle passes near a nucleus it undergoes a deflection which, in most cases, is accompanied by a negligible (approximately zero) loss of energy. This phenomenon, called elastic scattering, is caused by the same electric interaction between the passing particle and the Coulomb field of the nucleus. The global effect is that the path of the particle becomes a random walk (Figure 1.5), and information on the original direction is partly lost – this fact can create problems for the reconstruction of direction in tracking detectors. For very-high energy hadrons, also hadronic cross section can contribute to the effect.

Summing up many relatively small random changes of the direction of flight for a thin layer of traversed material, the distribution of the projected scattering angle of a particle of unit charge can be approximated by a Gaussian distribution of standard deviation (projected on a plane: one has to multiply by $\sqrt{2}$ to determine the variance in space):

$$\theta_0 = \frac{13.6\,\text{MeV}}{\beta c p} z_p \sqrt{\frac{x}{X_0}} \left[1 + 0.038 \ln \frac{x}{X_0}\right].$$

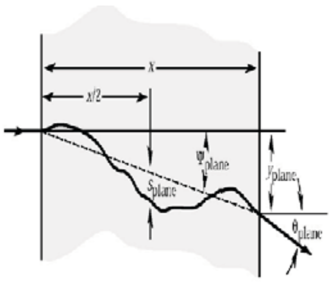

Electron bremsstrahlung and radiation length

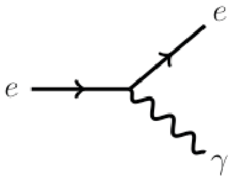

- As pair production, forbidden in vacuo by 4-momentum conservation
  - Requires interaction with the medium
- Photons of momentum $q<E_e$ emitted with probability ~proportional to 1/q
  - (and collimated: ~ m_e/E)

  ie, energy emission is ~constant for each interval of photon energy; total is propto E
  - The dependence on the material appears through the radiation length Xo:

    $dE_e/dx = -1/X_o$
  - Xo can be found in tables. It is ~400 m for air at NTP, ~43 cm for water; for density 1 g/cm^3
  - Collision energy loss is almost constant (plateau)

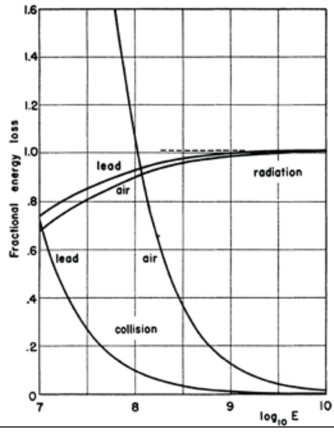

Cherenkov radiation (ß>1/n)

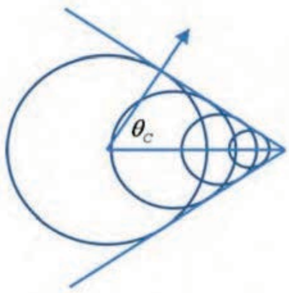

When ß>1/n in a medium, light is emitted in a coherent cone at an angle such that

$$\cos\theta_c = \frac{1}{n\beta}$$

from the direction of the emitting particle. The presence of a coherent wavefront can be easily derived by using the Huygens–Fresnel principle. The number of photons produced per unit path length and per unit energy interval of the photons by a particle with charge z_p at the maximum (limiting) angle is

$$\frac{d^2N}{d\lambda dx} \simeq \frac{2\pi\alpha z_p^2}{\lambda^2}\sin^2\theta_c$$

- The total energy radiated is small, some 10^{-4} times the energy lost by ionization. In the visible range (300–700 nm), the total number of emitted photons is about 40/m in air, about 500/cm in water.
- Due to the dependence on λ , it is important that Cherenkov detectors be sensitive close to the ultraviolet region. However, both n and the absorption probability of light can depend strongly on λ

Hadronic interactions

- The nuclear or hadronic force is felt by hadrons, charged and neutral; at high energies (above a few GeV) the inelastic cross section for hadrons is dominated by nuclear interaction
  - Above some 100 EeV, the "hadronic" component of photons dominates their behavior, and this becomes also the most important interaction for photons
- High-energy nuclear interactions can be characterized by an inelastic interaction length λ_H . Values for $\rho\lambda_H$ are typically of the order of 100 g/cm^2 ; a listing for some common materials is provided in the PDG — where the inelastic length λ_I and the total length λ_T are separately listed, and the rule for the composition is

$$1/\lambda_T = 1/\lambda_H + 1/\lambda_I \ .$$

- The final state products of inelastic high-energy hadronic collisions are mostly pions, since these are the lightest hadrons. The rate of positive, negative, and neutral pions is more or less equal—as we shall see, this fact is due to an important approximate symmetry of hadronic interactions, called the isospin symmetry.

Just for fun, neutrino cross sections

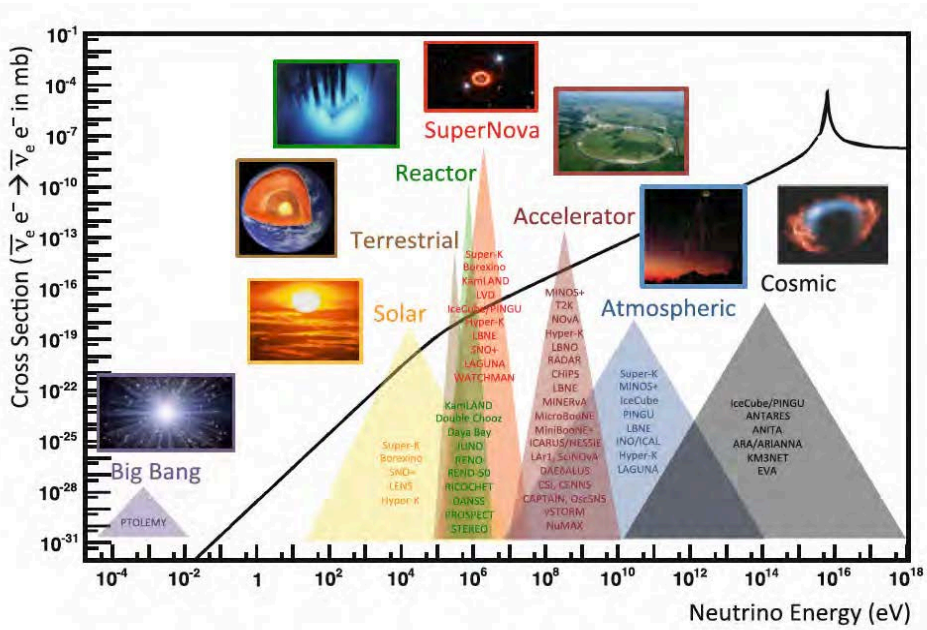

Bruno Rossi (founder of the Dipartimento)

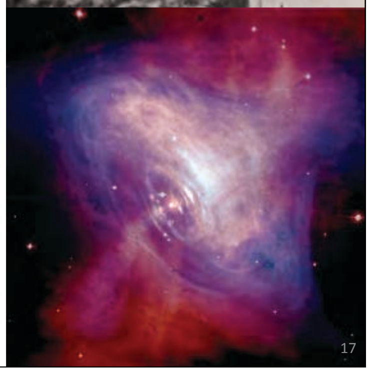

- Expelled from Italy in 1938 with a bad treatment, moved to US
- Toward the end of the 1950s, as accelerator experiments came to dominate particle physics, Bruno Rossi turned to space research
- At MIT he initiated a program of detector development and rocket experiments aimed astrophysics (but the excuse was the control of nuclear explosions above the atmosphere)
- To implement his ideas about X-ray astronomy, Rossi addressed the young Giacconi (Giacconi & Rossi (1960): “A ‘Telescope’ for Soft X-Ray Astronomy”) and they obtained support for rocket experiments from the Air Force. After two failures, the third satellite, launched in 1962, discovered a bright X-ray source.
- Giacconi won the Nobel prize in 2002 (Rossi died in 1993).

Multiplicative showers (Rossi 1934)

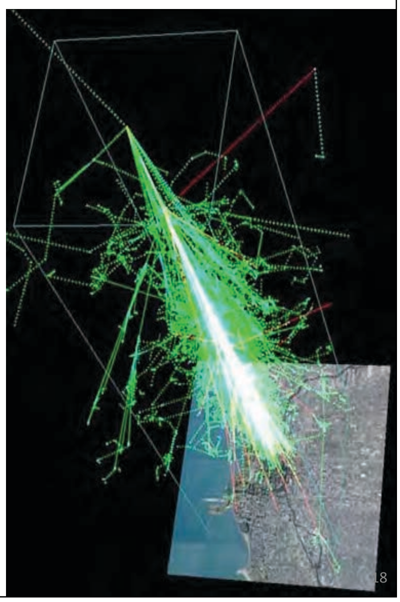

- Cascades of particles produced as the result of a primary high-energy particle interacting with matter
  - The incoming particle interacts, producing multiple new particles with lesser energy; each of these interacts in turn, a process that continues until many particles are produced. These are then stopped in the matter and absorbed
- 2 basic types of showers:
  - electromagnetic showers are produced by a particle that interacts via the electromagnetic force, a photon or electron
  - Hadronic showers are produced by hadrons, and proceed via the strong nuclear and the electromagnetic forces

Electromagnetic showers

- When a high-energy e or γ enters an absorber, it initiates an em cascade as pair production and bremsstrahlung generate more e and γ with lower energy
- The ionization loss becomes dominant < the critical energy E_c
  - E_c ~ 84 MeV in air, ~73 MeV in water; ~ (550/Z)MeV
    - Approximate scaling in $y = E/E_c$
  - The longitudinal development ~scales as the radiation length in the material: $t = x/Xo$
  - The transverse development scales approximately with the Moliere radius R_M ~ (21 MeV/E_c) Xo
    - In average, only 10% of energy outside a cylinder w/ radius R_M
    - In air, R_M ~ 80 m; in water R_M ~ 9 cm
- Electrons/positrons lose energy by ionization during the cascade process
- Not a simple sequence: needs Monte Carlo calculations

A simplified approach (Heitler)

- If the initial electron has energy E_0>>E_C , after t Xo the shower will contain 2^t particles. ~equal numbers of e+, e-, γ, each with an average energy

  $E(t) = E_0/2^t$

- The multiplication process will cease when $E(t)=E_C$

$$t_{max} = t(E_C) \equiv \frac{\ln(E_0/E_C)}{\ln 2},$$

and the number of particles at this point will be

$$N_{max} = \exp(t_{max} \ln 2) = E_0 / E_C$$

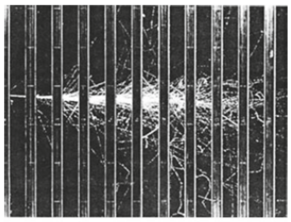

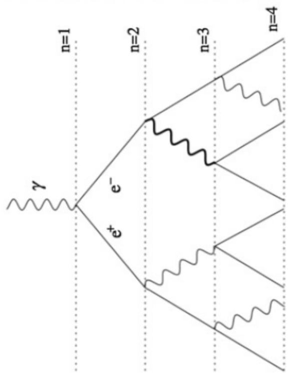

An analytic model: Rossi's "approximation B"

- Rossi in 1941 published an analytical formulation for the shower development as a set of 2 integro-differential equations under the approximation that:
  - Electrons lose energy by ionization & bremsstrahlung; asymptotic formulae hold
  - Photons undergo pair production only; asymptotic formulae hold ($E > 2\,m_e$)
- Very good approximation until $E \sim E_c$

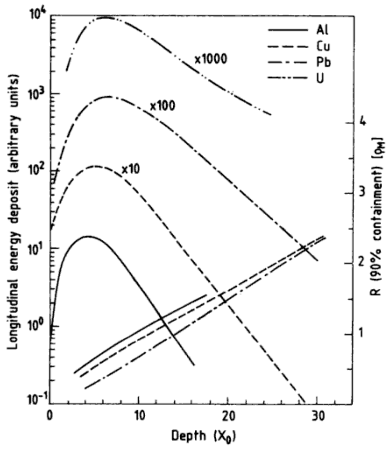

	Incident electron	Incident photons
Peak of shower, t_{max}	$1.0 \times (\ln y - 1)$	$1.0 \times (\ln y - 0.5)$
Centre of gravity, t_{med}	$t_{max} + 1.4$	$t_{max} + 1.7$
Number e^+ and e^- at peak	$0.3\,y \times (\ln y - 0.37)^{-1/2}$	$0.3\,y \times (\ln y - 0.31)^{-1/2}$
Total track length T	y	y

(Rossi-Greisen 1941, Rev. Mod. Phys. 13, 240)

$$\frac{\partial\pi(E,t)}{\partial t} = 2\int_0^1 \gamma\left(\frac{E}{u},t\right)\psi_0(u)\frac{du}{u} - \int_0^1\left[\pi(E,t) - \frac{1}{1-v}\pi\left(\frac{E}{1-v},t\right)\right]\varphi_0(v)dv + \epsilon\frac{\partial\pi(E,t)}{\partial E}.$$

$$\frac{\partial\gamma(W,t)}{\partial t} = \int_0^1 \pi\left(\frac{W}{v},t\right)\varphi_0(v)\frac{dv}{v} - \sigma_0\gamma(W,t)$$

Energy measurement

- The calorimetric approach: absorb the shower
  - As much as possible… But the logarithmic behavior helps
  - Typically (20-30) Xo give an almost full containment up to hundreds of GeV
    - But sometimes it is difficult (calorimeters in space)
  - Errors asymptotically dominated by statistical fluctuations:

$$\frac{\sigma_E}{E} \cong \frac{k_E}{\sqrt{E}} \oplus c$$

k can be a few per cent for a compact calorimeter

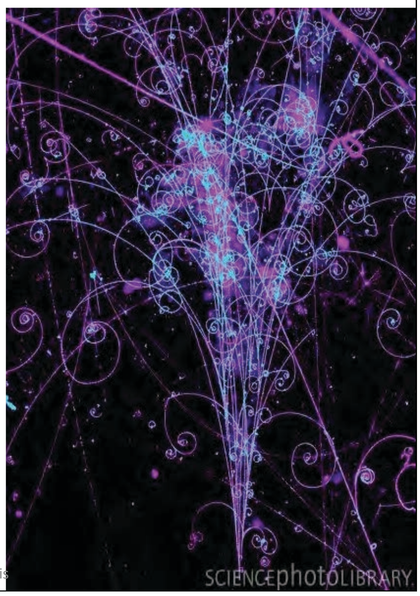

Hadronic showers and calorimeters

- Although hadronic showers are qualitatively similar to em, shower development is more complex because many different processes contribute
  - Larger fluctuations
- Some of the contributions to the total absorption may not give rise to an observable signal in the detector
  - Examples: nuclear excitation and leakage of secondary muons and neutrinos
- Depending on the proportion of π^0s produced in the early stages of the cascade, the shower may develop predominantly as an electromagnetic one because of the decay $\pi^0 \to \gamma\,\gamma$
- The scale of the shower is determined by the nuclear absorption length λ_H
  - Since typically λ_H > Xo, hadron calorimeters are thicker than em ones
- The energy resolution of calorimeters is in general much worse for hadrons than for electrons and photons
  - Energy resolution typically a factor of 5–10 poorer than in em calorimeters

Extensive air showers (EAS)

- Showers due to the interaction of HE particles with the atmosphere.
- High-energy hadrons, photons, and electrons interact in the high atmosphere. The process is conceptually similar.
- For photons and electrons above a few hundred MeV, the cascade process is dominated by the pair production and the bremsstrahlung mechanisms.
- The maximum shower size occurs approximately ln(E/Eo) radiation lengths, the radiation length for air being about 37 g/cm^2 (approximately 300m at sea level and NTP). The critical energy is about 80 MeV in air.
- The hadronic interaction length in air is about 61 g/cm^2 for protons (500 meters for air at NTP), being shorter for heavier nuclei—the dependence of the cross section on the mass number A is approximately $A^{2/3}$.
- The transverse profile of hadronic showers is in general wider than for electromagnetic showers, and fluctuations are larger.
- Particles release energy in the atmosphere, which acts like a calorimeter, through different mechanisms—which give rise to a measurable signal.

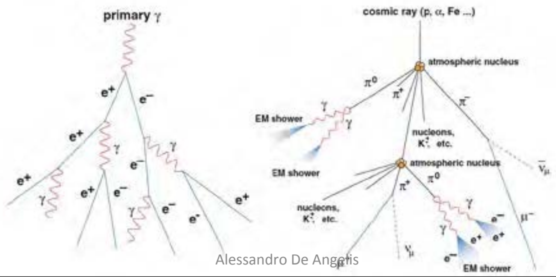

The events: Cosmic rays “rain”

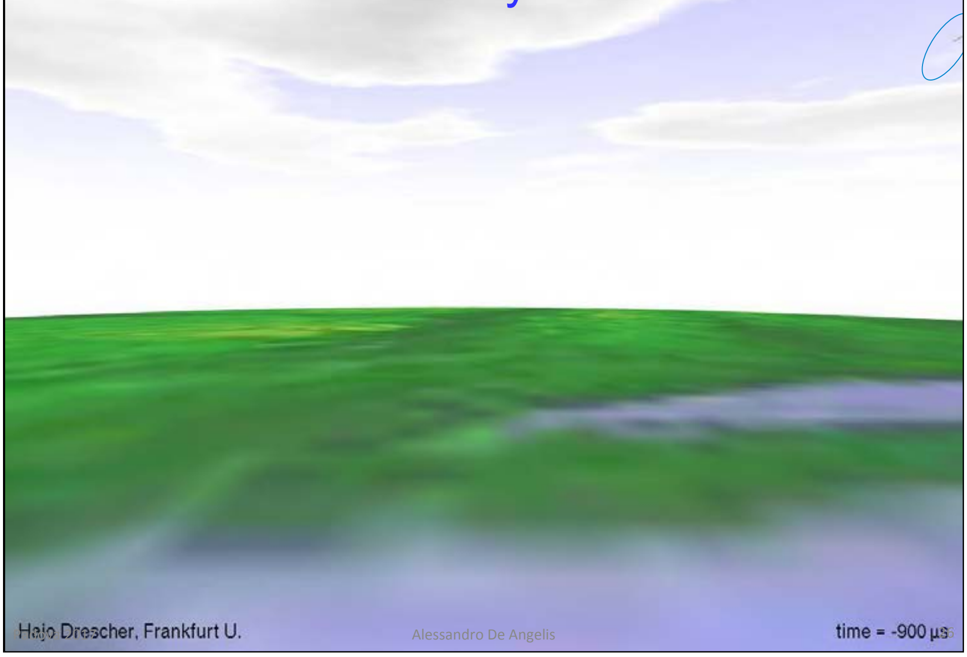

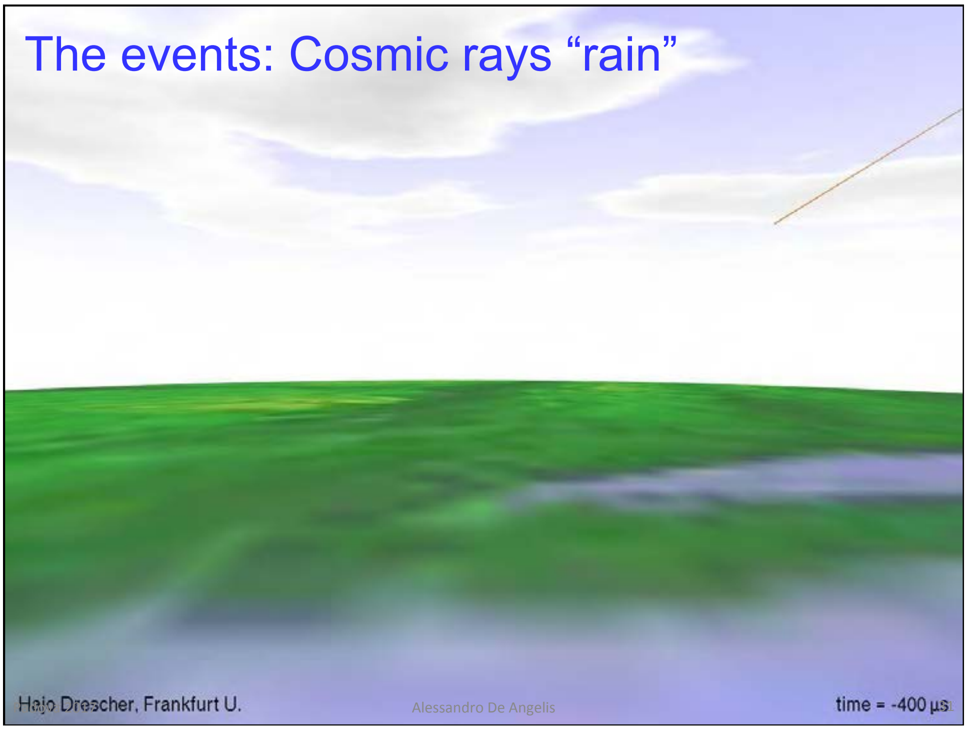
The events: Cosmic rays “rain”
Hajo Drescher, Frankfurt U.
Alessandro De Angelis
time = -400 µs

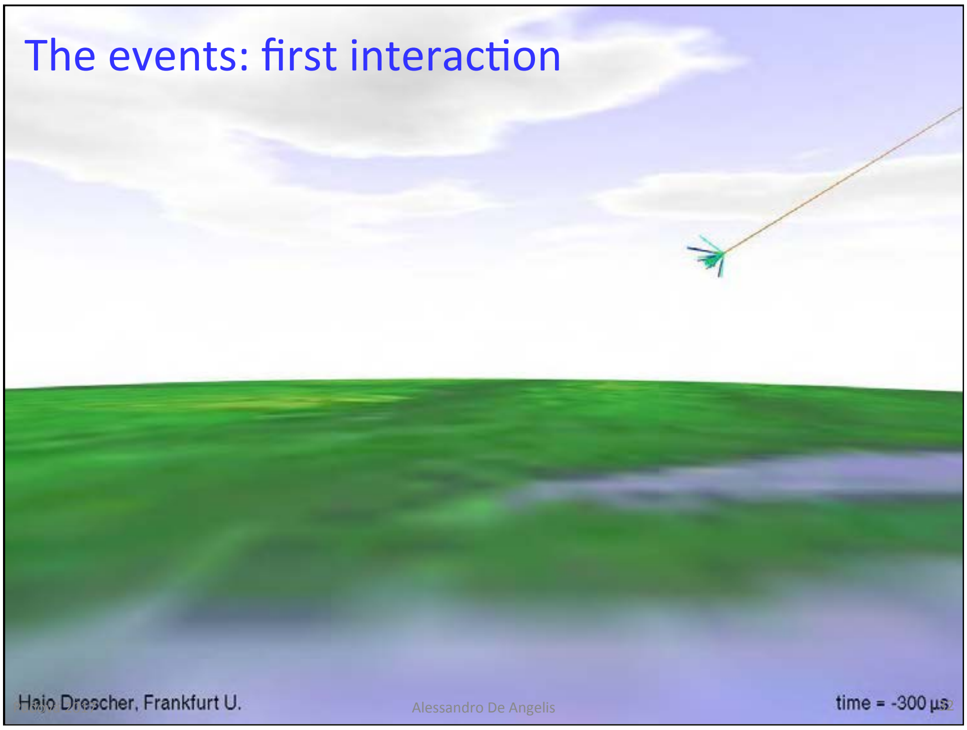
The events: first interaction
Hajo Drescher, Frankfurt U.
Alessandro De Angelis
time = -300 µs

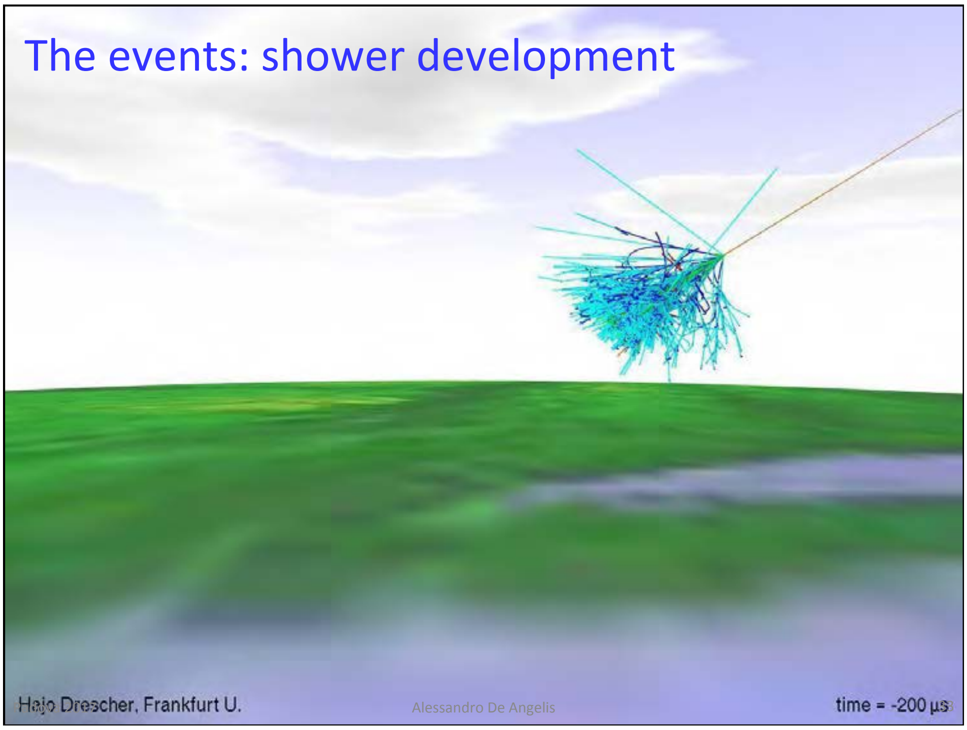
The events: shower development
Hajo Drescher, Frankfurt U.
Alessandro De Angelis
time = -200 µs

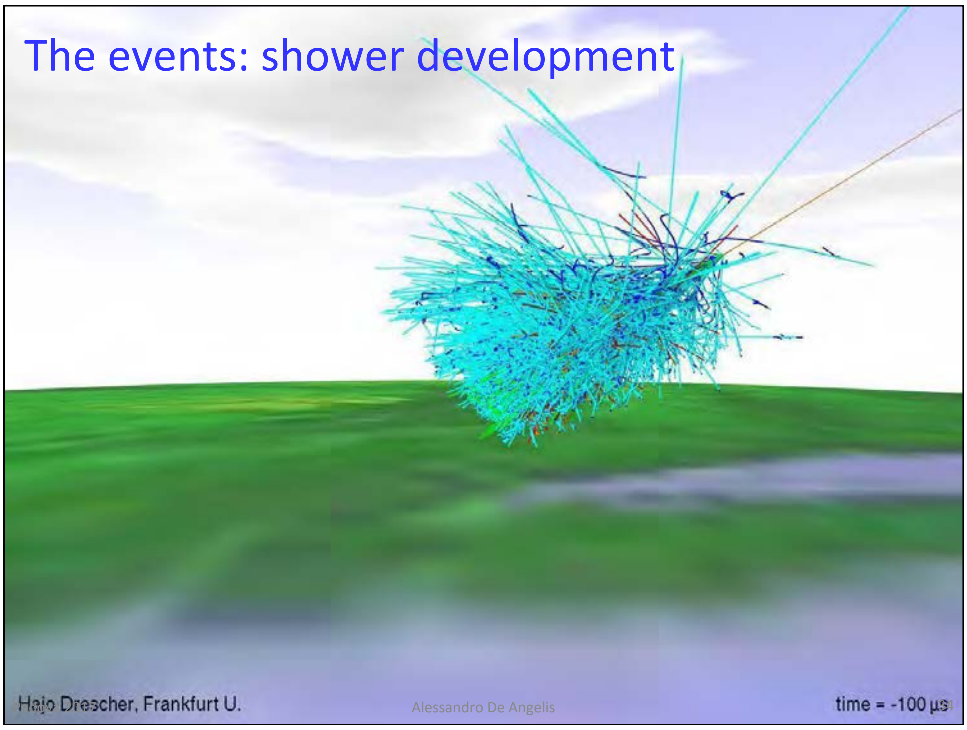
The events: shower development
Hajo Drescher, Frankfurt U.
Alessandro De Angelis
time = -100 µs

The events: shower hits Earth surface

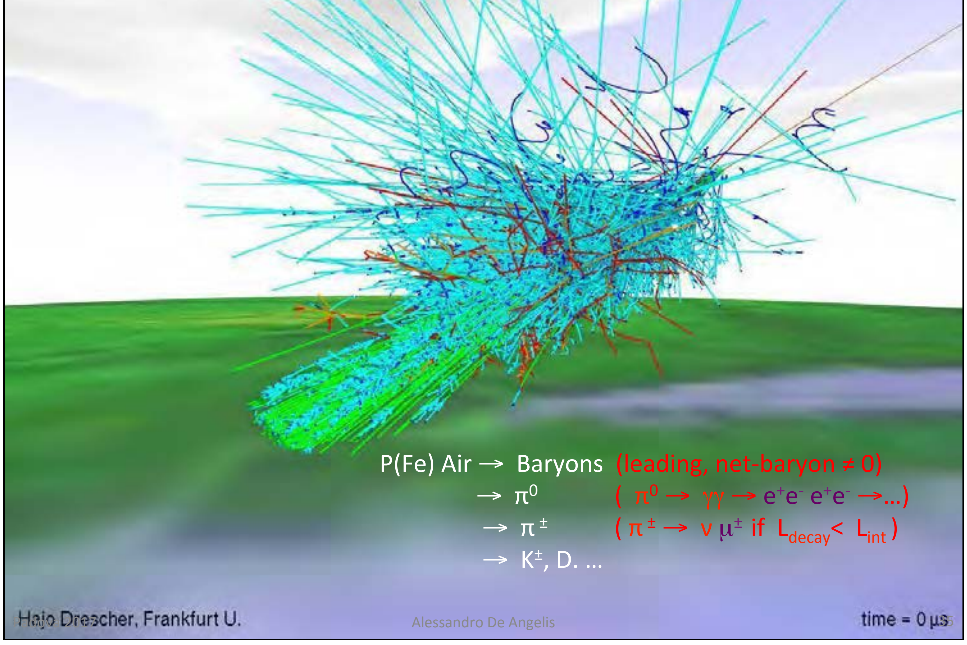

Photon-initiated shower in the atmosphere

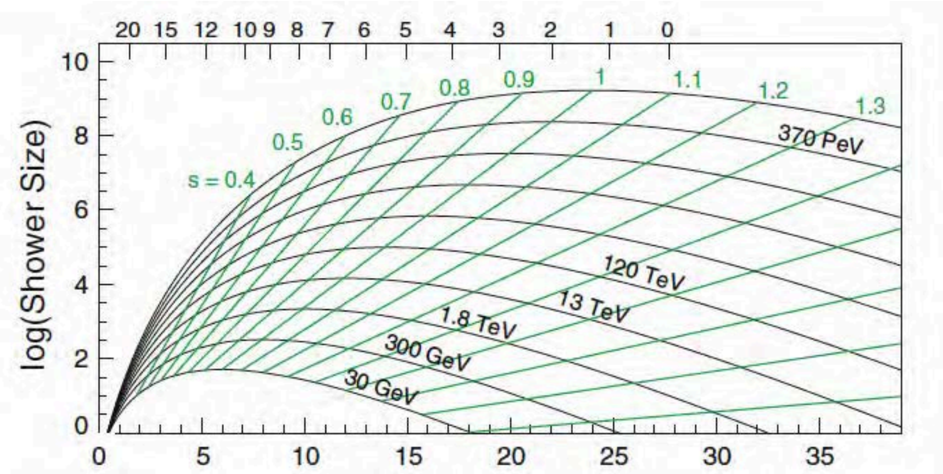

A frequent experimental problem: γ/hadron separation

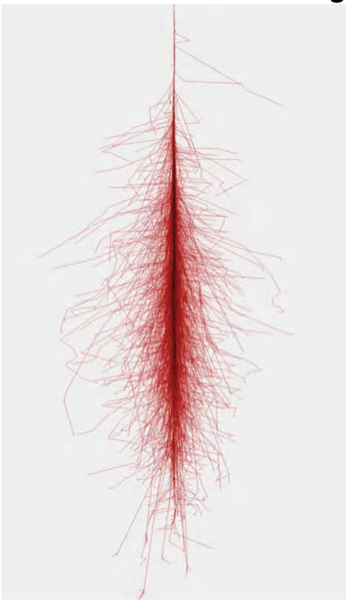

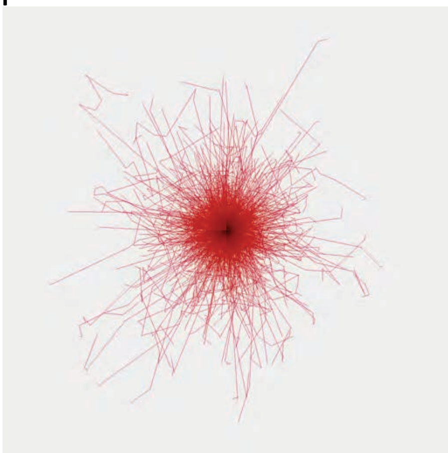

Simulated gamma
in the atmosphere:
50 GeV

Simulated gamma
1 TeV

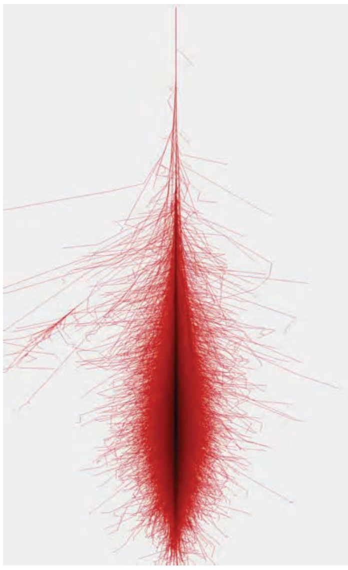

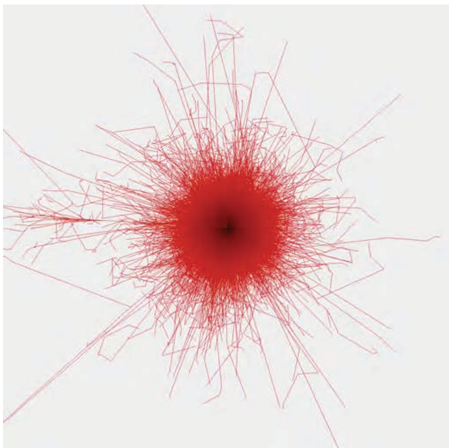

Simulated proton
100 GeV (the ennemy)

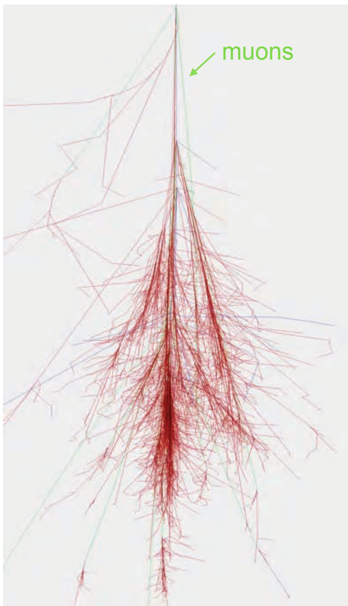

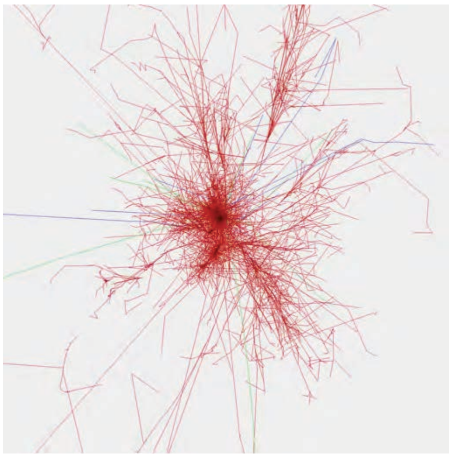

LET’S DETECT

Tracking detectors (charged particles)

- A tracking detector reveals the path taken by a charged particle by measurements of sampled points (hits). Momentum measurements can be made by measuring the curvature of the track in a magnetic field, which causes the particle to curve into a spiral orbit with a radius proportional to the momentum of the particle. This requires the determination of the best fit to a helix of the hits (particle fit). For a particle of unit charge

$$p\ (\mathrm{GeV}/c) \sim 0.3\ B_{\perp}(\mathrm{T})\ R\ (\mathrm{m})$$

- A source of uncertainty for this determination is given by the errors in the measurement of the hits; another (intrinsic) noise is given by multiple scattering. In what follows we shall review some detectors used to determine the trajectory of charged tracks.
- Prototype: the ionization tube (Geiger-Muller, …)

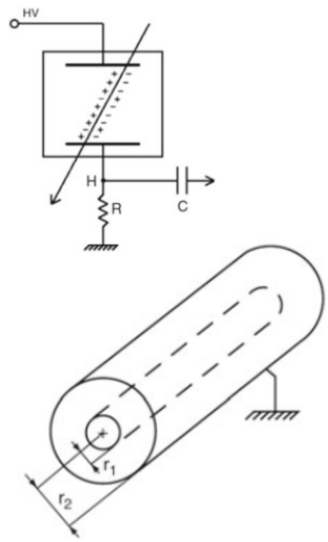

Tracking detectors (charged particles)

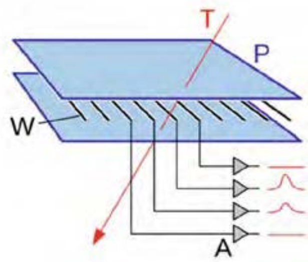

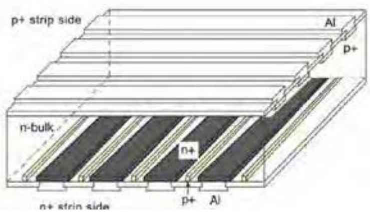

Detector type	Spatial resolution	Time resolution	Dead time
RPC	$\leq$10mm	$\sim$1ns (down to $\sim$50 ps)	–
Scintillation counter	10 mm	0.1 ns	10 ns
Emulsion	1 μm	–	–
Bubble chamber	10–100 μm	1 ms	50 ms–1 s
Proportional chamber	50–100 μm	2 ns	20–200 ns
Drift chamber	50–100 μm	few ns	20–200 ns
Silicon strip	Pitch/5 (few μm)	few ns	50 ns
Silicon pixel	10 μm	few ns	50 ns

Photodetectors

- Most detectors in particle physics and astrophysics rely on the detection of photons near the visible range, i.e., in the eV energy range. This range covers scintillation and Cherenkov radiation as well as the light detected in many astronomical observations.
- One needs to extract a measurable signal from a small number of incident photons. This can be achieved by generating a primary photoelectron or electron–hole pair by an incident photon (typically by photoelectric effect), amplifying the signal to a detectable level (usually by a sequence of avalanche processes), and collecting the secondary charges to form an electrical signal.
- The important characteristics of a photodetector include:
    - the quantum efficiency QE
    - the overall collection efficiency
    - the gain G
    - the dark noise DN , i.e. the electrical signal when there is no incoming photon;
    - the intrinsic response time of the detector.
- Prototype: the avalanche photomultiplier tube (PMT)

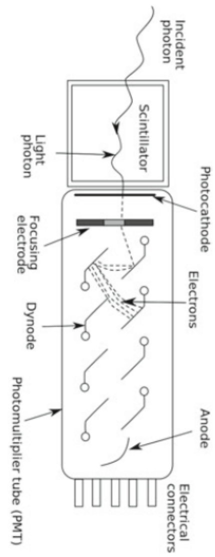

Photodetectors - II

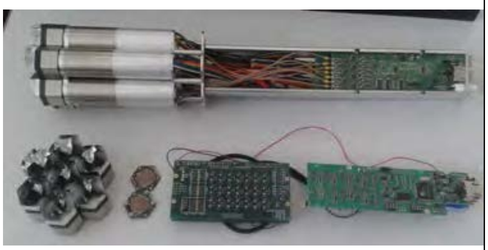

- Other photodetectors:
    - Gaseous detectors
    - Solid-state detectors (SiPM) – high fashion now

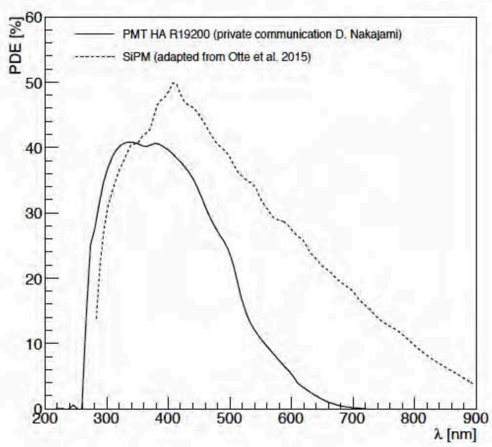

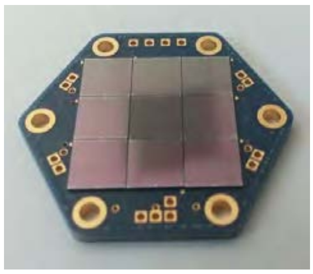

Corti, Rando+ (PD)

Exercises

1. *Cherenkov radiation.* A proton with momentum 1.0 GeV/c passes through a gas at high pressure. The index of refraction of the gas can be changed by changing the pressure. Compute: (a) the minimum index of refraction at which the proton will emit Cherenkov radiation; (b) the Cherenkov radiation emission angle when the index of refraction of the gas is 1.6.
2. *Photodetectors.* What gain would be required from a photomultiplier in order to resolve the signal produced by three photoelectrons from that due to two or four photoelectrons? Assume that the fluctuations in the signal are described by Poisson statistics, and consider that two peaks can be resolved when their centers are separated by more than the sum of their standard deviations.
3. *Cherenkov counters.* Estimate the minimum length of a gas Cherenkov counter used in the threshold mode to be able to distinguish between pions and kaons with momentum 20GeV. Assume that 200 photons need to be radiated to ensure a high probability of detection and that radiation covers thewhole visible spectrum (neglect the variation with wavelength of the refractive index of the gas).
4. Electromagnetic showers. If a shower is generated by a gamma ray of E = 1 TeV penetrating the atmosphere vertically, considering that the radiation length X0 of air is approximately 37 g/cm2 and its critical energy Ec is about 88 MeV, calculate the height hM of the maximum of the shower in the Heitler model and in the Rossi approximation B.
5. *Electromagnetic calorimeters.* Electromagnetic calorimeters have usually 20 radiation lengths of material. Calculate the thickness (in cm) for a calorimeters made of of BGO, $PbWO_4$ (as in the CMS experiment at LHC), uranium, iron, tungsten and lead. Take the radiation lengths from Appendix B or from the Particle Data Book.
6. *Muon energy loss.* A muon of 100 GeV crosses a layer of 1 m of iron. Determine the energy loss and the expected scattering angle.

PART 2
LET'S BUILD COMPLEX DETECTORS, NOW!

Charged particles: for astrophysics, the bigger the better

- Detect EAS at ground (mostly detect the charged particles in the shower)
- Go as high as possible (~4km)
- You can sample
- You can use simple detector units
  - Water pools (Cherenkov effect in water) with PMT(s)
  - Scintillators
  - RPC
- Your results are "dirty": difficult to identify the cosmic ray – also its charge

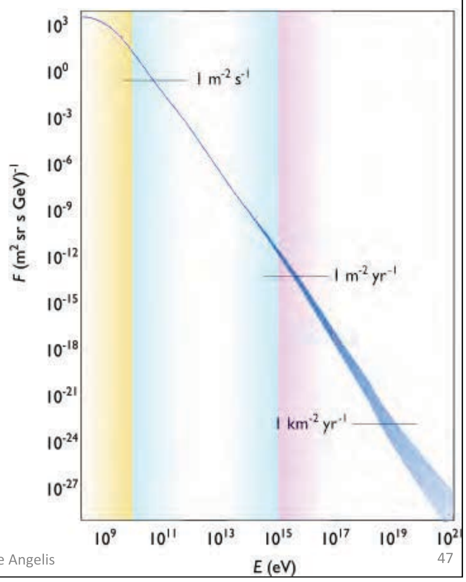

Padova 2017 Alessandro De Angelis 47

The Auger experiment in Argentina

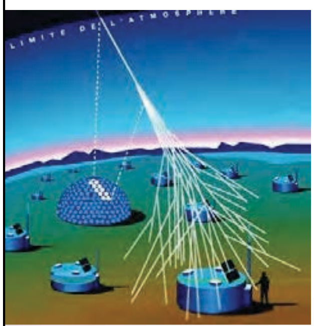

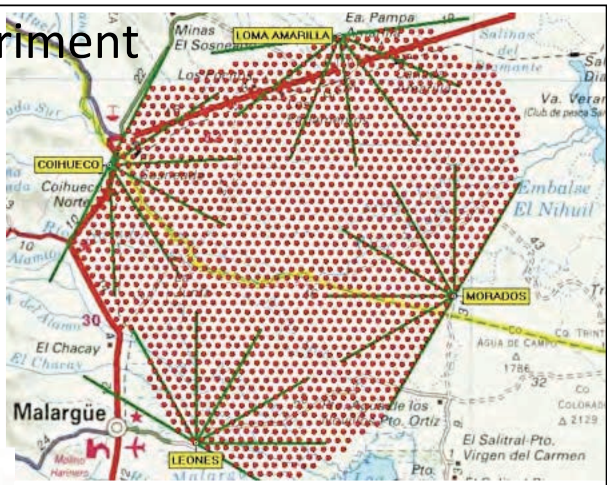

The largest in the world: surface of 3000 km^2 (Veneto: 18000 km^2)

1600 surface detectors & 4 telescopes

Still not enough for astronomy

Padova 2017 Alessandro De Angelis 48

If you want to identify particles (eg for DM studies), the only solution is going to space

- Need magnetic field
- Need power
- Maximum area ~ $1m^{2}$,
  Maximum weight ~ 1 ton
  Maximum power ~ 1kW
  => Maximum E ~ 1 TeV

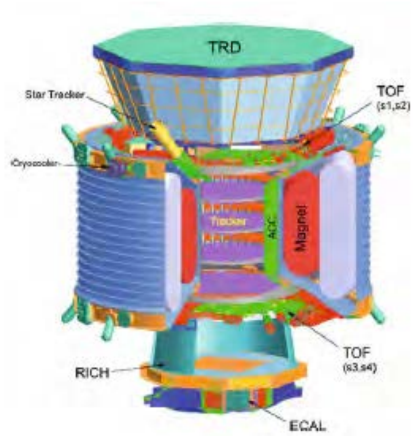

AMS-02 onboard the ISS
Launched by the Space Shuttle
May 2011

Another frontier of large detectors: neutrinos

- You need cubic kilometers to (possibly) do astrophysics…

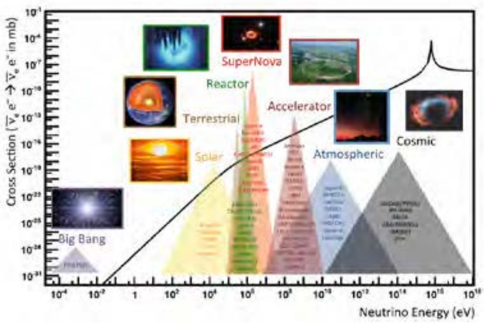

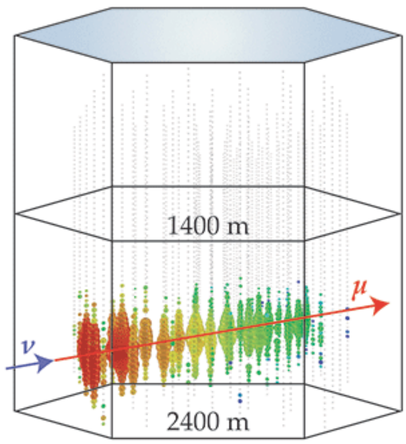

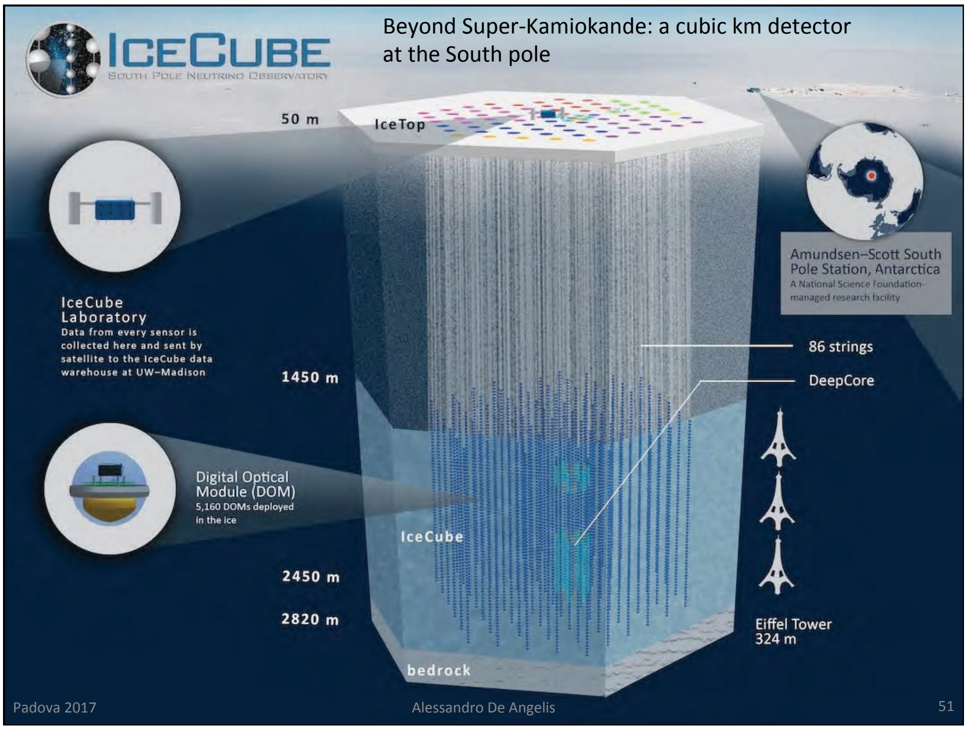

Deploying a (string of) photosensors

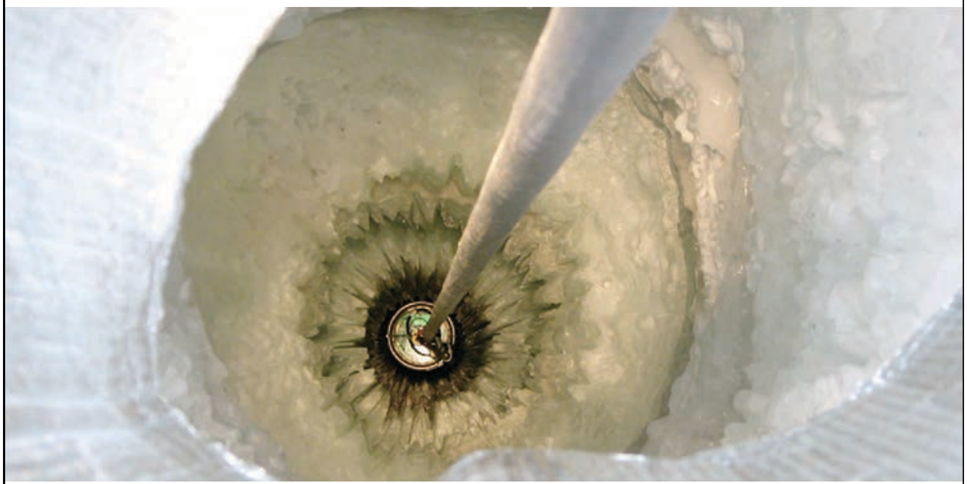

Padova 2017 Alessandro De Angelis 52

…and in the Mediterranean sea

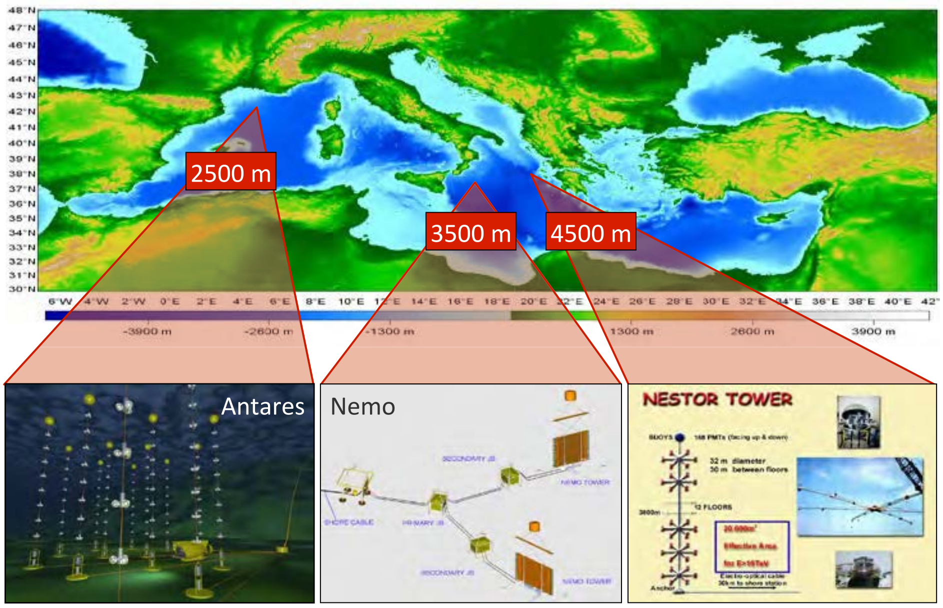

Photons in the nonthermal region

- LE or MeV : 0.1 (0.03) -100 (30) MeV
- HE or GeV : 0.1 (0.03) -100 (30) GeV
- VHE or TeV : 0.1 (0.03) - 100 (30) TeV
- UHE or PeV : 0.1 (0.03) -100 (30) PeV

- LE,HE domain of space-based astronomy
- VHE+ domain of ground-based astronomy

- When no ambiguity, we call "HE" all the HE and VHE+

Transparency of the atmosphere

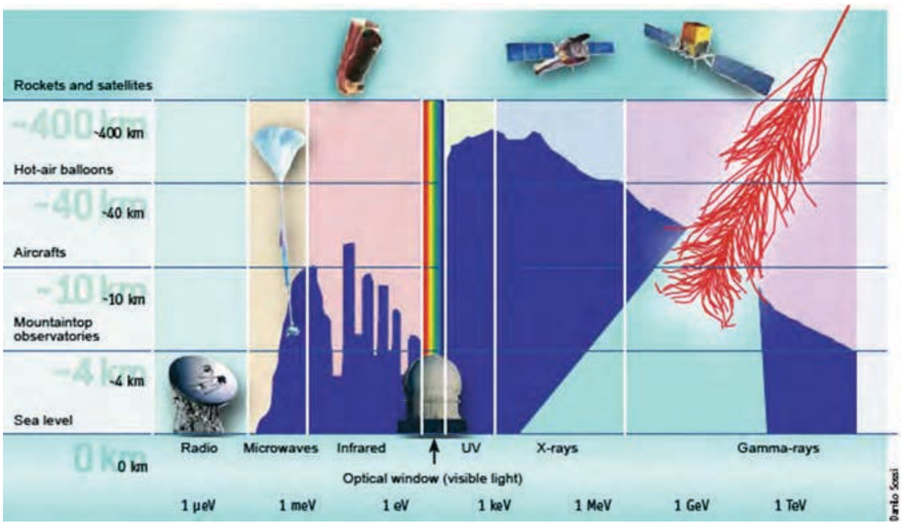

Padova 2017 Alessandro De Angelis 55

Detectors

Precision Si-strip Tracker (TKR)
18 XY tracking planes
Single-sided silicon strip detectors 228 μm pitch, 8.8 10^5 channels
Measure the photon direction

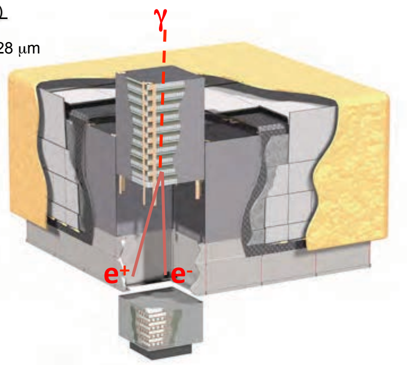

- MeV satellites
- GeV Satellites (AGILE, Fermi, DAMPE)
  - Silicon tracker (+calorimeter)
- Cherenkov telescopes (H.E.S.S., MAGIC, VERITAS)
- Extensive Air Shower detectors (HAWC): RPC, scintillators, water Cherenkov

HEP detectors!

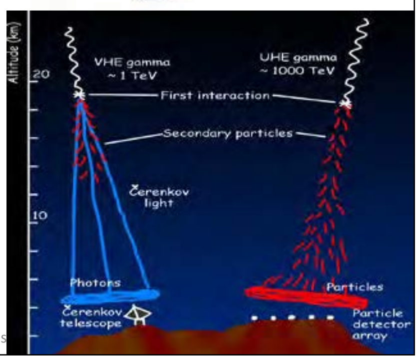

Padova 2017 Alessandro De Angelis

MeV photon detectors

- The MeV region is crucial for nuclear physics
- An “easy” way to do MeV photon detectors
  - Scintillating crystals
- But:
  - Bad directionality
  - No polarization information
- Typically used in Gamma-Ray Burst monitors

Fermi GBM detectors

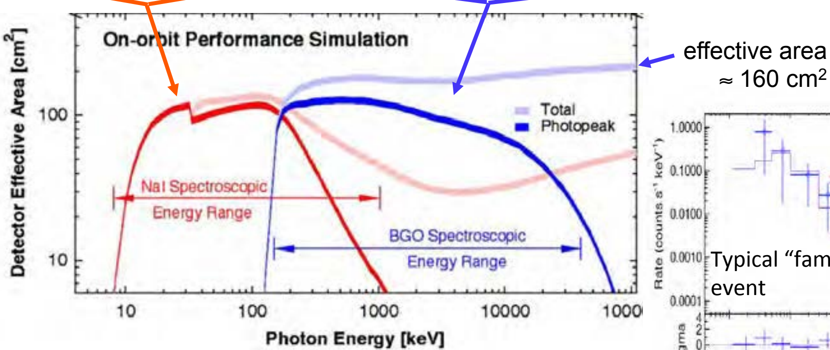

C. Meegan et al. 2009, ApJ, 702,

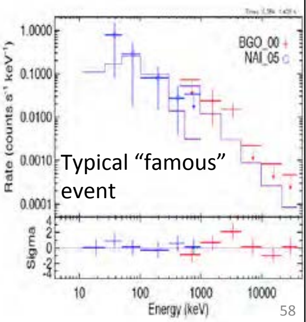

MeV photon detectors: the hard way

- Specific Compton detectors
- Need accurate tracking of the directionality of the scattered photon or of the ejected electron, if any
- The COMPTEL onboard the CGRO (1991-2000) was the last example. Now we could do better thanks to Si technology…

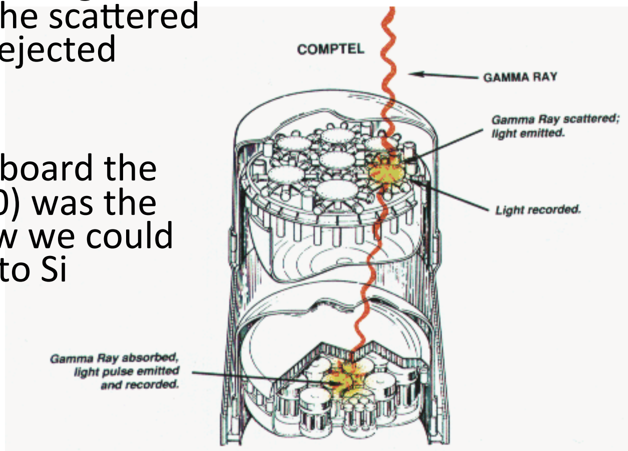

The GeV (pair production): Fermi and the LAT

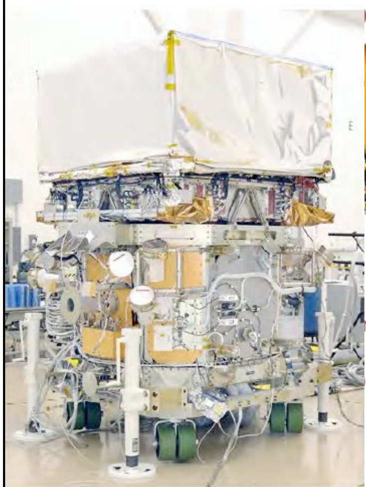

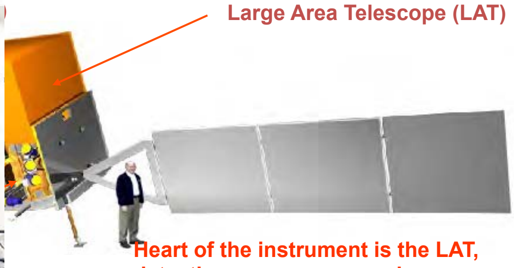

Heart of the instrument is the LAT, detecting gamma conversions γ

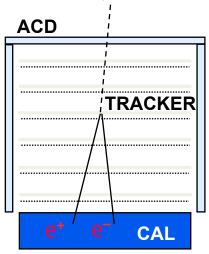

International collaboration USA-Italy-France-Japan-Sweden

Fermi-LAT launched June 2008

LAT overview

Si-strip Tracker (TKR)
18 planes XY ~ 1.7 x 1.7 m² w/ converter
Single-sided Si strips 228 μm pitch, ~10⁶ channels
Measurement of the gamma direction

AntiCoincidence Detector (ACD)
89 scintillator tiles around the TKR
Reduction of the background from charged particles

Astroparticle groups INFN/University Bari, Padova, Perugia, Pisa, Roma2, Udine/Trieste

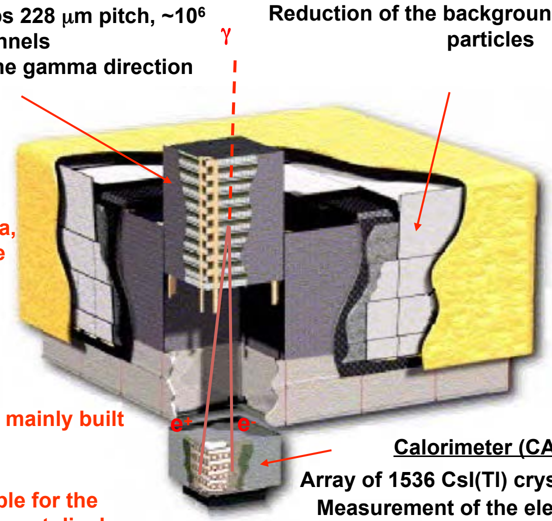

The Silicon tracker is mainly built in Italy

Calorimeter (CAL)
Array of 1536 CsI(Tl) crystals in 8 layers
Measurement of the electron energy

Italy is also responsible for the detector simulation, event display and GRB physics

Detection of a gamma-ray

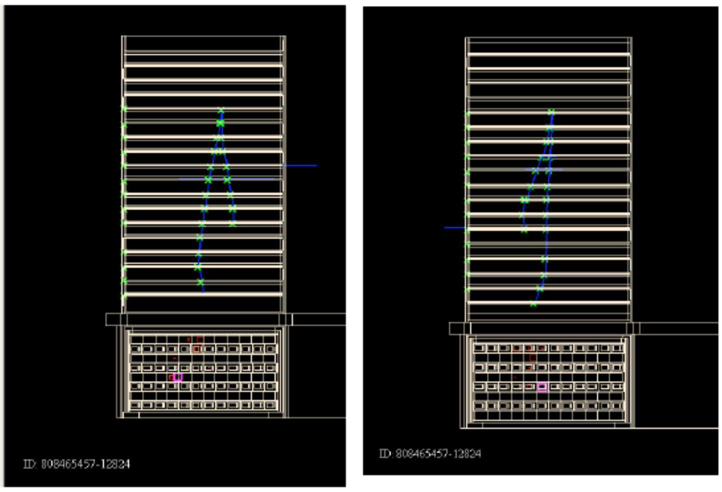

LAT 4-year Point Source Catalog (3FGL)

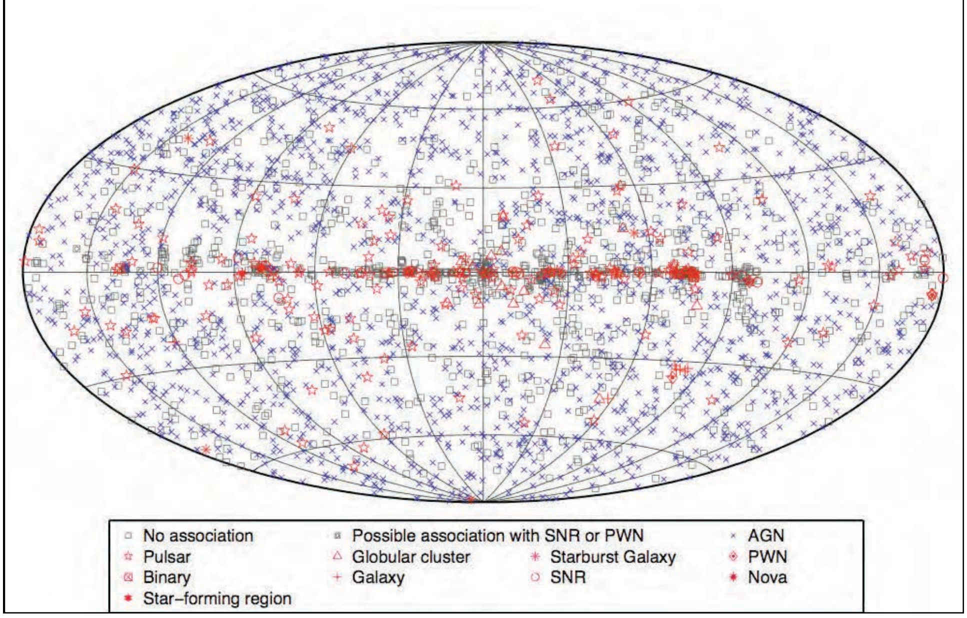

AGILE & DAMPE

- 2 more instruments in space
- The all-Italian telescope AGILE
  - A Fermi precursor: see Fermi, 16 times smaller
  - Launched April 2007
  - Pointing systems has some problems
- The Chinese-Italian-Swiss DAMPE
  - ~AGILE
  - Launched December 2015
  - Better calorimetry than Fermi

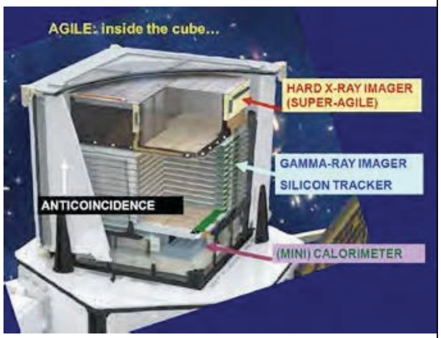

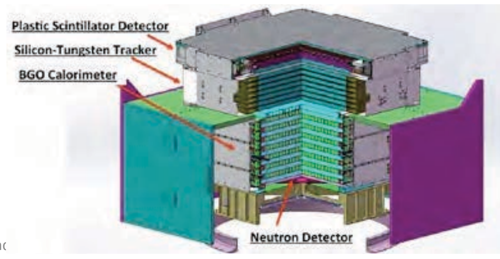

Performance of Fermi (Pass 8)

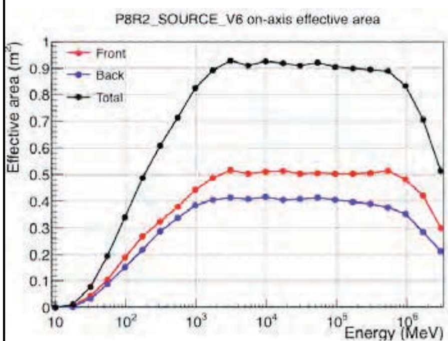

Effective area (Area x efficiency)

~ $1 m^2$

Grows as k lnE from 2 MeV to 2 GeV
Then ~$0.9 m^2$ from 2 GeV to 700 GeV
Then decreases as k' lnE

Acceptance: 2.5 sr

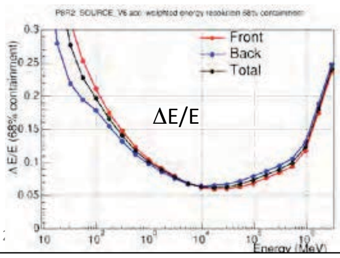

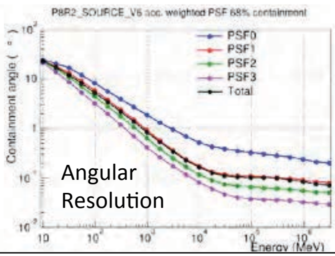

Why detection at ground?

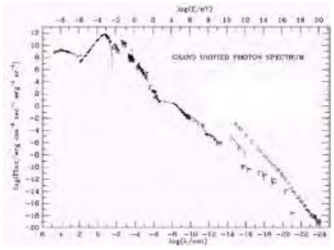

- High energies
  - Only way to build sensitive >TeV instruments
  - Maximum flux < 1 photon/h/m^2 above 200 GeV in Fermi
- High statistics /short timescales
  - Large collection areas O(km^2)
- Precision (Imaging Air Cherenkov telescopes, IACTs)
  - Superior angular resolution
- Limitations?
  - IACTs
    - Smaller duty cycle
    - Smaller field of view
  - EAS ground particle detectors
    - Modest resolution and background rejection power
  - Complementary approaches

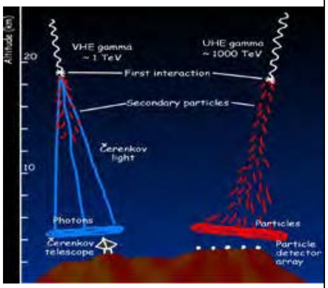

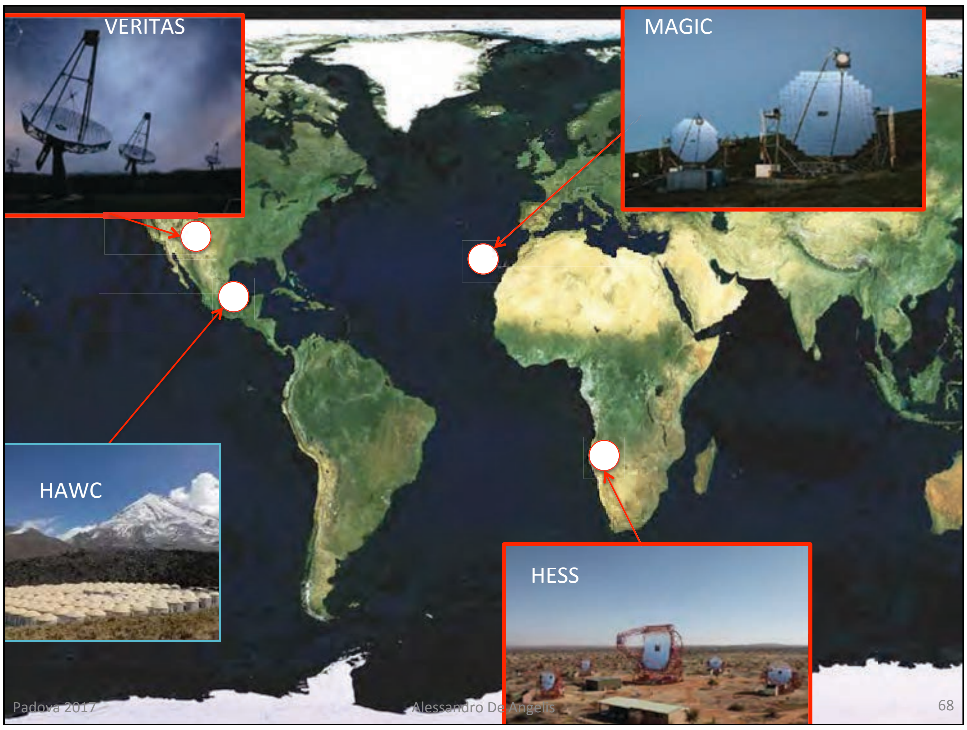

Highlight in γ-ray astrophysics (mostly HESS, MAGIC, VERITAS)

- Thanks mostly to Cherenkov telescopes, imaging of VHE (> 30 GeV) galactic sources and discovery of many new galactic and extragalactic sources: ~ 200 (and >200 papers) in the last 9 years
  - And also a better knowledge of the diffuse gammas and electrons
- A comparable success in HE (the Fermi realm); a 10x increase in the number of sources
- A new tool for cosmic-ray physics and fundamental physics

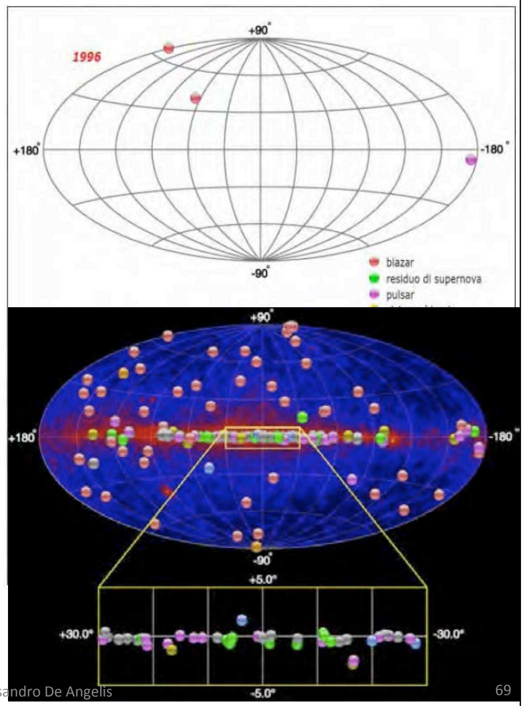

Padova 2017 Alessandro De Angelis 69

TeVCat

~200 sources detected by ground-based instruments

Not impressive versus 3FGL (O(2K)), **but**…

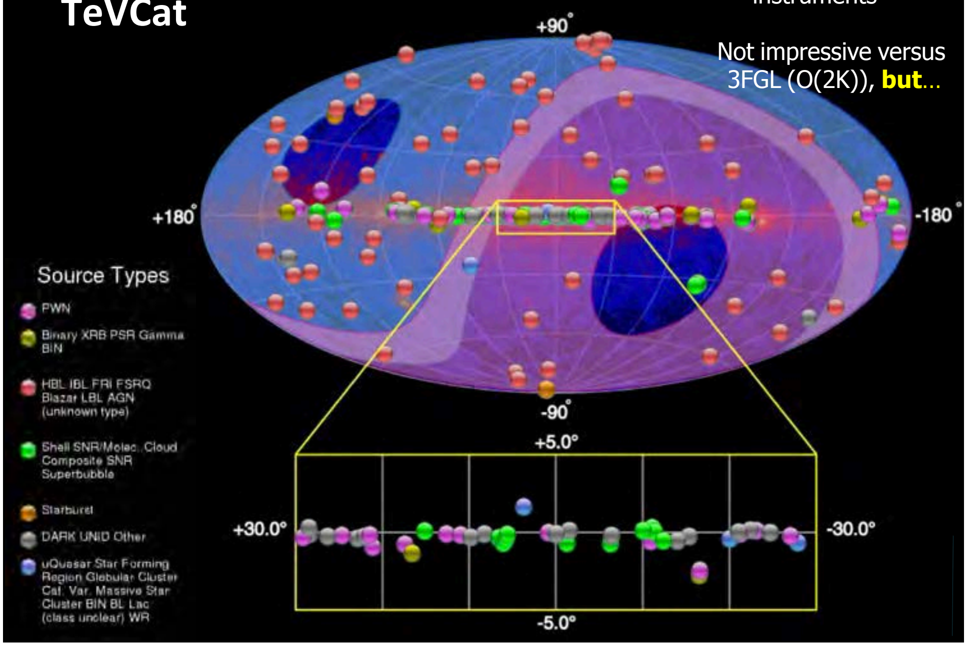

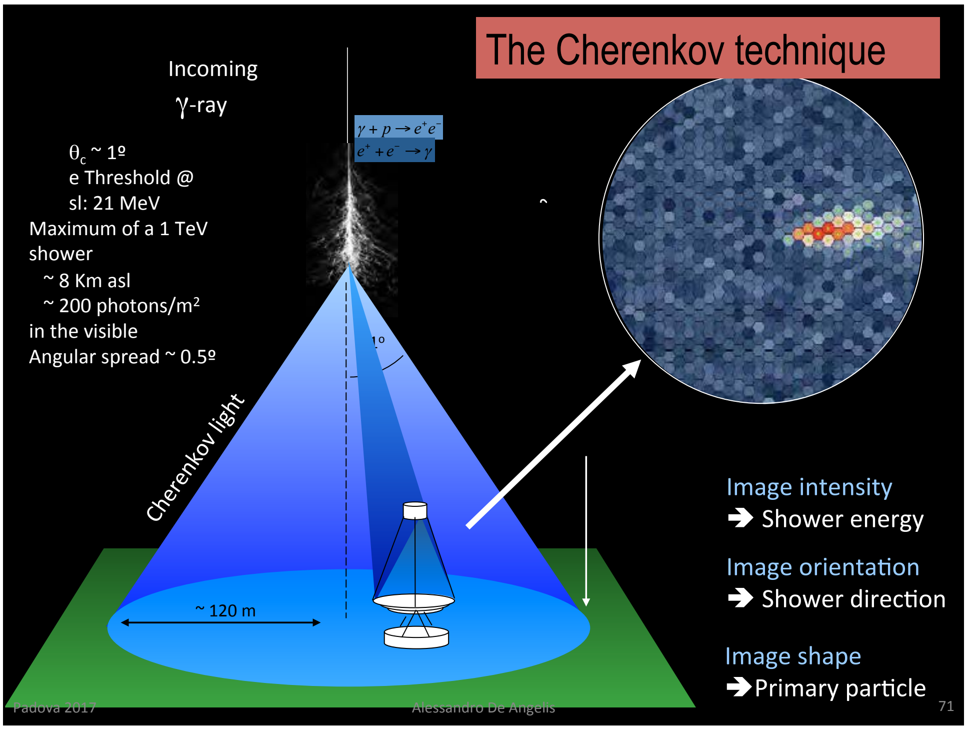

Signal duration: ~ 3ns

Padova 2017 Alessandro De Angelis 72

γ/h Separation

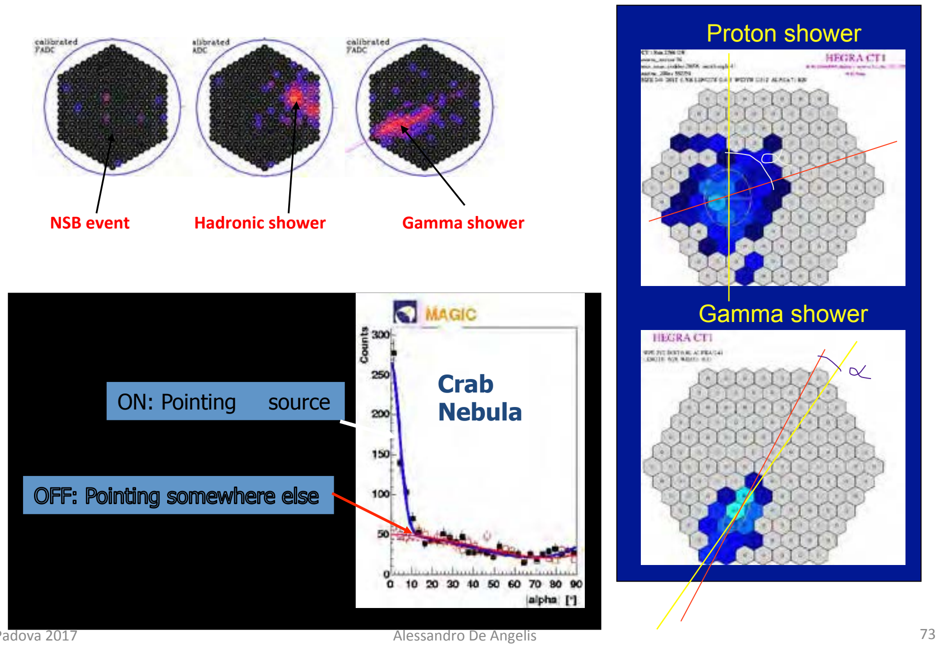

Systems of Cherenkov telescopes

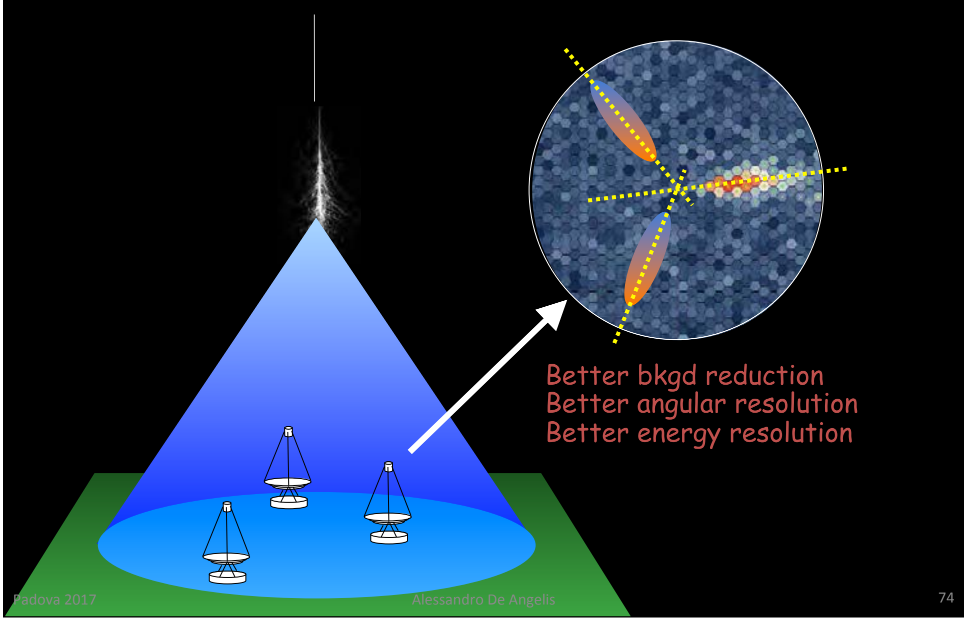

Instr.	Tels. #	Tel. A (m^2)	FoV (°)	Tot A (m^2)	Thresh. (TeV)	PSF (°)	Sens. (%Crab)
H.E.S.S.	4	107	5	428	0.1	0.06	0.7
MAGIC	2	236	3.5	472	0.05(0.03)	0.06	0.8
VERITAS	4	106	4	424	0.1	0.07	0.7

Plus a 600 m2 telescope (CT5) operating since 2015

(0.03 for CT5)

HESS (Namibia)

4 telescopes (~12m) operational since 2003

HESS 2: 5th telescope (26-28m) commissioned in 2015

MAGIC: Two 17m Ø Imaging Atmospheric Cherenkov Telescopes
1st telescope since 2004, 2nd since 2009, upgrade in 2013

~160 physicists from 10 countries:
Bulgaria, Croatia, Finland, Germany, India, Italy, Japan, Poland, Spain, Switzerland

Canary island of La Palma

at 2400 m a.s.l.

The level of perturbations is 1600 m => 650 m b

Key elements

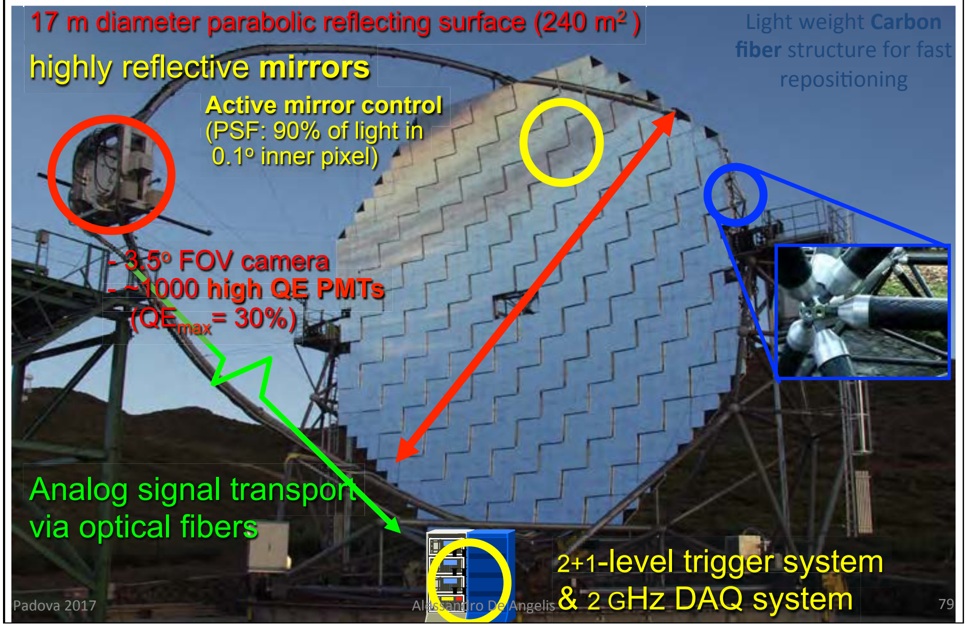

Operated from a control room

Main parameters & performance

- **Light-weight**: ~60 T
- **Fast re-positioning** to any coordinates in the sky: ~ 25 s /180°
- Optimized electro-optical design providing ~ 2.5 ns FWHM pulses
- Data digitized by using 2 GSample/s DRS4 chips
- Producing ~ 1 TB data per observation night

arXiv:1409.5594

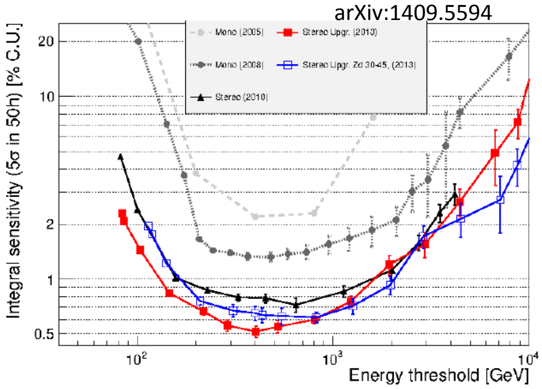

Energy threshold:
50 GeV
30 GeV Sum-Trigger

Energy resolution:
15% (@ 1 TeV) – 20% (@100 GeV)

Angular resolution:
0.06° @ 1 TeV , 0.1° @ 100 GeV

Best **sensitivity**: 0.5% of Crab Nebula flux
in 50 hours obs. @ E ~ 400 GeV

Fast and smooth repointing (< 30 s)

Adjustement (active control)

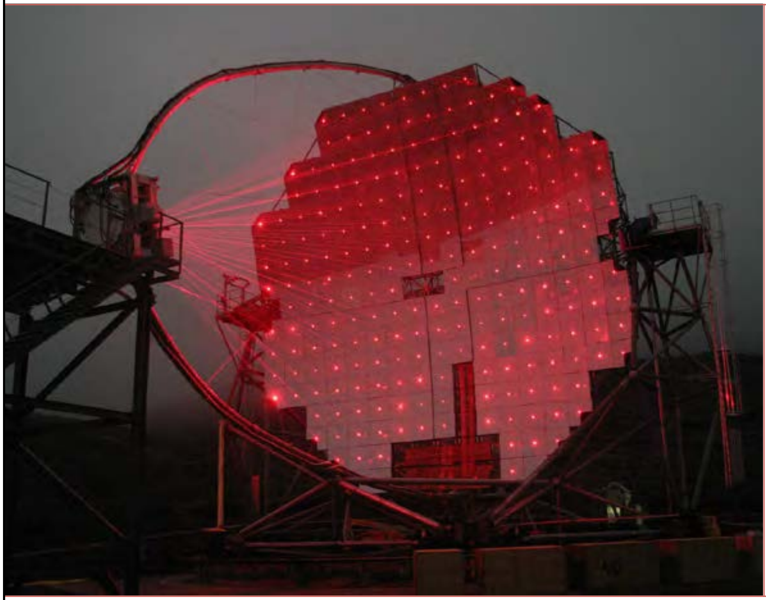

All AMC Lasers switched on during foggy night

(nice propaganda picture; does never look like that during operation ...)

Why bigger and bigger?

Figures of merit of a Cherenkov telescope

- Sensitivity: effective area (effective area covered, => ~ number of telescopes)
- Angular resolution: number N of telescopes
- Serendipity: FoV, Duty Cycle
- Still we use small N (cost: 1-10 MEUR/telescope)

Figures of merit - II

- The threshold is

$$E_{threshold} \propto \sqrt{\frac{\phi \Omega \tau}{\epsilon A}}$$

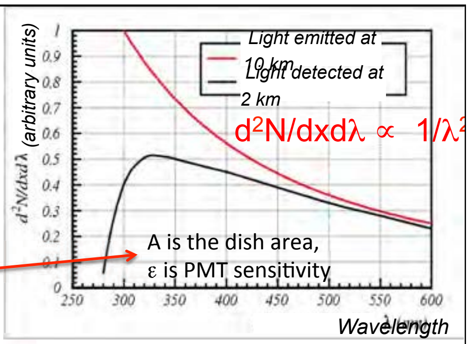

The Vela pulsar seen with CT5

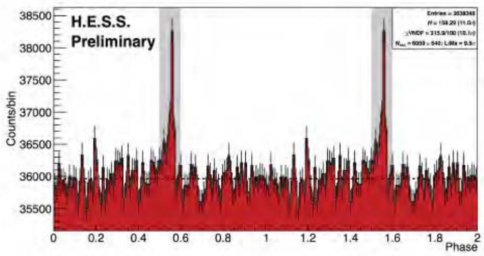

Energy distribution

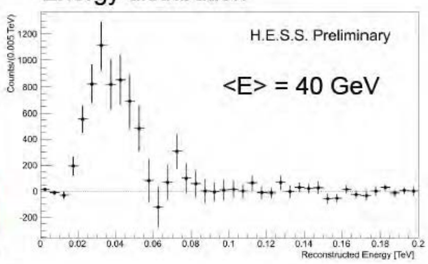

Higher energies: EAS detectors

(Cost of covering 1 km^2 with Cherenkov telescopes > 100 MEUR)

Tibet – AS gamma: scintillators

EAS detectors

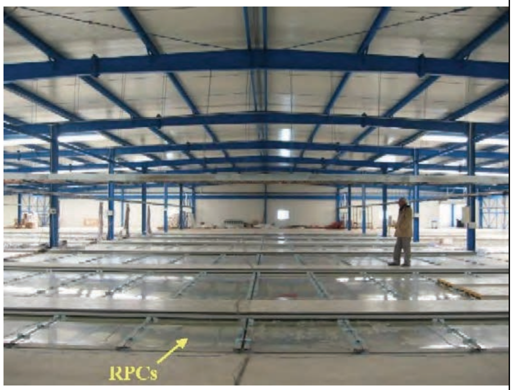

- Pro: wide field of view, continuous operation, cheap to instrument large areas
- Minus: Resolution is worse => more background, higher threshold

- Transients: plus is serendipity, can be the trigger; minus is sensitivity

The present

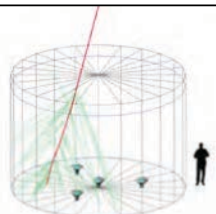

The HAWC Observatory

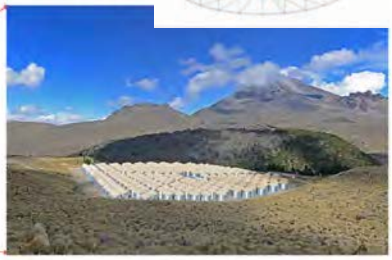

- Located at **4100 m** a.s.l. in Mexico near Pico de Orizaba at 19ºN
- Effective Area: **~22,000 m²**
- Instantaneous field of view **2 sr**; daily coverage of **2/3** of the sky.
- 300 Water Cherenkov Detectors (WCDs)
- Declinations from **-26º to 64º** (***Part of Northern Fermi Bubble visible***)
- Inaugurated in **March 2015**, taking science data since **2013**.

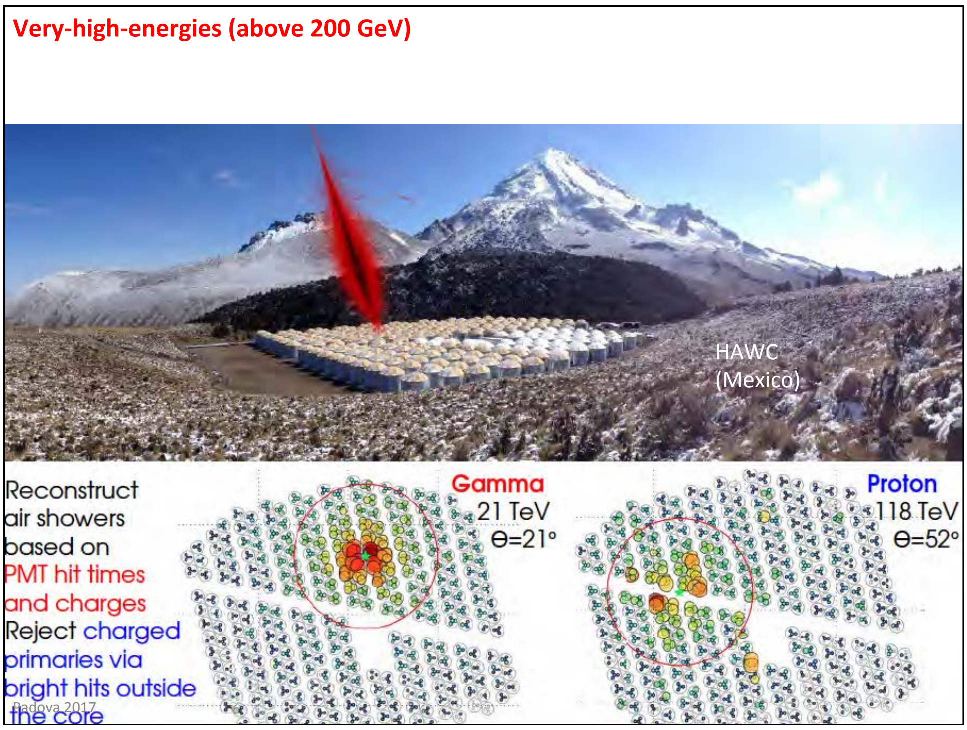
Very-high-energies (above 200 GeV)
HAWC
(Mexico)
Reconstruct air showers based on PMT hit times and charges
Reject charged primaries via bright hits outside the core
Gamma
21 TeV
Θ=21°
Proton
118 TeV
Θ=52°
Padova 2017

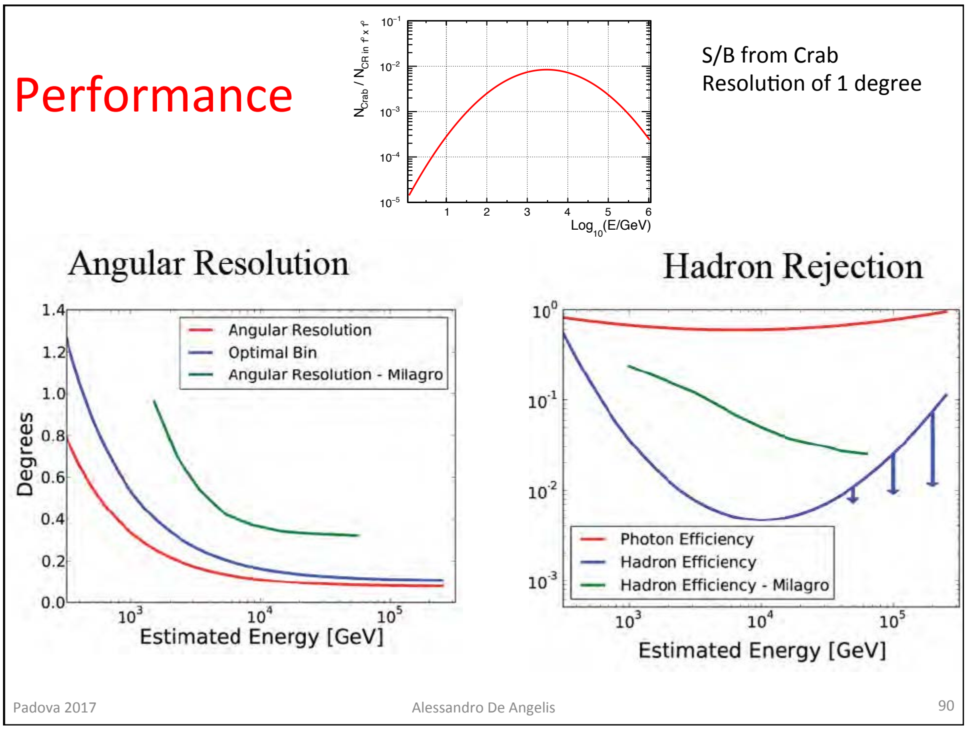
Performance
S/B from Crab
Resolution of 1 degree
Log10(E/GeV)
Angular Resolution
Angular Resolution
Optimal Bin
Angular Resolution - Milagro
Degrees
Estimated Energy [GeV]
Hadron Rejection
Photon Efficiency
Hadron Efficiency
Hadron Efficiency - Milagro
Estimated Energy [GeV]
Padova 2017
Alessandro De Angelis
90

HAWC-250 150-Day TeV Sky Survey (38σ Crab)

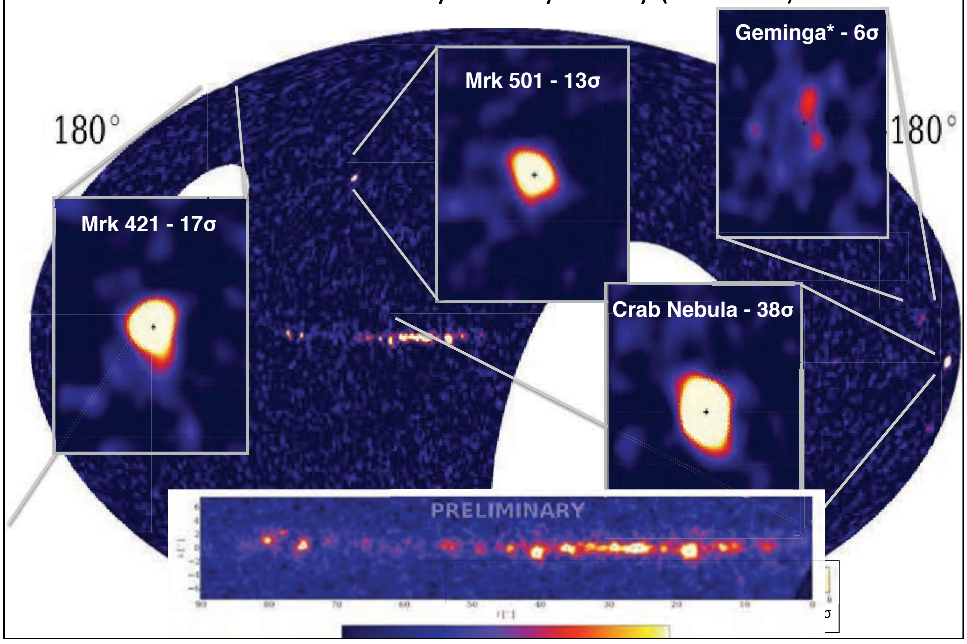

Detection of Cherenkov radiation vs. direct sampling

$$\theta_c = \frac{1}{n\beta}$$

from the direction of the emitting particle. The threshold velocity is thus $\beta = 1/n$, where n is the refractive index of the medium.

The number of photons produced per unit path length and per unit energy interval of the photons by a particle with charge $z_p e$ is

$$\frac{d^2N}{dEdx} \simeq \frac{\alpha z_p^2}{\hbar c} \sin^2\theta_c \simeq 370 \sin^2\theta_c \, \mathrm{eV}^{-1}\mathrm{cm}^{-1} \qquad (4.6)$$

or equivalently

$$\frac{d^2N}{dEd\lambda} \simeq \frac{2\pi\alpha z_p^2}{\lambda^2} \sin^2\theta_c \qquad (4.7)$$

(the index of refraction n is in general a function of photon energy E).

- For a particle unit charge: ~40 photons/m between 300nm and 700nm in air
  Total energy loss is about 10^{-4} the ionization loss
- Attenuation length is ~ 3 km
  The scale of attenuation of the shower is 10 times smaller!!! Direct sampling disfavored

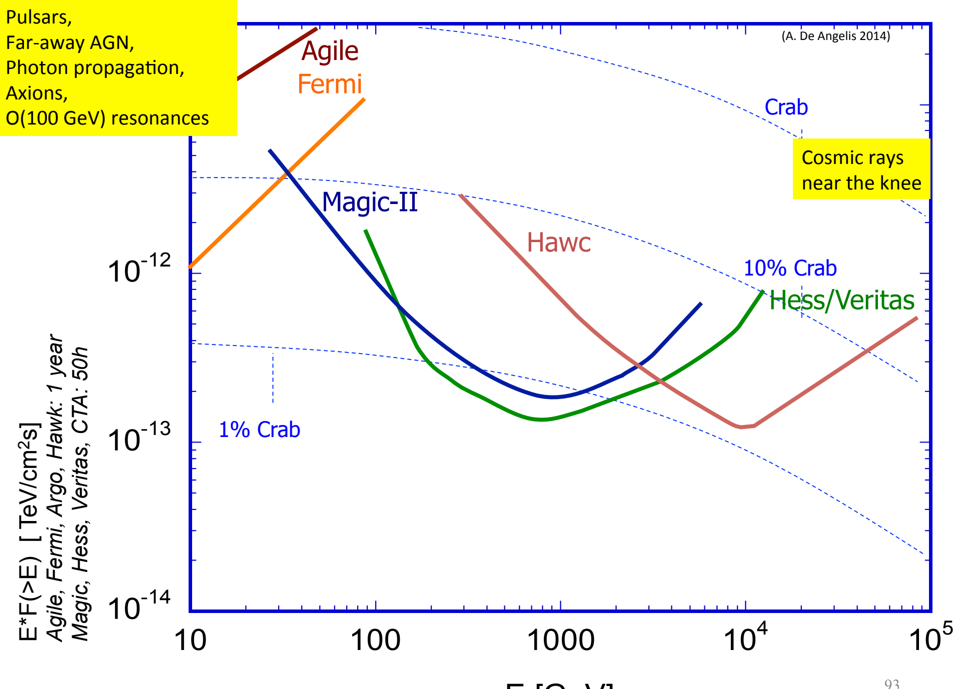

Padova 2017 Alessandro De Angelis 93

Performance of different types of HE gamma detectors

Table 4.5 A comparison of the characteristics of Fermi, the IACTs and of the EAS particle detector arrays. Sensitivity computed over one year for Fermi and the EAS, and over 50 h for the IACTs

Quantity	Fermi	IACTs	EAS
Energy range	20 MeV – 200 GeV	100 GeV – 50 TeV	400 GeV – 100 TeV
Energy res.	5–10 %	15–20 %	$\sim$ 50 %
Duty cycle	80 %	15 %	$>$ 90 %
FoV	$4\pi/5$	5 deg $\times$ 5 deg	$4\pi/6$
PSF (deg)	0.1	0.07	0.5
Sensitivity	1 % Crab (1 GeV)	1 % Crab (0.5 TeV)	0.5 Crab (5 TeV)

Padova 2017 Alessandro De Angelis 94

Gamma rays above the keV: an overall picture

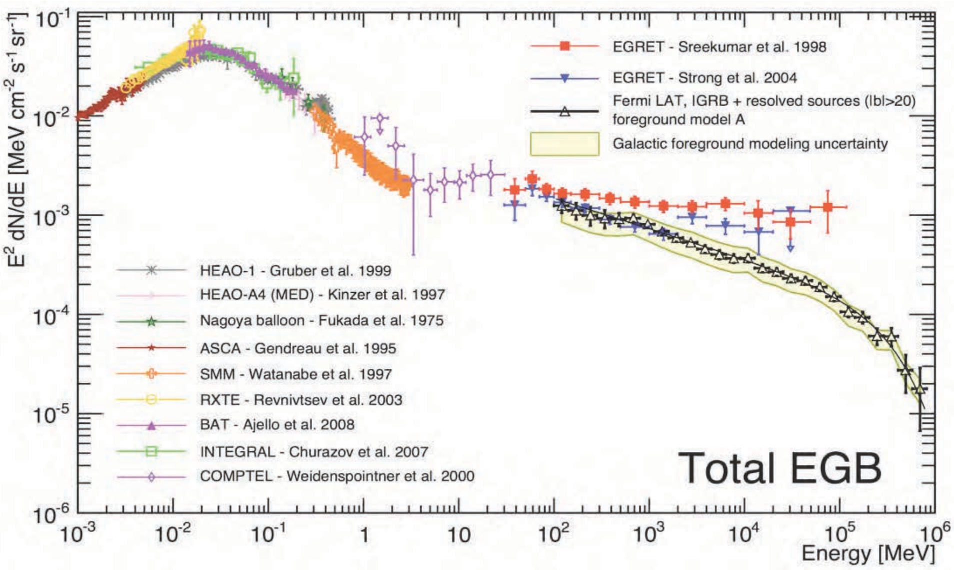

Summary of lectures 2 and 3

- Detectors for charged cosmic rays: (1) need large effective area for the UHE, (2) smart instruments on satellite for particle identification. For (1) we are close to the limit (Auger) unless we change technology, for (2) we are close to the limit
- Astrophysical neutrino detectors: we need several km3; we are close to the limit (Icecube) but still improving (Antares -> km3)
- Photons:
  - In the MeV region, instruments did not reach the technological limit, yet
  - In the GeV region, Fermi is close to the technological limit
  - In the TeV region, the Cherenkov technique reigns. HESS, MAGIC and VERITAS have still potential, and there is room for improvement by "brute force"
  - In the PeV region, only one detector presently active, and there is room for improvement by "brute force".

Exercises - II

1. *Cherenkov telescopes.* Suppose you have a Cherenkov telescope with 7m diameter, and your camera can detect a signal only when you collect 100 photons from a source. Assuming a global efficiency of 0.1 for the acquisition system (including reflectivity of the surface and quantum efficiency of the PMT),what is the minimum energy (neglecting the background) that such a system can detect at a height of 2 km a.s.l.?
2. *Cherenkov telescopes.* Show that the image of the Cherenkov emission from a muon in the focal plane of a parabolic IACT is a conical section (approximate the Cherenkov angle as a constant).
3. *Energy loss.* In the Pierre Auger Observatory the surface detectors are composed by water Cherenkov tanks 1.2m high, each containing 12 tons of water. These detectors are able to measure the light produced by charged particles crossing them. Consider one tank crossed by a single vertical muon with an energy of 5 GeV. The refraction index of water is n 1.33 and can be in good approximation considered constant for all the relevant photon wavelengths. Determine the energy lost by ionization and compare it with the energy lost by Cherenkov emission.

Multimessenger astroparticle physics

Alessandro De Angelis, INFN/INAF Padova and LIP/IST Lisboa

Lecture 6: Science

How high-energy photons are produced: acceleration sites. Propagation of high-energy photons.
WIMPs and high-energy astrophysics.

TeV Impact

Highlights from **HESS, MAGIC, VERITAS & MILAGRO**

- *Microquasars:* Science 309, 746 (2005), Science 312, 1771 (2006)
- *Pulsars:* Science 322, 1221 (2008), Science 334, 69 (2011)
- *Supernova Remnants:* Nature 432, 75 (2004)
- *The Galactic Centre:* Nature 439, 695 (2006)
- *Surveys:* Science 307, 1839 (2005), PRL 95, 251103 (2005)
- *Starbursts:* Nature 462, 770 (2009), Science 326,1080 (2009)
- *AGN:* Science 314,1424 (2006), Science 325, 444 (2009)
- *EBL:* Nature 440, 1018 (2006), Science 320, 752 (2008)
- *Dark Matter:* PRL 96, 221102 (2006), PRL 106, 161301 (2011)
- *Lorentz Invariance:* PRL 101, 170402 (2008)
- *Cosmic Ray Electrons:* PRL 101, 261104 (2009)

Padova 2017

Thermal radiation: Blackbody Spectra

CMB:
2.7 K

A Galactic gas cloud
60 K

Dim star in the Orion Nebula:
600 K

The Sun:
6000 K

Cluster of very bright stars, Omega Centauri:
60 000 K

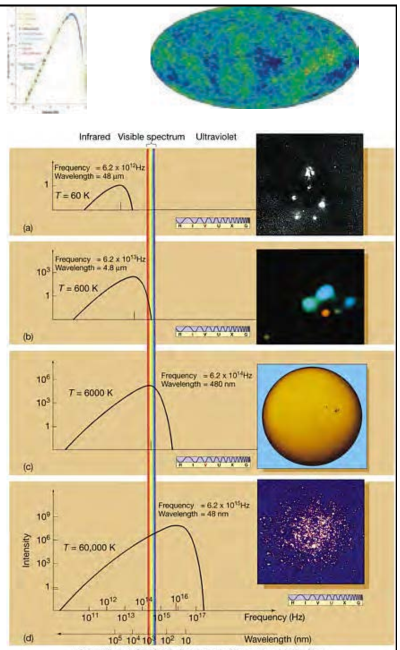

Accretion near BHs: below the keV

γ rays: non-thermal Universe

- Particles accelerated in extreme environments interact with medium
  - Gas and dust; Radiation fields – Radio, IR, Optical, …; Intergalactic Magnetic Fields, …
- Gamma rays traveling to us!
- No deflection from magnetic fields, gammas point ~ to the sources
  - Magnetic field in the galaxy: ~ 3μG
    Gamma rays can trace cosmic rays at energies ~10x
- Large mean free path
  - Regions otherwise opaque can be transparent to X/γ

Studying Gamma Rays allows us to see different aspects of the Universe

Examples of known extreme environments

GRB

SuperNova Remnants
Pulsars

Active Galactic Nuclei

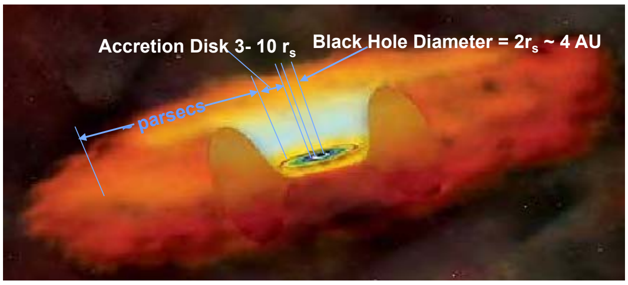

SOURCES OF GAMMA RAYS
RELATION WITH COSMIC RAY PHYSICS

Sources of gamma radiation (and CR?)

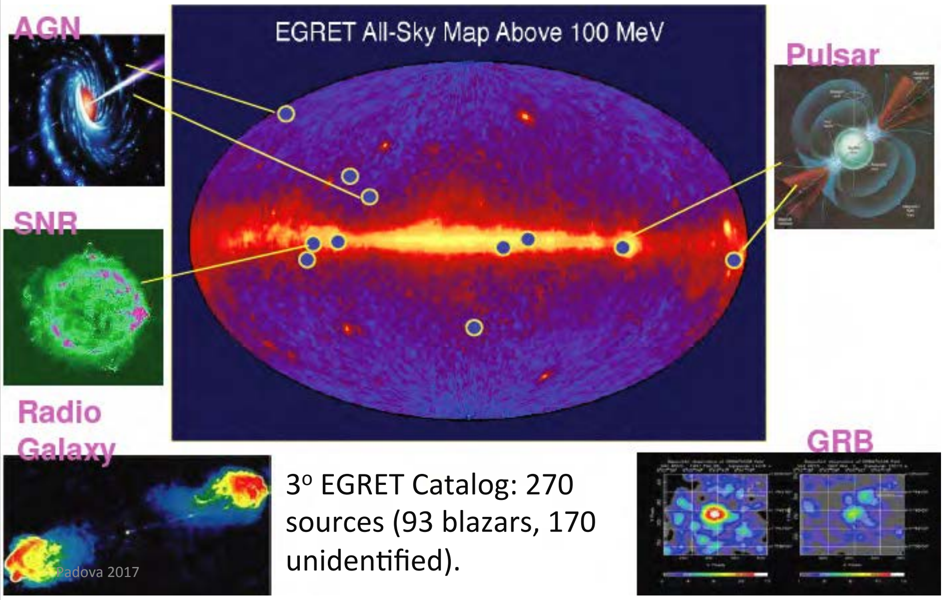

3° EGRET Catalog: 270 sources (93 blazars, 170 unidentified).

γ-rays production@sources

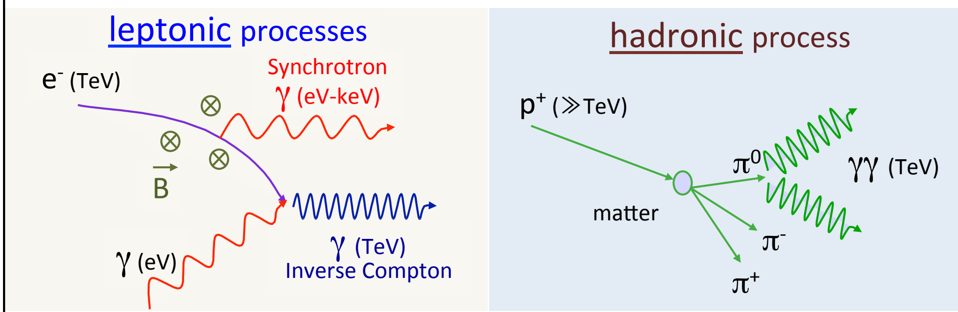

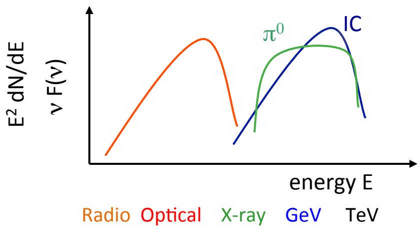

To distinguish between hadronic/leptonic origin the Spectral Energy Distribution (SED) must be studied with different experimental techniques

Padova 2017

4

interactions with matter

E-M: VHE

		VHE	
bremsstrahlung:	e N(e) => e' γ N (e)	*	$E\gamma \sim 1/2E_e$
pair production	γ N(e) => e^+e^- N (e)	*	
e+e- annihilation	e^+e^- => $\gamma\gamma$ (511 keV line)		
Strong/week:	pp (A) => π, K, Λ, ...	**	$E\gamma \sim 1/10E_p$
	π, K, Λ => γ, ν, e, μ		
	μ => ν		

also in the low energy region

Nuclear: p A => A* => A' γ, n

n p => D γ (2.2 MeV line)

interactions with radiation and B-fields

Radiation field		**VHE**	
E-M:			
inverse Compton:	e γ (B) => e' γ	**	$E\gamma \sim \varepsilon(Ee/mc^2)^2$ (T) to ~Ee (KN)
$\gamma\gamma$ pair production	$\gamma\gamma$ (B) => e^+e^-	**	
Strong/week	p γ => π, K, Λ, ...	*	
	π, K, Λ => γ, ν, e, μ		$E\gamma \sim 1/10Ep$
	μ => ν		
	A γ => A* => A' γ	*	$E\gamma \sim 1/1000A\ Ep$
B-field			
synchrotron	e (p) B => γ	*	$E\gamma \sim BE_e^2$; $h\nu_{max} \sim \alpha^{-1} mc^2$
pair production	γ B => e+e-	*	

Emission models

- Leptonic model (needs B field to generate synchrotron radiation)
- Also hadronic mechanism (needs matter as a target with density > ISM (1p/cm^3), or radiation fields)

In both cases,

$$\boxed{\frac{dN_\gamma}{dE_\gamma} \propto \frac{dN_{p,e}}{dE_{p,e}}}$$

Padova 2017

The SED (Spectral Energy Distribution)

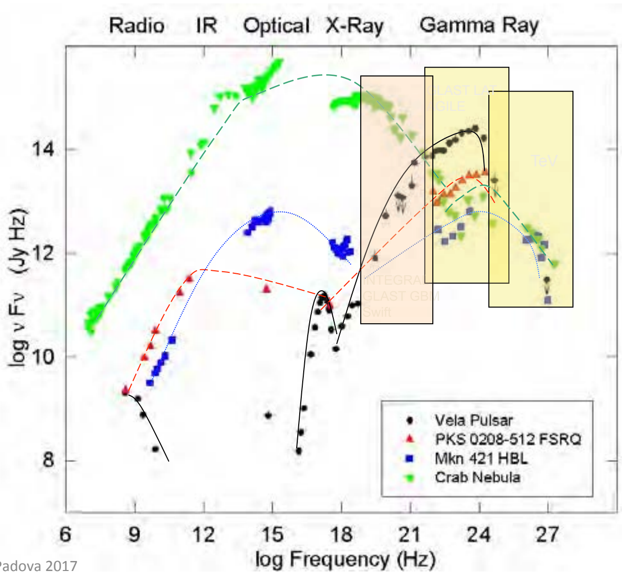

- γ sources are nonthermal (ie, no blackbody)
- γ sources however manifest themselves also in other wavelengths
- The high-energy mechanisms will probably manifest themselves also through different messengers

Padova 2017

The observed photon spectrum extends over 30 decades (measurements up to 1 TeV)

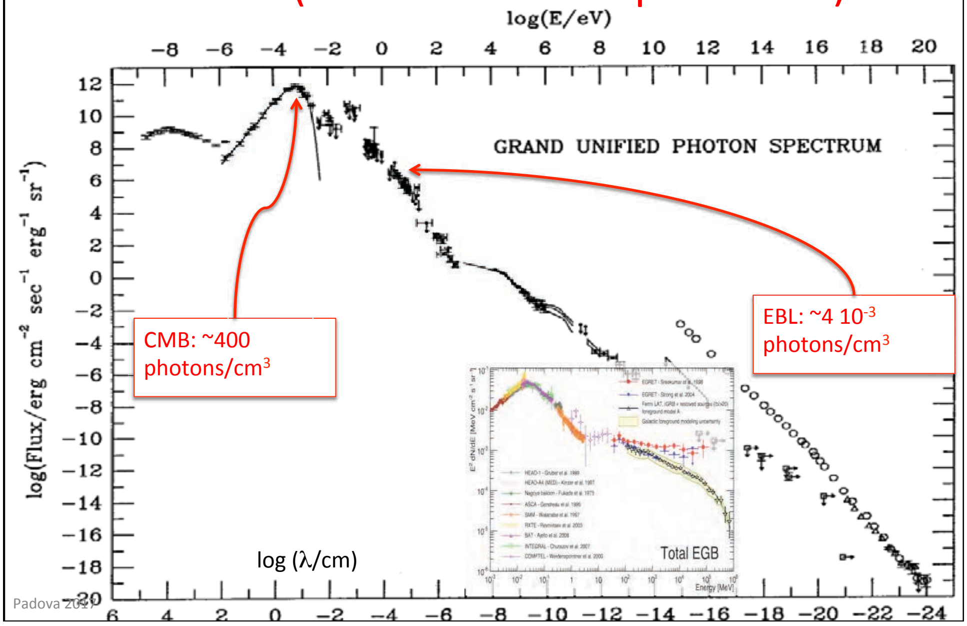

Padova 2017

Sources = signal – diffuse background

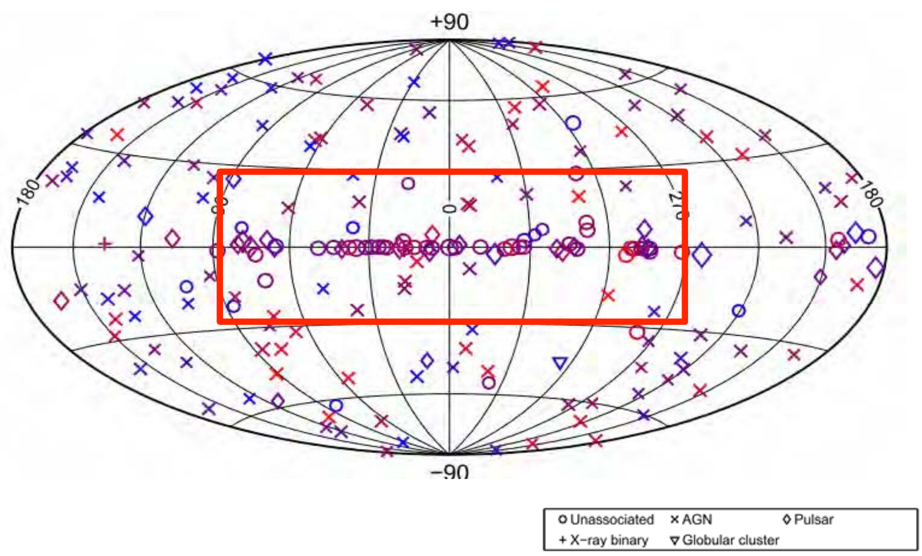

Padova 2017

GeV γ-rays sky by Fermi

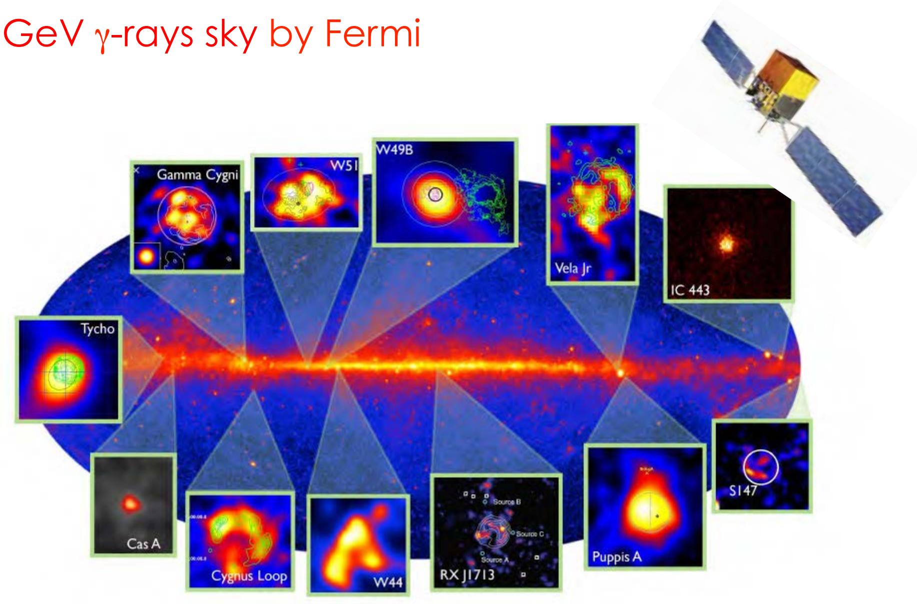

arXiv :1304.4153

Padova 2017

LAT 4-year Point Source Catalog (3FGL)

Fermi-LAT Third Source Catalog (4y) arXiv:1501.02003v3

3033 sources above 100 MeV

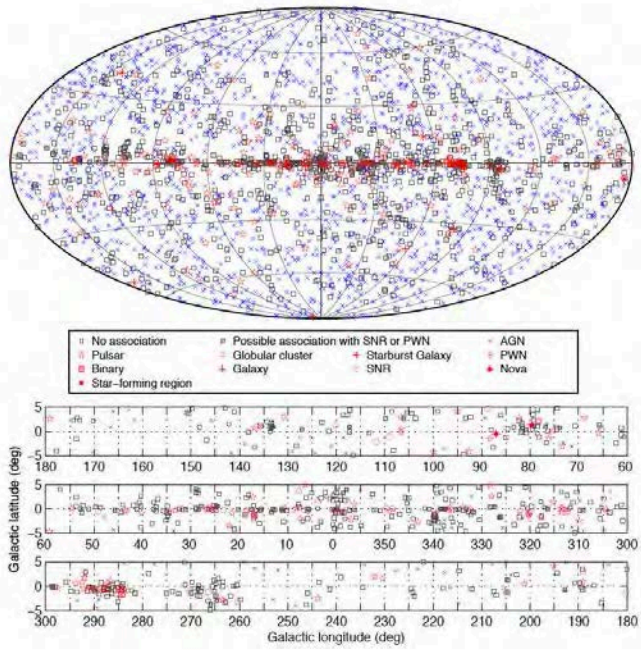

Padova 2017

Description	Identified Designator	Identified Number	Associated Designator	Associated Number
Pulsar, identified by pulsations	PSR	143	...	...
Pulsar, no pulsations seen in LAT yet	...	...	psr	24
Pulsar wind nebula	PWN	9	pwn	2
Supernova remnant	SNR	12	snr	11
Supernova remnant / Pulsar wind nebula	...	...	spp	49
Globular cluster	GLC	0	glc	15
High-mass binary	HMB	3	hmb	0
Binary	BIN	1	bin	0
Nova	NOV	1	nov	0
Star-forming region	SFR	1	sfr	0
Compact Steep Spectrum Quasar	CSS	0	css	1
BL Lac type of blazar	BLL	18	bll	642
FSRQ type of blazar	FSRQ	38	fsrq	446
Non-blazar active galaxy	AGN	0	agn	3
Radio galaxy	RDG	3	rdg	12
Seyfert galaxy	SEY	0	sey	1
Blazar candidate of uncertain type	BCU	5	bcu	568
Normal galaxy (or part)	GAL	2	gal	1
Starburst galaxy	SBG	0	sbg	4
Narrow line Seyfert 1	NLSY1	2	nlsy1	3
Soft spectrum radio quasar	SSRQ	0	ssrq	3
Total	...	238	...	1785
Unassociated	...	...	...	1010

Energy spectral index

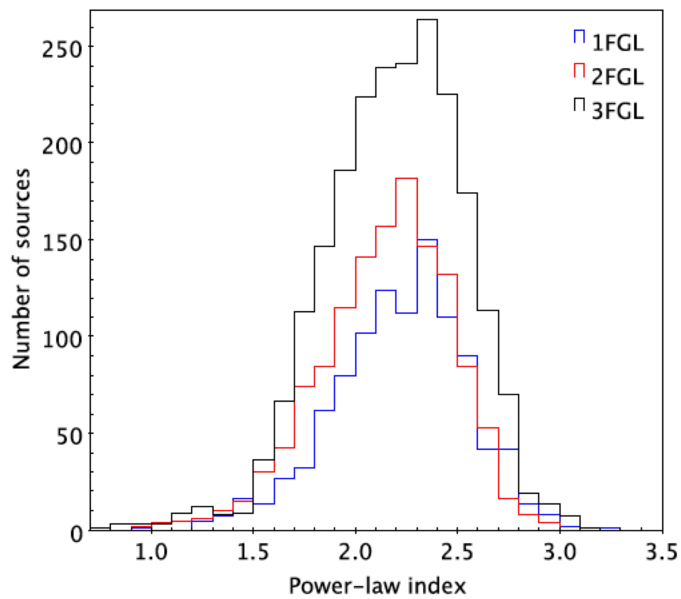

Fermi hard sources sky >50 GeV (2FHL)

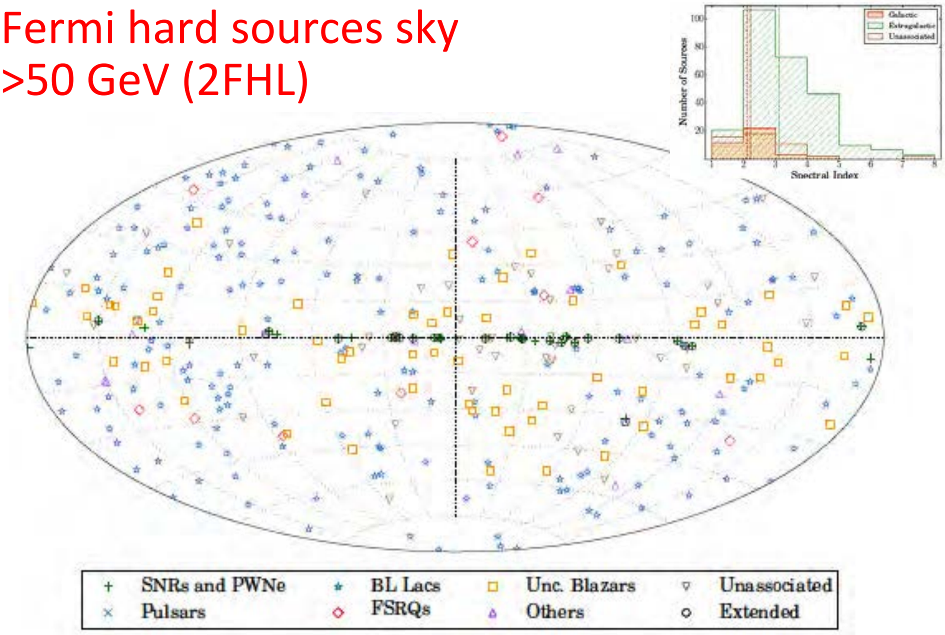

360 sources in 80 months, arXiv :1508.04449v1

TeV sources tevcat.uchicago.edu

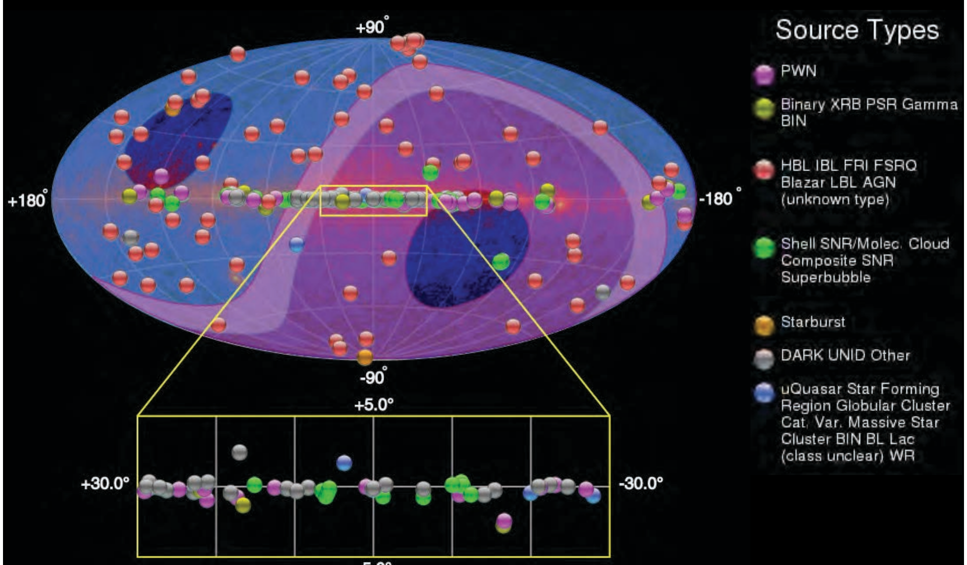

(>200)

Padova 2017

Type	Designator	Objects	Representatives
Pulsar wind nebula	PWN	31	Crab, Geminga, Vela X
Supernova remnant with shell	Shell	11	See Table 9.2
Supernova remnant with mol. clouds	SNR/Mol. Cloud	8	W28, W51
Binary systems	Binary	5	LS 5039, LSI +61 303
Massive star clusters, globular cl.	-	5	-
HBL Lac type of blazar	HBL	41	Mrk 421, Mrk 501
IBL Lac type of blazar	IBL	7	Bl Lac, W Comae
LBL Lac type of blazar	LBL	1	-
FSRQ type of blazar	FSRQ	3	3C 279
FRI type of blazar	FRI	3	Centaurus A, M87
Starburst galaxy	Starburst	2	
Unidentified	UNID	28	-
Total		145	

Table 9.1. Number of object catalogued in the TeVCat in Winter 2013. From [9w1]

Galactic sources

- Remnants of SN explosions (shells, pulsar wind nebulae, pulsars themselves)
- Gamma-rays binaries
- The Galactic Center

- **And a lot of unassociated sources**

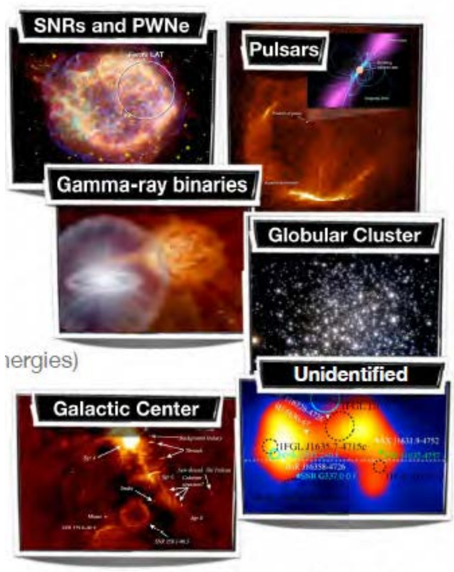

Most are remnants of supernova (including PWN)

- Most of the VHE gamma emission in the Galaxy can be associated to “SNR”.
- Shell Supernova Remnants (SNR). As the shockwave from a SN explosion plows through space, it produces a big shell of hot material in space. This process can continue up to 10^4–10^5 years before the energy release becomes negligible. Magnetic field strengths are estimated to be B ~ 10 µG to 1 mG.
- Pulsar Wind Nebulae (PWN) are SNR with a young pulsar slowing down in rotation: the typical rate of decrease of kinetic energy lies in the range dE/dt ~ 10^{32}–10^{39} erg/s. In most cases only a negligible fraction of this energy goes into the pulsed electromagnetic radiation observed from the pulsar, whereas most of it is deposited into an outflowing relativistic magnetized particle wind
  - Pulsars - When a star collapses into a neutron star, its size shrinks to some 10–20 km, with a density of 5 10^{17} kg/m3 . Since angular momentum is conserved, the rotation can become very fast, with periods of the order of a few ms up to 1 s. Neutron stars in young SNRs are typically pulsars
  - Can be derived from simple physics arguments, see the text
  - Pulsars have typical cutoffs at ~10 GeV, with two notable exceptions (Crab and Vela)

Jets in astrophysics

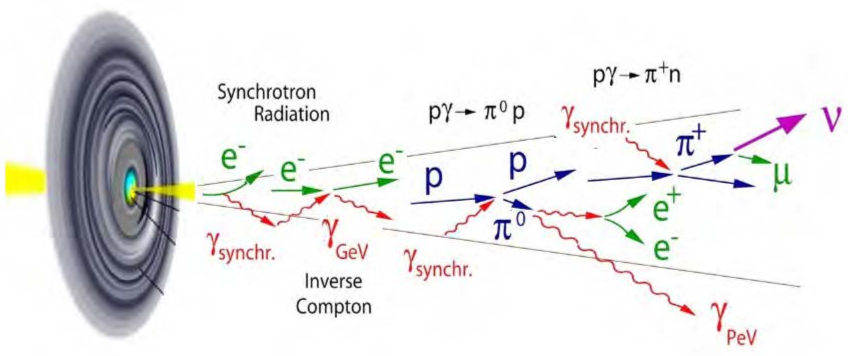

An example of a different galactic emitter: microquasars and binaries

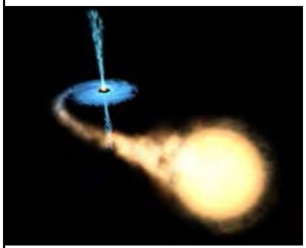

- Like quasars (AGN), they have strong and variable emissions, often in jets, abd an accretion disk surrounding a Black Hole
- In the quasars, the BH is supermassive (>10^6 solar masses) while in microquasars it is of few solar masses
- Accretion comes usually at the expense of a normal star and emission is visible in the optical and X-ray regions
- The emission is periodical (days, months)

What sort of compact object?

How are the particles accelerated?

Are there different types of such high-mass binary systems?

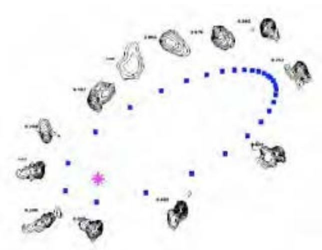

Something special: the Fermi bubbles

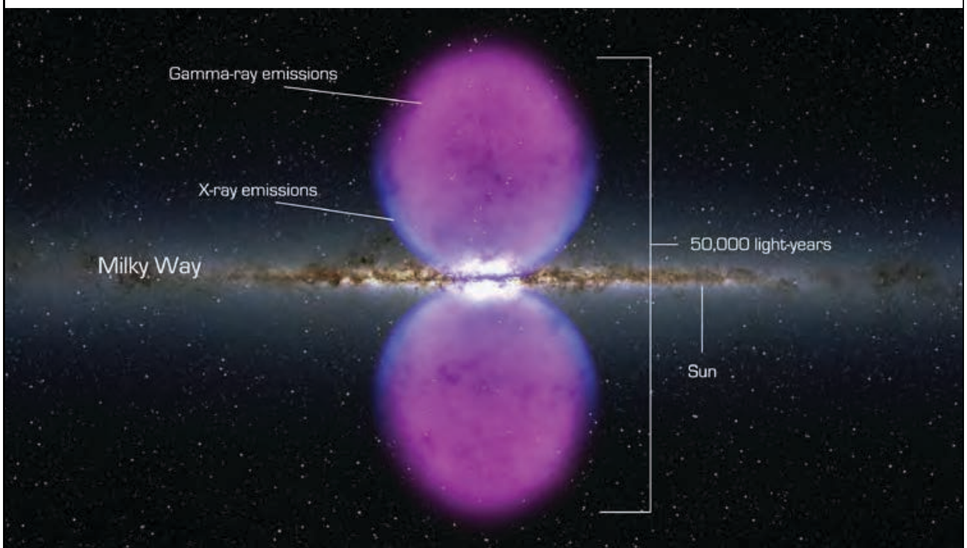

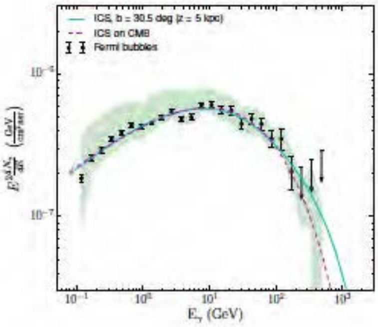

- Each bubble has a major axis ~25 kpc
- γ-ray emission has a significantly harder spectrum ($dN/dE \sim E^{-2}$) than IC emission from galactic electrons, or γ-rays produced by decay of pions from CR-ISM collisions
- Bubbles are spatially correlated with the hard-spectrum microwave excess known as the "WMAP haze". Edges are correlated with X-ray emission detected by ROSAT.
- May have been created by some large episode of energy injection in the Galactic center, such as past accretion events onto the central massive black hole, or a nuclear starburst in the last ~ 10 Myr.
    - Other alternatives: in situ acceleration in shocks at the edge of the bubble, steady wind of particles from galactic center…
- The brightness of the emission is not uniform across the bubbles: excess of emission on the S-E side of the bubbles (referred to as the cocoon). Otherwise, the 2 bubbles are consistent.

Padova 2017

Extragalactic emitters: AGN

(we don't have the resolution to see structures in HE)

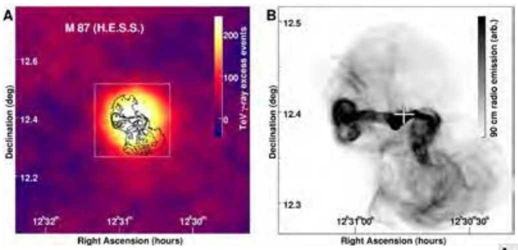

M87: Image from HESS and radio image

M87 variability in the TeV

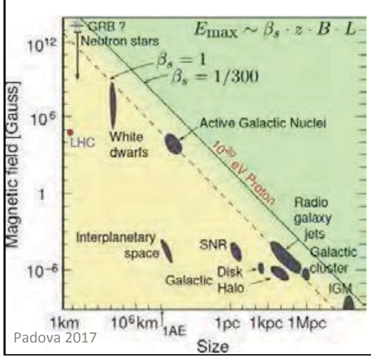

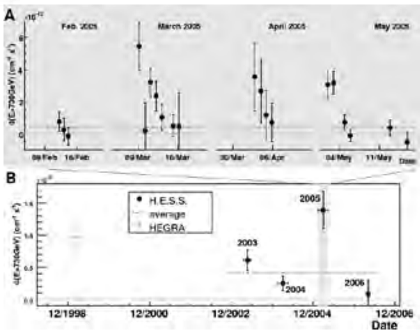

Padova 2017

Variability

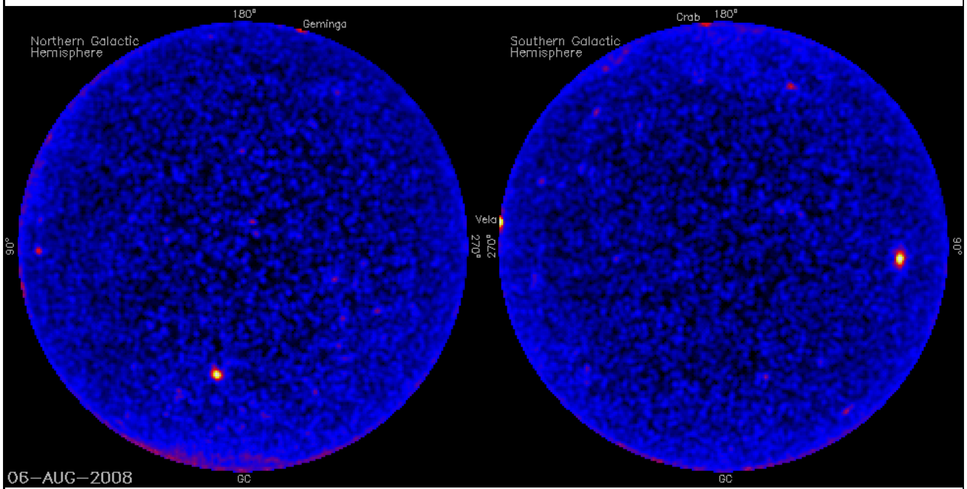

Padova 2017

Rapid variability

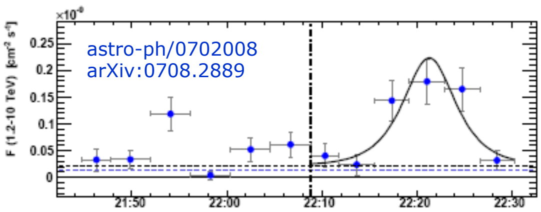

MAGIC, Mkn 501
Doubling time ~ 2 min

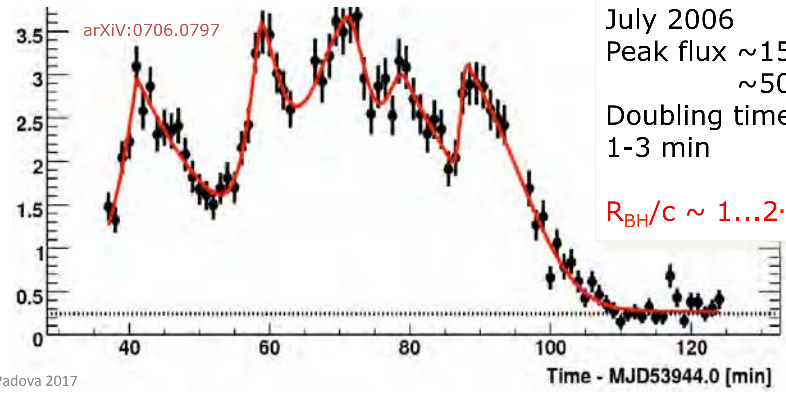

HESS PKS 2155
z = 0.116

July 2006
Peak flux ~15 x Crab
~50 x average
Doubling times
1-3 min

$R_{BH}/c \sim 1...2 \cdot 10^4$ s

Padova 2017

Classification of AGN

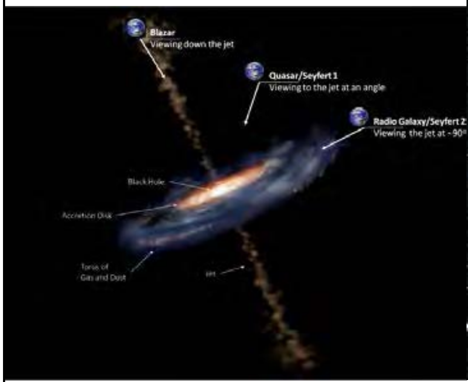

Centaurus A

Most extragalactic sources are blazars

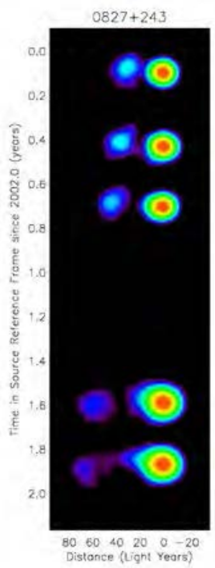

- AGN with the accretion jets pointing towards us

What do the combined radio/gamma-ray observations tell us about particle acceleration and interaction – processes, location?

What can this information reveal about jet formation and collimation?

VLBI image

The spectral energy distributions of blazars

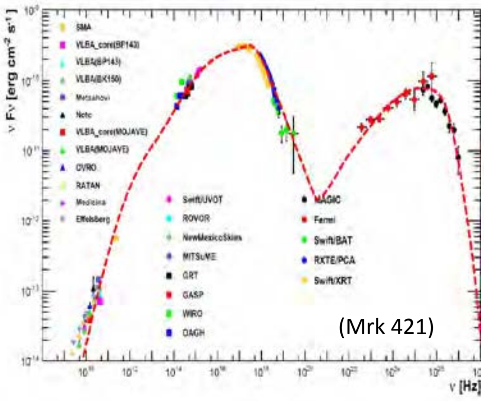

The "blazar sequence"

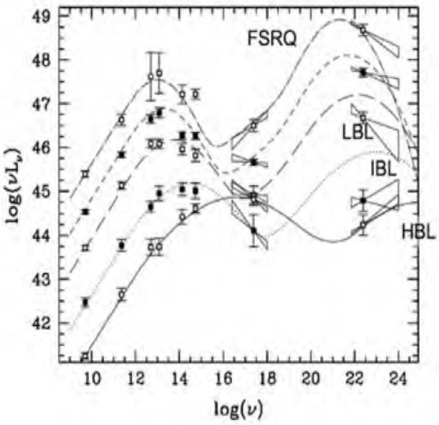

But: some indications of "orphan" flares

Padova 2017

Gamma Ray Bursts (GRBs)

Transient Sources

- Frequently they have a delayed high-energy emission (afterglow)

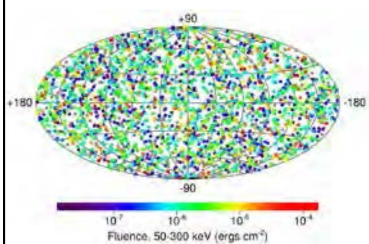

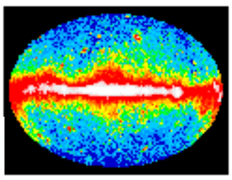

BATSE on CGRO

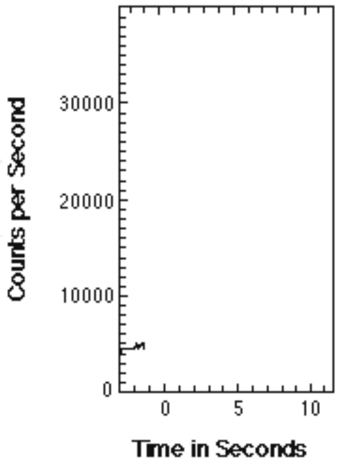

Isotropical => Extragalactic origin

Padova 2017

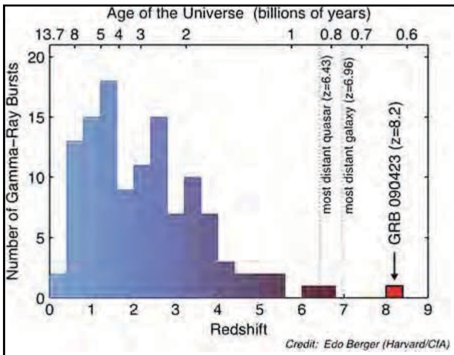

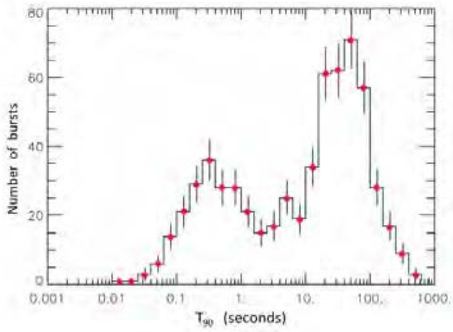

- GRBs are detected roughly once per day, from random directions in the sky by satellite experiments. They are typically far away
- Lasting anywhere from a few milliseconds to several minutes, GRBs shine hundreds of times brighter than a typical supernova, making them briefly the brightest source of cosmic gamma-ray photons in the observable Universe.
- GRBs are separated into two classes: long- and short-duration bursts.
  - Long duration last more than 2 seconds and short-duration less.
  - Short GRBs are difficult to associate

But the time profile can be very different from one GRB to another

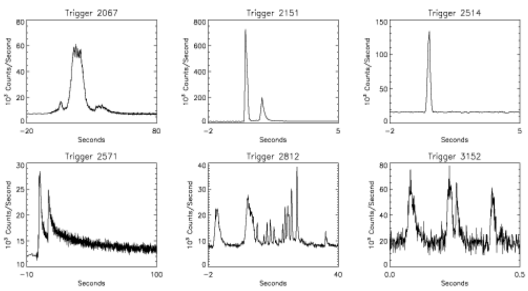

A sampling of the large variety of GRB time profiles, as detected from the CGRO satellite

Long and short GRBs

- Long and short duration GRBs are created by fundamentally different physical mechanisms
- Possible candidates for short GRBs are mergers of neutron star (NS) binaries or NS-BH binaries, which lose angular momentum and undergo a merger
  - Remember the recent gravitational wave event?
- Possible candidates for long GRBs: core collapse of a very massive star, a very energetic supernova (the "hypernova", 100 times the SN). Seen in association!
  - The explosion originates at the center of these massive stars. While a BH forms from the collapsing core, this explosion sends a blast wave moving through the star at speeds close to c. The gamma rays are created when the blast wave collides with stellar material still inside the star.
  - Erupting through the star surface, the blast wave of stellar material sweeps through space, colliding with intervening gas and dust, producing additional emission of photons. These emissions are believed responsible for the "afterglow" of progressively less energetic photons

The Fireball model

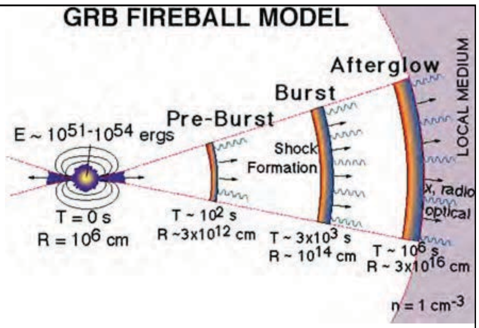

- First the BH formed (or accreted) starts to pull in more stellar material; quickly an accretion disk forms, with the inner portion spinning around the BH at a relativistic speed. This creates a B field which blasts outward two jets of electrons, positrons and protons at ultrarelativisic speed in a plane out of the accretion disk. Photons are formed in this pre-burst.
- Step two is the fireball shock. Each jet behaves in its way as a shockwave, plowing into and sweeping out matter like a "fireball". Gamma rays are produced as a result of the collisions of blobs of matter; light escapes in the direction of motion of the jet, ahead of the shock front.
- From the point of view of the observer, the photons first detected are emitted by a particle moving at relativistic speed, resulting in a Doppler blueshift to the highest energies. This is the GRB.
- An afterglow results when material escaped from the fireball collides with the interstellar medium and creates photons. The afterglow can persist for months as the energies of photons decrease.

Leptonic vs. hadronic models

Multifrequency/multimessenger observation required
Use galactic sources (morphology)

The reference source: Crab

Nebula

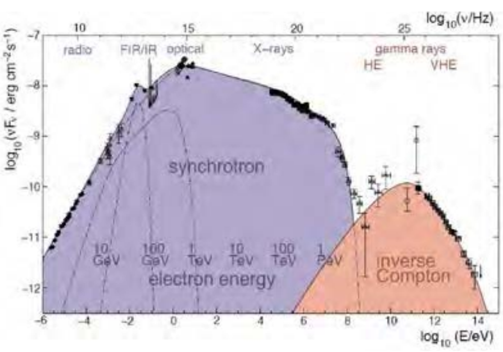

Pulsar

ApJ, vol. 708, p1254 (2010).

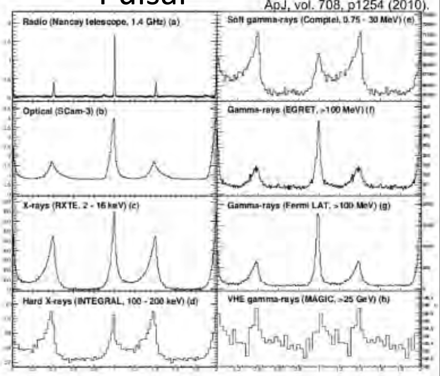

The Crab Pulsar and Nebula are a remnant of the supernova SN1054, (observed on Earth in the year 1054).
The Pulsar was discovered in 1968, and it was the first to be connected with a supernova remnant (PWN).

Crab: well modeled by leptonic emission

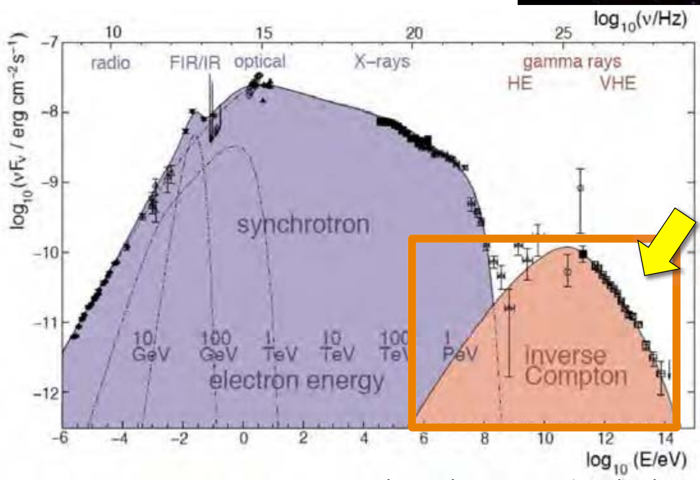

Nebula: Synchrotron + IC emission. e- up to PeV, accelerated at termination shock.

Padova 2017

A >TeV accelerator

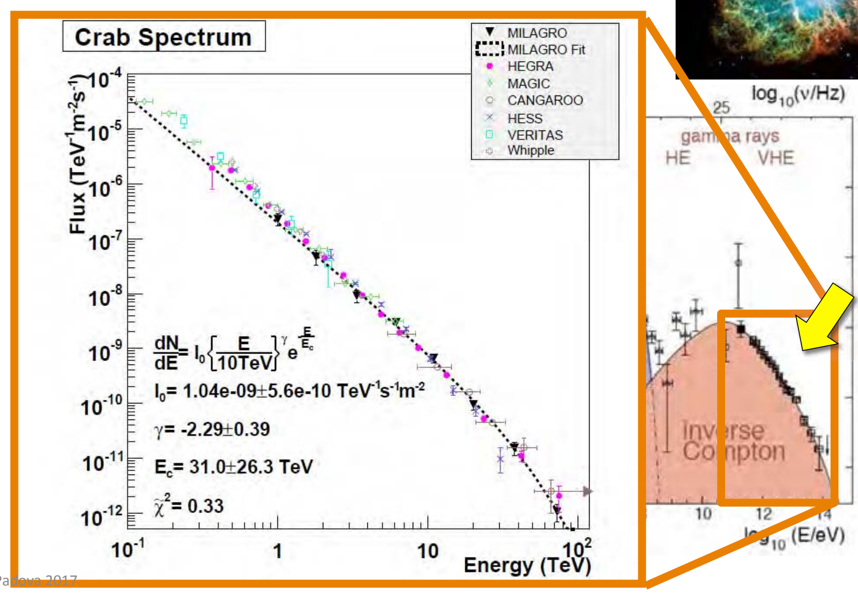

Padova 2017

Supernova remnants - the sources of CRs?

Strong Correlation with X-ray Intensities

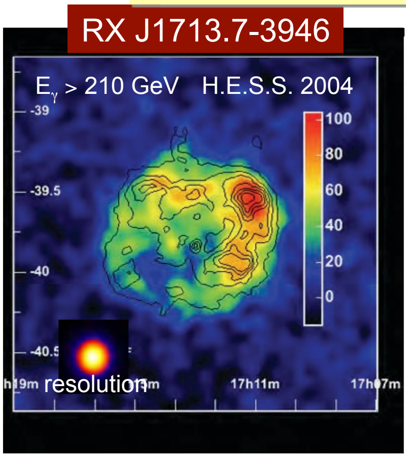

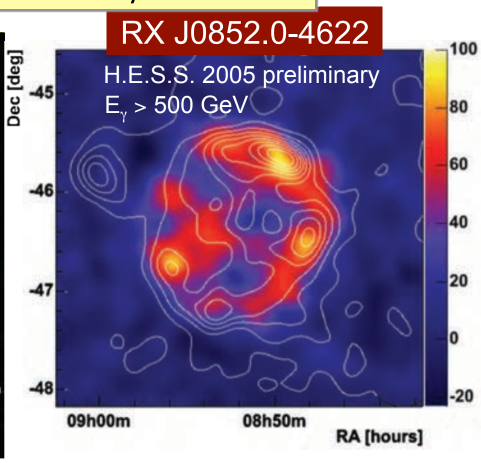

- SN-Shells accelerate particles up to 100 TeV at least
- Are the accelerated particles protons or electrons?

Interaction with molecular clouds or gammas in the ambient

- Evidence that SNR are sources of CR up to ~1000 TeV (almost the knee) came from morphology studies of RX J1713-3946 (H.E.S.S. 2004) with photons
- Striking evidence from the morphology of SNR IC443 (MAGIC + Fermi/Agile 2010)

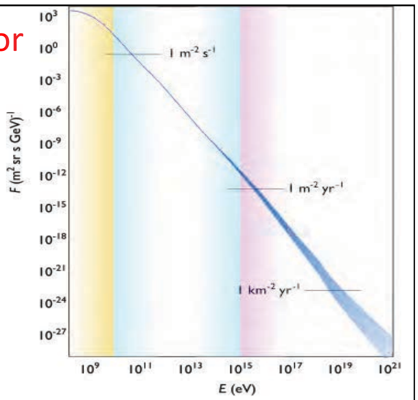

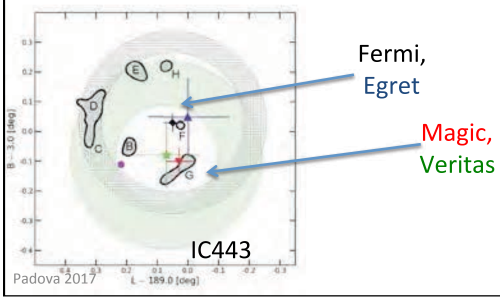

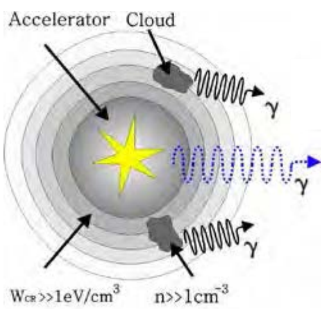

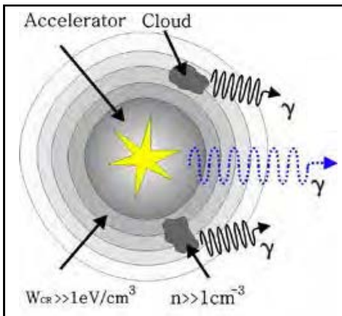

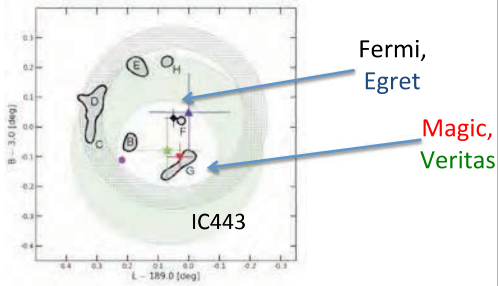

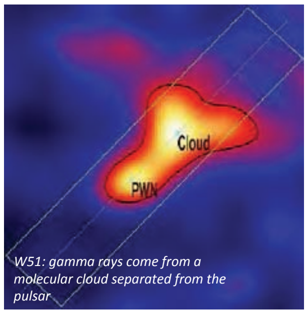

W51: gamma rays come from a molecular cloud separated from the pulsar

Padova 2017

Spatially resolved spectra of RX J1713.7-3946

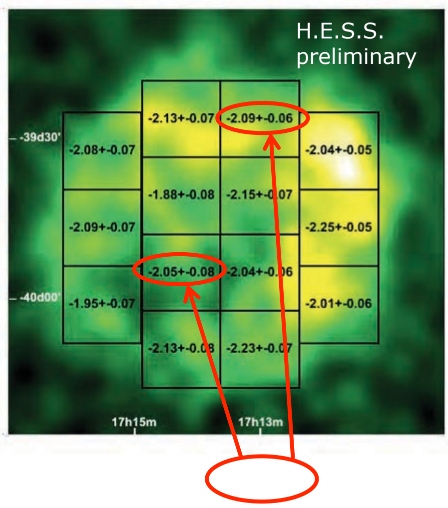

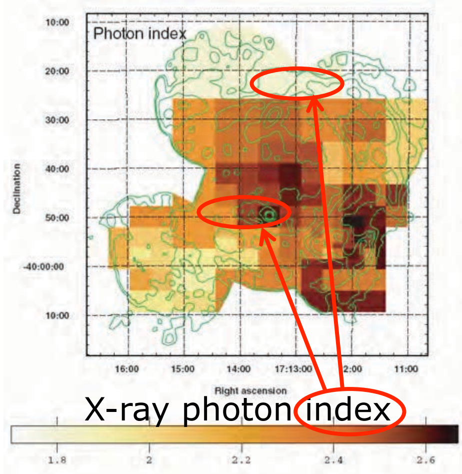

TeV / X-ray intensities correlate, but NOT the spectral shapes
⇒ very hard to understand for pure electron accelerator !

Padova 2017

The SNR RX J1713.7-3946

SN remnant
RX J1713.7-3946
age: 1.6 kyr,
distance: 1 kpc

Funk, 2007- Pre FERMI era

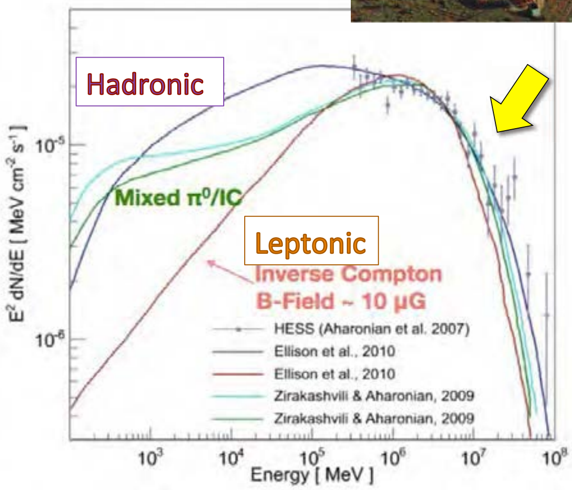

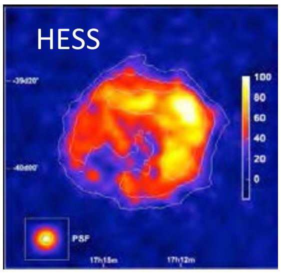

Padova 2017

Hadrons ! (February 2013)

CRs acceleration sites first time detected in Supernova remnants:

IC 443: gas densities n = 20 cm^{-3} , d=1.5 kpc
(W44: n = 100 cm^{-3}, d= 2.9 kpc)

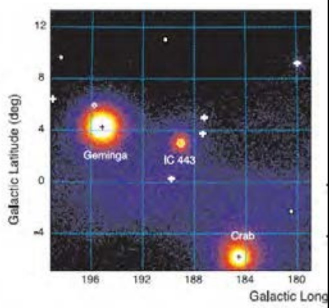

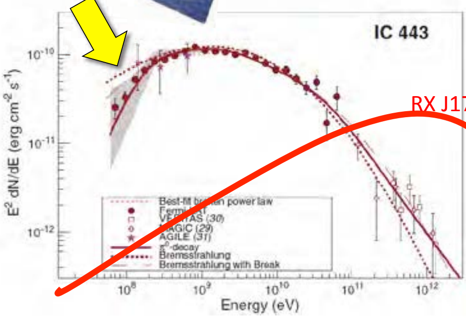

γ-rays produced in nearby clouds of higher matter density than ISM

Ackermann et al. 2013, Science, 339, 807

•Compare with the measured spectrum from RX 1713.7-3946 !

Padova 2017

Not a PeVatron

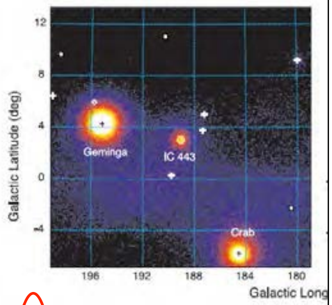

- Photon flux >1 TeV negligible → CR up to few TeV
- Proton spectrum: many objects (~10^4) should contribute to the CR

Ackermann et al. 2013, Science, 339, 807

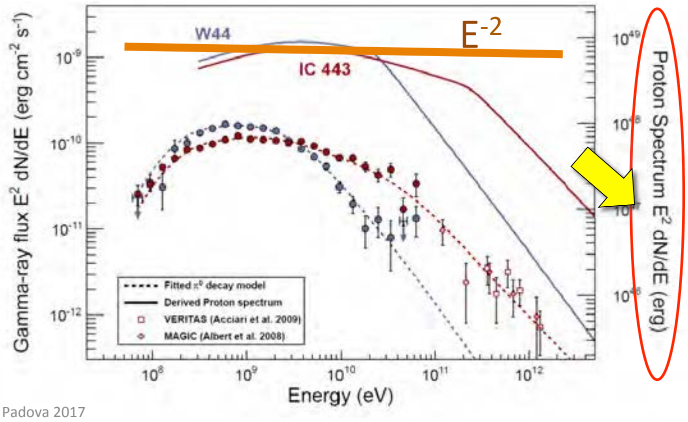

The Galactic Center

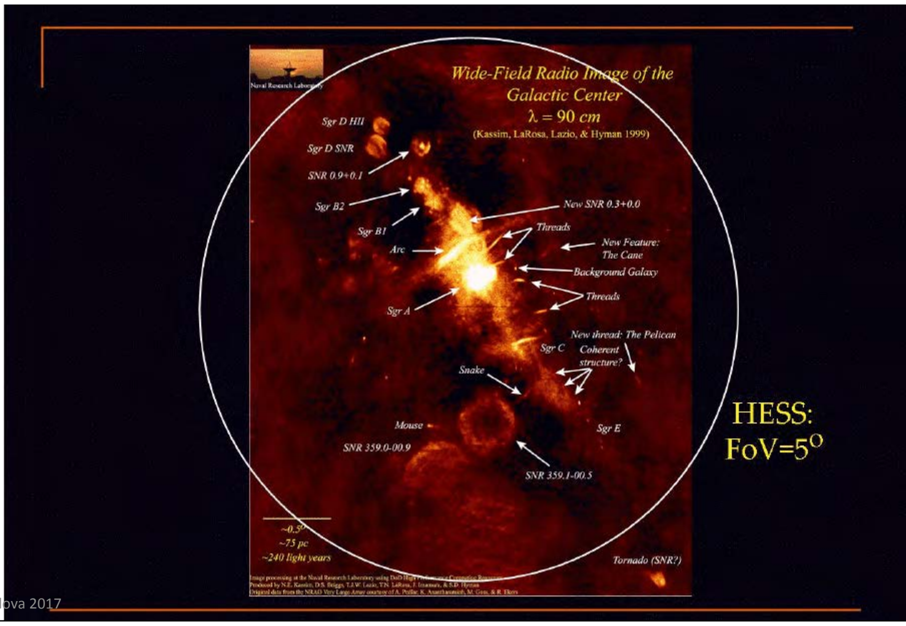

The Galactic center above 50 GeV (Fermi) and in TeV (HESS)

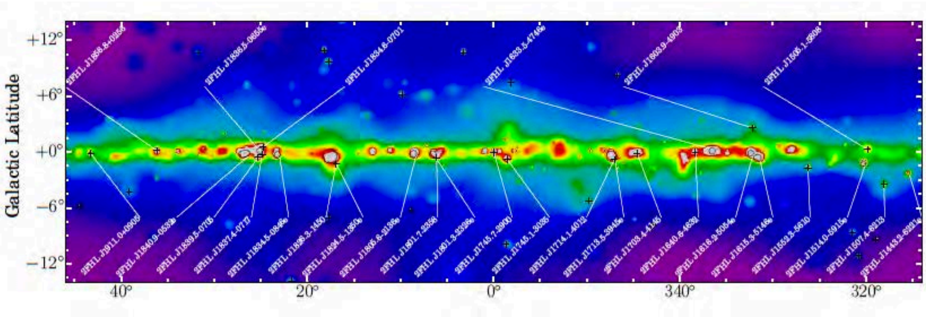

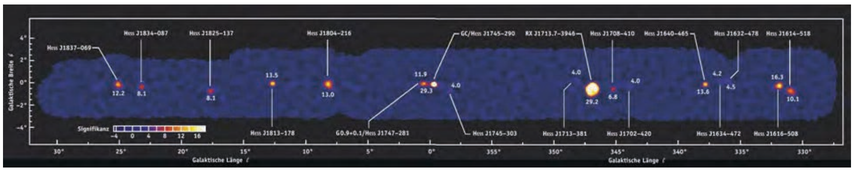

A PeVatron in the GC? (Nature 2016)

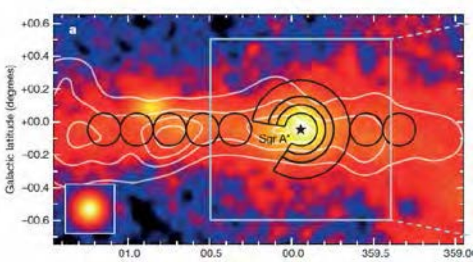

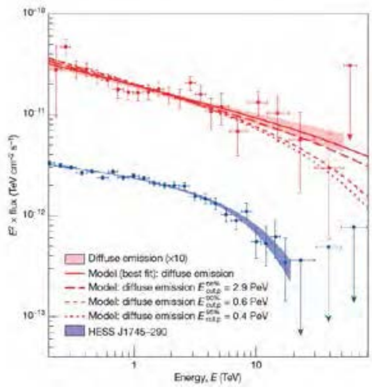

- Diffuse emission from the decay of π^0 produced in pp interactions can reach some 50 TeV => primary energy ~ 1 PeV

PROPAGATION OF PHOTONS

Attenuation of γ−rays

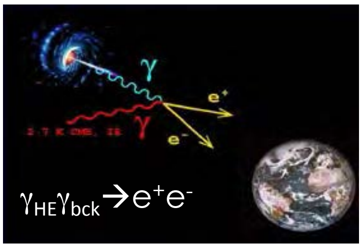

- γ-rays are effectively produced in EM and hadronic interactions
  - Energy spectrum at sources E^{-2}
- are effectively detected by space- and ground-based instruments
- effectively interact with matter, radiation ($\gamma\gamma \rightarrow e^+e^-$) and B-fields
- The interaction with background photons in the Universe attenuates the flux of gamma rays
- The “enemies” of VHE photons are photons near the optical region (Extragalactic Background Light, EBL)

$\gamma_{VHE}\gamma_{bck} \rightarrow e^+e^-$

$\sigma(\beta) \sim$ $$1.25 \cdot 10^{-25}(1-\beta^2) \cdot \left[2\beta(\beta^2-2)+(3-\beta^4)\ln\left(\frac{1+\beta}{1-\beta}\right)\right] \mathrm{cm}^2$$

Max for: $$\epsilon \simeq \frac{2m_e^2c^4}{E} \simeq \left(\frac{500\,\mathrm{GeV}}{E}\right)\mathrm{eV}$$

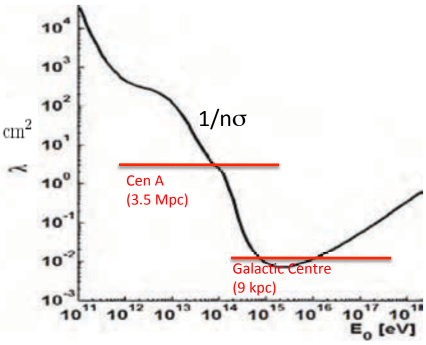

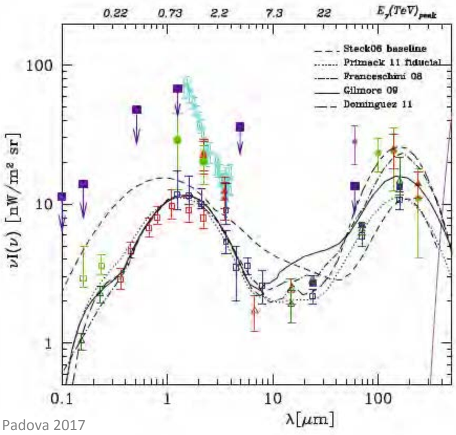

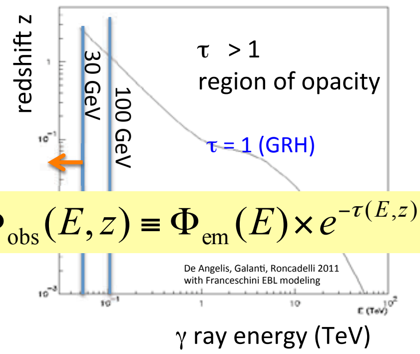

$$\Phi_{\mathrm{obs}}(E,z) \equiv \Phi_{\mathrm{em}}(E) \times e^{-\tau(E,z)}$$

Padova 2017

- The diffuse extragalactic background light (EBL) is all the accumulated radiation in the Universe due essentially to star formation processes
- This radiation covers a wavelength range between ~0.1 and 600 μm (consider the redshift and the reprocessing)
- After the CMB, the EBL is the second-most energetic diffuse background
- The understanding of the EBL is fundamental
  - To know the history of star formation
  - To model VHE photon propagation for extragalactic VHE astronomy. VHE photons coming from cosmological distances are attenuated by pair production with EBL photons. This interaction is dependent on the SED of the EBL.
- Therefore, it is necessary to know the SED of the EBL in order to study intrinsic properties of the emission in the VHE sources.

Padova 2017

The γ horizon: nuisance and resource

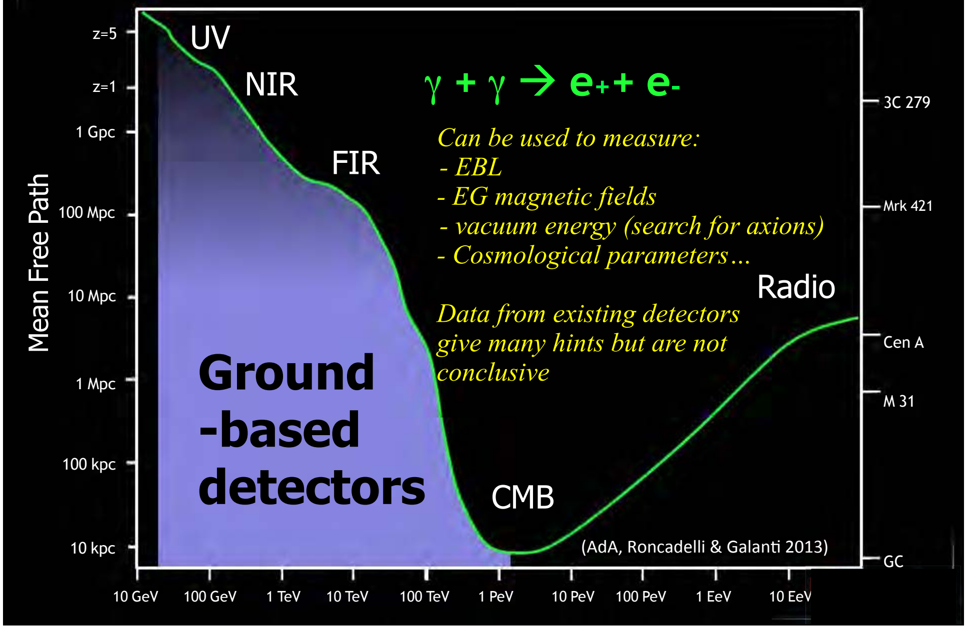

EBL

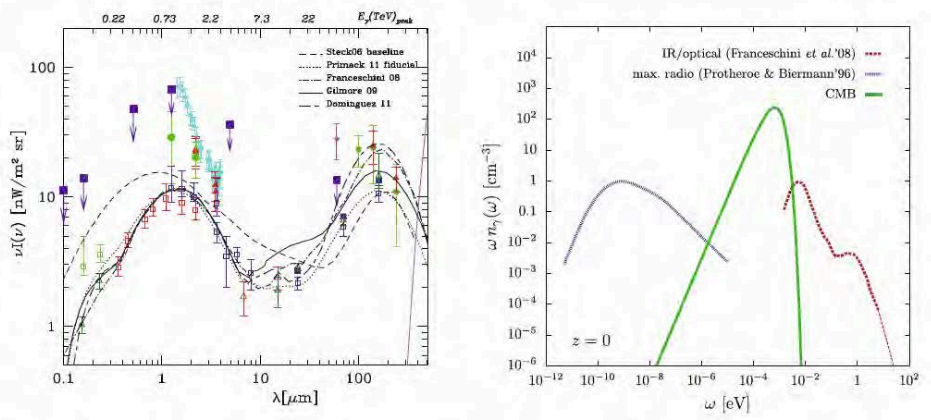

The EBL affects in particular the signal from extragalactic sources

Fermi 2FHL and gamma horizon

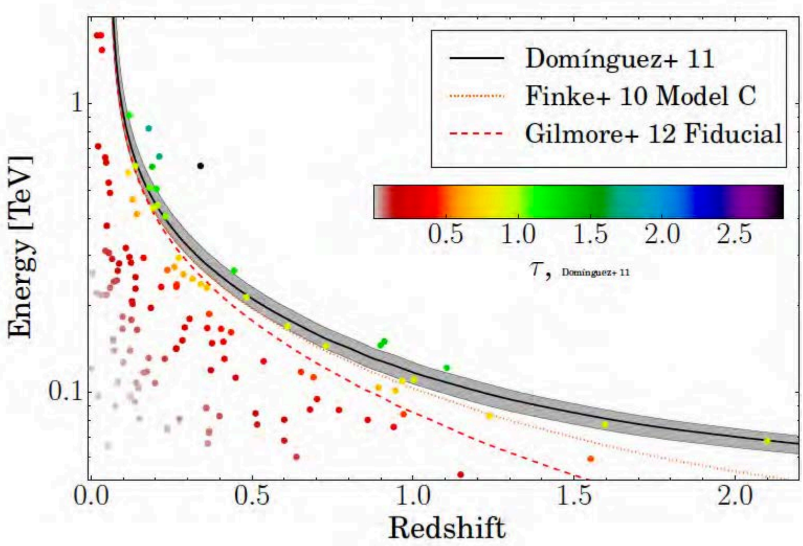

Padova 2017

DARK MATTER

Padova 2017

Evidence and features of Dark Matter

*Comprises **majority** of **mass** in Galaxies*
Missing mass on Galaxy Cluster scale
Zwicky (1937)

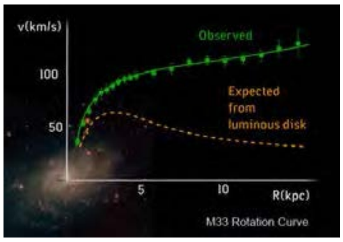

*Large **halos** around Galaxies*
Rotation Curves
Rubin+(1980)

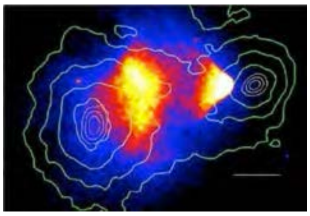

Low cross section
Bullet Cluster
Clowe+(2006)

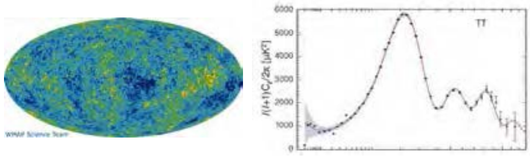

Non-Baryonic
Big-Bang Nucleosynthesis,
CMB Acoustic Oscillations
WMAP(2010), *Planck*(2015)

Constraints on Dark Matter

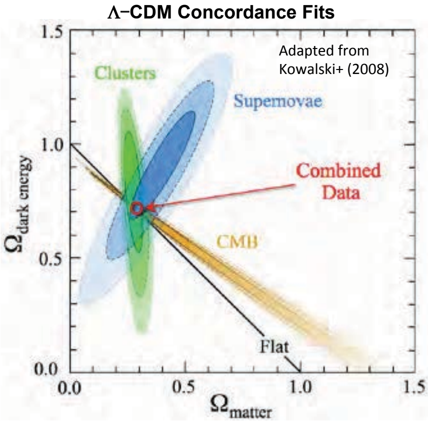

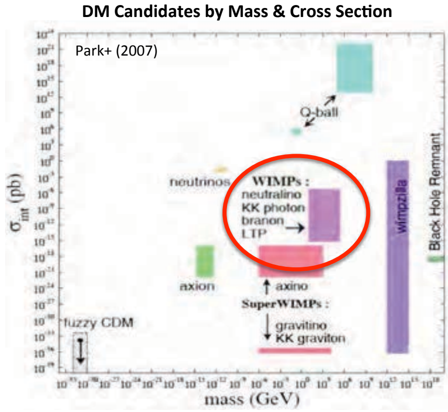

- No SM particle matches the known properties of dark matter
- Many candidate particles have been proposed and have implications in multimessenger astrophysics:
  - WIMPs
  - WISPs (axion-like particles, etc.)
  - Super-heavy particles

Average density $\rho_{DM} \sim 5\rho_B$ (1.5 GeV/m^3)
Near the Sun, $\rho_{DM} \sim 0.4$ GeV/cm^3

WIMP Dark Matter as a thermal relic

DM Density v. Temperature

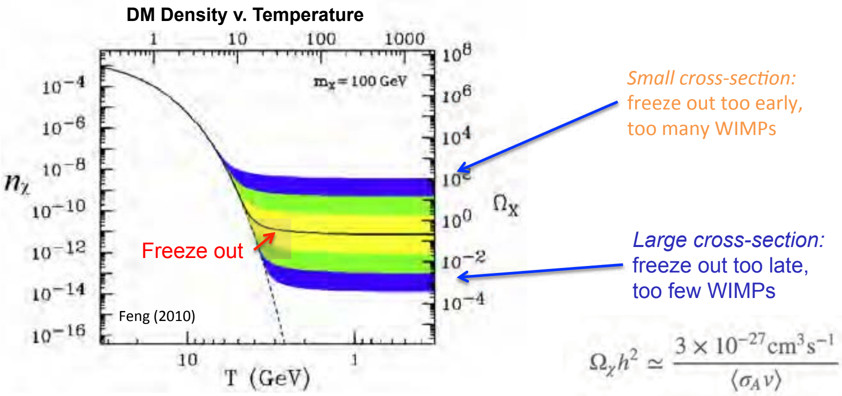

$$\Omega_\chi h^2 \simeq \frac{3 \times 10^{-27} \mathrm{cm}^3 \mathrm{s}^{-1}}{\langle \sigma_A v \rangle}$$

- The calculation of the thermal-averaged cross-section $<\sigma v>$ needed to obtain the relic density gives $<\sigma v> \sim 3\ 10^{-26}\ \mathrm{cm}^3\mathrm{s}^{-1}$ at freeze-out
- At that cross-section the entire class of particle models that would generate GeV-to-TeV dark matter would be in reach in the next 10 years

DM Structures are present on many scales

Zoom Sequence of DM Structure on 100 Mpc Scales

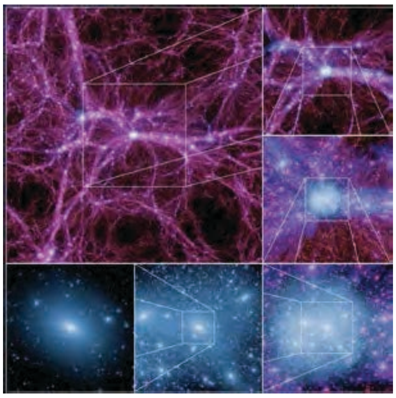

Milky Way-like Halo and Several Sub-Halos

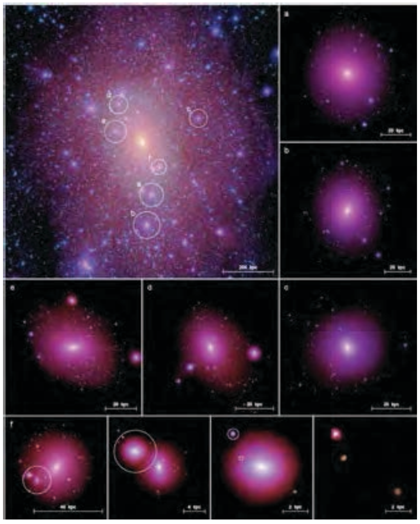

- We can probe DM by looking for signal contributions from halos:
  - On cosmological scales (left)
  - In the Milky Way virial radius (~300 kpc = ~1 MLY, right) (Visible size of MW = ~ 20 kpc)

Left: Boylan-Kolchin+ 2009MNRAS.398.1150B
Right: Springel+ 2008MNRAS.391.1685S

Padova 2017

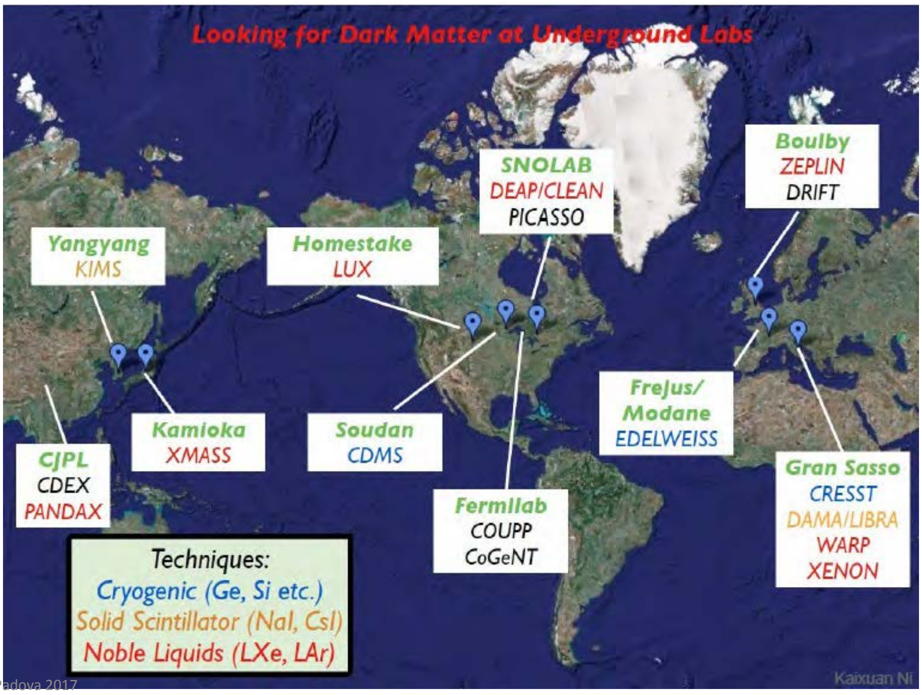

Padova 2017

Signals?

DAMA/LIBRA Annual Modulation

R. Bernabei et al. EPJ C 56, 333 (2008), arxiv:0804.2741
EPJ C 67, 39 (2010), arxiv:1002.1028

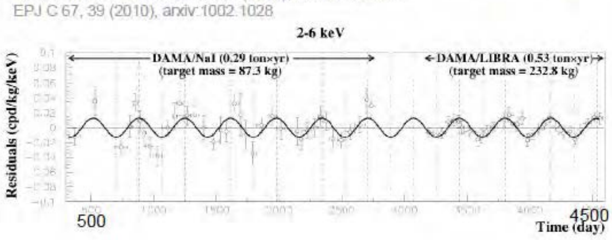

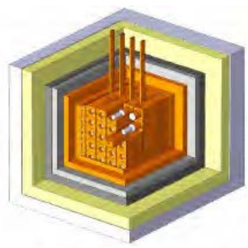

- ~250 kg of NaI counters
- 1.17 ton-year exposure (2010)

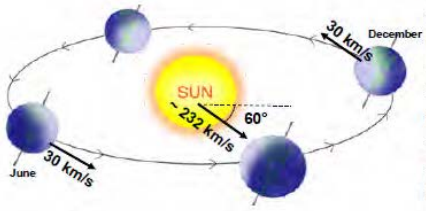

- Modulation in 2-6 keV single hits: 8.9 σ
- Mostly in 2-4 keV, ~0.02 cts/d/kg/keV
- Total single rate ~1 cts/d/kg/keV
- Standard DM distribution: < ~5% modulation
- Period & phase about right for DM.
- No annual modulation in 6-14 keV.
- No annual modulation in multiple hits. (which?)
- **DM detection?**
- Conflict with other experiments in standard scenarios that test the larger steady state effect.

Drukier, Freese, Spergel PRD 86
Freese et al. PRD 88

Padova 2017

Exclusion/Signal region

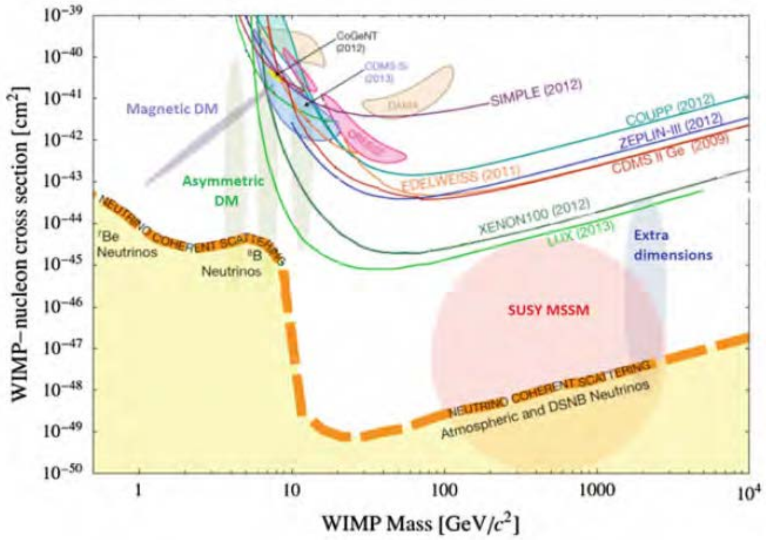

Padova 2017

The indirect detection of DM

- **WIMP Annihilation** Typical final states include heavy fermions, gauge or Higgs bosons

- **Fragmentation/Decay** Annihilation products decay and/or fragment into combinations of electrons, protons, deuterium, (and their antiparticles), gamma-rays and neutrinos

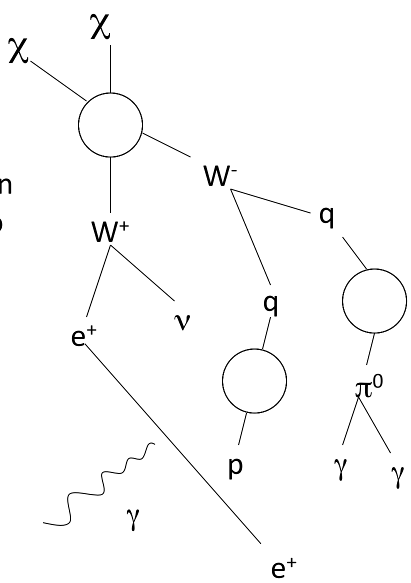

Padova 2017

- **Gamma Rays** from annihilations in the galactic halo, near the galactic center, in dwarf galaxies, etc. Drawback: Unknown astrophysical background.
- **Neutrinos** from annihilations in the core of the Sun or in the sama sources as gamma rays (IceCube, Antares). Not the sensitivity, yet
- **Positrons/Antiprotons** from annihilations throughout the galactic halo. Drawback: Unknown astrophysical background.
  - Measured in space–based detectors: Fermi (gammas), PAMELA, AMS (antimatter) or in atmospheric Cherenkov telescopes: MAGIC

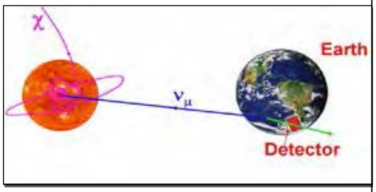

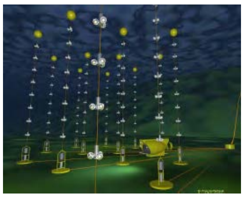

The Key Formula for WIMP Searches

Particle Physics **Astrophysics (*J*-Factor)**

$$\frac{d\Phi_\gamma}{dE_\gamma}(E_\gamma,\phi,\theta) = \boxed{\frac{1}{4\pi}\frac{<\sigma_{ann}v>}{2m^2_{WIMP}}\sum_f \frac{dN^f_\gamma}{dE_\gamma}B_f} \boxed{\int_{\Delta\Omega(\phi,\theta)} d\Omega' \int_{los} \rho^2(r(l,\phi'))dl(r,\phi')}$$

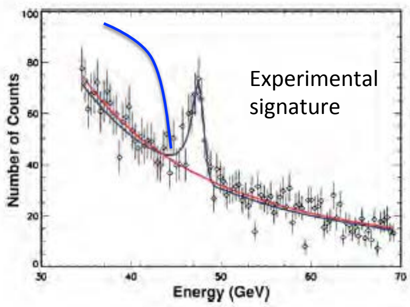

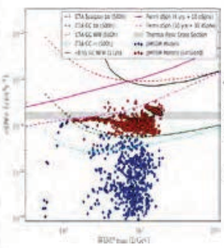

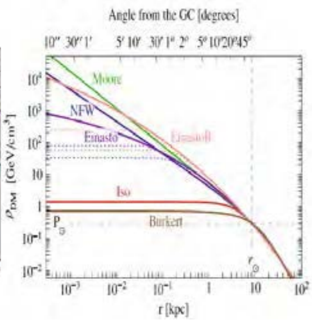

- *J*-factor includes distance, i.e., *J*-factor would decrease by four if a point-like source were twice as far away => look as close as possible
- The factor of $1/m_\chi^2$ is due to the fact we express the *J*-factor as a function of mass density (which we can measure), not number density
- We usually call χ the generic WIMP, like the SUSY neutralino, but it's more general

Role of Indirect Detection Dark Matter Searches

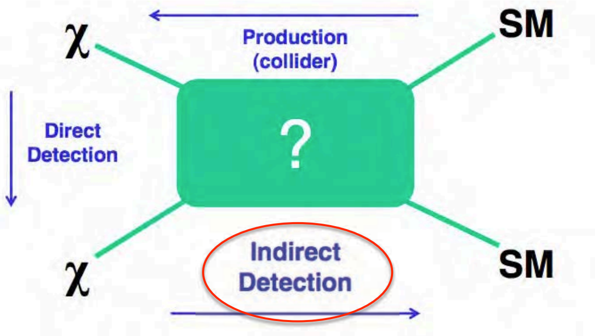

- *Compared to collider searches*: indirect detection is sensitive to high mass scales (particles already exist, stable final state particle spectrum peaks at ~10% of m_χ)
- *Compared to direct detection*: indirect detection is sensitive to annihilation rather than scattering off of nuclei (i.e., more sensitive when χ couples more to heavy quarks and vector bosons than to light quarks and gluons)

Antimatter measured by PAMELA - pbar

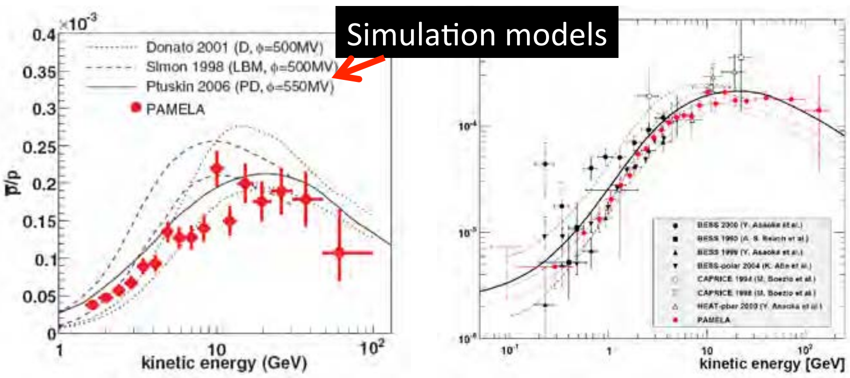

- PAMELA results are consistent with pure secondary production of antiprotons during the propagation of cosmic rays in the galaxy

Positron fraction:PAMELA/AMS02

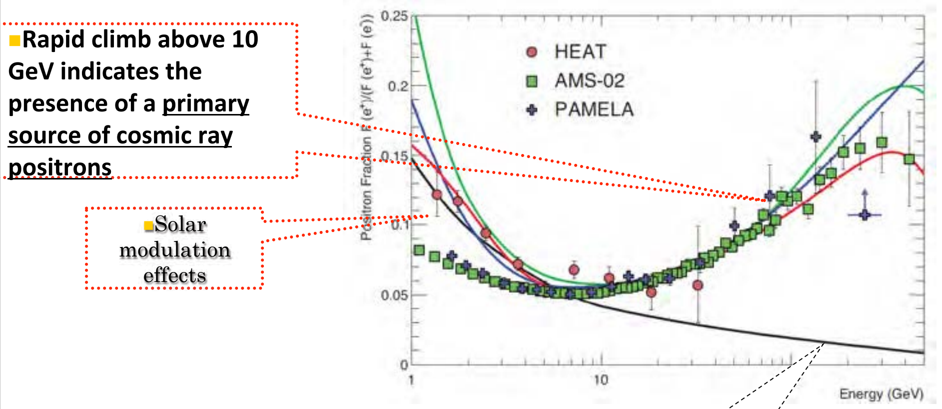

- Explanations*:
  - Dark matter;
  - Astrophysical processes
  - ??

HE positrons from nearby pulsars?

- Pulsars accelerate electrons to VHE
- Very young pulsars (<10,000 years) are typically surrounded by a pulsar wind nebula, which can produce energetic pairs

Two promising candidates:

- **Geminga** (157 pc away, 370,000 years old)
- **B0656+14** (290 pc, 110,000 years)

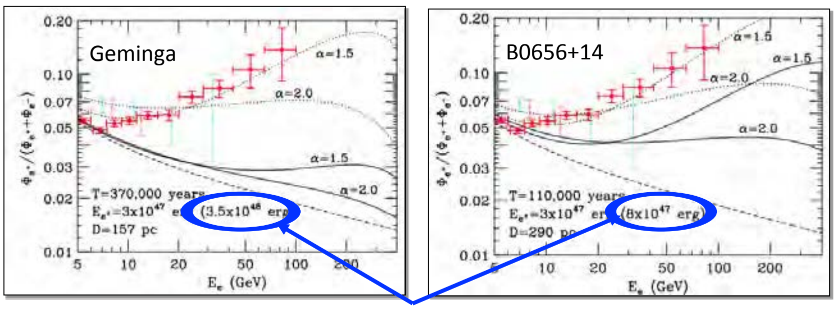

A few percent of the total spindown energy is needed in high energy e^+e^- pairs

Hooper, P. Blasi, P. Serpico, JCAP, arXiv:0810.1527

Search in the γ channel (waiting for neutrinos)

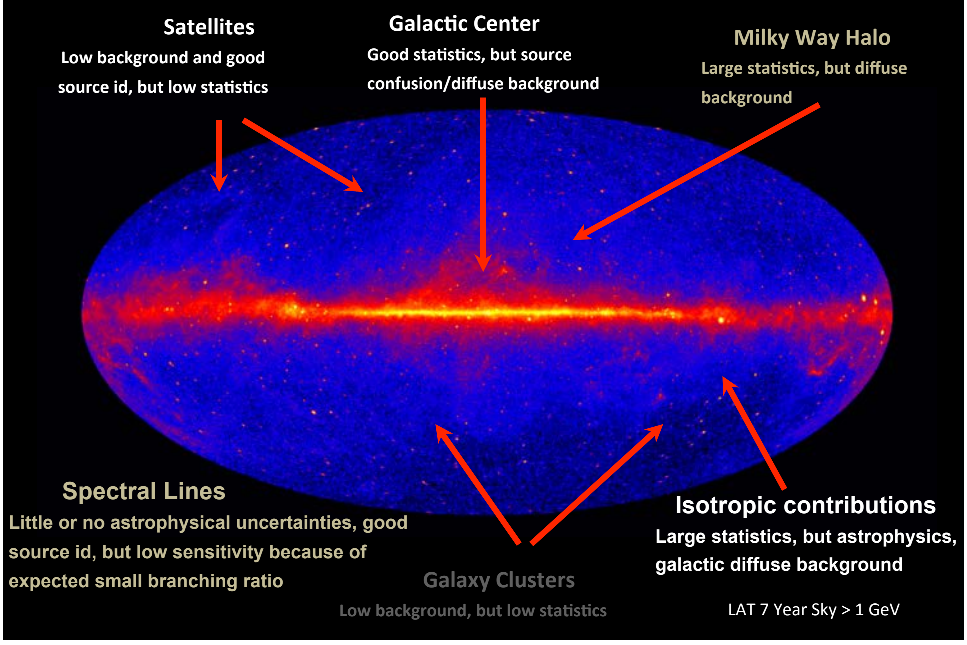

Observing the Inner Galaxy

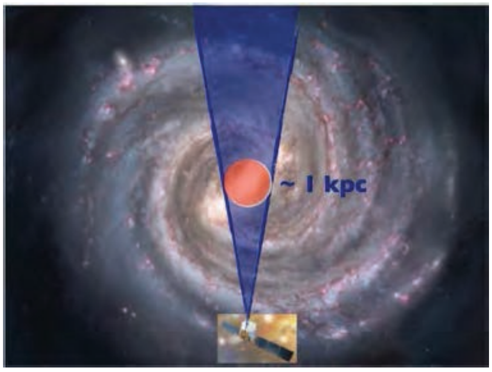

LAT Intensity: 7 years, > 1 GeV, 15°x15°

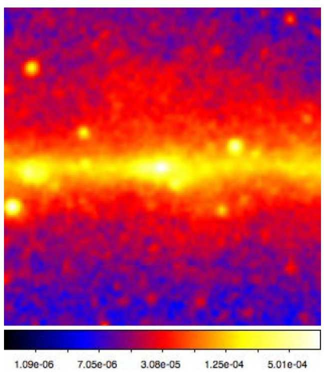

- Observations of the inner Galaxy include strong astrophysical foreground and backgrounds along the line of sight
- Because of the large astrophysical foregrounds, we must first understand the γ-ray emission from the Galaxy and from known source classes
  - In the 1-100 GeV energy band these account for ~85% of the γ-rays in a 15°x15° box around the Galactic center

Galactic Center GeV Excess

- Modeling the diffuse γ-ray emission from cosmic ray interactions with matter and radiation fields in the galaxy is challenging (see extra slides)
- Spatially extended excess around the Galactic center at a few GeV has been report in several papers

LAT Residuals (counts): 5 years, > 1.6-10 GeV, 15°x15°

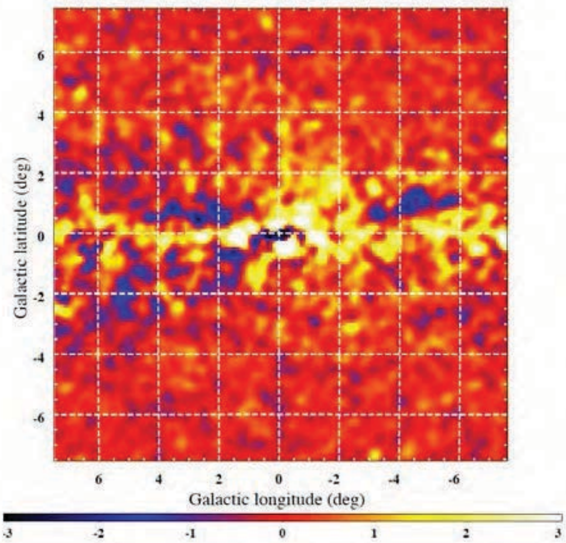

Ajello+ [LAT Clb] 2016ApJ...819...44A

Spectrum of the Galactic Center Excess

Spectral Energy Density for Galactic Center Excess Compared to Several Models

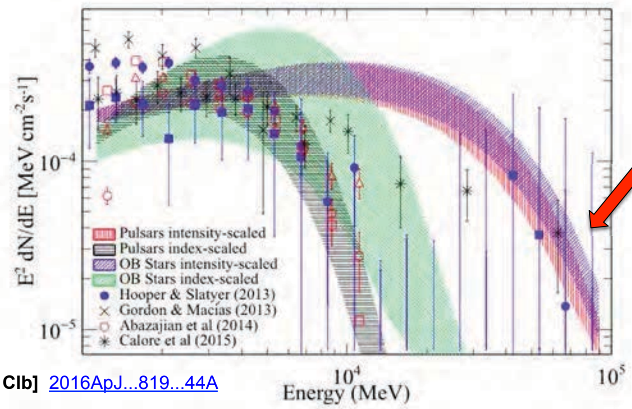

Emission above 50 GeV not from 50 GeV dark matter

Ajello+ [LAT Clb] 2016ApJ...819...44A

- The presence for an γ-ray excess with respect to the modeled diffuse emission at the Galactic center at a few GeV is well established
- However, the details (and the interpretation) of the excess depend on the modeling of the astrophysical fore/background

Radial Profile of Galactic Center Excess

Radial profile of GC Excess (at 2 GeV) Compared to Predictions From N-Body Simulations

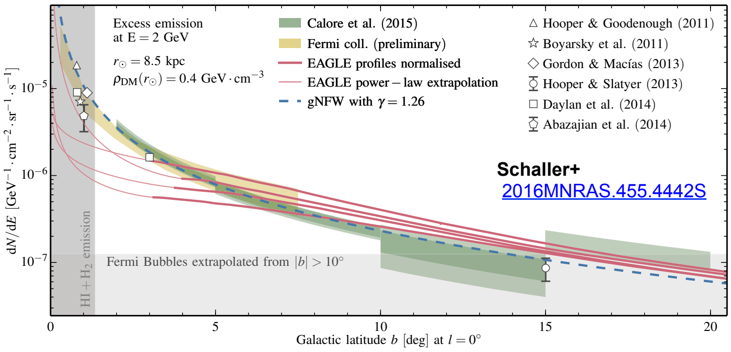

- The interpretation of the excess is unclear (similar size excesses attributed to local sources of cosmic rays are present elsewhere)
- The radial profile is of the GC excess is broadly consistent with dark matter expectations for N-body (red lines above)
  - N-body simulations of Milky-Way like galaxies tend to show less DM signal in the inner few degrees than observations of the Galactic center (grey shaded region)

Dwarf Spheroidal Satellites of the Milky Way

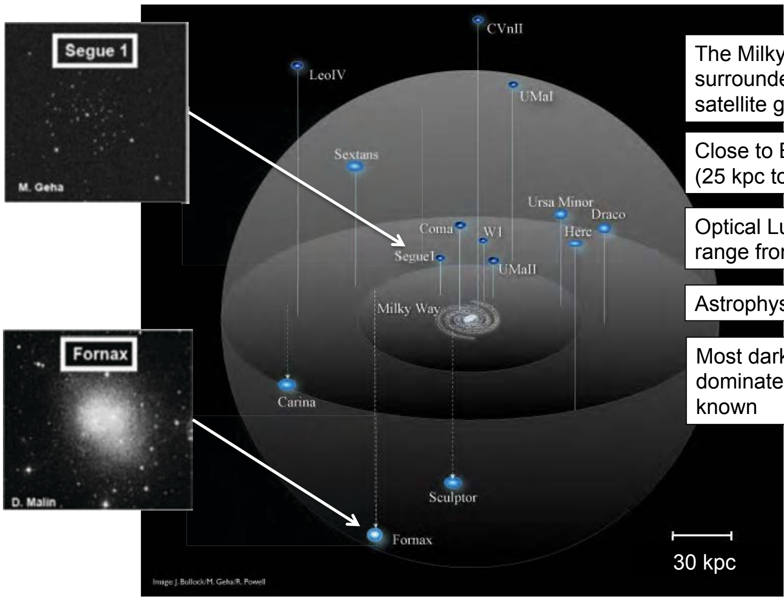

The Milky Way is surrounded by small satellite galaxies

Close to Earth (25 kpc to 250 kpc)

Optical Luminosities range from 10^3 to 10^7 $L_\odot$

Astrophysically inactive

Most dark matter dominated objects known

Dwarf Spheroidal Satellites of the Milky Way

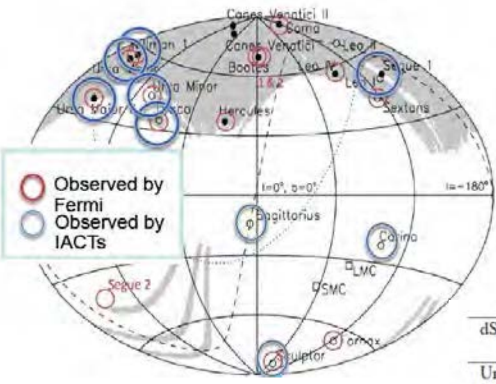

dSph	Dec. [deg]	D [kpc]	J [$\mathrm{GeV^2\,cm^{-5}}$]	Profile
Ursa Minor	+44.8	66	2.2×10^{18}	NFW
Draco	+34.7	87	7.1×10^{17}	NFW
Sculptor	−83.2	79	8.9×10^{17}	NFW
			2.7×10^{17}	ISO
Carina	−22.2	101	2.8×10^{17}	NFW
Segue 1	+16.1	23	1.7×10^{19}	Einasto
Willman 1	+51.1	38	8.4×10^{18}	NFW
Coma Berenices	+23.6	44	3.9×10^{18}	NFW

You don't expect gamma emission, unless from DM

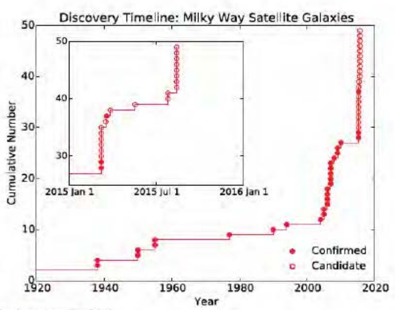

k. bechtol 2015

J-factors – K. Hayashi et al 2015

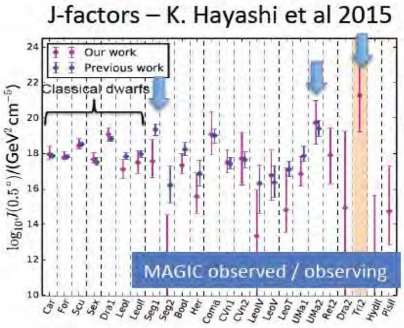

- The framework for particle dark matter particles is still very open, given the scarce guidelines from cosmology or accelerator physics
- Plans to observe Triangulum II
  Distance = 30 kparsec
  Mass/light = 3600
- Caveat: big uncertainties in J-factor estimations

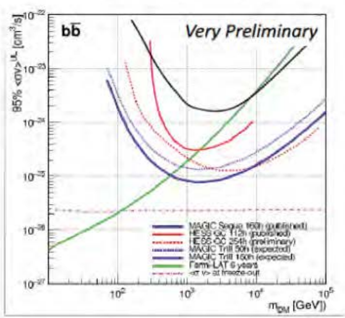

Searches for DM in satellite galaxies

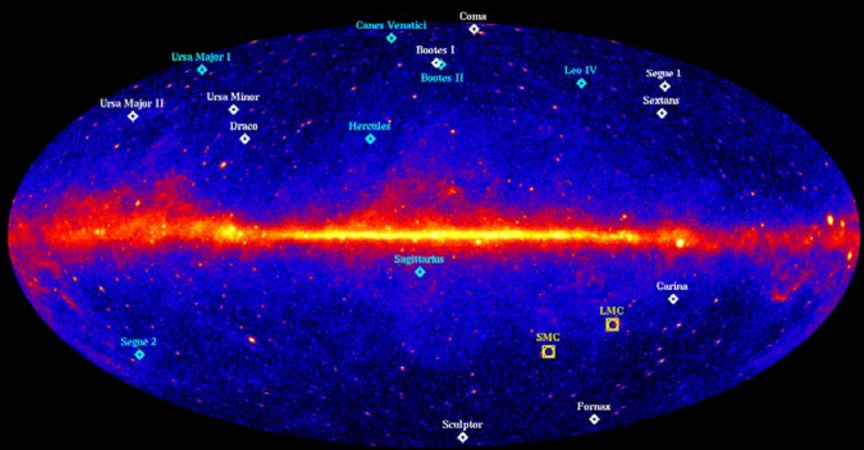

- Roughly two dozen Dwarf spheroidal (dSph) satellite galaxies of the Milky Way known up to the DES era
- Negligible astrophysical γ-ray production expected

Upper Limits from Dwarf Galaxies

$\chi\chi$ -> bb channel

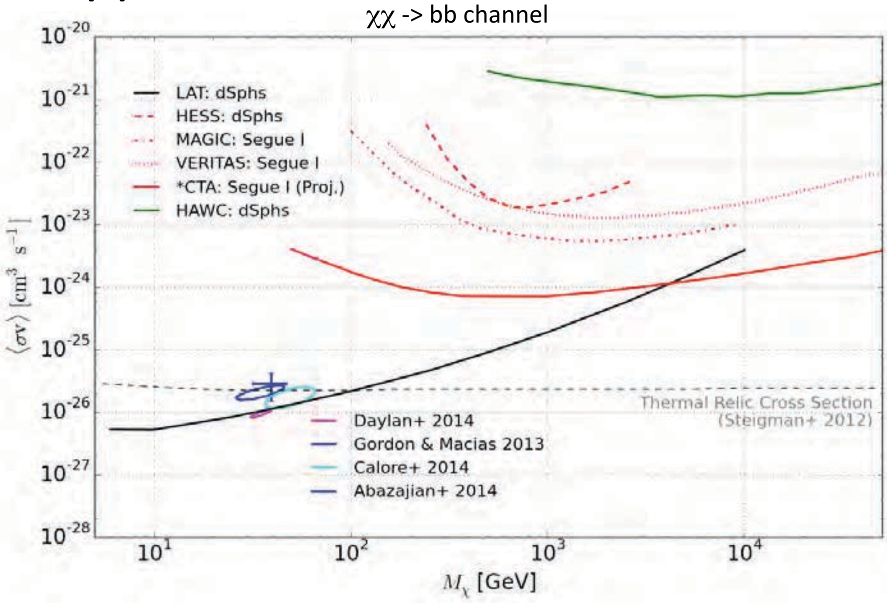

Interplay with other indirect detection methods

Comparison of LAT Projected Limits with Other Indirect-detection Limits for b-quark Channel

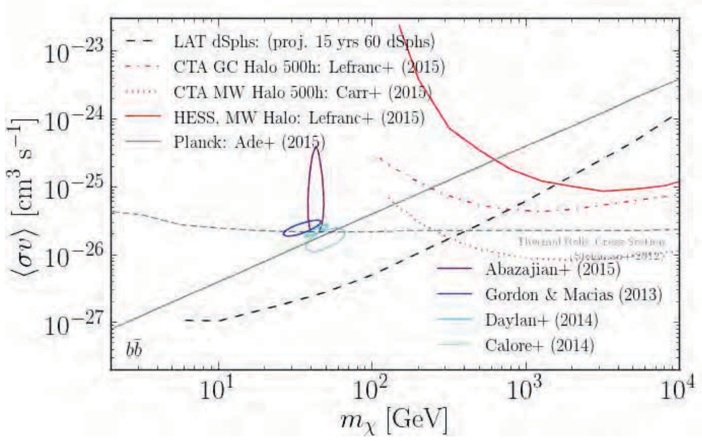

- With 15 years of data the LAT would:
  - Have the best sensitivity for indirect detection up to 800 GeV (b-quark channel)
  - Probe the thermal relic cross section up to > 400 GeV (b-quark channel)
  - Confirm or rule out a DM-interpretation of the GeV excess

Search for annihilation lines

- A few hints from time to time (recently Fermi, 130 GeV)
- Not supported by data as today (Fermi), although a feature is there

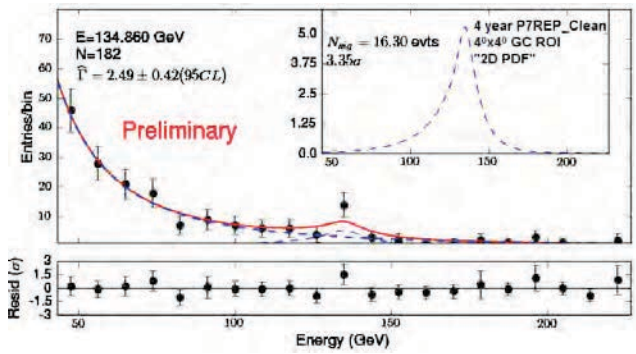

Summary of Lecture 6

- During the recent years, we discovered thousands of astrophysical gamma-ray emitters in the HE region and >200 in the VHE region
  - New emitters and new classes of emitters
  - A diffuse background up to the TeV, maybe the sum of unresolved point-like emitters
- Both the leptonic and the hadronic gamma-ray mechanisms at work
  - Identified mechanisms of emission explaining cosmic rays up to the PeV
- The SED of many emitters can be modeled in an effective way
- Although we are able to detect effectively gamma rays, the interaction with background photons in the Universe attenuates the flux of gamma rays
  - The "enemies" of VHE photons are photons near the optical region (Extragalactic Background Light, EBL)
- Interesting perspects for fundamental physics from astroparticle physics
- Dark matter:
  - A standard WIMP below 400 GeV is on reach for HE gamma detectors, if the particles was in thermal equilibrium and $\langle \sigma v \rangle$ is the same as at freeze-out
    - Dwarph spheroidals (no need for background models) and the GC region (a mess from the point of view of astronomy) are the favorite targets

  Needs a laboratory experiment to confirm

Exercises

- *Photon spectrum in hadronic cascades.* Show that in a decay $\pi^0 \to \gamma\gamma$, once boosted for the energy of the emitting π^0, the probability to emit a photon of energy E_γ is constant over the range of kinematically allowed energies.
- *$\gamma\gamma$-> e+e-*. Compute the energy threshold for the process as a function of the energy of the target photon, and compare it to the energy for which the absorption of extragalactic gamma-rays is maximal.
- *Acceleration and propagation.* The transparency of the Universe to a given particle depends critically on its nature and energy. In fact, whenever it is possible to open an inelastic channel of the interaction between the traveling particle and the CMB, its mean free path diminishes drastically. Assuming that the only relevant phenomena that rules the mean free path of the traveling particle is the CMB (CνB), estimate the order of magnitude energies at which the transparency of the Universe changes significantly, for:
  - Photons;
  - Protons;
  - Neutrinos.

Multimessenger astroparticle physics

Alessandro De Angelis, INFN/INAF Padova and LIP/IST Lisboa

Lectures 7a: Science

Anomalous propagation of photons. Axion-Like Particles. Testing relativity and cosmology with photons. VHE neutrinos.

Detection of WISPs from photon propagation

Are our AGN observations consistent with theory (1) ?

- For each AGN detected, a corresponding lower limit on the optical depth τ is calculated using a minimum EBL model
- Nonparametric test of consistency
- Disagreement with data: overall significance of 4.2 σ

=> Understand experimentally the outliers

(Horns, Meyer 2011)

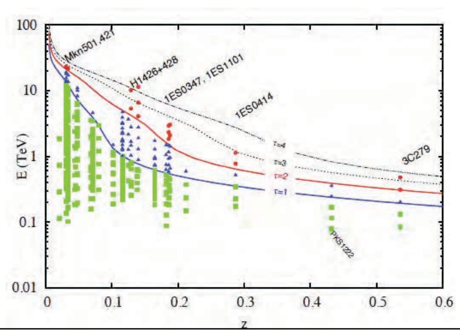

Are our AGN observations consistent with theory?

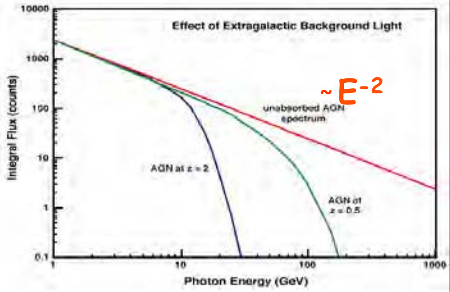

Measured spectra affected by attenuation in the EBL:

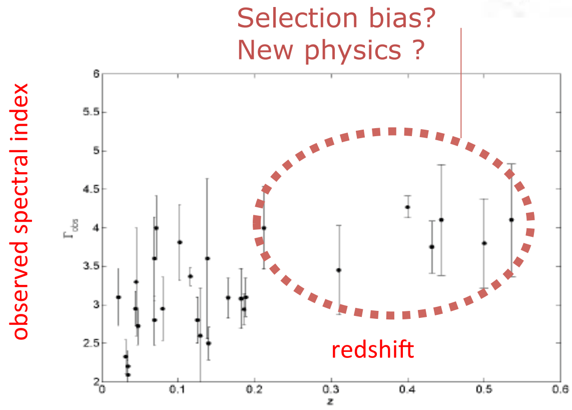

(DA, Galanti, Roncadelli; PRD 2011)

A reminder: EBL rather well constrained, and SED extrapolation from Fermi is possible

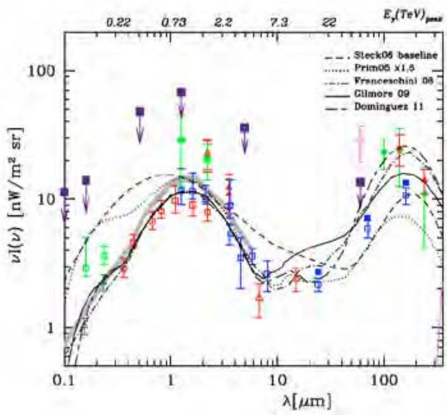

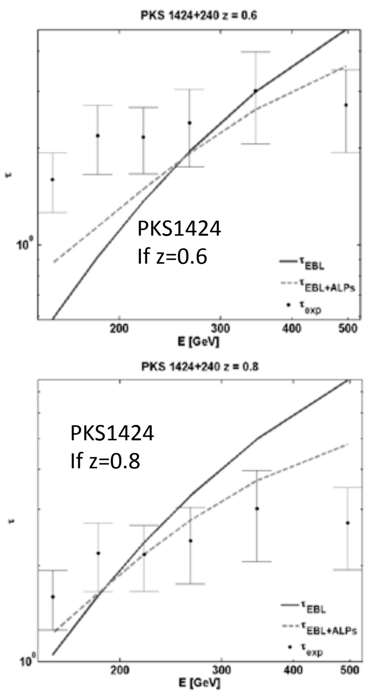

If there is a problem

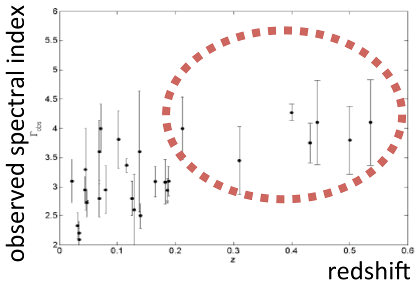

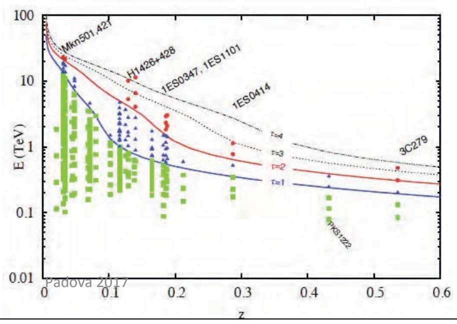

Explanations from the standard ones

- very hard emission mechanisms with intrinsic slope < 1.5 (Stecker 2008)
- Very low EBL, plus observational bias, plus a couple of "wrong" outliers

to almost standard

- γ-ray fluxes enhanced by relatively nearby production by interactions of primary cosmic rays or ν from the same source

to possible evidence for new physics

- Oscillation to a light particle coupled to the photon?

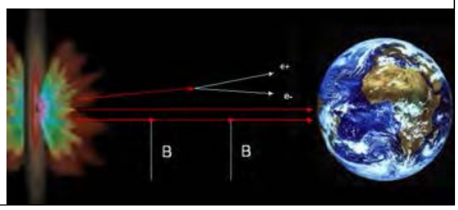

Axions and ALPs

- The "strong CP problem": CP violating terms exist in the QCD Lagrangian, but CP appears to be conserved in strong interactions
- Peccei and Quinn (1977) propose a solution: clean it up by an extra field in the Lagrangian
  - Called the "axion" from the name of a cleaning product
  - Pseudoscalar, neutral, stable on cosmological scales, feeble interaction, couples to the photon
    - Can make light shine through a wall
  - The minimal (standard) axion coupling $g \propto m$; however, one can have an "ALP" in which $g = 1/M$ is free from m
- $m_a < 0.02$ eV (direct searches)
- $g < 10^{-10}$ GeV^{-1} from astrophysical bounds
- Production is not thermal, and it might be cold (ALPs can be a DM candidate)

Padova 2017

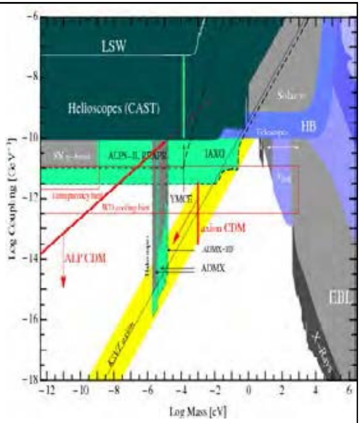

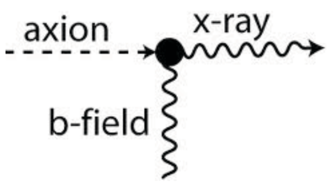

$$\frac{m}{1\,\mathrm{eV}} \simeq \frac{1}{M/6\times10^{6}\,\mathrm{GeV}}$$

The photon-axion mixing mechanism

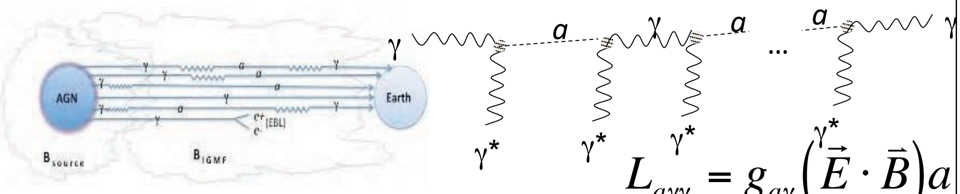

$$L_{a\gamma\gamma} = g_{a\gamma}\left(\vec{E}\cdot\vec{B}\right)a$$

- Magnetic field 1 nG < B < 1fG (AGN halos). Cells of ~ 1 Mpc

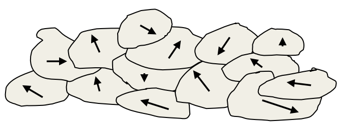

$$P_{\gamma \to a} \approx NP_1$$

$$P_1 \approx \frac{g_{a\gamma}^2 B_T^2 s^2}{4} \approx 2\times 10^{-3}\left(\frac{B_T}{1\text{nG}}\frac{s}{1\text{Mpc}}\frac{g_{a\gamma}}{10^{-10}\,\text{GeV}^{-1}}\right)^2$$

- Photons-ALP mixing could enhance the transparency of the Universe:
  - Photon/ALP mixing in the intergalactic space (DA, Roncadelli & MAnsutti [DARMA], PRD2007)
  - Conversion into axion at the source, reconversion in the Milky Way (Hooper, Simet, Serpico 2008)Axion emission (Simet+, PRD2008)
  - A combination of the above

Padova 2017

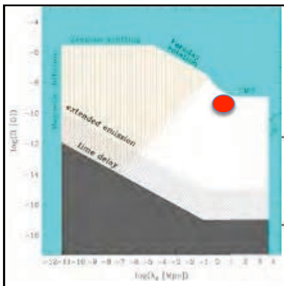

Preferred values for m, g (DARMA)

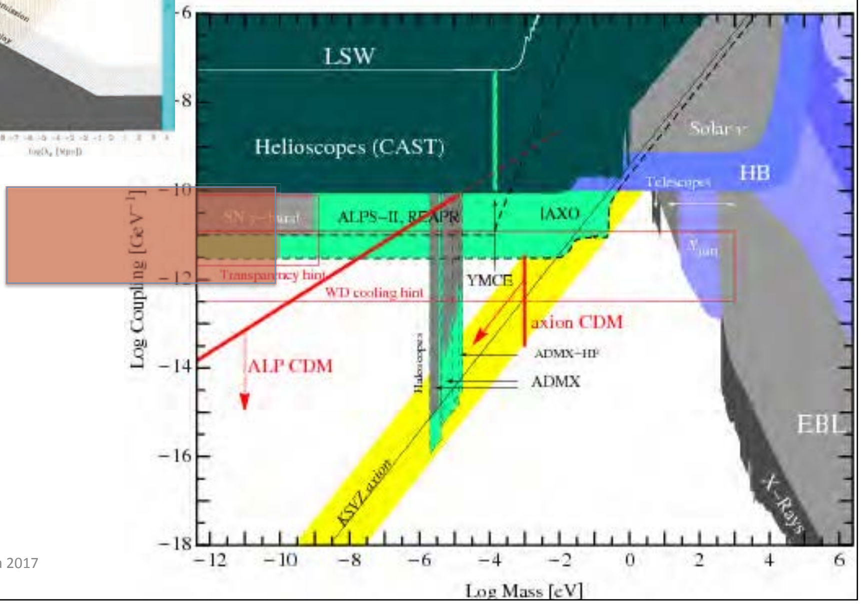

Padova 2017

VERY EXOTIC PHYSICS
(VIOLATION OF THE LORENTZ INVARIANCE+)

Is Lorentz invariance exact?

- For longtime violating Lorentz invariance/Lorentz transformations/Einstein relativity was a heresy
  - Is there an aether? (Dirac 1951)
  - Many preprints, often unpublished (=refused) in the '90s
- Then the discussion was open
  - Trans-GZK events? (AGASA collaboration 1997-8)
  - LIV => high energy threshold phenomena: photon decay, vacuum Cherenkov, GZK cutoff (Coleman & Glashow 1997-8)
  - GRB and photon dispersion (Amelino-Camelia et al. 1997)
  - Framework for the violation (Colladay & Kostelecky 1998)
  - LIV and gamma-ray horizon (Kifune 1999)
  - ...

LIV? New form of relativity?

- Von Ignatowsky 1911: {relativity, omogeneity/isotropy, linearity, reciprocity} => Lorentz transformations with "some" invariant c (Galilei relativity is the limit c $\rightarrow\infty$)
- CMB is kind of an aether: give away isotropy?
- QG motivation: give away linearity? (A new relativity with 2 invariants: "c" and E_P)
- In any case, let's sketch an effective theory…
  - Let's take a purely phenomenological point of view and encode the general form of Lorentz invariance violation (LIV) as a perturbation of the Hamiltonian (Amelino-Camelia+)

A heuristic approach: modified dispersion relations (perturbation of the Hamiltonian)

- We expect the Planck mass to be the scale of the effect

$$E_P = \sqrt{hc/G} \cong 1.2\times 10^{19}\,\text{GeV}$$

$$H^2 = m^2 + p^2 \rightarrow H^2 = m^2 + p^2\left(1+\xi\frac{E}{E_P}+\dots\right)$$

$$H \xrightarrow[p>>]{} p\left(1+\frac{m^2}{2p^2}+\xi\frac{p}{2E_P}+\dots\right)$$

$$v = \frac{\partial H}{\partial p} \cong 1 - \frac{m^2}{2p^2} + \xi\frac{p}{E_P} \Rightarrow \boxed{v_\gamma \cong 1+\xi\frac{E}{E_P}}$$

=> effect of dispersion relations at cosmological distances can be important at energies well below Planck scale:

$$\boxed{\Delta t_\gamma \cong T\Delta E\frac{\xi}{E_P}}$$

Rapid variability is the name of the game

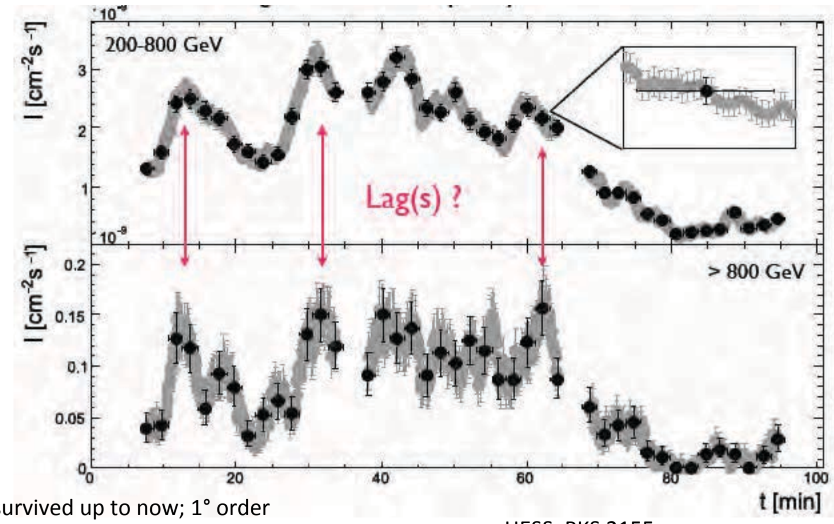

No claim survived up to now; 1° order effects unlikely

HESS, PKS 2155

Padova 2017

Apart from one positive claim (MAGIC, Mkn 501 2007)
Finally interpreted as a source effect

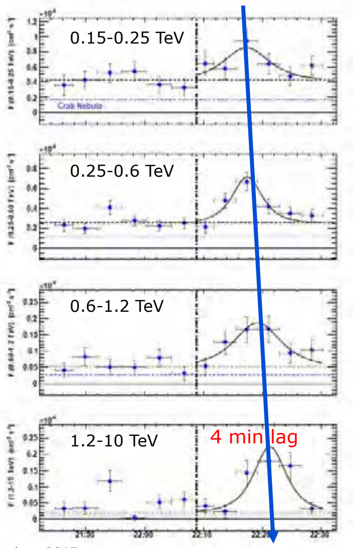

$E_{QG,1} > 7.6\ E_P$

$E_{QG,2} > 1.3\text{x}10^{11}$ GeV

Mostly based on one GRB from Fermi

2nd order? Cherenkov rules!

$$(\Delta t)_{obs} \cong \frac{3}{2}\left(\frac{\Delta E}{E_{s2}}\right)^2 H_0^{-1}\int_0^z dz' \frac{(1+z')^2}{\sqrt{\Omega_M(1+z')^3+\Omega_\Lambda}}$$

$E_{s2} > 10^{11}$ GeV (~10^{-9} M_P) (HESS, MAGIC, Fermi)

Padova 2017

Kifune 1999: modified GRH due to LIV (increases or decreases depending on the sign of ξ)

LIV provides effective mass to photons → $m_\gamma^2 = \xi \dfrac{E_\gamma^{2+\alpha}}{E_{LIV}^{\alpha}}$

Protheroe&Meyer, Phys.Lett.B 93 (2000)

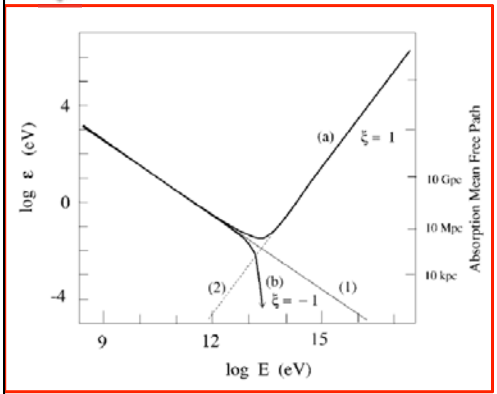

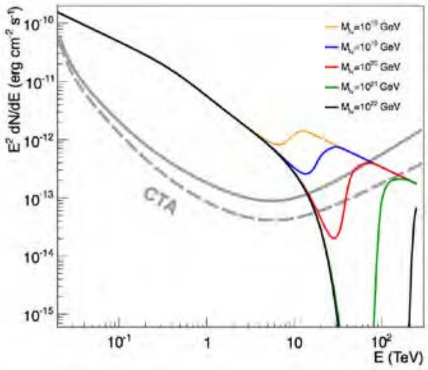

Fairbairn et al, arXiv:1401.8178 (2014)

But: factorization questioned (Liberati, Sonego, …)

A win-win game: if no anomalous physics, determination of cosmological parameters

- Fluxes of VHE photons reaching the Earth have been attenuated due to the EBL density from observed spectra

⇒ Determine cosmological constants from observed HE spectra vs. fitted from lower energy

(Blanch & Martinez 2005; Dominguez & Prada 2013)

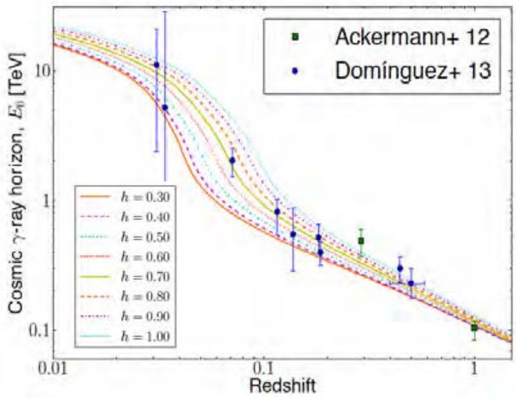

Cosmology

$$\tau(E,z) = \int_0^z \left(\frac{dl}{dz'}\right) dz' \int_0^2 d\mu \frac{\mu}{2} \int_{\varepsilon_{th}}^{\infty} d\varepsilon' \, \sigma_{\gamma\gamma}(\beta') n(\varepsilon', z')$$

$$\left|\frac{dt}{dz'}\right| = \frac{1}{H_0(1+z')E(z')}$$

$$E(z') \equiv \sqrt{\Omega_m (1+z')^3 + \Omega_\Lambda}$$

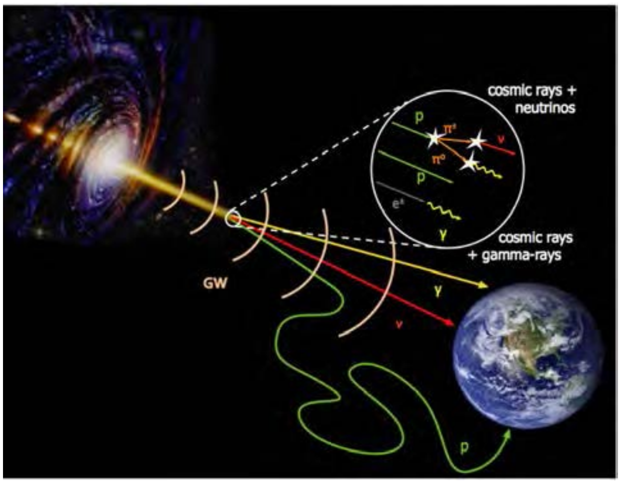

MULTIMESSENGER ASTROPHYSICS (Neutrinos and gravitational waves)

Why Neutrino Astronomy?

- Neutrino Astronomy is a quite recent and very promising experimental field.

Photon and proton mean free range path

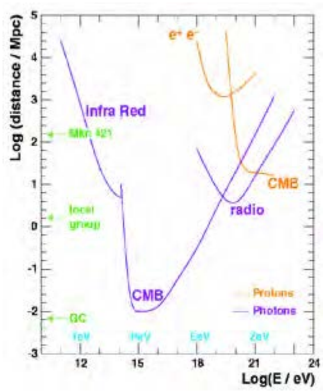

- Advantages:
  - Photons: interact with CMB and matter (r~10 kpc @100 TeV)
  - Protons: interact with CMB (r~10 Mpc @10^{11} GeV) and undergo magnetic fields ($\Delta\theta$>1º, E<$5\cdot10^{10}$ GeV)
  - Neutrons: are not stable (r~10 kpc @10^{9} GeV)
- Drawback: large detectors (~GTon) needed.

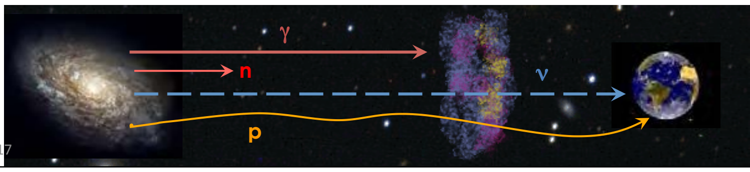

γ and ν in cosmic accelerators:

Hadronic mechanisms produce both

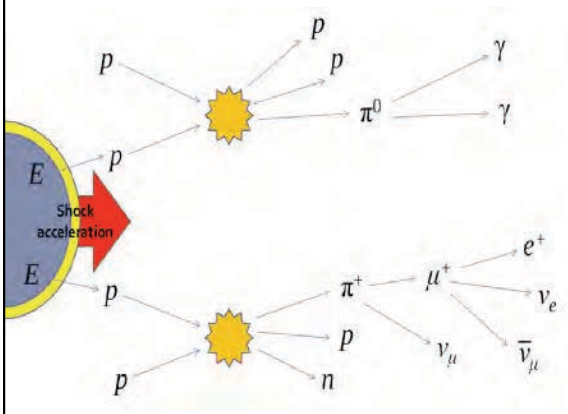

Neutral mesons decay in **photons**:
$\pi^0 \rightarrow \gamma\gamma$
charged mesons decay in **neutrinos**:
$\pi^+ \rightarrow \nu_\mu + \mu+$
$\mu^+ \rightarrow \nu_\mu + \nu_e + e^+$
$\pi^- \rightarrow \nu_\mu + \mu^-$
$\mu^- \rightarrow \nu_\mu + \nu_e + e^-$

#ν ~ 3#γ

Padova 2017

Astrophysical Sources: same as for gamma-rays

- Galactic sources: these are near objects (few kpc) so the luminosity requirements are much lower.
  - Supernova remnants
  - Micro-quasars
  - …
- Extra-galactic sources: Most powerful sources in the Universe
  - AGNs
  - GRBs

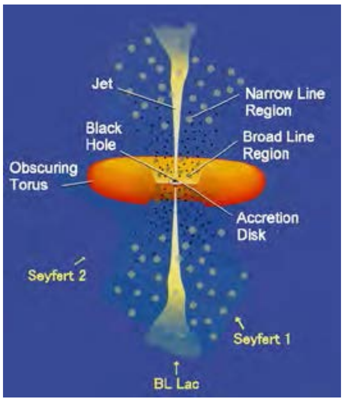

- Active Galactic Nuclei includes Seyferts, quasars, radio galaxies and blazars.
- Standard model: a super-massive (10^6-10^8 M_o) black hole towards which large amounts of matter are accreted.

Padova 2017

Need large volumes
Fight against background from atmospheric ν/μ
High energies (ν cross section)

- Atmospheric muons dominate by many order of magnitude the neutrino-induced muons.
- Upward-going particles are the best candidates for extraterrestrial ν .

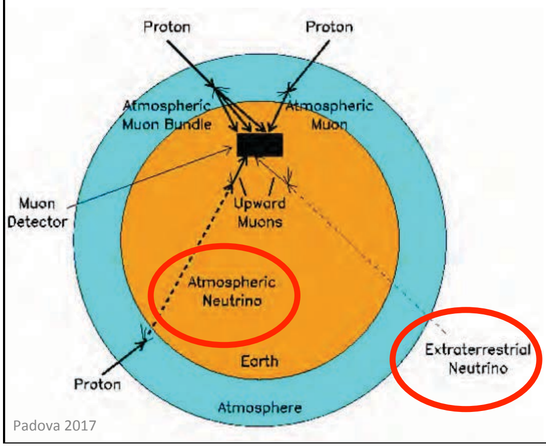

Atmospheric neutrinos represent the irreducible background for νT

Upward-going muons (or horizontal muons) ARE neutrino-induced!

But don't go much beyond 1 PeV, or Earth will become opaque

Padova 2017

A source candidate: RX J1713.7-3946

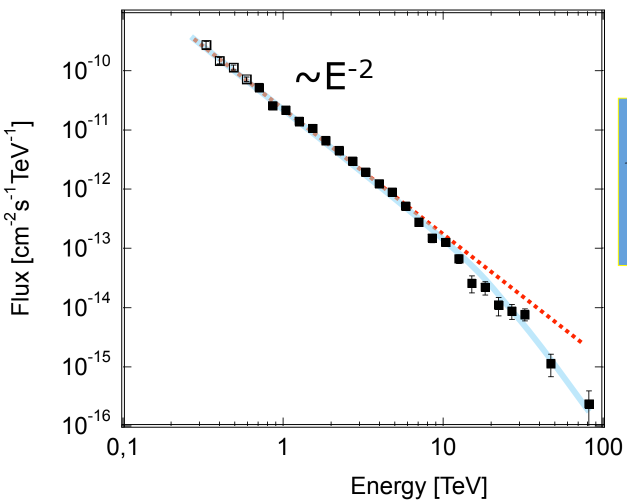

RX J1713.7-3946 seen by HESS (gamma rays)

$$E^2_{\nu,\gamma}\frac{d\Phi_{\nu,\gamma}}{dE_{\nu,\gamma}} = 10^{-11}\ \text{TeV cm}^{-2}s^{-1}$$

Padova 2017

Diffuse flux of cosmic ν

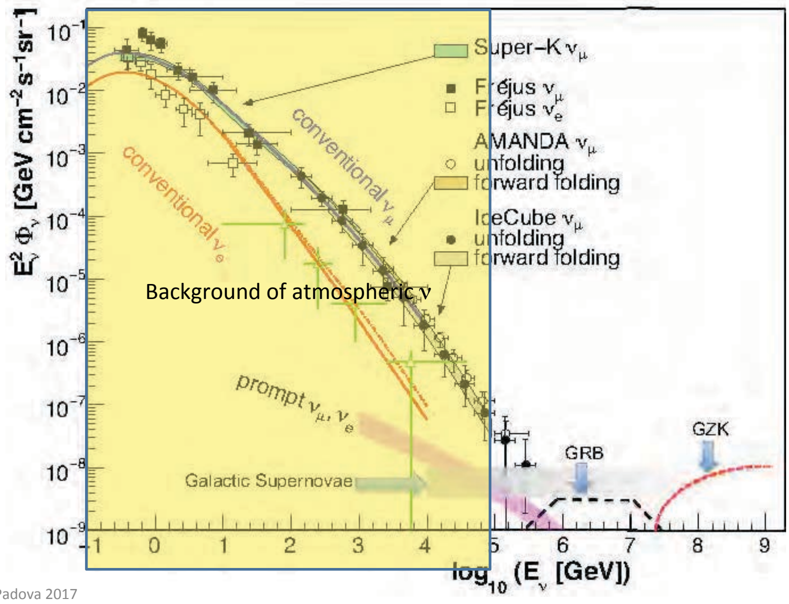

Padova 2017

Excess of HE events over the background (IceCube 2014)

- Atmospheric muons
- Atmospheric neutrinos

=> Yes, astrophysical neutrinos exist

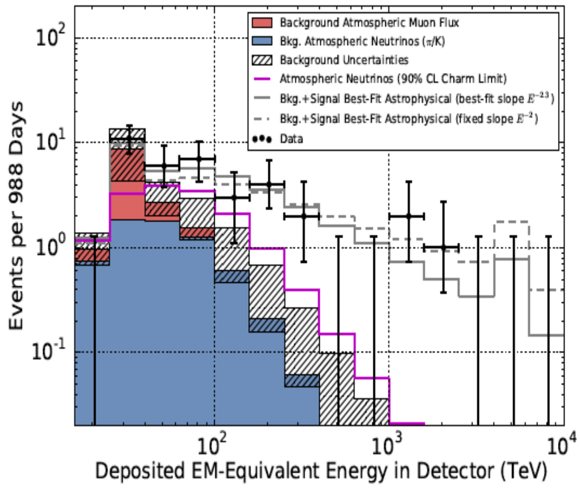

Excess of 22 events in 3 years from 30 TeV to 2 PeV (total of 37) with significance of 5.7σ;
3 events above 1 PeV

But their correlation with known or unknown sources is not significant

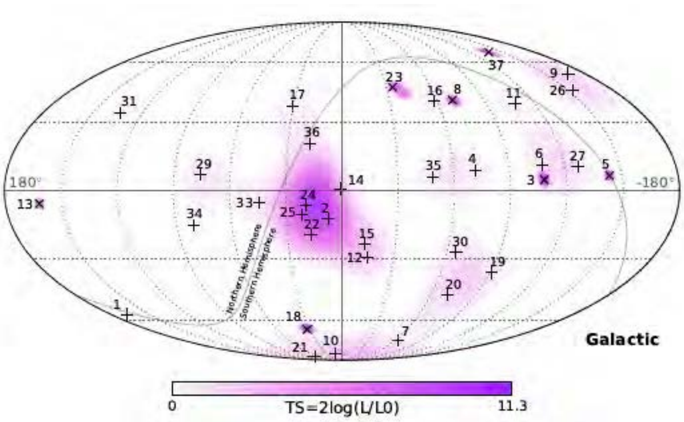

Gravitational waves

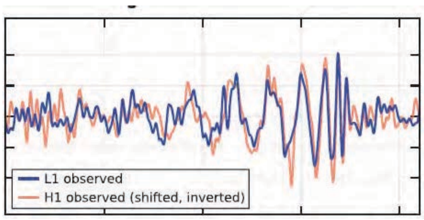

- A science experimentally started just now
- GW should be produced in binary mergers
  - Short GRBs?
  - Gammas delayed by ~ 1s?

- See next lecture

Summary of Lecture 7a

- Interesting perspects for fundamental physics from astroparticle physics
- Dark matter:
  - A standard WIMP below 400 GeV is on reach for HE gamma detectors, if the particles was in thermal equilibrium and <σ v> is the same as at freeze-out
    - Dwarph spheroidals (no need for background models) and the GC region (a mess from the point of view of astronomy) are the favorite targets

    Needs a laboratory experiment to confirm
  - Can find indirect evidence for ALPs, but then <u>badly</u> needs a laboratory experiment to confirm
- Tests of fundamental physics/LIV: linear models appear disfavored, and our sensitivity at 2° order is far from the Planck scale (but we can do cosmology)
- Multimessenger astrophysics (just starting) will teach us more…
  - Protons cannot be used for astronomy (but they give os O(100 TeV) c.m. energies
  - We just detected astrophysical neutrinos (<~8/year with 1km^3 detector), and we know that probably a several-km^3 detector is needed do to astronomy
  - Gravitational waves: maybe the answer is just around the corner

Exercises

1. *Neutrinos from SN1987A.* Neutrinos from SN1987A, at an energy of about 50 MeV, arrived in a bunch lasting 13 s from a distance of 50 kpc, 3 h before the optical detection of the supernova.What can you say on the neutrino mass? What can you say about the neutrino speed (be careful...)?
2. *Time lag in light propagation.* Suppose that the speed *c* of light depends on its energy E in such a way that

$$c(E) \simeq c_0\left(1+\xi\frac{E^2}{E_P^2}\right)$$

where E_P is the Planck energy (second-order Lorentz Invariance Violation). Compute the time lag between two VHE photons as a function of the energy difference and of the redshift *z*.

Gravitational waves searches

Claudia Lazzaro - Virgo group
Seminar 12 April 2017
Experimental astroparticle physics

Gravitational waves and General Relativity

- ✗ Gravity is a manifestation of curvature of space-time produced by matter-energy
- ✗ Linearized Einstein equations admit wave solutions, as perturbations to a background geometry. $g_{\nu\mu}=\eta_{\nu\mu}+h_{\nu\mu}$ $\quad h_{\nu\mu}\ll 1$

- ✗ Any rapidly moving mass generates fluctuations in spacetime curvature which propagate at the speed of light.

Gravitational waves

- ✗ Propagate with speed of light,
- ✗ Transverse, traceless
- ✗ Have two independent polarizations states "+" and "x"
- ✗ Can be detected by their effect on the relative motion of test masses (stress and compress spacetime in two directions)

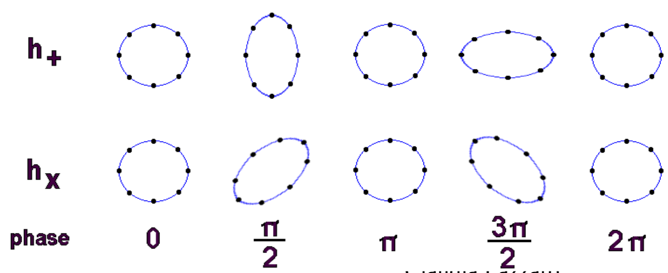

$$\frac{\Delta L}{L}\sim h$$

GW existence: Hulse and Taylor binary

GW emission has been indirectly demonstrated through the radiative energy loss of PSR191316

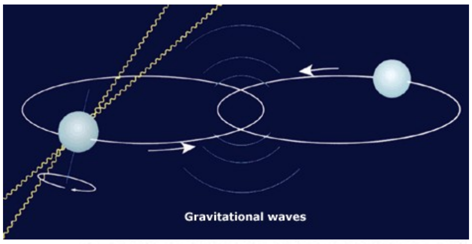

- ✗ Pulsar bound to a “dark companion”, 7kpc from Earth. (vmax/c ~10--3)
- ✗ GR predicts such a system to lose energy via GW emission: orbital period decrease
- ✗ Prediction of general relativity verified at 0.2% level

Symbol	Name	Value
m_1	primary mass	$1.441 M_\odot$
m_2	secondary mass	$1.387 M_\odot$
P_{orb}	orbital period	7.751939106 hr
a	semi-major axis	1.9501×10^9 m
e	eccentricity	0.617131
D	distance	21,000 lyr

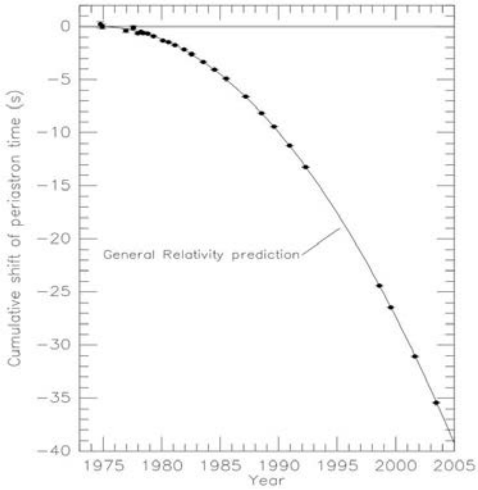

Claudia Lazzaro

GW amplitude

Mass quadrupole $Q_{\mu\nu}$

Radiated power $P=\frac{G}{5c^2}\dddot{Q}_{\mu\nu}\dddot{Q}^{\mu\nu}$

Amplitude $h_{\mu\nu}=\frac{2G}{c^4}\frac{1}{r}\ddot{Q}_{\mu\nu}$

$Q_{\mu\nu}!=0$

Efficient sources of GW must be asymmetric, compact and fast

GW detectors are sensitive to amplitude

h: 1/r attenuation

Possible GW source:

Transient signal from core collapse supernovae:

$$h \sim 6 \times 10^{-21} \left(\frac{E}{10^{-7}\,\mathrm{M_\odot} c^2}\right)^{\frac{1}{2}} \left(\frac{1\,\mathrm{ms}}{T}\right) \left(\frac{1\,\mathrm{kHz}}{f}\right) \left(\frac{10\,\mathrm{kpc}}{r}\right)$$

Continuous waves from non asymmetric spinning neutron stars

$$h_0 = \frac{4\pi^2 G I_{zz} f_{GW}^2}{c^4 r}\epsilon = (1.1 \times 10^{-24}) \left(\frac{I_{zz}}{I_0}\right) \left(\frac{f_{GW}}{1\,\mathrm{kHz}}\right)^2 \left(\frac{1\,\mathrm{kpc}}{r}\right) \left(\frac{\epsilon}{10^{-6}}\right) \qquad \epsilon \equiv \frac{I_{xx} - I_{yy}}{I_{zz}}$$

Even in optimistic case: $h \leqslant 10^{-20}$

Need to measure: $\Delta L \sim 10^{-18}$ m

Claudia Lazzaro

Michelson e Morley interferometers

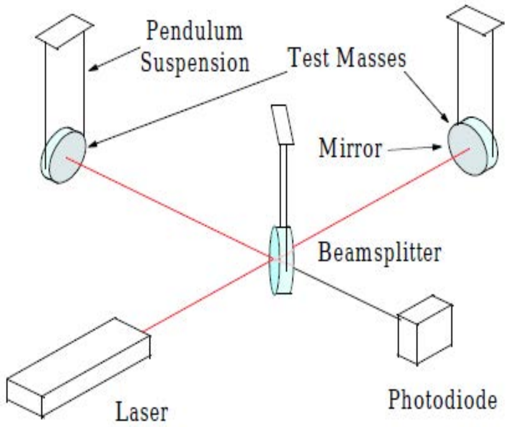

- ✗ Suspended mirrors act as “test-particles” (in “free-fall”)
- ✗ Sensitivity increases with L, then arms have kilometric scales length
- ✗ Laser beam is separated at the beamsplitter, in perpendicular directions. The light reflected on the mirrors returns backs and is collected to the photodetector
- ✗ Interferometer works in the dark fringe

$$\Delta\phi = 4\pi \frac{L h_+}{\lambda_{Laser}} \frac{\sin\left(\frac{\omega_{GW} L}{c}\right)}{\frac{\omega_{GW} L}{c}}$$

- ✗ Cut-off frequency $\Omega_{GW} L \sim \frac{\pi}{2} \Rightarrow L < \frac{\lambda_{\Omega_{GW}}}{4}$
- ✗ Broad-band response ~10 Hz to few kHz

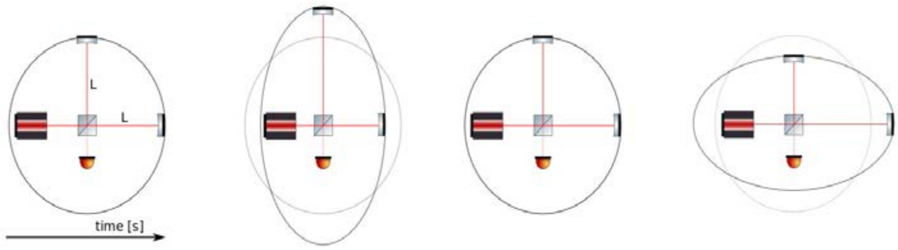

Interferometer response to h_+ . Anisotropic response and polarization sensitivity

Interferometers

Improving the sensitivity: Increase length of the interferometer arms, increase incident light power

Reaching h~10-22 would requires, kilometric arms scale and kilowatts of laser power

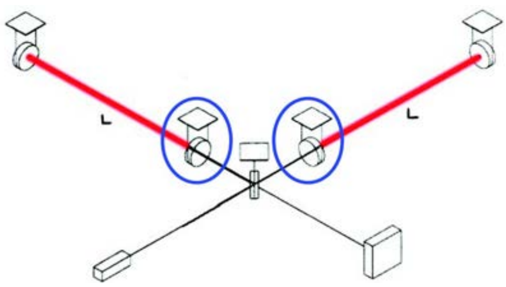

Fabry-Perot cavities

Effective light path length increased

Gain factor for Advanced Virgo ~300

Power recycling

$$P_{eff} = P_i * Recycling\ factor$$

Add recycling mirror between the input laser and the beamsplitter IFO, highly reflecting mirrors

gain~40 for Advanced Virgo

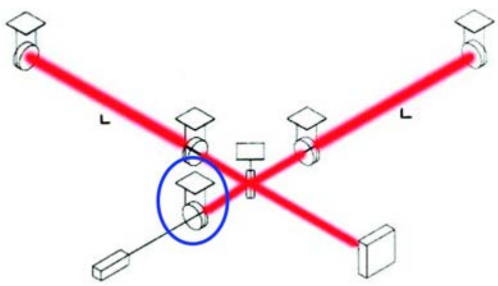

Additional improvement: Signal recycling mirror to be added in front of the dark port

Interferometers: optical layout

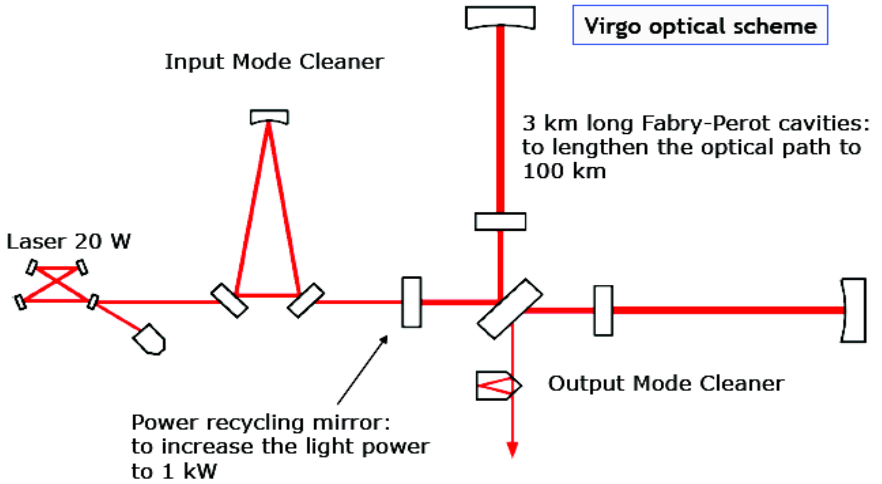

Operation conditions (Locking conditions):

- Keep the FP Cavities In resonance (Maximize the phase response);
- keep the PR cavity in resonance (Minimize the shot noise);
- Keep the output on the "dark fringe" (Reduce the dependence on power fluctuations)

-Keep the arm length constant within 10-15 m

Claudia Lazzaro

AdvVirgo interferometer

Arms:

3km length

Vaccum volume 7000 m^3 , 10^{-9} mbar

Claudia Lazzaro

AdvVirgo interferometer

Arms:
3km length
Vaccum volume 7000 m^3 , 10^{-9} mbar

Suspension
Super-seismic isolation (from initial Virgo)
Reduction 10^{-12} vibrations

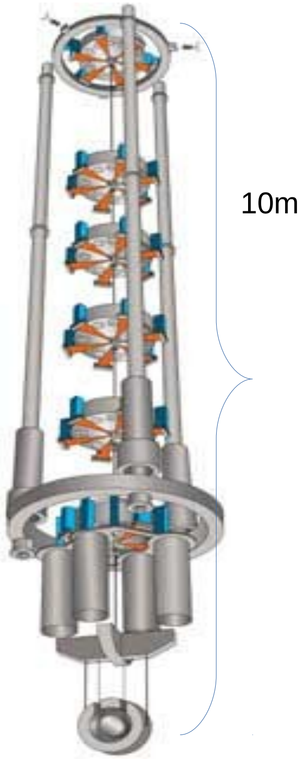

Claudia Lazzaro

AdvVirgo interferometer

Arms:
3km length
Vaccum volume 7000 m^3 , 10^{-9} mbar

Suspension
Super-seismic isolation (from initial Virgo)
Reduction 10^{-12} vibrations

Mirrors
- ✗ 42 kg, 35 cm diam., 20 cm thick
- ✗ Flatness < 0.5 nm rms
- ✗ Roughness < 0.1 nm rm
- ✗ Absorption < 0.5 ppm
- ✗ Low mechanical losses, Low optical absorption

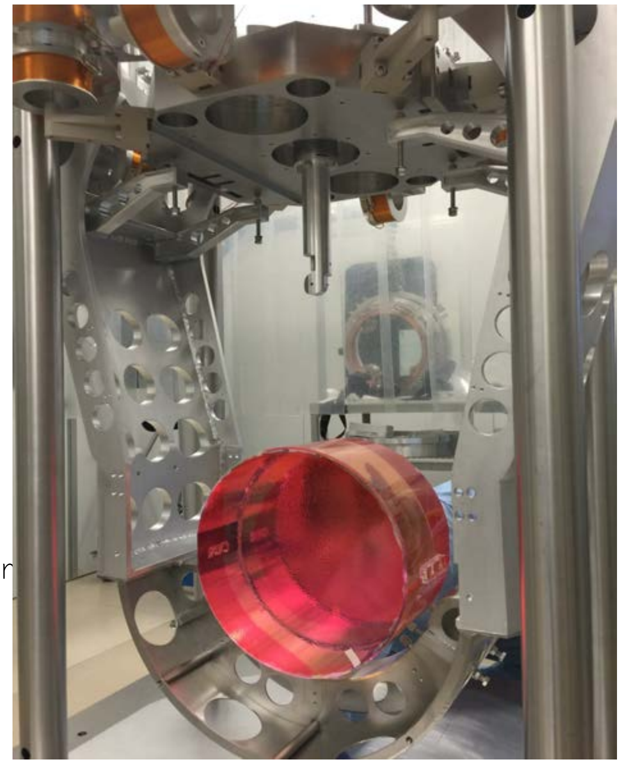

Claudia Lazzaro

Ground based interferometers: main noise source

IFO sensitivity: power spectrum density (PSD, unit: 1/√Hz)

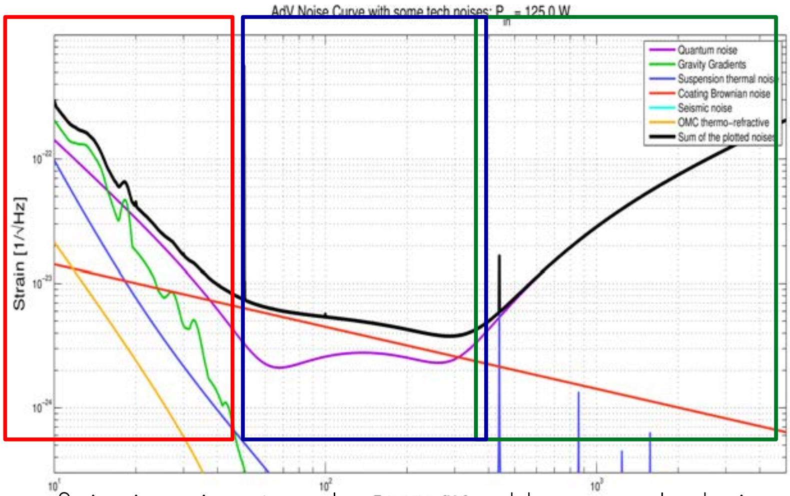

Fundamental Noise Sources:

- ✗ Seismic noise
- ✗ Newtonian noise/Gravity gradients
- ✗ Radiation pressure noise

- ✗ Thermal noise
- ✗ Mirror coatings
- ✗ Mirror substrates

- ✗ Quantum shot noise

- ✗ Seismic noise strongly suppressed by properly designed suspension systems).
- ✗ The two main thermal noise sources: wires suspending mirrors and mirrors themselves (mainly optical coatings on mirrors surface)
- ✗ Photon shot noise is due to the quantum nature of the light; it arise from statistical fluctuations in the number of detected photons.

Network of interferometers

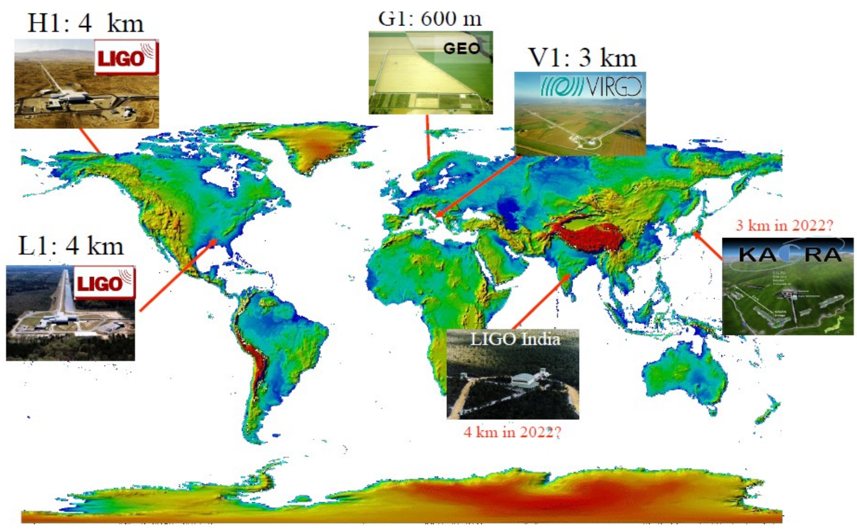

<u>Data taking:</u>
-LIGO Hanford (H1)
-LIGO Livingston
<u>Upcoming:</u>
-Virgo
<u>Future:</u>
-Kagra (2021)
-Ligo India (2022)

Advantages of multiple interferometer:

- ✗ Simultaneous detection, improve background rejection and detection confidence
- ✗ Duty cycle
- ✗ Enhanced network sky coverage, source parameter estimation(position and polarization)

Detector response to GW signal

Interferometer has non-uniform response in the sky

Direction to the source θ,ϕ and polarization angle Ψ define relative orientation of the detector and wave frames.

$$F_{+}=\frac{1}{2}(1+\cos^{2}\theta)\cos 2\phi\cos 2\psi-\cos\theta\cos 2\phi\cos 2\psi$$

$$F_{x}=\frac{1}{2}(1+\cos^{2}\theta)\cos 2\phi\sin 2\psi+\cos\theta\cos 2\phi\cos 2\psi$$

$$h(t)=F_{+}(\theta,\phi,\psi)h_{+}+F_{x}(\theta,\phi,\psi)h_{x}$$

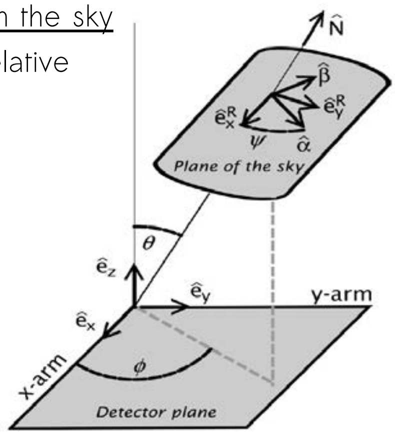

Astro-ph arXiv:1102.5421v2

F+ and F× antenna pattern depend on the source position in the sky and the interferometer plane:

- ✗ Maximal when perpendicular to this plane
- ✗ Blind region in the sky

Detector data: $x(t)=h(t)+n(t)$

Interferometer response to GW signal

noise

Amplitude GW wave

$$h^{2}=\int h_{+}^{2}+h_{x}^{2}$$

Claudia Lazzaro

Interferometers network response to GW signal

Multiple detector allows, improves:

- ✗ network sky coverage
- ✗ Source parameter estimation, polarization resolution

Network data allows coherent (not only coincident) analysis

Network response:

$$\begin{bmatrix} x_1 \\ x_2 \\ \vdots \\ x_N \end{bmatrix} = \begin{bmatrix} F_1^{+} & F_1^{\times} \\ F_2^{+} & F_2^{\times} \\ \vdots & \vdots \\ F_N^{+} & F_N^{\times} \end{bmatrix} \begin{bmatrix} h_{+} \\ h_{\times} \end{bmatrix} + \begin{bmatrix} n_1 \\ n_2 \\ \vdots \\ n_N \end{bmatrix}$$

Localization of the source position:

- ✗ Triangulation: measure time of flight with 2 or more detector sites and reconstruct ToF rings
- ✗ degeneracy along the rings can be reduce by using variability of antenna pattern

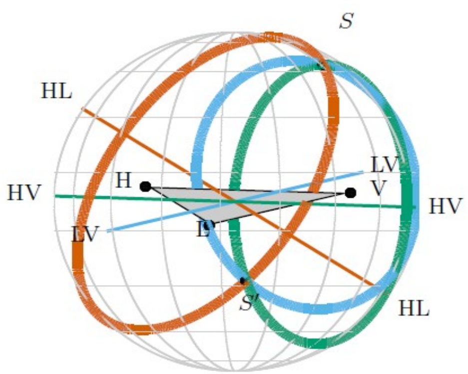

Claudia Lazzaro

Interferometers network response to GW signal

How describe the coverage capability of the network:

- ✗ Network sensitivity $S_{net}=\left(\sum_k S_k^{-1}\right)^{-1}$
- ✗ Network acceptance $F=\sqrt{|F_+^2|+|F_x^2|}S_{net}$
- ✗ Network alignment $A=|f_x|/f_+$

Mean F

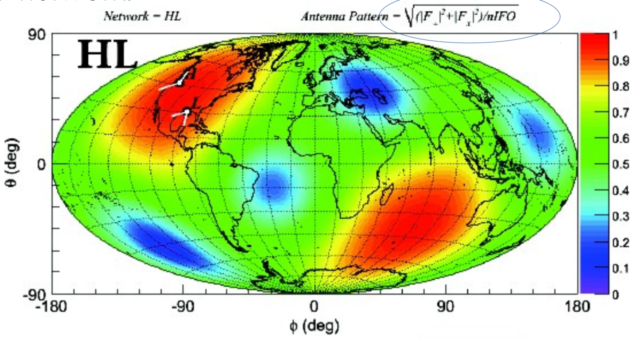

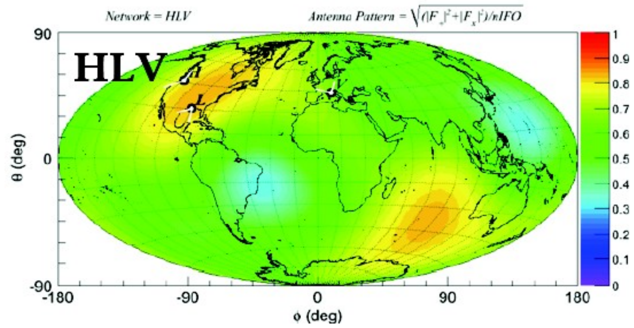

- ✗ multiple detectors improve coverage of the sky (acceptance & alignment) and strain sensitivity
- ✗ Even sensitive detectors, depending on source position, can act as spectator and not really participate in the measurement of event reconstruction
- ✗ Detectors with low sensitivity gives smaller contribution to the network SNR

NB: Hanford and Livigston are almost co-aligned

Interferometers network response to GW signal

...even 3 interferometers are not enough

LIGO H1+LIGO L1

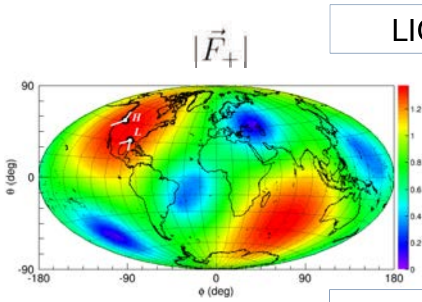

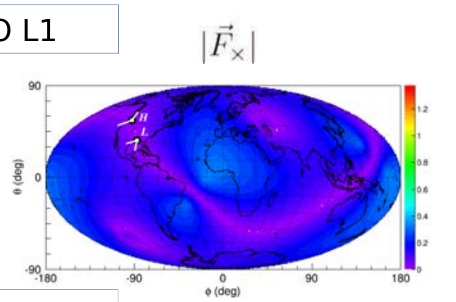

LIGO H1+LIGO L1+**Virgo**

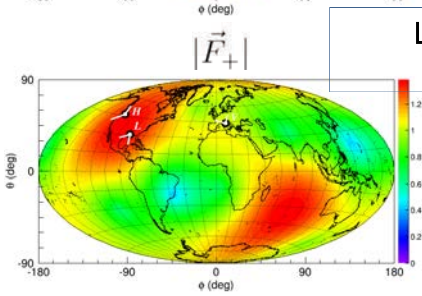

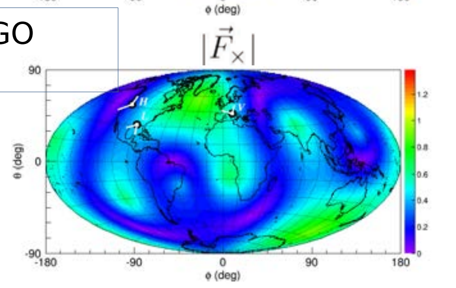

Astrophysical sources

Transient signals

Coalescing Compact Binary Systems (Neutron Star-NS, Black Hole-NS, BH-BH): Strong emitters, well modeled

Well known signals
Template search

Asymmetric Core Collapse Supernovae weak emitters, not well-modeled ('bursts'), transient
Cosmic strings, soft gamma repeaters,
pulsar glitches

Not known signals
burst search

Cosmological stochastic background (residue of the Big Bang, cosmic GW background, long duration)
Astrophysical stochastic background

Continuous signals

Spinning neutron stars (monotonic waveform, long/continuous duration)

known signals

Claudia Lazzaro

Astrophysical sources

Transient signals

Coalescing Compact Binary Systems (Neutron Star-NS, Black Hole-NS, BH-BH): Strong emitters, well modeled

Well known signals
Template search

Asymmetric Core Collapse Supernovae weak emitters, not well-modeled ('bursts'), transient
Cosmic strings, soft gamma repeaters,
pulsar glitches

Not known signals
burst search

Cosmological stochastic background (residue of the Big Bang, cosmic GW background, long duration)
Astrophysical stochastic background

Continuous signals

Spinning neutron stars (monotonic waveform, long/continuous duration)

known signals

Claudia Lazzaro

CBC search

Burst search

Stocastic search

Continuous search

CBC source

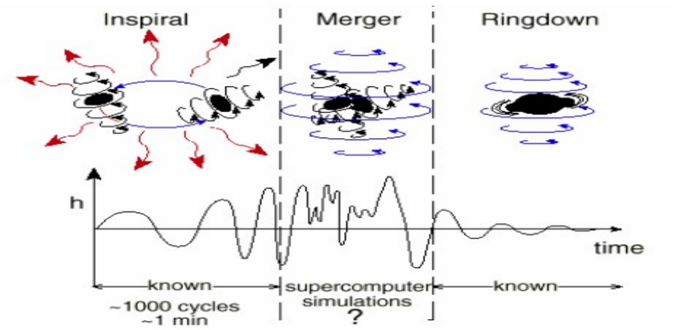

GW signal:

- ✗ Inspiral
- ✗ Merge
- ✗ ringdown

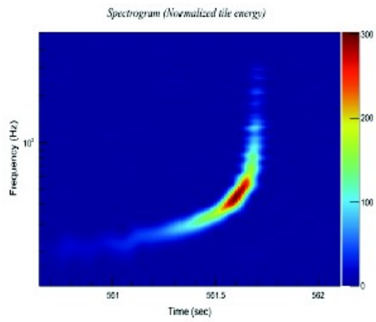

Till the ISCO (inner most circle orbital) characteristic frequency evolution in time: chirp signal

$$M_{chirp} = \frac{m_1 m_2^{3/5}}{m_1 + m_2^{1/5}} \qquad \dot{f}_{GW} = \frac{96}{5}\pi^{8/3}\left(\frac{GM_c}{c^3}\right)^{5/3} f_{GW}^{11/3}$$

The GW emission is not isotropic, it depends on line of sight and luminosity distance

$$h_+ = \frac{1}{D_L}\left(\frac{5}{c(t_c - t)^{1/4}}\right)\frac{1+cosi^2}{2}\cos[\Phi(t_c - t)] \qquad h_x = \frac{1}{D_L}\left(\frac{5}{c(t_c - t)^{1/4}}\right) cosi \sin[\Phi(t_c - t)]$$

Inclination of the orbital plane ι *& luminosity distance* D_l

Claudia Lazzaro

CBC (template) search

Need to build a bank of template that will cover the full parameter space:

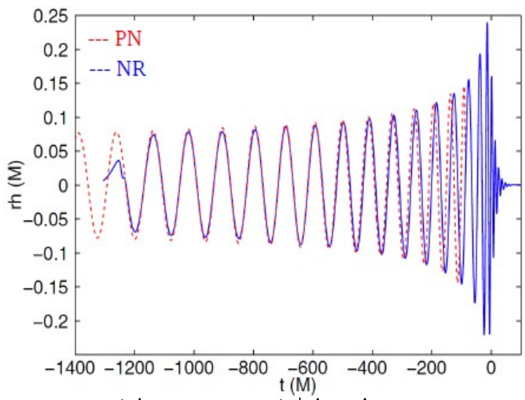

- ✗ To accurately calculate inspiral, merger and ring-down stage, “hybrid” waveforms are built. Post Newtonian approximation (PN) used for inspiral phase, Numerical relativity and perturbative theory for merger and ringdown phase
- ✗ Source parameters are encoded In detected waveforms., up to 15 parameters to include/estimate (chirp mass, component masses, spins,
- ✗ template not fully available for complex systems such as eccentric compact binaries, spinning ...

Template analysis search, main step (generic):

- ✗ matching filter for each template, find template that maximized matching template
- ✗ Same templates which are coincident in time (among the detector, including consistent time difference between sites) are combined in one event
- ✗ coincident triggers are ranked according to a detection statistic (combined SNR, weighted likelihood, ...)

Claudia Lazzaro

Burst sources

Possible sources

- ✗ core-collapse supernovae
- ✗ CBC signal: the merger phase of binary compactobjects. In particular the burst search is crucial for eccentric binary black holes, and high precessing, spinning system; in this cases the template are not well known.
  Post merger phase of NS-NS phase (equation of state of NS)
- ✗ neutron star instabilities, pulsar glitches
- ✗ accretion disk instabilities
- ✗ cosmic string cusps/kinks,
- ✗ ....the un-expected

Waveform morphologies is poorly modeled or fully unknown.
Short duration signal: hundreds milliseconds to a few seconds
Long duration: signals lasting from few seconds up to hours

Claudia Lazzaro

Burst searches

Burst search is performed without assumption (or minimal) on the phase evolution of the signal
Goal: cover wide range of parameters space (can overlap the modeled searches)

Burst analysis search, main step (generic):

- ✗ make time-frequency representation of the data, weight data by the noise at each frequency (whitening). Search for excess power in time-frequency domain, coincidently/coherently in different detectors data (considering time delay between detector sites and different antenna patterns of the detectors for any incoming direction).
- ✗ Coherent analysis of the triggers and estimation of the signal parameters. Different algorithms
- ✗ Ranked statistic

Claudia Lazzaro

Joint GW and high-energy astrophysics

GWs and photons provide complementary information on the astrophysics source (and maybe on the environment)

Gravitational waves signal ⟺ Electromagnetic signal

Two scenario:

➔GW triggered EM follow-up: low-latency GW data analysis pipelines promptly identify GW candidates and send GW alerts to trigger prompt EM observations

Low latency analysis, GW candidates, skymap ~minutes → Event validation Hours, days → EM followup

➔EM triggered GW: an EM transient event is detected and GW triggered searches are are performed to look for possible associated GW events.

➔even more: joint with neutrino, searches neutrino candidates with data of IceCube and ANTARES

Joint GW and EM, astrophysics motivation

<u>Coalescence of binary systems of NSs and/or BHs</u>

- Short GRBs:

  Prompt γ-ray emission (< 2 s)

  Multiwavelegth afterglow emission: X-ray, optical and radio (minutes, hours, days, months).

-Kilonova: optical (days-weeks).

<u>Core collapse of massive stars:</u>

Supernovae:

-X-rays, UV (minutes, days)

-optical (week, months)

-radio (years)

Long GRBs (massive rapidly spinning star Collapse ??)

<u>Isolated neutron stars</u>

-soft γ–ray repeaters

-radio/X-ray pulsar glitches

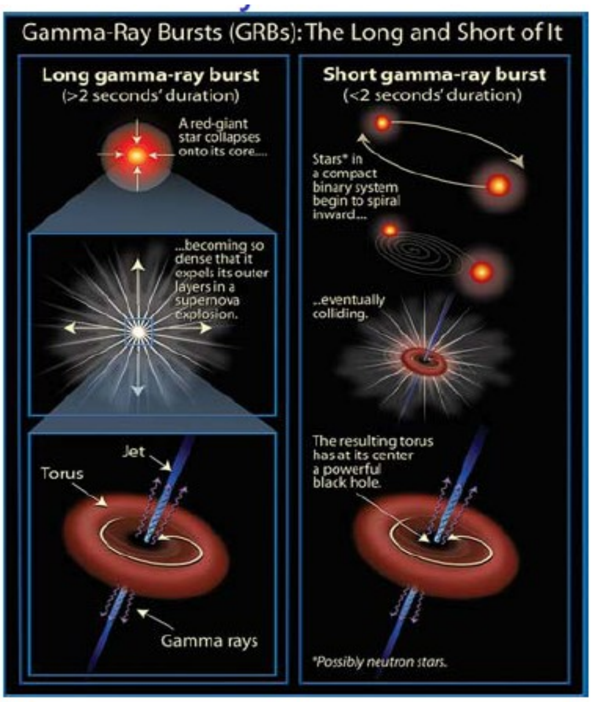

O1 data talking and sensitivity

September 12, 2015 - January 19, 2016
Total coincidence analysis time: 51.5 days
Total coincidence analysis time after removing noisy data: 48.6 days (~38%)

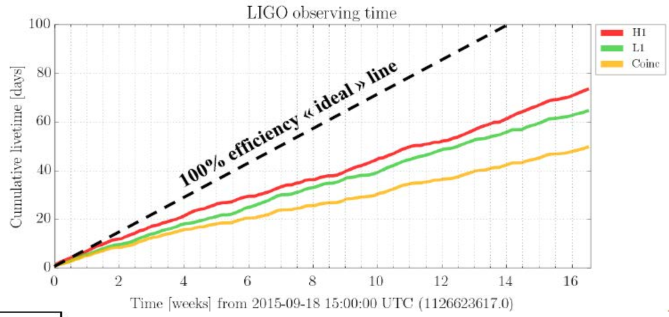

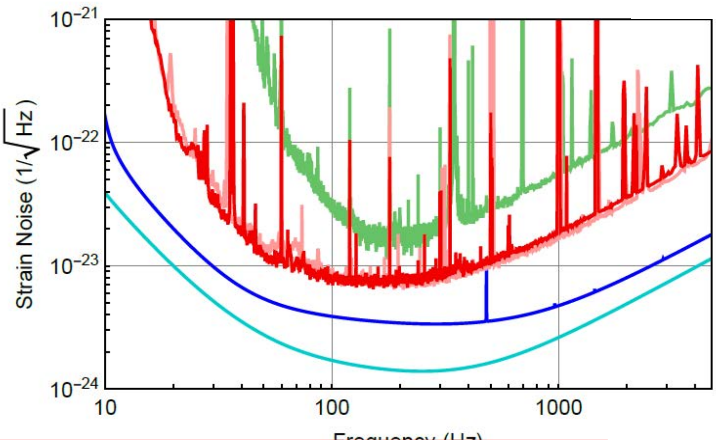

strain sensitivity during the First observation run (O1) of the Advanced LIGO detectors and during the last science run (S6) of the initial LIGO detectors.

– Hanford
– Livingston
– S6
– AdvancedLigo (design sensitivity)

GW150914: The Advanced LIGO Detectors in the Era of FirstDiscoveries (Phys. Rev. Lett. 116,131103)

Claudia Lazzaro

O1 analysis: binary black holes

Phys. Rev. X 6, 041015

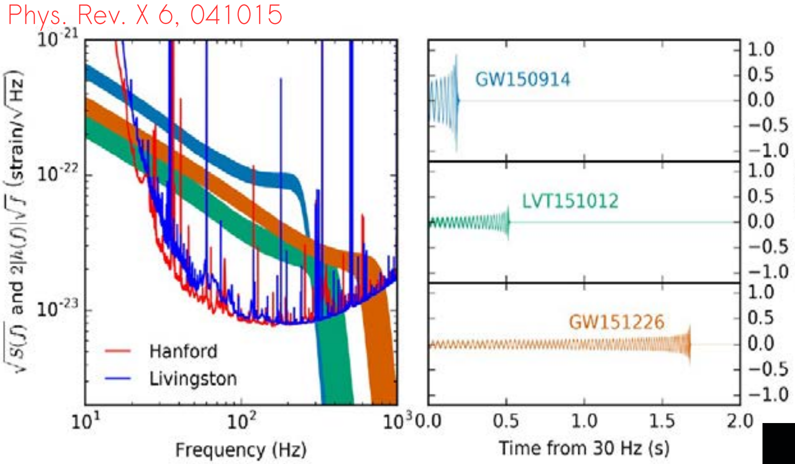

GW150914 (significance >5.3σ)
LVT151012 (Candidate 1.7σ)
GW151226 (significance>5.3σ)

Amplitude spectral density of the total strain noise of the H1 and L1 and the recovered signals

GW150914 - September 14, 2015 at 09:50:45UTC
- ✗ 29 and 36 Msun
- ✗ Duration ~ 0.2s

GW151226 December 26, 2015 at 03:38:53 UTC
- ✗ 7 and 14 Msun
- ✗ Duration ~ 1s

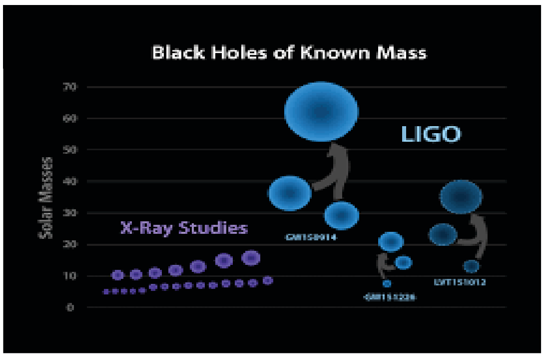

Claudia Lazzaro

O1 analysis: first detection

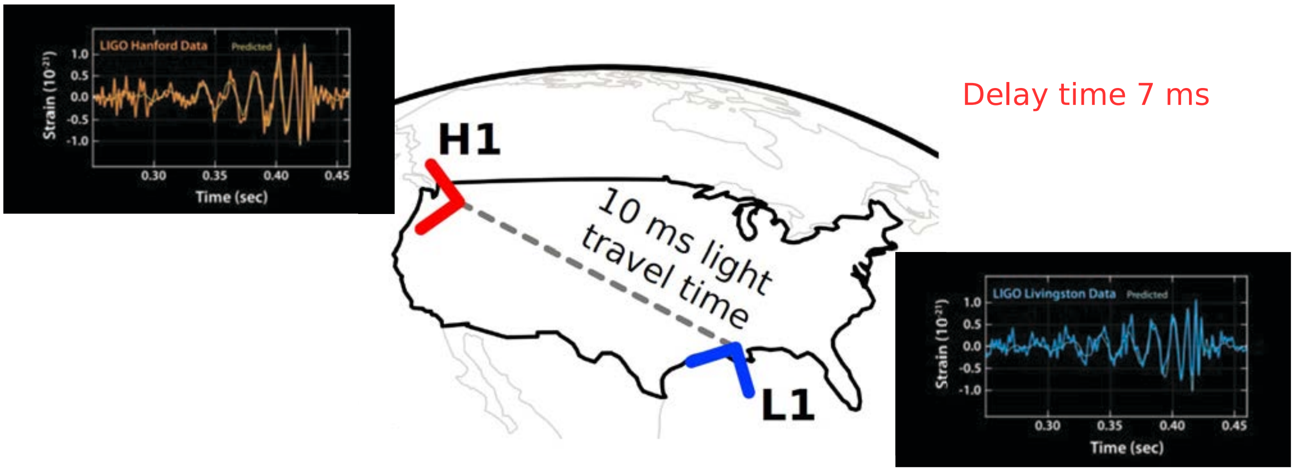

- ✗ 3 minutes alert from the low latency searches pipeline coherent Wave Burst (cWB) (Florida, Hannover, Padova/Trento)
- ✗ Two independent sky maps available in short time (cWB 17 min, LIB 14 hours) within 600 deg^2 (90% c.l.)
- ✗ As the preliminary estimate of the event significance overcomes the planned threshold (1/month) within 48 hours, allert sent via GCN circular to 62 astronomer partners (including INAF PD).

O1 analysis: first detection, confidence

The possibility that the transient GW150914 is due to environmental or instrumental excess noise is ruled out. 5.1 evidence of the astrophysical origin of the signal

Two independent data analysis pipelines used to estimate the confidential level

Template search,
Estimated False Alarm rates: <1/203000 years

Generic (burst) search,
Estimated False Alarm rates: <1/225000 years

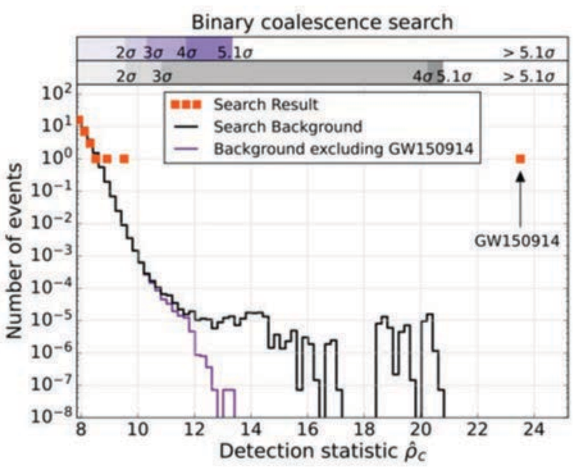

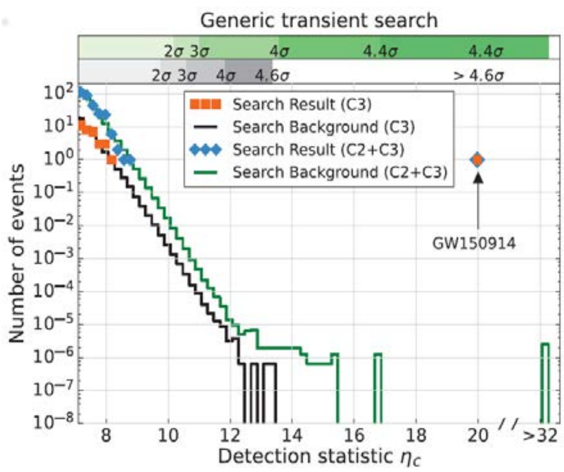

O1 analysis: first detection, binary parameters

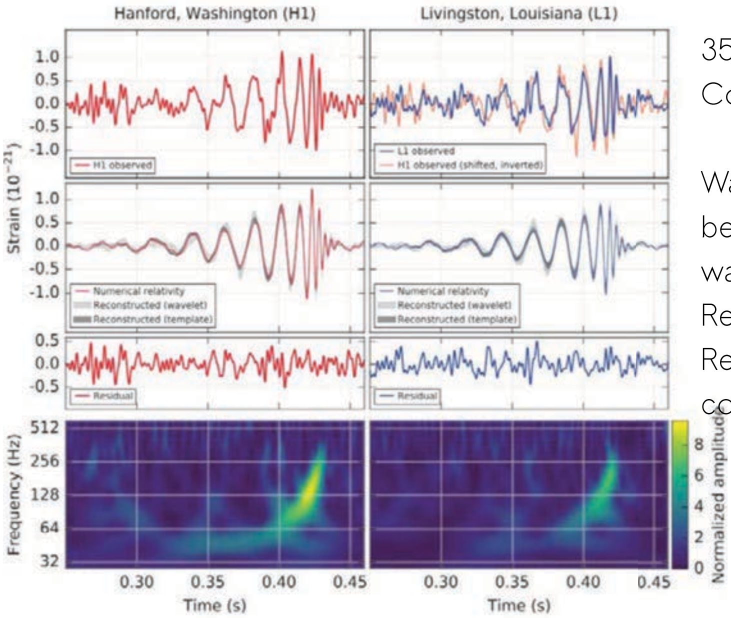

35 - 350 Hz band-passed strain time series. Coherent signals in both detectors

Waveform reconstruction, agreement between best fit theoretical waveforms, wavelet (unmodeled) and NR (Numerical Relativity)
Residual noise after waveform subtraction consistent with instrumental noise

Mass 1	$36.3^{+5.3}_{-4.5} M_\odot$
Mass 2	$28.6^{+4.4}_{-4.2} M_\odot$
Final mass	$62.0^{+4.4}_{-4.0} M_\odot$
Energy radiated in GW	$3.0^{+0.5}_{-0.5} M_\odot$
Spin magnitude $\|a1\|$	$0.32^{+0.45}_{-0.28}$
Spin magnitude $\|a2\|$	$0.57^{+0.40}_{-0.51}$
Final spin $\|a_f\|$	$0.67^{+0.06}_{-0.08}$
Luminosity distance	$410^{+160}_{-180} Mpc$

- ✗ The physical system is described by 8 parameters: $m_{1,2}$ and $S_{1,2}$
- ✗ 9 additional parameters are required Luminosity distance, celestial coordinates, orbit inclination, time and phase of coalescence.

O1 analysis: first detection, follow up

Electromagnetic follow up.

Covered sky map (contained probabillity):
GW
Gamma-ray: 100 %
Optical: over 50 %
Radio: 86 %
X-ray: 90 %

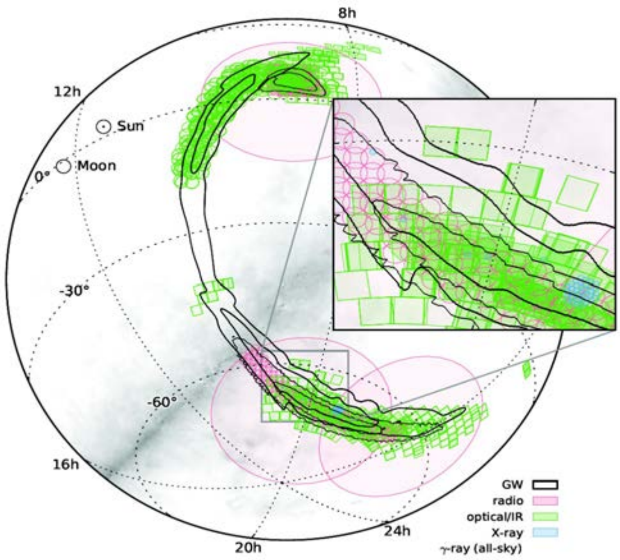

Neutrino joint analysis

Search for coincident neutrino candidates of IceCube and ANTARES (in 500s window):
-ANTARSE: 0 neutrino candidates:
-IceCube: : 3neutrino candidates, consistent with the expected background (No one directionally coincident with GW150914)

Interferometers network, second generation

Living Reviews in Relativity DOI 10.1007/lrr-2016-1

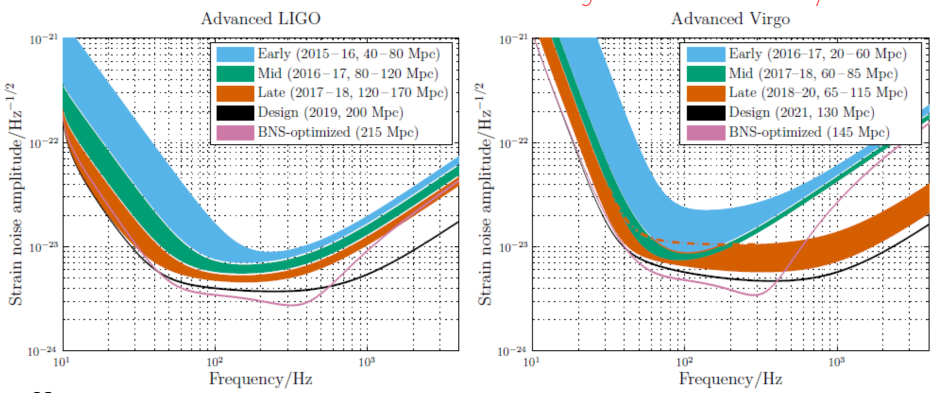

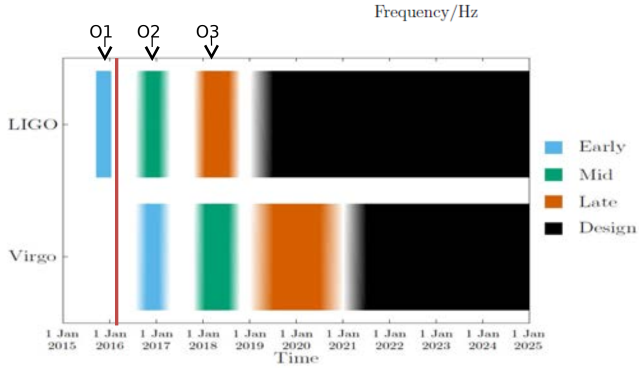

- Estimated BNS detection rate: 0.2-200 per year
- Sky position ~5 deg²

Claudia Lazzaro

Three detector localization

Living Reviews in Relativity DOI 10.1007/lrr-2016-1

Face-on BNS 80 Mpc

Face-on BNS 160 Mpc

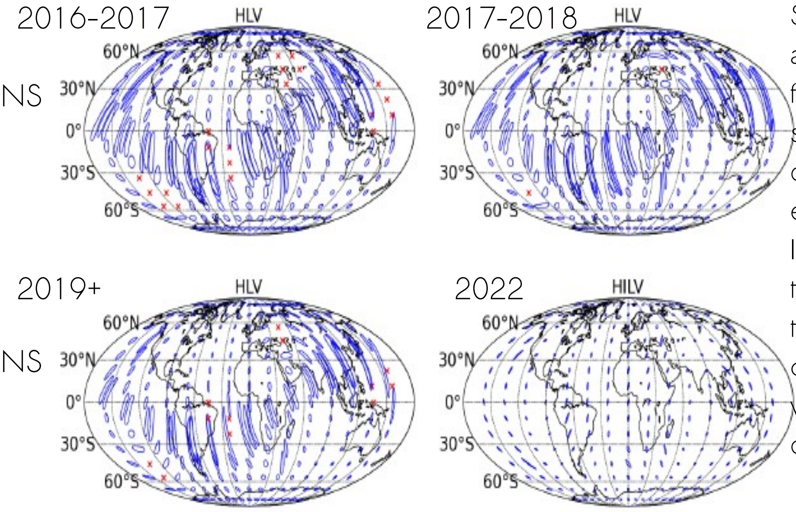

Schematic network sensitivity and localization accuracy for face-on BNS systems with advanced-detector networks. The ellipses show 90% confidence localization areas based upon timing triangulation alone, and the red crosses show regions of the sky where the signal would not be confidently detected.

GW150914

L1H1:600 deg²
If Virgo: L1H1V1: 90% probability sky area reduced by a factor 30

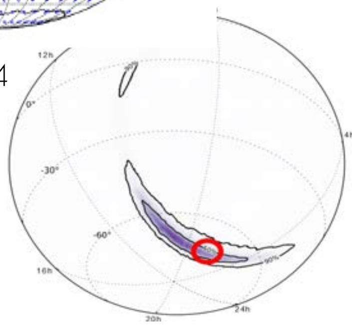

Claudia Lazzaro

GW spectrum

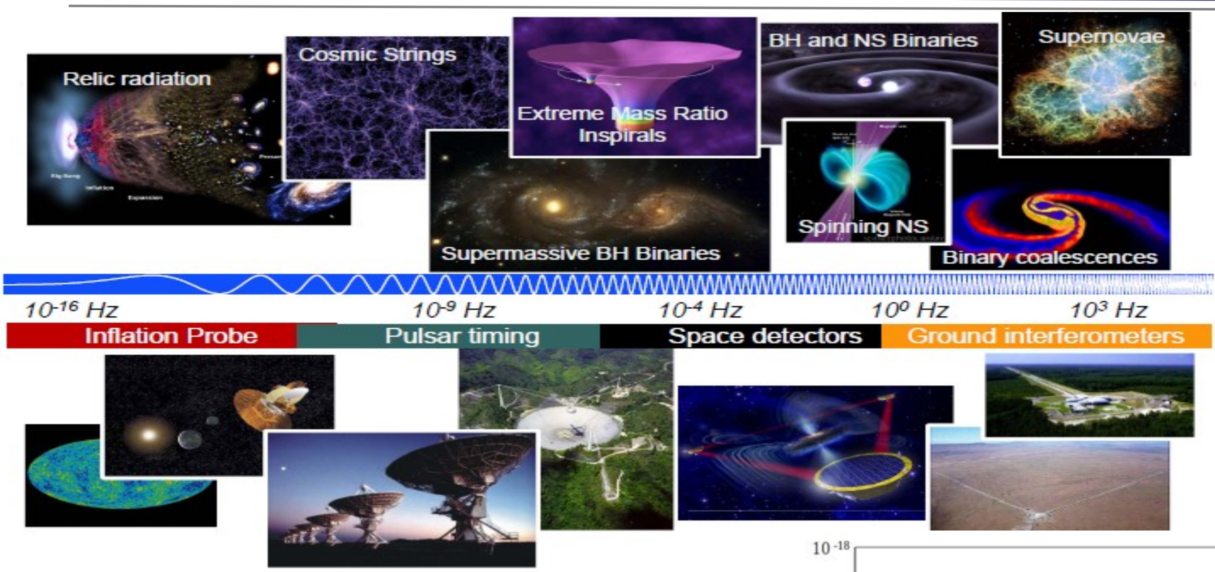

to “be sensitive” to GW spectrum:

✗ improve ground interferometers

✗ space interferometers

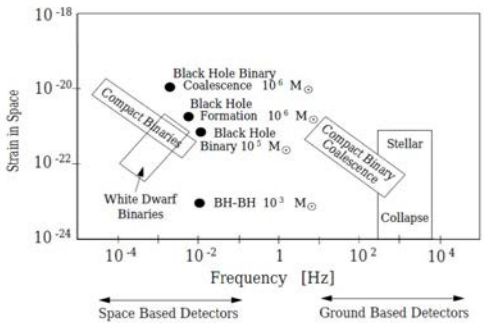

Claudia Lazzaro

Future

“Limit” to improvement of the second generation interferometer: length of the arms, seismic and newtonian noise, size of the beam (thermal noise), :

“3rd generation observatory”:

✗ Possible new technology: squeezed light, alternative wavelengths + cryogenics, longer arms, go underground (access low frequencies)

✗ Factor ~10 sensitivity increase over aLIGO (10 Hz - few kHz); sensitivity x10 ⇒volume $x10^3$

✗ Low frequency sensitivity (down to ~ 5 Hz)

Einstein telescope design studies

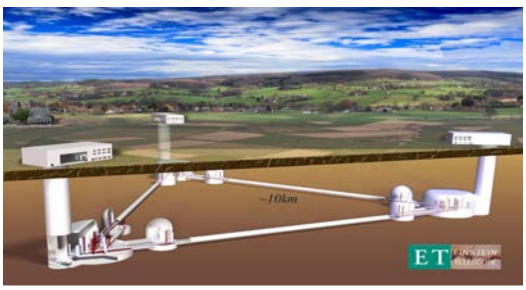

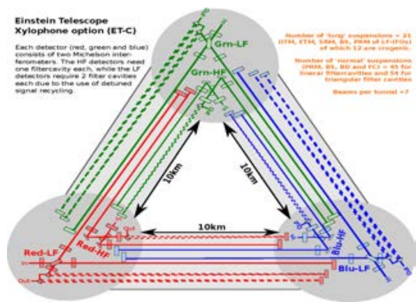

✗ 10 km arm length

✗ Underground, cryogenics

✗ New geometries or topologies, multiple interferometers

Claudia Lazzaro

Space interferometers

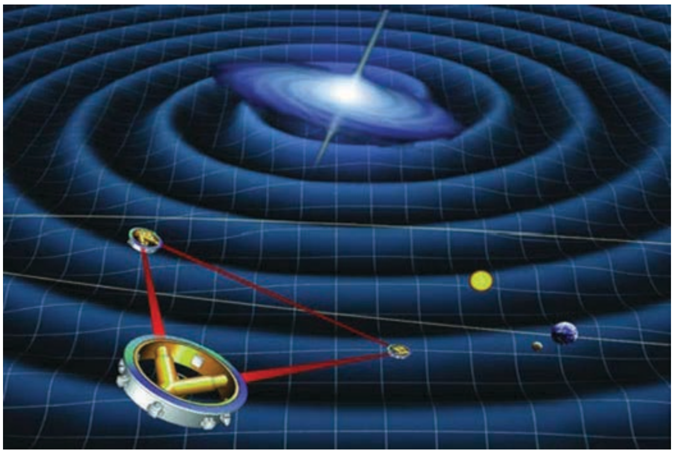

- ✗ 3 Spacecraft 2.5 Million-km arm-lengths
- ✗ Test masses in sub-femto-g free fall (10^{-15}m/s^2/√Hz)
- ✗ Laser interferometry between TMs

Successful LISA Pathfinder mission
Mission proposal submitted (arXiv:1702:00786)
Launch 2030-2034

Possible source:
massive black hole binaries (MBHBs) detection,
parameter estimation..and MBH formation.
Extreme mass ratio inspirals (EMRIs)
Cosmological background

Back up

Multimessenger astroparticle physics

Alessandro De Angelis, INFN/INAF Padova and LIP/IST Lisboa

Lecture 8

A look to the future.

Summary^2 of previous 2 lectures

- HE astrophysics is today essentially gamma astrophysics. Thousands of astrophysical gamma-ray emitters in the HE region and >200 in the VHE region
  - New emitters and new classes of emitters
  - A diffuse background up to the TeV, maybe the sum of unresolved point-like emitters
  - We have seen both the leptonic and the hadronic gamma-ray mechanisms at work
  - We have identified mechanisms of emission explaining cosmic rays up to the PeV – also in action, but (by far) not enough to explain the full flux
  - The SED of many emitters can be modeled in an effective way
  - Interesting perspects for fundamental physics. DM:
    - A standard WIMP below 400 GeV is on reach for HE gamma detectors, if just one WIMP and the particle was in thermal equilibrium
    - Dwarf spheroidals (no need for background models) and the GC region (a mess from the point of view of astronomy) are the favorite targets
    - Can find indirect evidence for Axion-Like Particles
- Multimessenger astrophysics (just starting) will teach us more, both from the point of view of astrophysics and of fundamental physics
  - We just detected astrophysical neutrinos [signal of (7±2)/year with 1km^3 detector, s/b ~ 2/1), and we know that probably a several-km^3 detector is needed do to astronomy
  - Gravitational waves: first signals (~2/year with two large interferometers)
  - Protons cannot be used for astronomy (but they give us O(100 TeV) c.m. energies)

Summary of older lectures

- Detectors for charged cosmic rays: (1) need large effective area for the UHE, (2) smart instruments on satellite for particle identification. For (1) we are close to the limit (Auger) unless we change technology, for (2) we are close to the limit (AMS-02)
- Astrophysical neutrino detectors: we need several km^3; we are close to the limit (IceCube) but still improving (Antares -> km^{3}NeT)
- Photons:
  - In the MeV region, instruments did not reach the technological limit, yet (no new instrument since COMPTEL, 1991-2000)
  - In the GeV region, Fermi is close to the technological limit
  - In the TeV region, the Cherenkov technique reigns. HESS, MAGIC and VERITAS have still potential, and there is room for improvement by "brute force"
  - In the PeV region, only one detector presently active, and there is room for improvement by "brute force" – plus something

3k HE and >200 VHE photon emitters

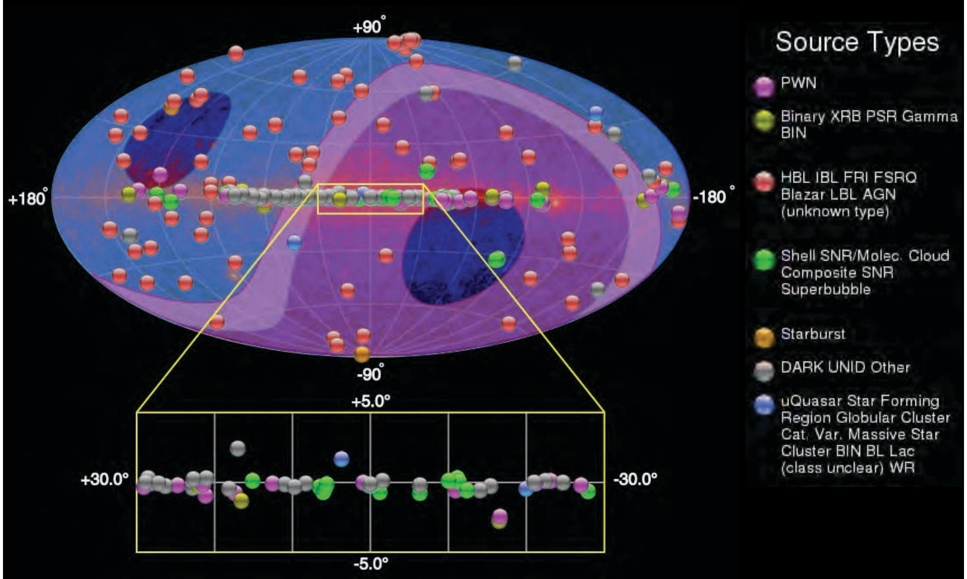

The TeV gamma region: CTA

The 20 GeV- 100 TeV region: how to do better with traditional IACT?

- More events
  - More photons = better spectra, images, fainter sources
    - Larger collection area for gamma-rays
- Better events
  - More precise measurements of atmospheric cascades and hence primary gammas
    - Improved angular resolution
    - Improved background rejection power

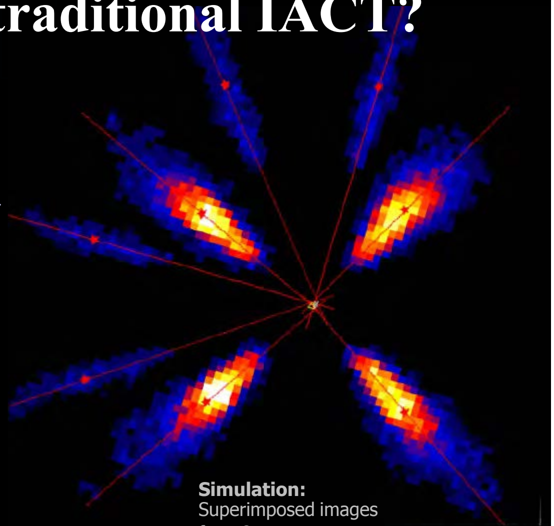

Simulation: Superimposed images from 8 cameras

☛ The CTA solution: More telescopes !

What is CTA? A multi-telescope Cherenkov array

Low energies
Energy threshold 20 GeV
23 m diameter
4 telescopes
(LST)

Medium energies (MST)
100 GeV – 10 TeV
9.5 to 12 m diameter
25 single-mirror telescopes
up to 24 dual-mirror telescopes
mCrab sensitivity in 50h at 0.1-10 TeV

High energies
10 km² area at few TeV
4 to 6 m diameter
70 telescopes
(SST)

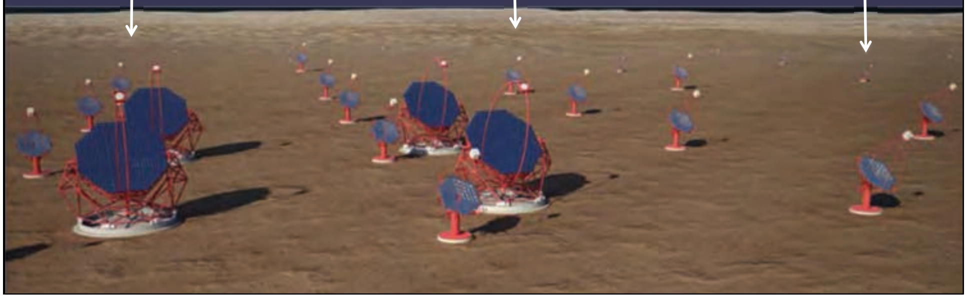

CTA sensitivity in units of Crab flux

for 5 σ detection & $N_\gamma > 10$ in each 0.2-dex bin in E, in 50 h

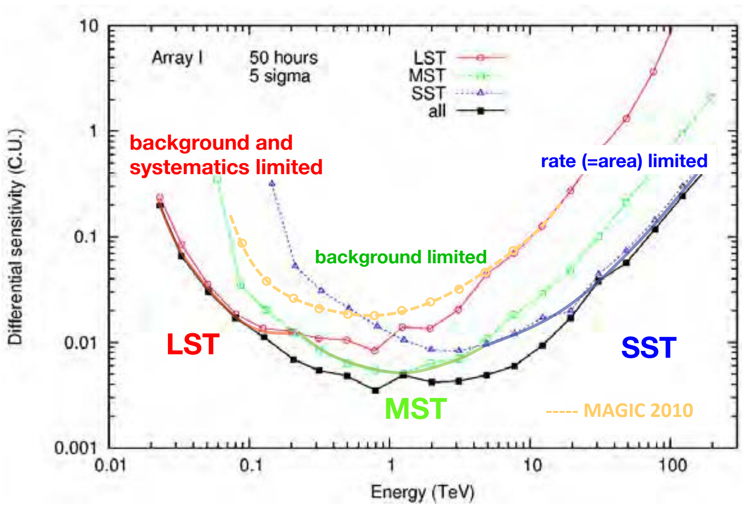

CTA consortium: a world-wide effort

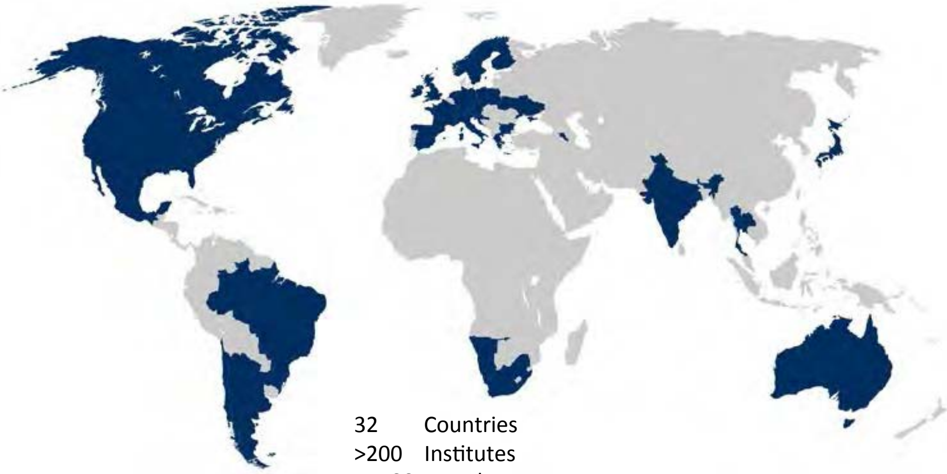

32 Countries
>200 Institutes
>1500 Members

All-sky coverage: two observatories

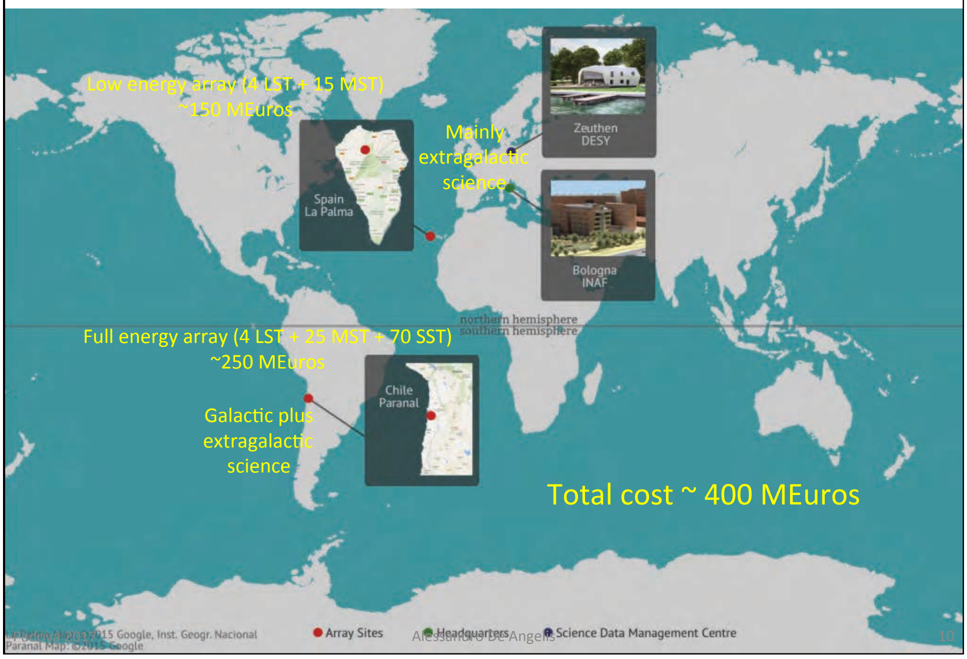

array layoutS

Reference (baseline) layouts

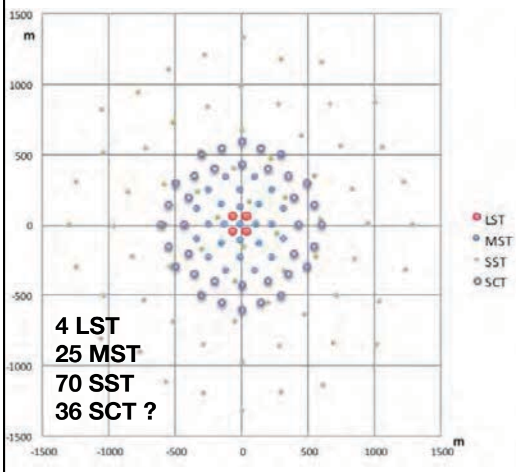

CTA-South

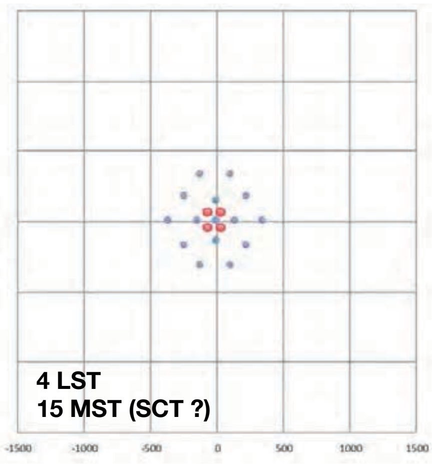

CTA-North

Sensitivity for North and South

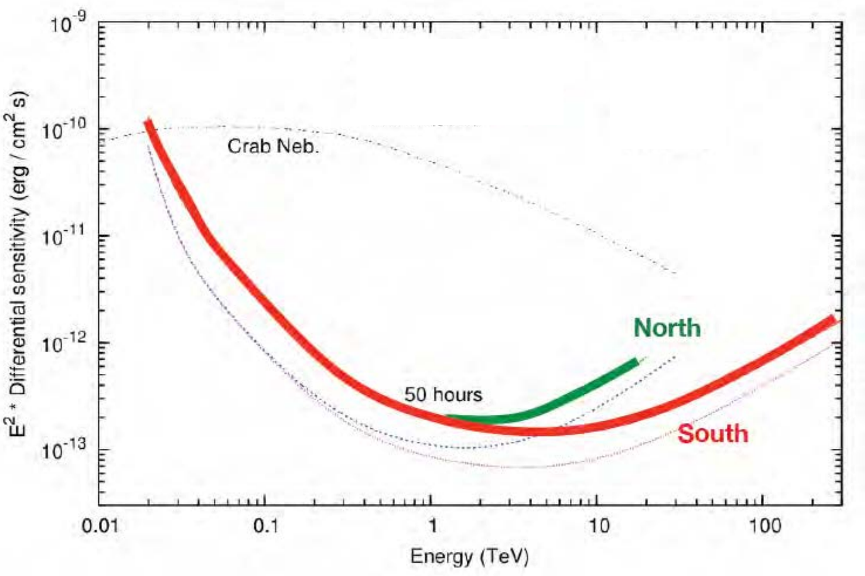

Telescope Specifications

SiPM Cameras

3 SST types

	LST "large"	MST "medium"	SCT "medium 2-M"	SST "small"
Number	**4 (S) 4 (N)**	**25 (S) 15 (N)**	**≤ 24 (S and N)**	**70 (S)**
Energy range	20 GeV to 1 TeV	200 GeV to 10 TeV	200 GeV to 10 TeV	> few TeV
Effective mirror area	> 330 m²	> 90 m²	> 50 m²	> 5 m²
Field of view	> 4.4°	> 7°	> 7°	> 8°
Pixel size ~PSF θ_{80}	< 0.12°	< 0.18°	< 0.07°	< 0.25°
Positioning time	50 s, 20 s goal	90 s, 60 s goal	90 s, 60 s goal	90 s, 60 s goal
Target capital cost	7.4 M€	1.6 M€	< 2.0 M€	500 k€

LST

(optimized for the 20 GeV-200 GeV range)

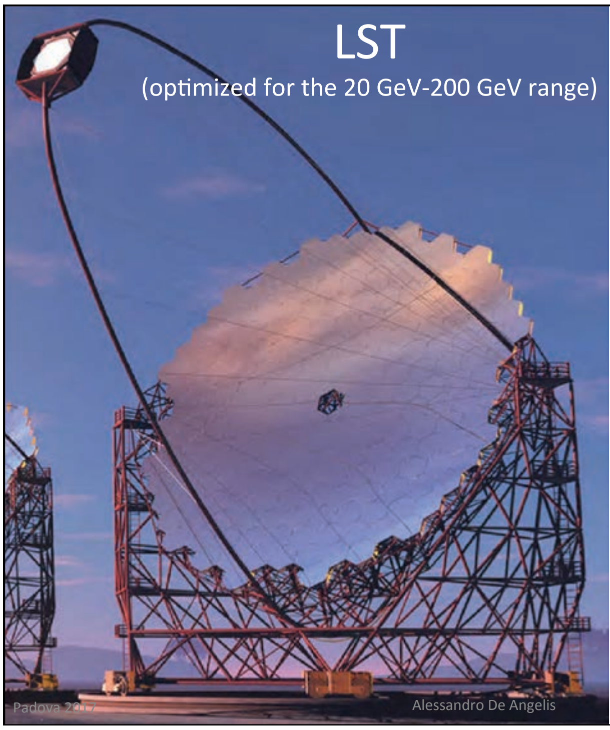

- 23 m diameter (400 m² dish area)
- 28 m focal length
- 200x2m² hexagonal mirrors
- 4.5 deg FoV
- 0.1° pixels, camera diam. 2m
- Light structure for 20 s positioning
- AMC
- 4 LSTs on North site, 4 LSTs on South site
- Prototype = 1st telescope at La Palma.
- Foundations finished end 2016
- Inauguration expected Nov 15, 2017
- Japan, Germany, INFN Italy, Spain, IN2P3 France, India, Brazil, Croatia, Sweden

LST1 construction (webcam live)

MEDIUM-SIZED 12 M TELESCOPE

OPTIMIZED FOR THE 100 GEV TO ~10 TEV RANGE

cta cherenkov telescope array

100 m² dish area
16 m focal length
1.2 m mirror facets

8° field of view
~2000 x 0.18° pixels

25 MSTs on South site
15 MSTs on North site

Berlin
MST prototype
operational

Two-Mirror Telescopes

Schwarzschild-Couder (SC) Design

Vassiliev, Fegan, Brousseau
Astropart.Phys.28:10-27,2007

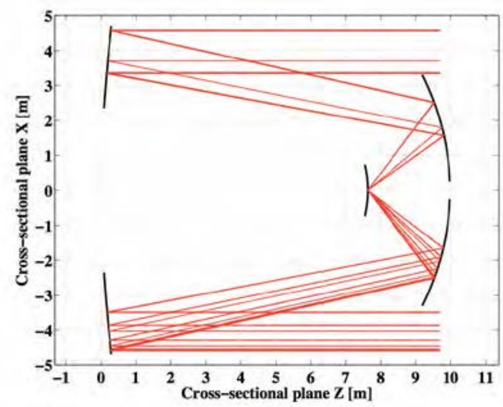

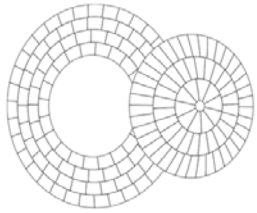

- Reduced plate scale
- **Improved PSF**
- **Uniform PSF across f.o.v.**

➜ Low-cost small telescopes with compact sensors (SST-2M)

➜ Higher-performance, cost-effective, medium telescope (MST-SCT)

3 telescope prototypes within CTA are using two mirror designs

Medium Telescope 2-mirror (SCT)

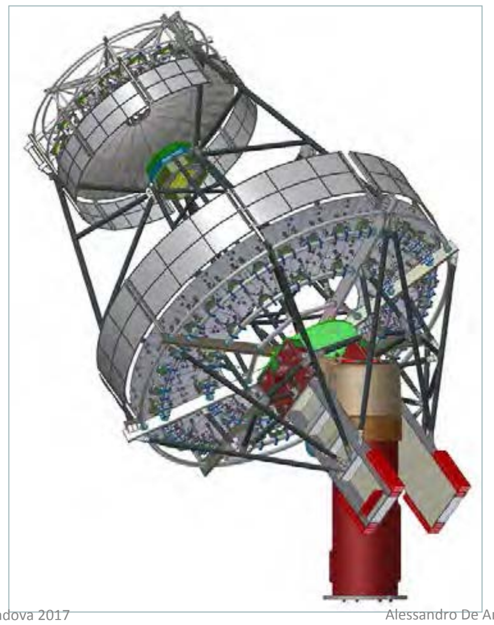

9.7 m primary
5.4 m secondary
5.6 m focal length, f/0.58
50 m^2 mirror dish area
PSF better than 4.5′
across 8° FOV

8° field of view
11328 x 0.07° SiPMT pixels
TARGET readout ASIC

SCTs can augment / replace MSTs in either S or N
→ proposed US contribution

➜ Increased γ-ray collection area
➜ Improved γ-ray ang. resolution
➜ Improved DM sensitivity

pSCT construction near Tucson (webcam live)

SST: HIGH THRESHOLD, OPTIMIZED FOR LOW COST
(SST-1M inauguration, Krakow June 2014)

CTA TELESCOPE DESIGN & PROTOTYPING: SST-1M

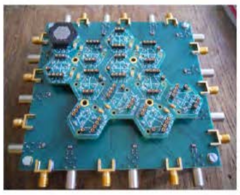

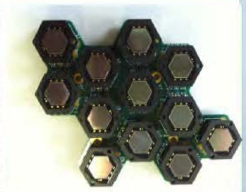

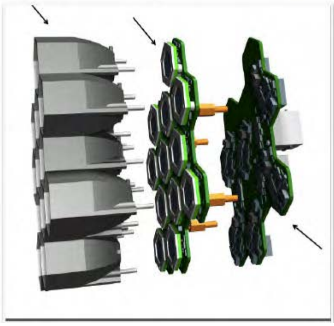

Small Telescope 2-mirror (SST-2M)

SST-2M –ASTRI Mechanical Prototype Inauguration, 24 Sept 2014 (Serra La Nave, Sicily)

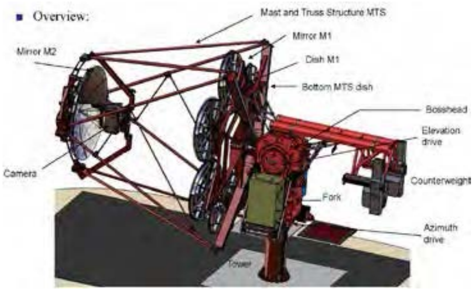

SST-2M-GCT (Gate Telescope) Inaugurated in June 2016 Saw already 1st light

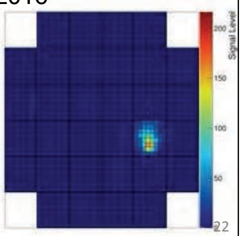

Both 2-mirror SST designs: compact, Silicon-PM cameras

CAMERAS

NectarCam cooling studies

FlashCam 144 pixel focal plane

LST camera cluster

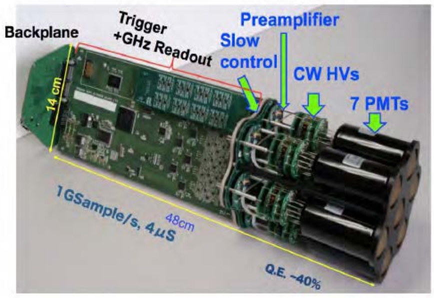

SiPM: the technological challenge for small cameras

Cameras need high granularity, and typical PMT size of 5-6 mm

Difficult to do with standard PMT

New detectors (SiPM) under development

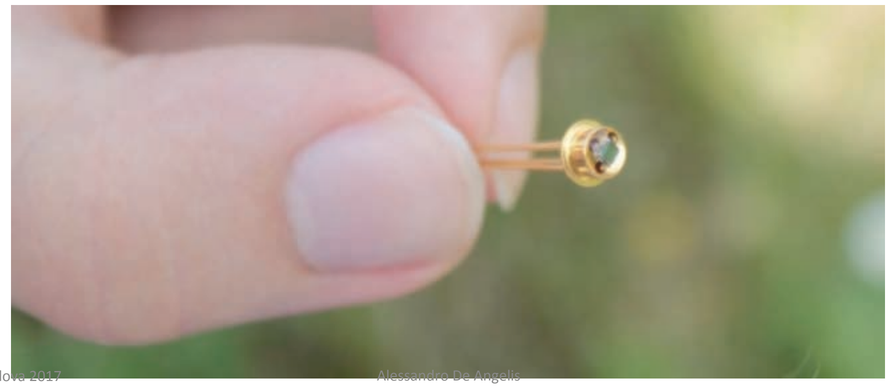

LST in the future: large surface SiPM?

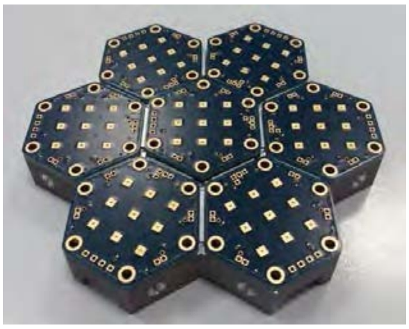

Challenge: single sensor with large area (1 inch diameter)
Amplify-and-sum stage, one output per pixel

Prototype of analog sum scheme will be tested in MAGIC

Prototype cluster using Hamamatsu and developed by MPI mounted on MAGIC Jun 15

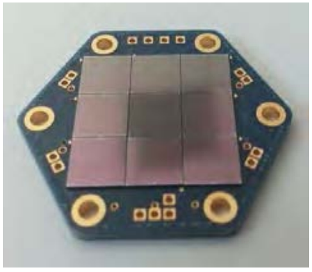

9 FBK 6x6 mm^2 sensors
Sensor electronics by INFN Padova
MAGIC cluster control electronics and

Signal: 2 mV per phe; noise: 0.5 mV rms
Linearity: ok to >200 phe

Assembly and test now,; installed in MAGIC October 2015 for comparison with the standard PMT clusters (and with the similar Max Planck SiPM cluster, just installed)

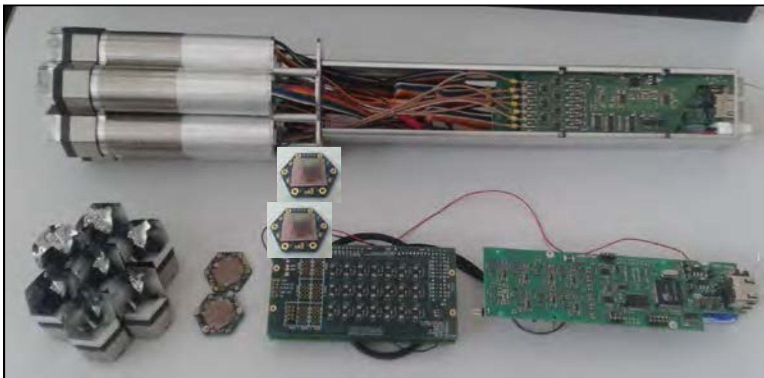

In picture:
Top: standard MAGIC PMT cluster
Bottom: components for SiPM cluster, mechanical structure removed

CTA-N: rendering

LST1 to commissioned in 2018 (inauguration end 2017?)
LST2-4 commissioned in 2020?
First 5 MST commissioned in 2022?

CTA-S in Paranal: rendering (works starting in 2018?)

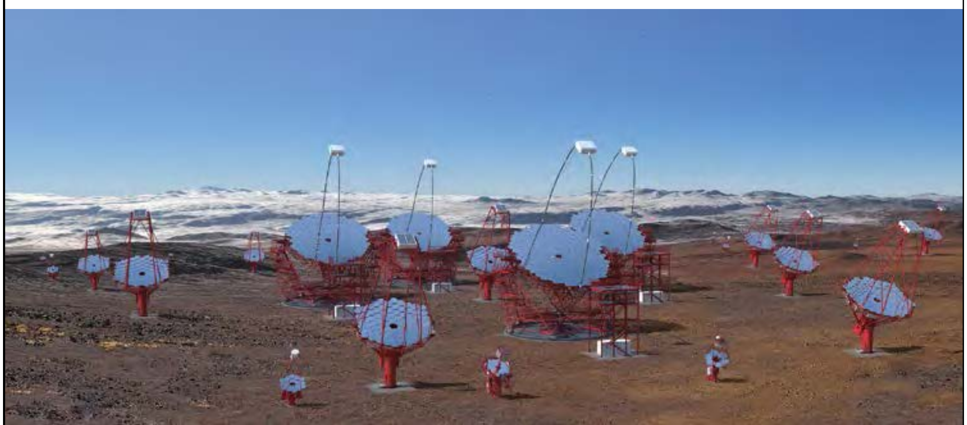

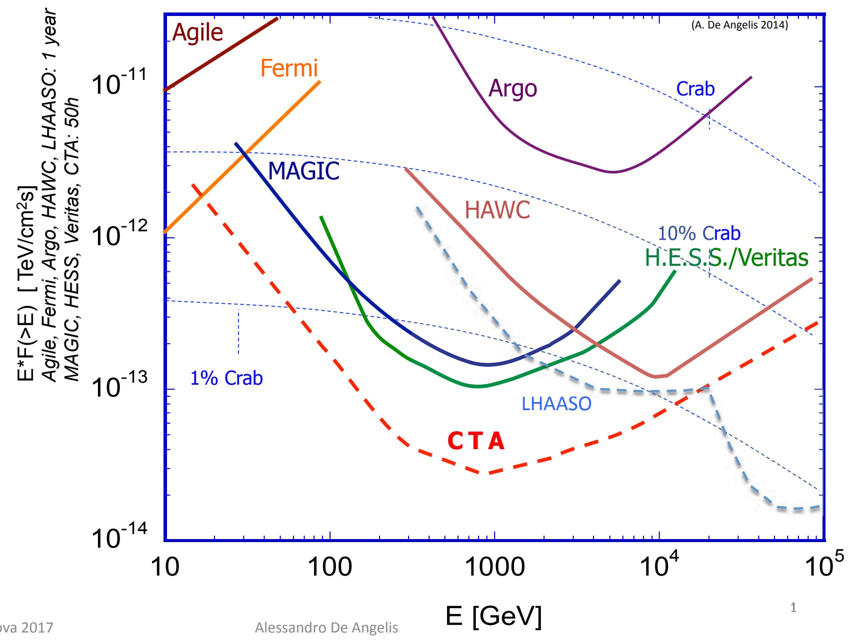

Guaranteed Science with CTA

An advanced Facility for ground-based gamma-ray Astronomy

~200 -> ~2000 sources above 100 GeV

- Study of sources and propagation of high energy particles in the Cosmos, on scales ranging from compact objects to large scale structures
  - Pulsars
  - Pulsar wind nebulae
  - Stellar winds
  - Supernova remnants
  - Diffuse emission
  - Galactic center region
  - Starburst galaxies
  - Clusters of galaxies
- Black holes and their environment
  - Stellar-mass black holes
  - Supermassive black holes

Simulation of the visibility of the Galaxy

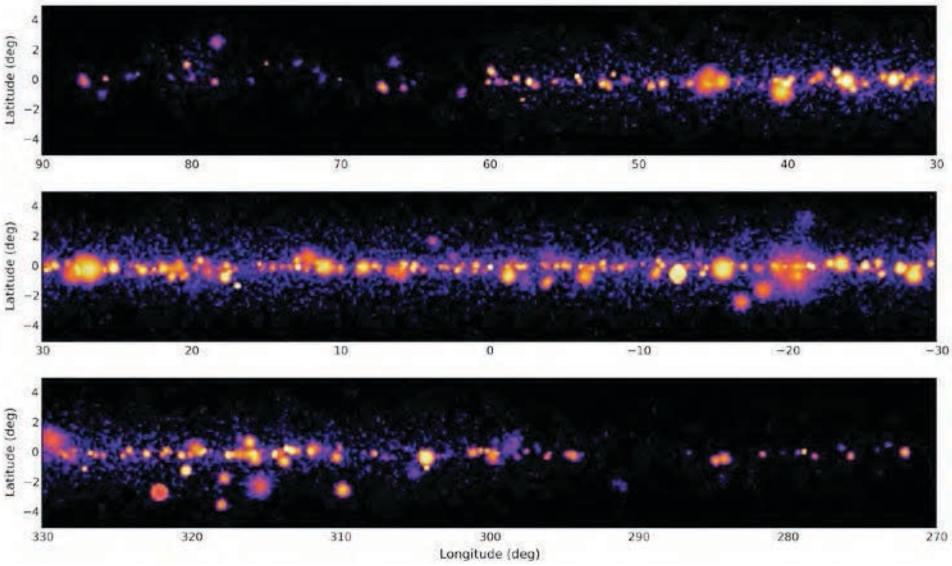

OTHER POSSIBLE DESIGNS FOR VHE GAMMA ASTROPHYSICS

An experimentalist's view of gamma rays: different energy regions

1. MeV: 30 keV to 30 MeV
2. GeV: 30 MeV to 30 GeV
3. TeV: 30 GeV to 30 TeV
4. PeV : 300- GeV - 30+ TeV

CTA

- (subjectively) chosen from the requirements of
  - (i) detection specifics and
  - (ii) principal scientific issues
- Can CTA be helped in regions 1., 2. and 4. ?

EAS-type designs (serendipity => GRB, unexpected…)

- CTA can be non optimal for PeV detection
- EAS can be the key for Pevatron studies

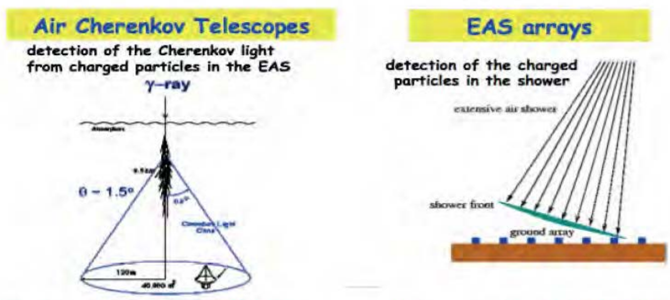

Air Cherenkov Telescopes	EAS arrays
Very low energy threshold (≈50 GeV)	Higher energy threshold (≈300 GeV)
Excellent bkg rejection (>99%)	Good bkg rejection (>80%)
Excellent angular resolution (≈0.05 deg)	Good angular resolution (0.2-0.8 deg)
Good energy resolution (≈15%)	Modest energy resolution (≈50%)
High Sensitivity (< % Crab flux)	Good Sensitivity (5-10% Crab flux)
Low duty-cycle (≈10%)	High duty-cycle (≈100%)
Small field of view (4-5 deg)	Large field of view (≈2 sr)

HAWC: most VHE triggered showers energy falls outside of the array

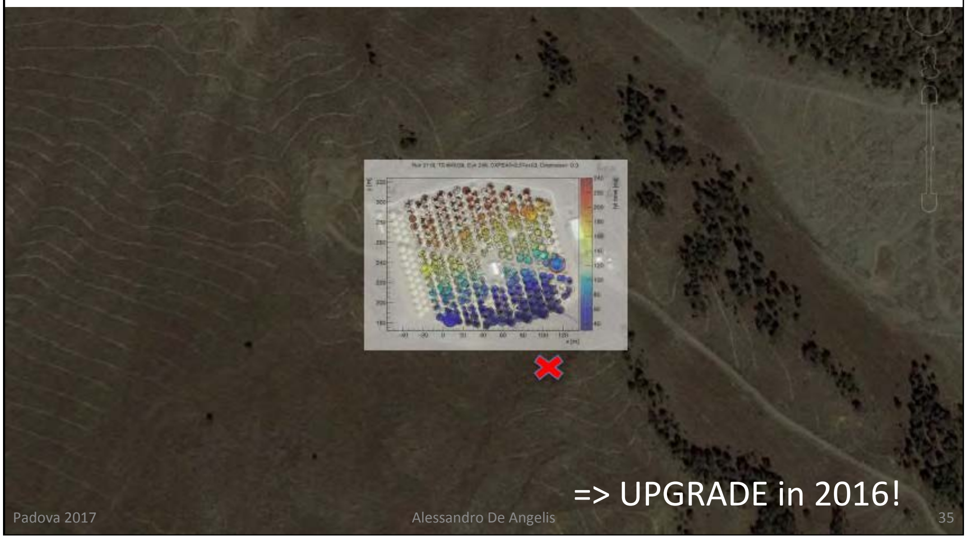

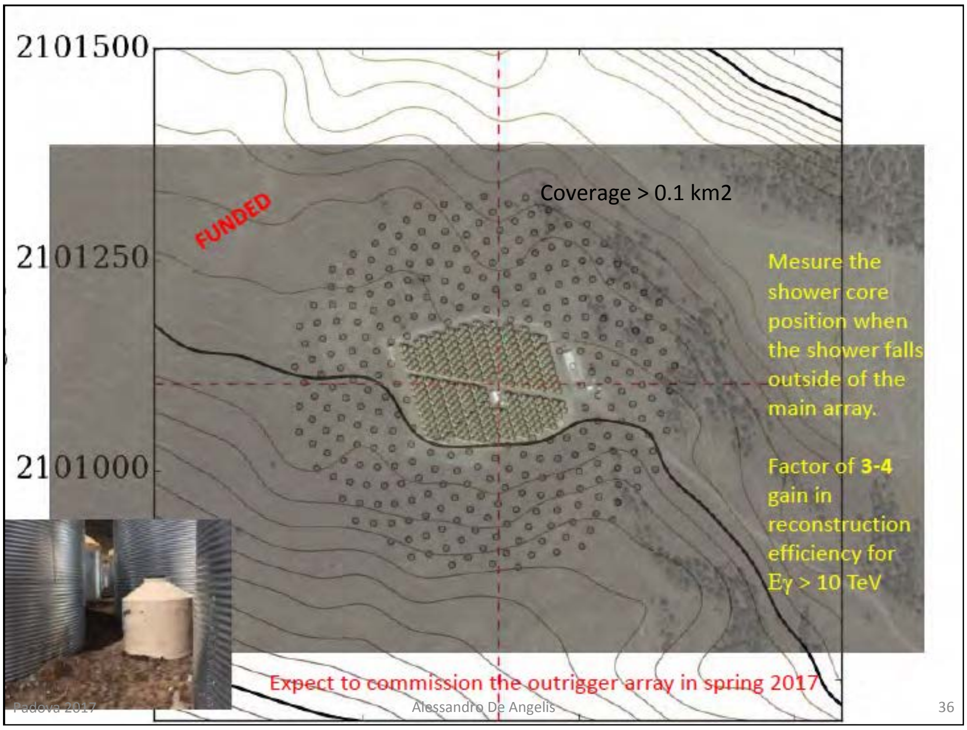

The LHAASO project

The Large High Altitude Air Shower Observatory (LHAASO) project is a new generation all-sky instrument to perform a combined study of cosmic rays and gamma-rays in the wide energy range 10^{11} -- 10^{17} eV.

The experiment will be located at 4300m asl (606 g/cm^2) in the Sichuan province

1 KM2A:
5635 EDs
1221 MDs

WFCTA:
24 telescopes
1024 pixels each

WCDA:
3600 cells
90,000 m^2

SCDA:
452 detectors

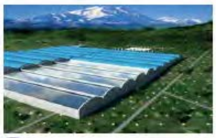

Coverage area: 1.3 km^2

Francesco Simeone - The Future of Research on Cosmic Gamma Rays - 28/8/2015 3

Padova 2017 Alessandro De Angelis 37

LHAASO

- Phase-0: Large Area Water Cherenkov Array (LAWCA)
  - YangBaJing, Tibet: around the ARGO detector
  - Completion end 2014
- Phase-1
  - Final site: Shangri-La
    - 4.3 km altitude
  - Sensitivity?
    - Will depend on background rejection power achieved in practice, but will be a **very** powerful instrument

Angular resolution:

30 TeV ~0.4°

100TeV ~0.3 °

Energy relsolution:

30 TeV ~30%

100 TeV ~20%

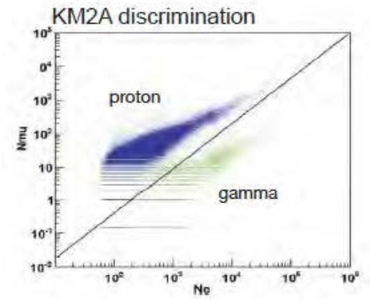

2018: start scientific operation of the first quarter of LHAASO.
2021: conclusion of the installation of all main components.

For Galactic objects, energies > 300 TeV are not impossible to detect

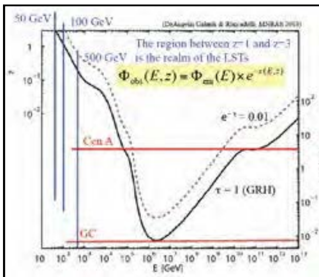

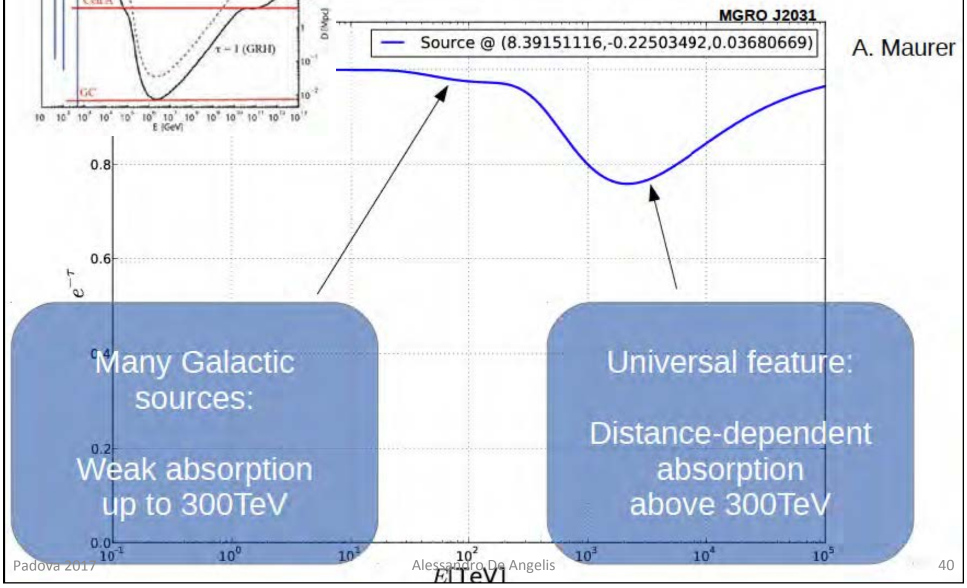

Flux limitations => large area is the key: HiSCORE

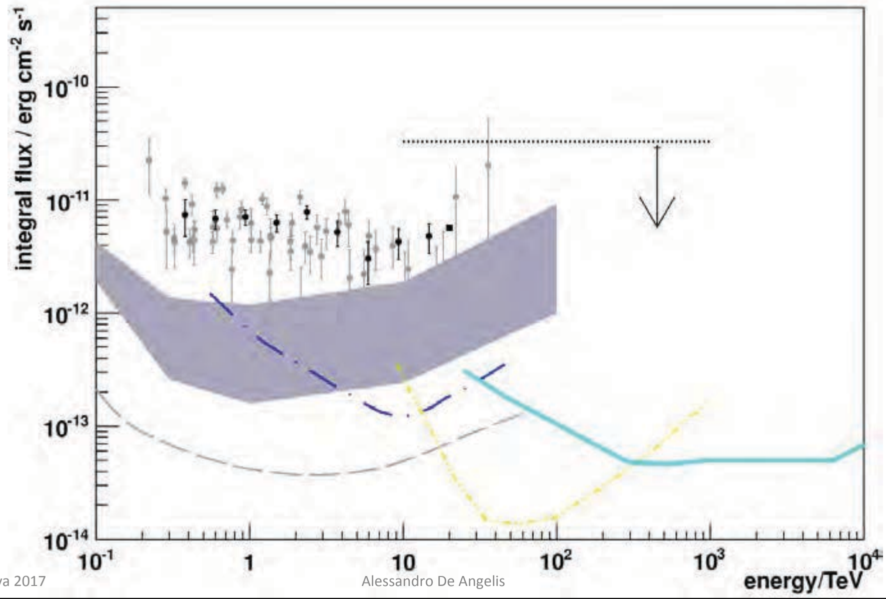

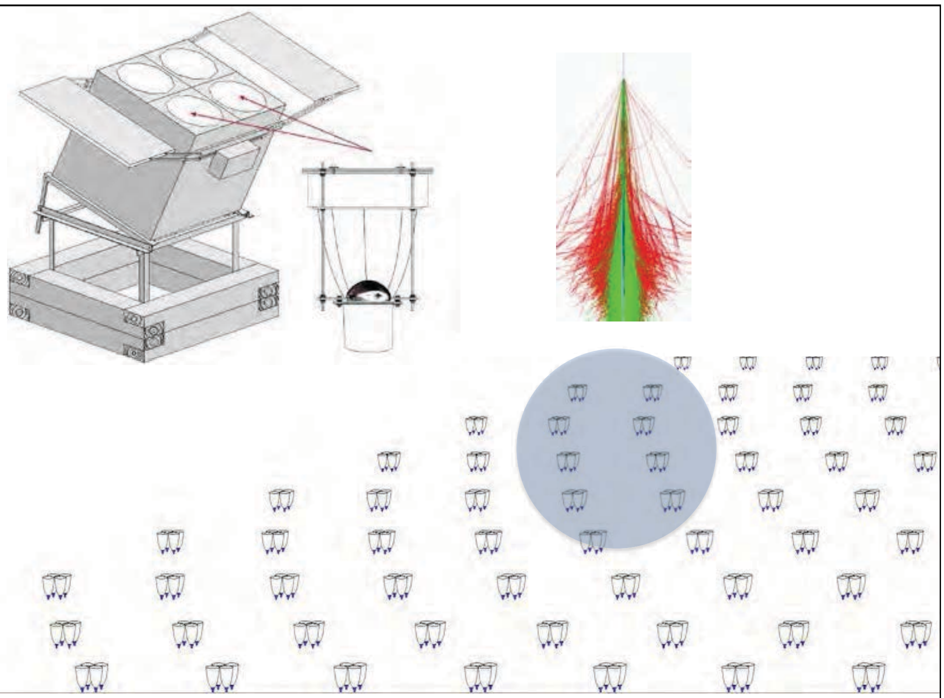

Tunka-HiSCORE → TAIGA

Tunka Advanced Instrument for Gamma ray and cosmic ray physics

10/2014: extension

- Total: 29 stations
- Tilting mode
- 0.25 km²

2015+:

- First telescope
- Hybrid timing+imaging
- In total 10 telescopes planned
- Muon detectors

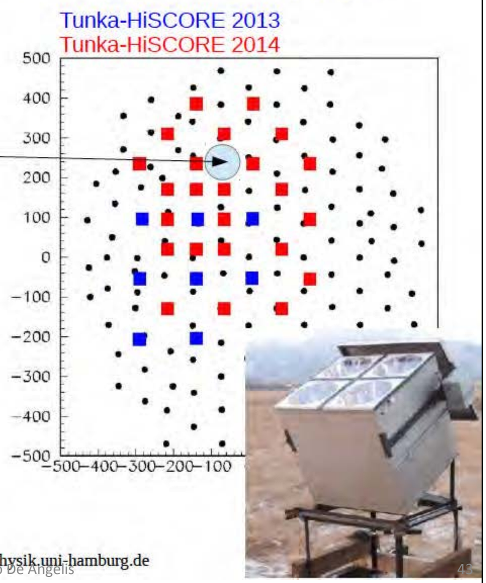

TAIGA Telescopes

- Dish: Davies-cotton tesselated, 34 mirrors (60cm)
- 4.3 m dish diameter
- 4.75 m focal length
- F/D ~ 1.2
- 397 PMT camera foV 8° (0.38° / pixel)
- Proven design components

September 3, 2014 martin.tluczy

- Planned: equip 0.2% of array area with Muon detectors

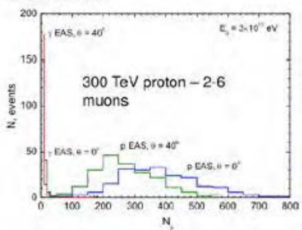

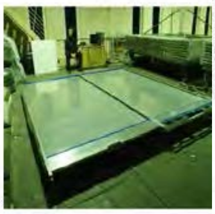

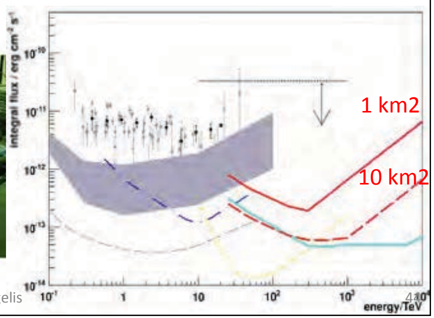

HAWC+, LHAASO, HiSCORE ~ funded, but there is a strong case for a sub-PeV experiment in the Southern hemisphere

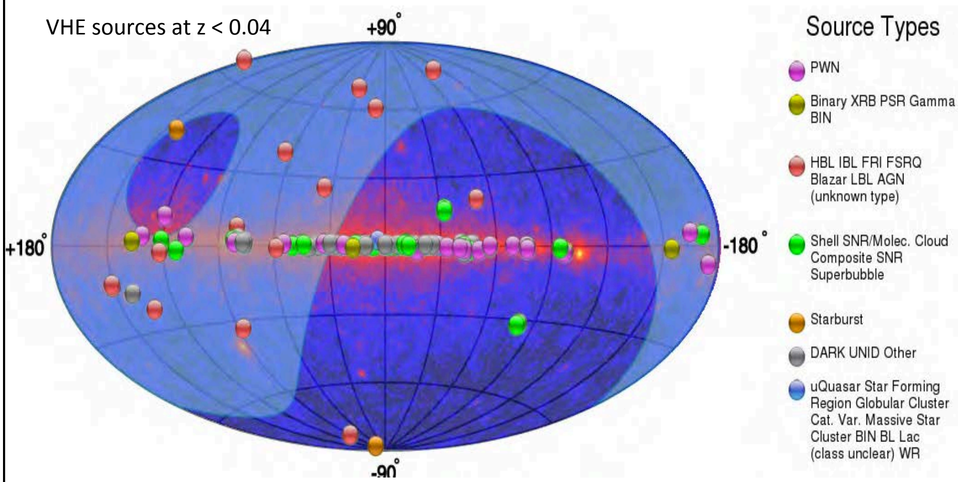

HAWC South

- 3rd generation water Cherenkov detector
- higher altitude, more sensitive than HAWC
- for example at the Alma site at 5,000 masl

Large Array Telescope for Tracking Energetic Sources (LATTES)

- Instrument a large area with closed-loop RPCs
  - Under test (MARTA)
- and Cherenkov tanks
  - Cherenkov can be water or glass, under test (CESAR)
- Proposal by CBPF Rio, LIP Lisboa, Univ. Padova & Udine (2014; to be reiterated in 2017)
- Possible sites
  - Argentina
  - Bolivia (Chacaltaya site, latitude 16.3 S, altitude 5200 m asl)
  - Chile (Atacama destert, latitude 23.7 S, altitude 5060 m asl)

The qualities of LATTES

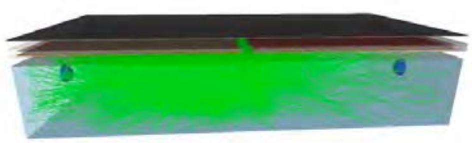

Figure 2: Basic detector station, with one WCD covered with RPCs and a thin slab of lead. The green lines show the tracks of the Cherenkov photons produced by the electron and positron from the conversion of a photon in the lead (for better visualisation the Tyvek's reflectivity was scaled by 1/10).

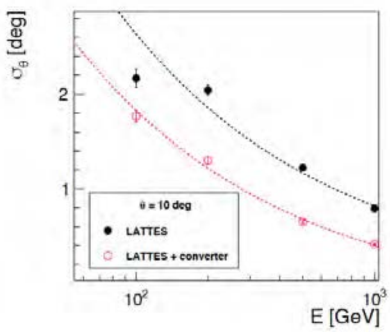

Goal: to reach sensitivity in the 100 GeV – 30 TeV region

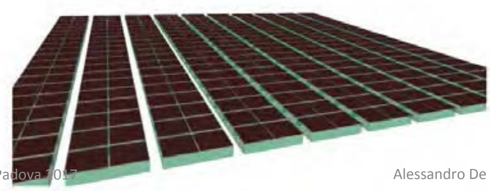

LOWER ENERGIES (GeV and MeV)

GeV region from space

- Fermi can fly till 2028 (granted till 2020)
- Difficult to find a successor…
- Only one super-Fermi project on the field: the Chinese-Italian HERD
  - A Fermi with better calorimetry
  - A few years after the CSS
  - Approved in 2017
- Also useful for observing charged cosmic rays up to ~ the knee

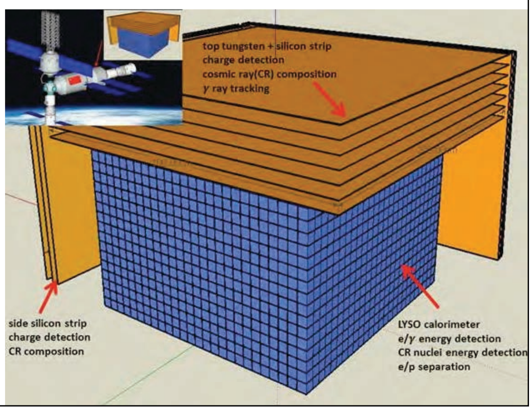

The MeV energies

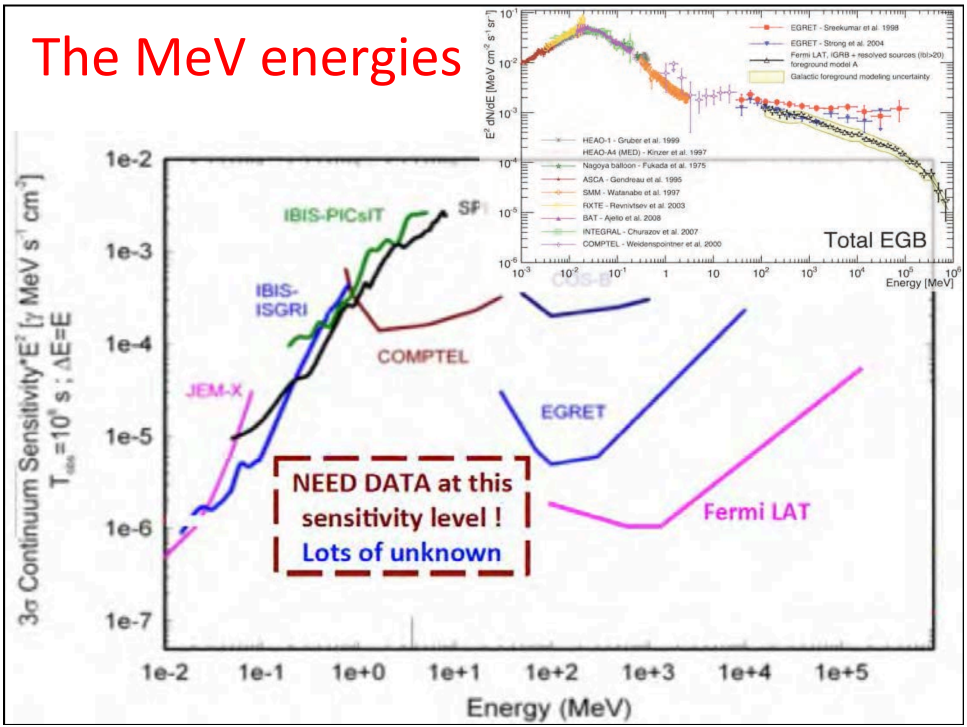

O(1 MeV)

- The MeV region is the less known, and its knowledge has large impact on the modeling of SEDs

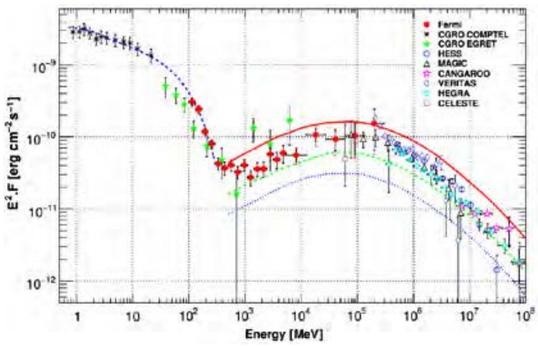

- As a bonus, Compton photons are naturally polarized

e-ASTROGAM (Europe, De Angelis et al.) and AMEGO (US, McEnery et al.) – 2028/29

1. Processes at the heart of the extreme Universe (AGNs, GRBs, microquasars): prospects for the Astronomy of the 2030s
   - Multi-wavelength, multi-messenger coverage of the sky (with CTA, SKA, eLISA, ν detectors...), with special focus on transient phenomena
2. The origin of high-energy particles and impact on galaxy evolution, from cosmic rays to antimatter
3. Nucleosynthesis and the chemical enrichment of our Galaxy

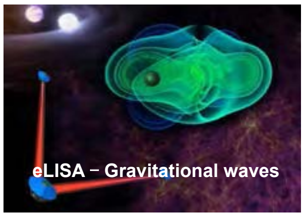

Km3Net/IceCube-Gen2 - ν

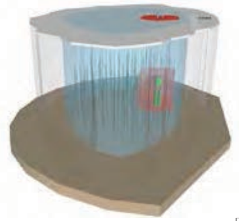

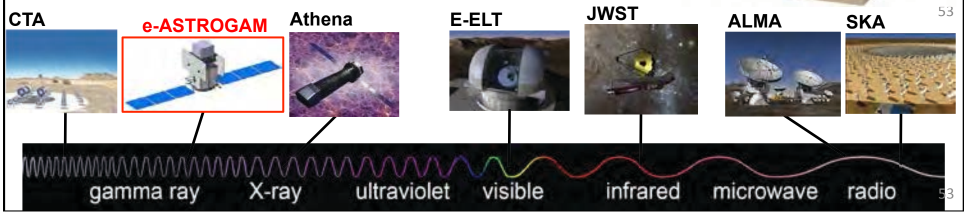

e-ASTROGAM scientific requirements

1. Achieve a sensitivity better than that of INTEGRAL/CGRO/COMPTEL by a factor of 20 - 50 – 100 in the range 0.2 – 30 MeV
2. Fully exploit gamma-ray polarization for both transient and steady sources
3. Improve significantly the angular resolution (to reach, e.g., ~ 10' at 1 GeV)
4. Achieve a very large field of view (~ 2.5 sr) ⇒ efficient monitoring of the γ-ray sky
5. Enable sub-millisecond trigger and alert capability for transients

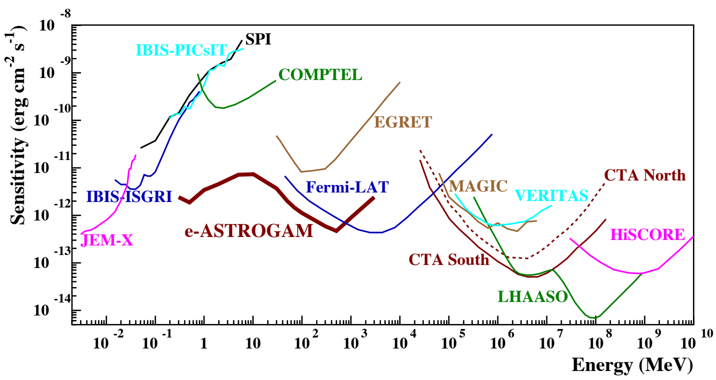

A. De Angelis, 1st e-ASTROGAM Workshop, Padova

How to measure gamma rays in the MeV-GeV?

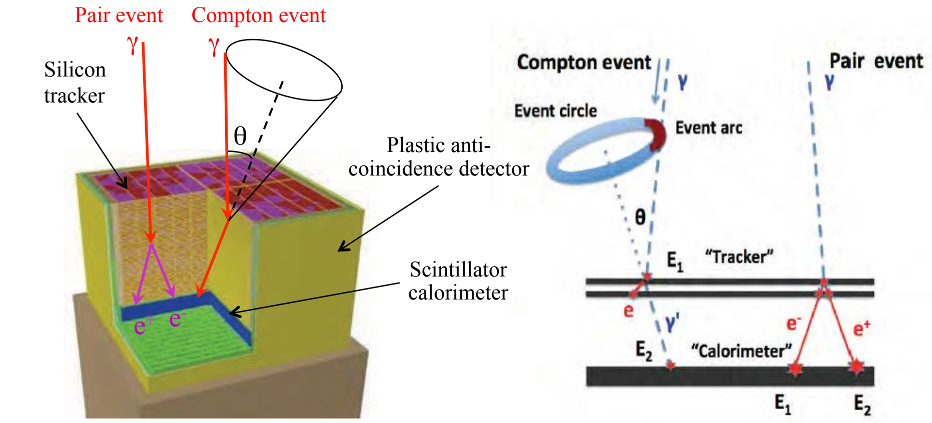

- **Tracker** – Double sided Si strip detectors (DSSDs) for excellent spectral resolution and fine 3-D position resolution (1m^2, 500 μm thick, 0.3 Xo in total)
- **Calorimeter** – High-Z material for an efficient absorption of the scattered photon $\Rightarrow$ CsI(Tl) scintillation crystals readout by Si drift detectors or photomultipliers for best energy resolution. 8 cm (4.3 Xo)
- **Anticoincidence detector** to veto charged-particle induced background $\Rightarrow$ plastic scintillators readout by Si photomultipliers

e-ASTROGAM discovery space

- Over 2/3 of the 3033 sources from the 3rd *Fermi* LAT Catalog (3FGL) have power-law spectra (E_γ > 100 MeV) steeper than E_γ^{-2}, implying that their peak energy output is below 100 MeV

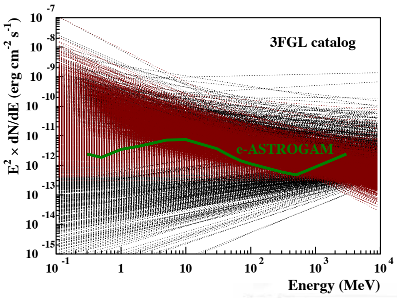

- These includes about 1100 (candidate) blazars and more than **720 unassociated sources**
- Most of these sources will be detected by **e-ASTROGAM** $\Rightarrow$ large discovery space for new sources and source classes

Type	3 yr	New sources
Total	3000 – 4000	~1800 (including GRBs)
Galactic	~ 1000	~400
MeV blazars	~ 350	~ 350
GeV blazars	1000 – 1500	~ 350
Other AGN (<10 MeV)	70 – 100	35 – 50
Supernovae	10 – 15	10 – 15
Novae	4 – 6	4 – 6
GRBs	~600	~600

UHE COSMIC RAYS

Upgrade of Auger (funded, to be completed in 2018)

- Auger's surface (3000 km2) unbeatable
- Upgrade in the next years: scintillators coupled to the tanks to improve the capability of hadron classification, presently based on the shower shape

New concepts: space

- Increase the effective area by looking from space
- Problem: lower threshold at some EeV
- The JEM-EUSO concept
- No clear schedule

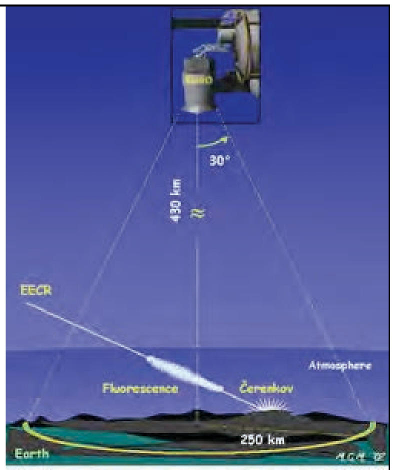

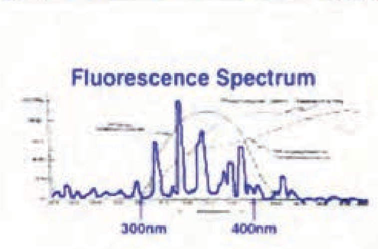

ASTROPHYSICAL NEUTRINOS

IceCube-Gen2, a ten-cubic-kilometer detector

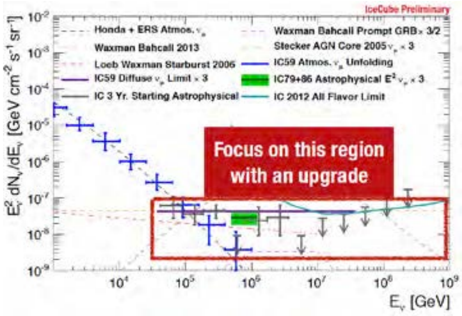

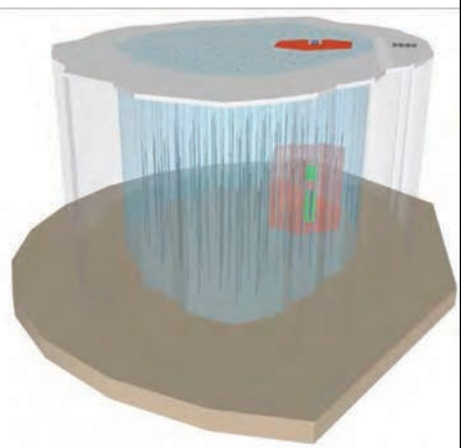

- Spacing between light sensors to exceed 250 meters, instead of the current 125 meters in IceCube. The IceCube-Gen2 instrumented volume might rapidly grow at modest costs.
- By roughly doubling the instrumentation already deployed, the telescope will achieve a tenfold increase in volume to about 10 cubic kilometers, aiming at an order of magnitude increase in neutrino detection rates.

Km3Net in the Mediterranean Sea

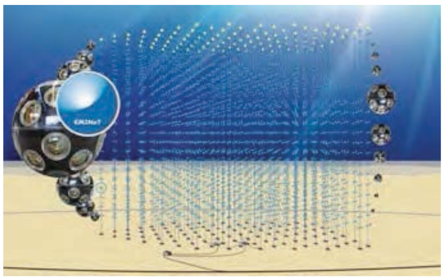

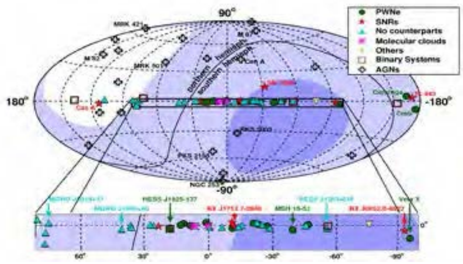

- Plan to reach ~5km^3
- Better angular resolution
- Better visibility of the GC region

Source Name	Source radius (°)	Visibility	Number of events per year For E_ν> 5 TeV	
			Signal ν	Atm ν
RX J1713.7–3946	0.7	0.74	4 – 11	6.4
RX J0852.0–4622	1.0	0.84	2 – 6	17
HESS J1745–303	0.2	0.66	0 – 22	1.4
HESS J1626–490	< 0.1	0.91	4 – 9	1.6
Vela X	0.4	0.81	4 – 15	3.5
Crab Nebula	< 0.1	0.39	1 – 3	0.8

CONCLUSIONS

- Gamma rays:
  - A rich panorama of gamma experiments at VHE gamma proposed for the future. CTA will lead the field.
    - Besides CTA, new techniques. Exploration of the PeV region is fundamental – and feasible. Northern projects approved, will produce nice science. Need to converge to a Southern 100 GeV-100 TeV EAS array.
  - In the longer term, need taking care of multiwavelength aspects: priorities are
    - A MeV mission (room for smart improvement; 2 missions proposed)
    - A successor of Fermi
- Multimessenger astronomy gamma/neutrinos can help our understanding of cosmic accelerators, of physics under extreme environments and of fundamental particle physics
  - Neutrino detectors will grow (at high price), and we know what we can get for astronomy
  - In a few years we'll know the impact of GW (cfr the dedicated lecture)
  - Auger to be upgraded, but new technologies look far away in time

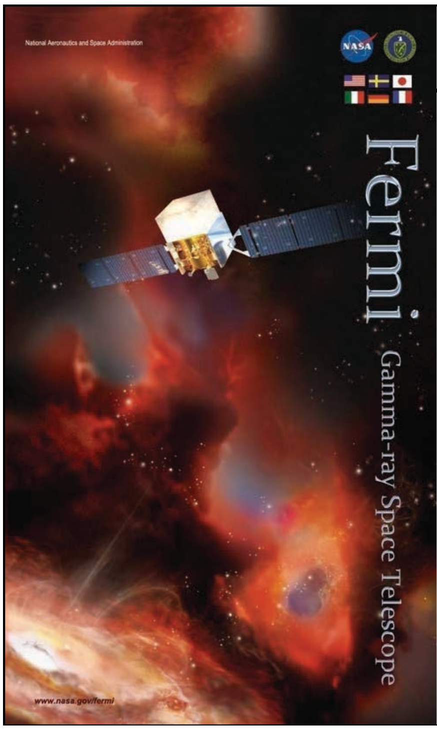

Tutorial on Fermi-LAT data analysis the case of 3c454.3

Francesco Longo
(University of Trieste and INFN Trieste)

Material from P.Bruel, M.Razzano, S.Buson and R.Desiante

PhD course 2017 – Padova

Outline

- Overview of the Fermi Large AreaTelescope
  - How it works
  - LAT data
  - LAT performance
- Fermi Science Tools
  - General Introduction
- Maximum Likelihood Overview
  - Source modeling
- One study case:
  - 3c454.3: analysis tutorial

2

Organization

- **Today**
  - Introduction to the LAT data analysis
  - LAT data introduction
  - LAT data exploration
  - LAT data preparation
  - Preparation of Sky models

- **Tomorrow**
  - Likelihood analysis of LAT data
  - Hands-on on an Extragalactic source
    - General LAT analysis with gtlike
    - Light curve with aperture photometry
    - SED (possibly)

The observatory

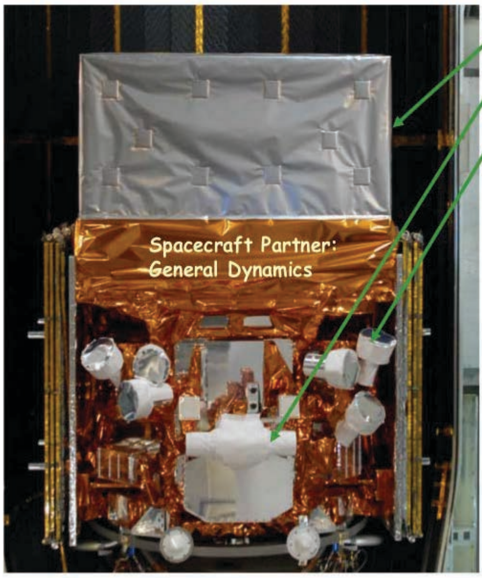

Large AreaTelescope (LAT)
20 MeV - >300 GeV

Gamma-ray Burst Monitor (GBM)
NaI and BGO Detectors
8 keV - 30 MeV

KEY FEATURES

- Huge field of view
  - –LAT: 20% of the sky at any instant; in sky survey mode, expose all parts of sky for ~30 minutes every 3 hours. GBM: whole unocculted sky at any time.
- Huge energy range, including largely unexplored band 10 GeV - 100 GeV. Total of >7 energy decades!
- Large leap in all key capabilities. Great discovery potential.

2

How the LAT works

- Precision Si-strip Tracker (TKR) Measure the photon direction; gamma ID.
- Hodoscopic CsI Calorimeter (CAL) Measure the photon energy; image the shower.
- Segmented Anticoincidence Detector (ACD) Reject background of charged cosmic rays; segmentation removes self-veto effects at high energy.
- Electronics System Includes flexible, robust hardware trigger and software filters.

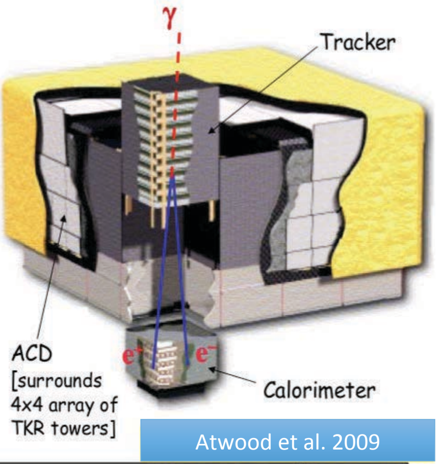

Systems work together to identify and measure the flux of cosmic gamma rays with energy 20 MeV - >300 GeV.

5

Operating Mode

- Primary observing mode is Sky Survey
  - Full sky every 2 orbits (3 hours)
  - Uniform exposure, with each region viewed for ~30 minutes every 2 orbits
  - Best serves majority of science, facilitates multiwavelength observation planning
  - Exposure intervals commensurate with typical instrument integration times for sources
  - EGRET sensitivity reached in days

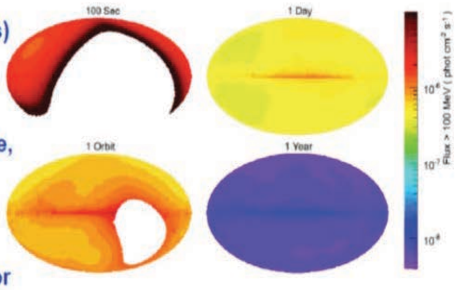

- Pointed observations when appropriate (selected by peer review in later years) with automatic earth avoidance selectable. Target of Opportunity pointing.
- Autonomous repoints for onboard GRB detections in any mode.

6

The Fermi Sky

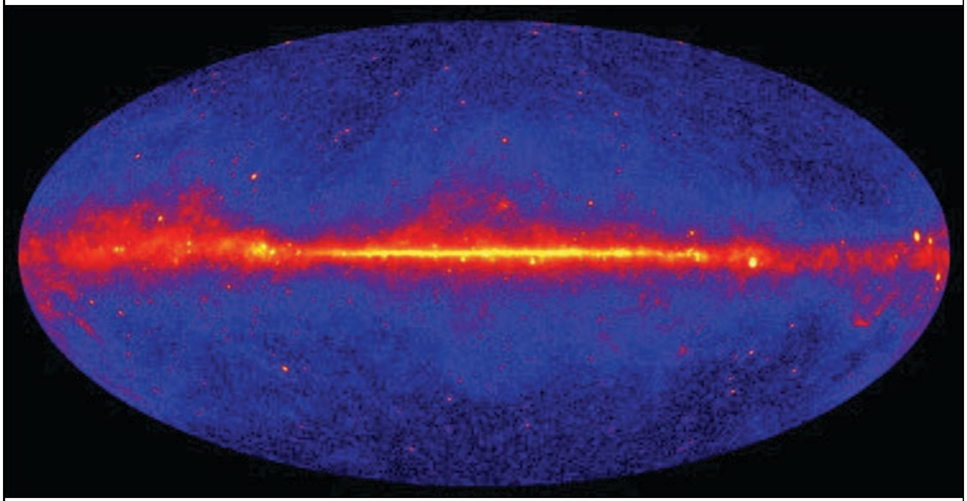

7

What do you need for the analysis

LAT DATA ARE PUBLIC!!

- **Data ...of course!**
  - LAT detected events
  - Spacecraft related stuff
  - Extras (Backgrounds , catalog sources, timing..)
- **Fermi Science Tools**
  - http://fermi.gsfc.nasa.gov/ssc/data/analysis/software/
- **Other ancillary tools**
  - ftools, HEASOFT, DS9 etc..
  - http://heasarc.gsfc.nasa.gov/docs/software.html
- **Lots and lots of scripts!**
  - Fermi tools are already scriptable
  - You can also use your favourite scripting language... but ..
  - Science Tools can be imported as Python modules!

8

4

LAT data analysis references

Fermi Data Analysis: starting points

Fermi Science Support Center: http://fermi.gsfc.nasa.gov/ssc/

Fermi Newsletters: http://fermi.gsfc.nasa.gov/ssc/resources/newsletter/

Fermi Data Access: http://fermi.gsfc.nasa.gov/cgi-bin/ssc/LAT/LATDataQuery.cgi

Fermi Science Tools Reference Manual:
http://fermi.gsfc.nasa.gov/ssc/data/analysis/scitools/references.html

Fermi Analysis Threads:
http://fermi.gsfc.nasa.gov/ssc/data/analysis/scitools/
http://fermi.gsfc.nasa.gov/ssc/data/analysis/documentation/Cicerone/

Fermi - LAT Likelihood Algorithm description
http://fermi.gsfc.nasa.gov/ssc/data/analysis/documentation/Cicerone/Cicerone_Likelihood/
Cash W. 1979, ApJ 228, 939
Mattox J. R. et al 1996, ApJ 461, 396
Protassov et al. 2002, ApJ 57, 545

LAT Performance Page: http://www-glast.slac.stanford.edu/software/IS/glast_lat_performance.htm
The Large Area Telescope on the Fermi Gamma-Ray Space Telescope Mission, W.B. Atwood, et. al., ApJ, 2009, 695, 1071.
The On-orbit Calibrations for the Fermi Large Area Telescope, A.A. Abdo, et al. arXiv:0904.2226v1

How to access LAT Data

http://fermi.gsfc.nasa.gov/ssc/data/analysis/

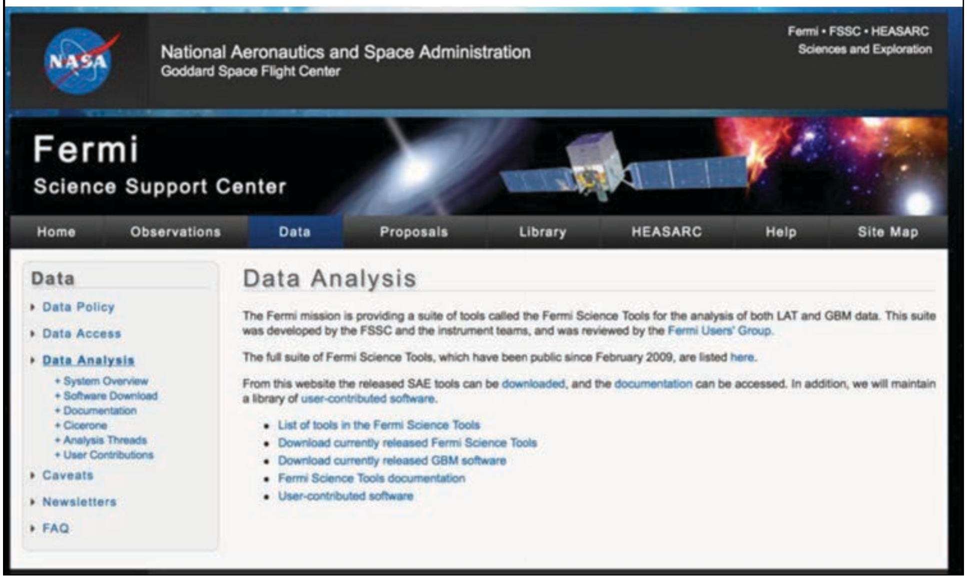

5

LAT Data

•LAT data products can be downloaded by the FSSC website

–**LAT Data server** http://fermi.gsfc.nasa.gov/cgi-bin/ssc/LAT/LATDataQuery.cgi

–**Archive of weekly files**

–ftp://legacy.gsfc.nasa.gov/fermi/data/

•Two main data products (stored in FITS format)

–**Events file (FT1)**

–**i. e. "what the LAT sees"**

– (photons, their energy, coordinates, time, event classes etc..)

–**Spacecraft files (FT2)**

–**i. e. "where the LAT is"**

– (position, angles..)

11

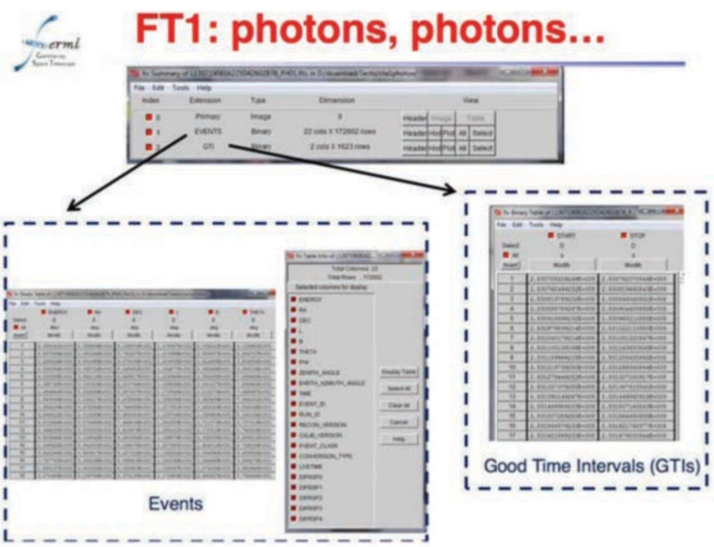

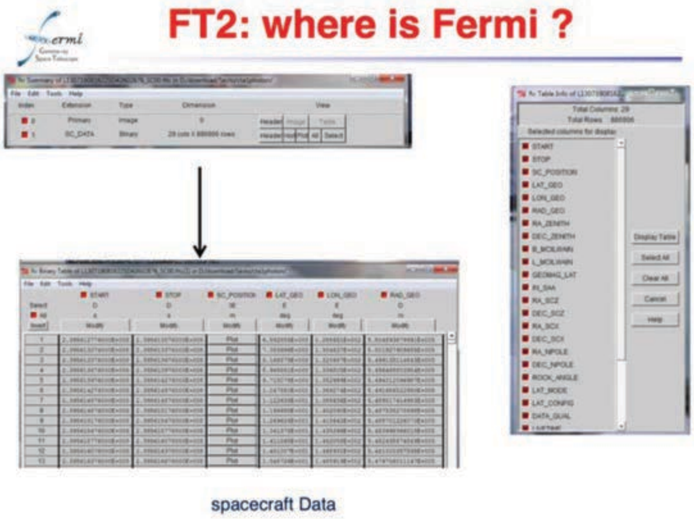

Extras - IRFs

- LAT Instrument Response Functions (IRFs)
  - Point Spread Function (PSF)
  - Effective Area
  - Energy Resolution

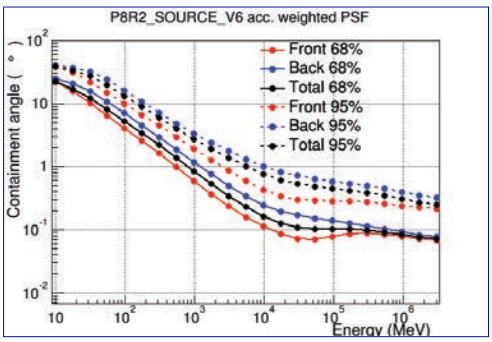

- Highly dependent on energy
- and arrival direction of incident
- photon

- Fundamental for analysis!!

- http://www.slac.stanford.edu/exp/glast/groups/canda/lat_Performance.htm

16

Pass8 (?)...

New Pass8 data


Fermi
Science Support Center

Home | Observations | Data | Proposals | Library | HEASARC | Help | Site Map

Data
- Data Policy
- Data Access
- Data Analysis
  - System Overview
  - Software Download
  - Documentation
  - Cicerone
  - Analysis Threads
  - User Contributions
- Caveats
- Newsletters
- FAQ

Using LAT's New Pass 8 Data

The FSSC is now serving Pass 8 LAT data for analysis. The new version of LAT data provides a number of improvements over the reprocessed Pass 7 data, and is considered the best dataset for all types of LAT analysis. As of the release date (June 24, 2015) reprocessed Pass 7 data is no longer being served. However, existing Pass 7 reprocessed data has been archived and is available from the FSSC's FTP server.

Pass 8 provides a full reprocessing of the entire mission dataset, including improved event reconstruction, a wider energy range, better energy measurements, and significantly increased effective area. In addition, the events have been evaluated for their measurement quality in both position and energy. This allows the user to select a subset of the events if appropriate to improve analysis results. To support the use of these data selections, there have been some structural changes to the *Fermi* Science Tools.

Here we discuss the changes to the data and tools, and how they affect your analysis.

Pass 8 Bottom Line

Pass 8 contains a lot of changes, and the rest of this page may seem overwhelming. If you just want to get started doing a standard LAT analysis, here's the bottom line:

- Recommended event class for source analysis is "P8 Source" class (*evclass*=128).
- Add evtype parameter to your gtselect call (*convtype* parameter is deprecated). Recommended event type for source analysis is "FRONT+BACK" (*evtype*=3).
- Recommended zenith angle cut to eliminate Earth limb events ("zmax") is 90 degrees for events at 100 MeV and above.
- Recommended source list for analysis is the 3FGL Catalog. A python script is available at the User-Contributed Tools page that creates XML model files using the 3FGL catalog FITS file.

http://fermi.gsfc.nasa.gov/ssc/data/analysis/documentation/Pass8_usage.html

Fermi Gamma-ray Space Telescope

Pass 8 introduction

What does Pass mean?

- Each pass corresponds to a version of the Fermi LAT data
- It implies a whole package:
  - Intrument simulation
  - Reconstruction code
  - Event selection
  - Instrument Response Functions (IRFs)
  - Systematic uncertainties
  - Isotropic template (which includes the cosmic-ray residual background)
  - And sometimes more (Galactic diffuse model, Earth limb template, Sun+Moon template)
- It's only when we have validated the whole package that we can release it to the public.

Fermi Gamma-ray Space Telescope

Pass8 introduction

From Pass 6 to Pass 8

- Pass 6 (launch time)
  - Pass 6 reconstruction
  - Pass 6 selection
  - Based on pre-launch instrument simulation
  - First data revealed the issue of out-of-time pile-up (aka ghosts)
  - New: instrument simulation with ghosts -> correct IRFs
- Pass 7
  - Pass 6 reconstruction
  - New: Pass 7 selection optimized with simulations with ghosts
- Pass 8
  - New: improved instrument simulation
  - New: Pass 8 reconstruction, as ghost-proof as possible
  - New: Pass 8 selection

9

Pass8 Introduction

Pass 8 improvements

- Ghost handling
  - Tracker: ignoring ghost hits
  - ACD: partial deghosting
  - Calorimeter: clustering and cluster classification
- Improved direction measurement
  - Tree-based track finder
- Improved energy measurement
  - Extension of the energy range: from ~10 MeV to ~3 TeV
- Improved track/ACD matching information
  - Using the uncertainty of the tracker direction
- Improved event selection
  - Using the ROOT TMVA package (tmva.sourceforge.net)
- Additional sub-classes of events

Pass8 performance

http://www.slac.stanford.edu/exp/glast/groups/canda/lat_Performance.htm

Effective Area

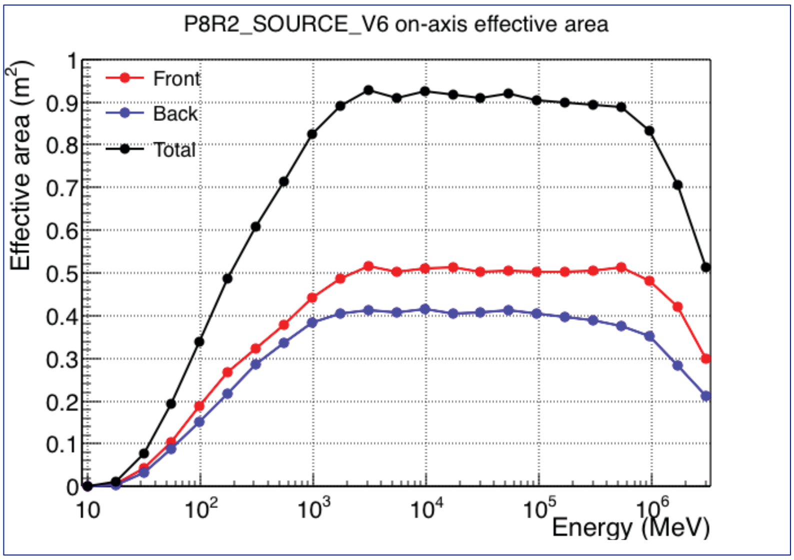

Pass8 Effective Area

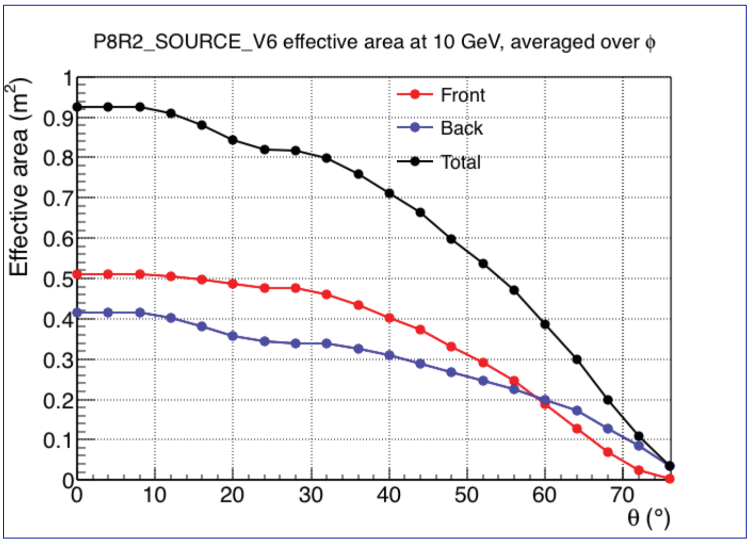

11

Point Spread Function

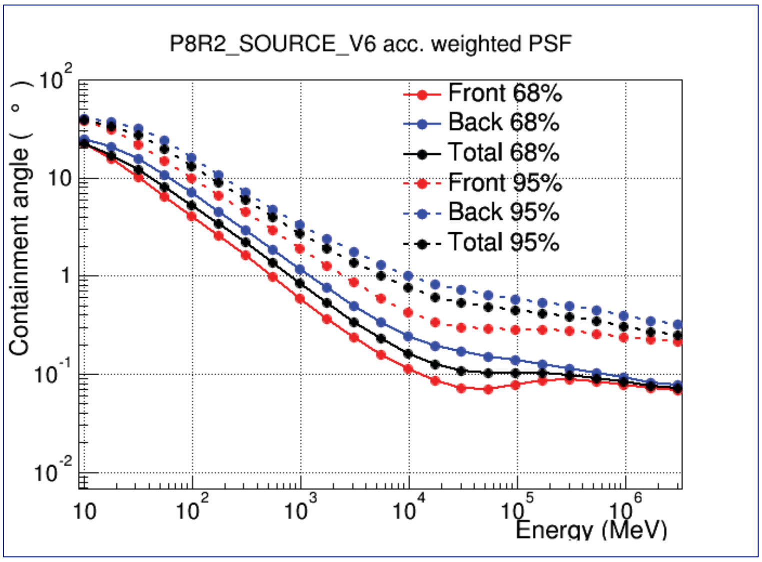

Point Spread Function

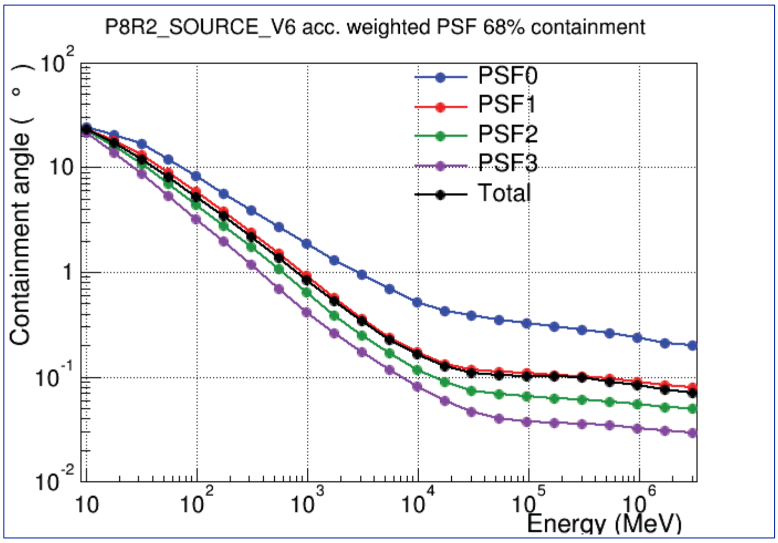

Energy resolution

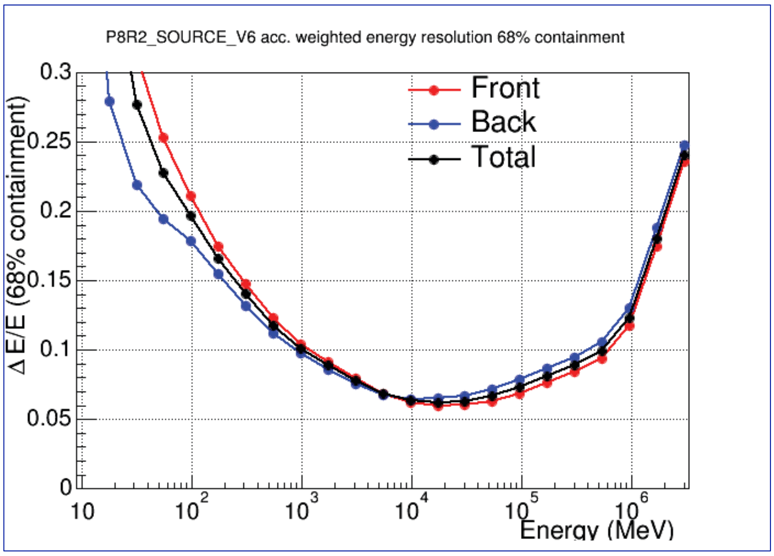

Energy resolution

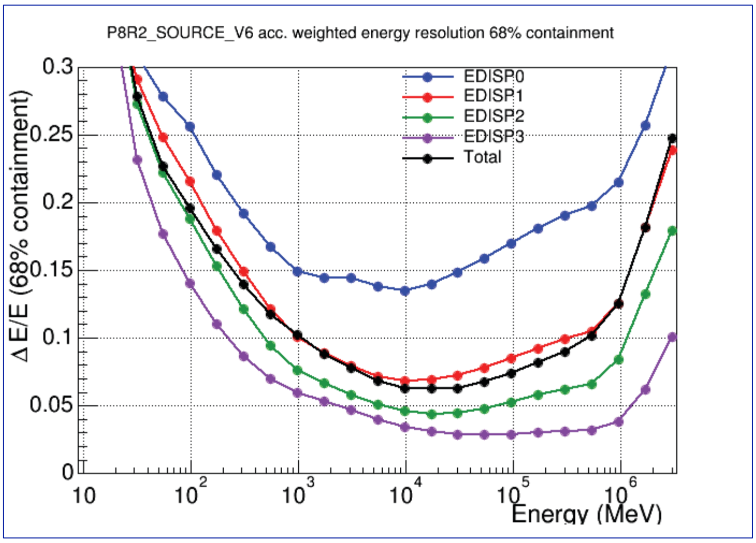

Extras

•Diffuse models (.txt & FITS files)

–To correctly take into accounts the galactic and extagalactic backgrounds

–http://fermi.gsfc.nasa.gov/ssc/data/access/lat/BackgroundModels.html

• Source Catalogs (3FGL, 3FHL, PSRs, GRB, SNR …)

• Region of Interest model definition (stored in XML files)

- More on this later …

•Choose the proper combination of

- event classes based on the probability of being a photon and background level
  - TRANSIENT (for very short events)
  - SOURCE (suggested for source analysis)
  - CLEAN and ULTRACLEAN (lowest particle contamination – for diffuse sources analysis)
- Event types based on conversion point or PSF or Energy reconstruction

36

LAT background models

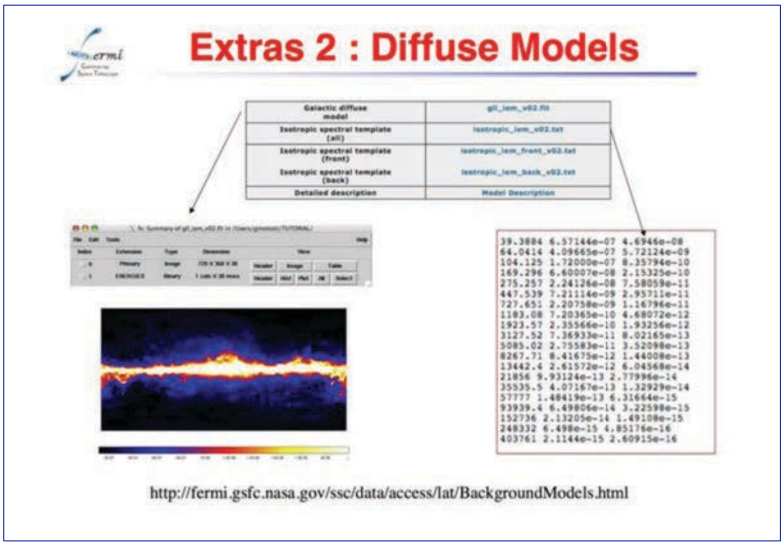

LAT background models

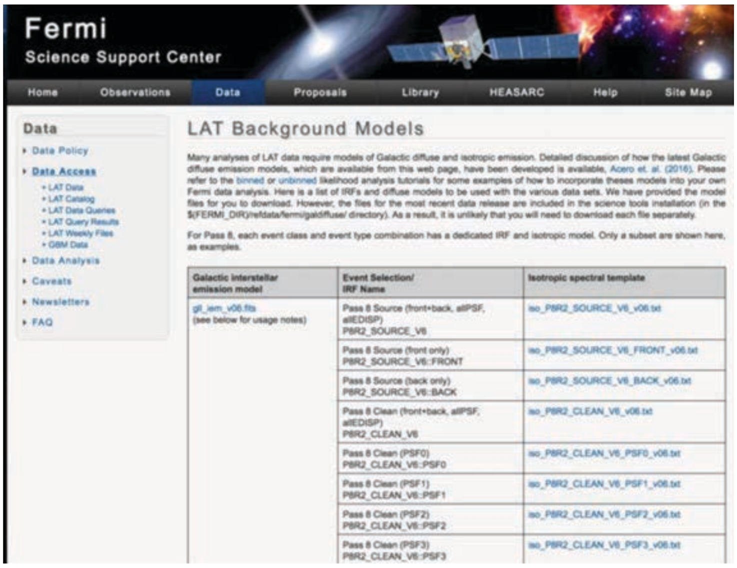

Fermi
Science Support Center

Home | Observations | Data | Proposals | Library | HEASARC | Help | Site Map

Data
- Data Policy
- Data Access
  - LAT Data
  - LAT Catalog
  - LAT Data Queries
  - LAT Query Results
  - LAT Weekly Files
  - GBM Data
- Data Analysis
- Caveats
- Newsletters
- FAQ

LAT Background Models

Many analyses of LAT data require models of Galactic diffuse and isotropic emission. Detailed discussion of how the latest Galactic diffuse emission models, which are available from this web page, have been developed is available, Acero et. al. (2016). Please refer to the binned or unbinned likelihood analysis tutorials for some examples of how to incorporate theses models into your own Fermi data analysis. Here is a list of IRFs and diffuse models to be used with the various data sets. We have provided the model files for you to download. However, the files for the most recent data release are included in the science tools installation (in the $(FERMI_DIR)/refdata/fermi/galdiffuse/ directory). As a result, it is unlikely that you will need to download each file separately.

For Pass 8, each event class and event type combination has a dedicated IRF and isotropic model. Only a subset are shown here, as examples.

Galactic interstellar emission model	Event Selection/ IRF Name	Isotropic spectral template
gll_iem_v06.fits (see below for usage notes)	Pass 8 Source (front+back, allPSF, allEDISP) P8R2_SOURCE_V6	iso_P8R2_SOURCE_V6_v06.txt
	Pass 8 Source (front only) P8R2_SOURCE_V6::FRONT	iso_P8R2_SOURCE_V6_FRONT_v06.txt
	Pass 8 Source (back only) P8R2_SOURCE_V6::BACK	iso_P8R2_SOURCE_V6_BACK_v06.txt
	Pass 8 Clean (front+back, allPSF, allEDISP) P8R2_CLEAN_V6	iso_P8R2_CLEAN_V6_v06.txt
	Pass 8 Clean (PSF0) P8R2_CLEAN_V6::PSF0	iso_P8R2_CLEAN_V6_PSF0_v06.txt
	Pass 8 Clean (PSF1) P8R2_CLEAN_V6::PSF1	iso_P8R2_CLEAN_V6_PSF1_v06.txt
	Pass 8 Clean (PSF2) P8R2_CLEAN_V6::PSF2	iso_P8R2_CLEAN_V6_PSF2_v06.txt
	Pass 8 Clean (PSF3) P8R2_CLEAN_V6::PSF3	iso_P8R2_CLEAN_V6_PSF3_v06.txt

LAT catalogs

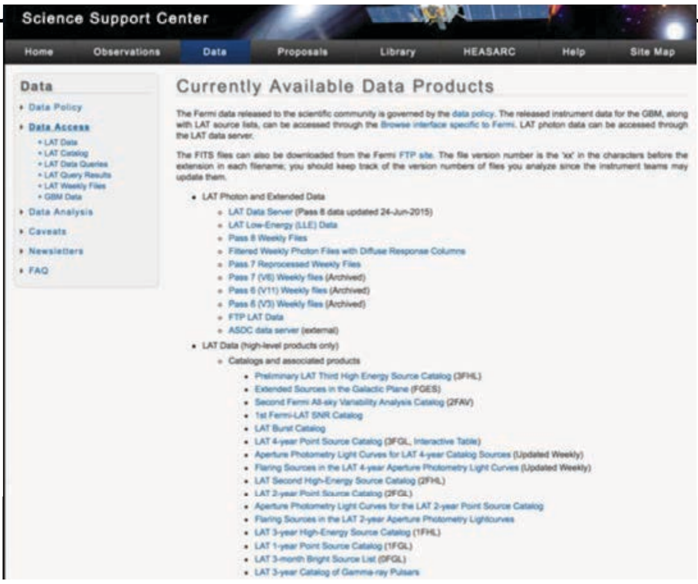

Science Support Center

Home | Observations | Data | Proposals | Library | HEASARC | Help | Site Map

Data
- Data Policy
- Data Access
  - LAT Data
  - LAT Catalog
  - LAT Data Queries
  - LAT Query Results
  - LAT Weekly Files
  - GBM Data
- Data Analysis
- Caveats
- Newsletters
- FAQ

Currently Available Data Products

The Fermi data released to the scientific community is governed by the data policy. The released instrument data for the GBM, along with LAT source lists, can be accessed through the Browse interface specific to Fermi. LAT photon data can be accessed through the LAT data server.

The FITS files can also be downloaded from the Fermi FTP site. The file version number is the 'xx' in the characters before the extension in each filename; you should keep track of the version numbers of files you analyze since the instrument teams may update them.

- LAT Photon and Extended Data
  - LAT Data Server (Pass 8 data updated 24-Jun-2015)
  - LAT Low-Energy (LLE) Data
  - Pass 8 Weekly Files
  - Filtered Weekly Photon Files with Diffuse Response Columns
  - Pass 7 Reprocessed Weekly Files
  - Pass 7 (V6) Weekly files (Archived)
  - Pass 6 (V11) Weekly files (Archived)
  - Pass 6 (V3) Weekly files (Archived)
  - FTP LAT Data
  - ASDC data server (external)
- LAT Data (high-level products only)
  - Catalogs and associated products
    - Preliminary LAT Third High Energy Source Catalog (3FHL)
    - Extended Sources in the Galactic Plane (FGES)
    - Second Fermi All-sky Variability Analysis Catalog (2FAV)
    - 1st Fermi-LAT SNR Catalog
    - LAT Burst Catalog
    - LAT 4-year Point Source Catalog (3FGL, Interactive Table)
    - Aperture Photometry Light Curves for LAT 4-year Catalog Sources (Updated Weekly)
    - Flaring Sources in the LAT 4-year Aperture Photometry Light Curves (Updated Weekly)
    - LAT Second High-Energy Source Catalog (2FHL)
    - LAT 2-year Point Source Catalog (2FGL)
    - Aperture Photometry Light Curves for the LAT 2-year Point Source Catalog
    - Flaring Sources in the LAT 2-year Aperture Photometry Lightcurves
    - LAT 3-year High-Energy Source Catalog (1FHL)
    - LAT 1-year Point Source Catalog (1FGL)
    - LAT 3-month Bright Source List (0FGL)
    - LAT 3-year Catalog of Gamma-ray Pulsars

https://fermi.gsfc.nasa.gov/ssc/data/access/

Event types

P8R2 Event Type Name	Event Type Partition	Event Type Value (evtype)
FRONT	Conversion Type	1
BACK	Conversion Type	2
PSF0	PSF	4
PSF1	PSF	8
PSF2	PSF	16
PSF3	PSF	32
EDISP0	EDISP	64
EDISP1	EDISP	128
EDISP2	EDISP	256
EDISP3	EDISP	512

Event classes

P8R2 IRF name	Event Class (evclass)	Class Hierarchy	Photon File	Extended File
P8R2_ULTRACLEANVETO_V6	1024	Standard	X	X
P8R2_ULTRACLEAN_V6	512	Standard	X	X
P8R2_CLEAN_V6	256	Standard	X	X
P8R2_SOURCE_V6	128	Standard	X	X
P8R2_TRANSIENT010_V6	64	Standard		X
P8R2_TRANSIENT020_V6	16	Standard		X
P8R2_TRANSIENT010E_V6	64	Extended		X
P8R2_TRANSIENT020E_V6	8	Extended		X
P8R2_TRANSIENT015S_V6	65536	No-ACD		X

Recommendations

Event Selection Recommendations (P8R2)

Analysis Type	Minimum Energy (emin)	Maximum Energy (emax)	Max Zenith Angle (zmax)	Event Class (evclass)	IRF Name
Galactic Point Source Analysis	100 (MeV)	500000 (MeV)	90 (degrees)	128	P8R2_SOURCE_V6
Off-plane Point Source Analysis	100 (MeV)	500000 (MeV)	90 (degrees)	128	P8R2_SOURCE_V6
Burst and Transient Analysis (<200s)	100 (MeV)	500000 (MeV)	100 (degrees)	16	P8R2_TRANSIENT020_V6
Galactic Diffuse Analysis	100 (MeV)	500000 (MeV)	90 (degrees)	128	P8R2_SOURCE_V6
Extra-Galactic Diffuse Analysis	100 (MeV)	500000 (MeV)	90 (degrees)	1024	P8R2_ULTRACLEANVETO_V6
Impulsive Solar Flare Analysis	100 (MeV)	500000 (MeV)	100 (degrees)	65536	P8R2_TRANSIENT015S_V6

Caveats

Caveats About Analyzing LAT Pass 8 Data

These caveats are relevant for the P8R2 version of the Pass 8 photon dataset. They are an updated version of previous sets of caveats for analysis of Pass 7 reprocessed (P7REP), Pass7 (P7_V6) and Pass 6 (P6_V3 and P6_V11) event selections and Instrument Response Functions (IRFs).

The LAT team is still working to validate all aspects of Pass 8 data and analysis. As a consequence it is expected that, in the coming year, the range of application of Pass 8 data will be increased, the tools and files will be improved and the systematic uncertainties will be decreased. These caveats will be modified accordingly.

The P8R2_V6 IRFs are defined between 5.62 MeV and 3.16 TeV but that does not mean that they have been fully validated over this whole energy range. Following the Pass 7 validation effort, the LAT team has started performing studies in order to check the consistency and precision of the instrument simulation and the instrument response representation provided by the IRFs. These studies are based on the analysis of Vela (E < 10 GeV), bright AGN (3 GeV < E < 100 GeV) and the Earth limb (E > 10 GeV). They include:

- comparing the distributions of reconstructed quantities between data and the simulation of the instrument for a given selection (e.g. SOURCE class)
- comparing the fraction of events of a loose selection (e.g. TRANSIENT020 class) that are accepted in a more stringent selection (e.g. SOURCE class) in data and as predicted by the instrument simulation or the IRFs
- comparing the fraction of events in each event type for a given selection in data and as predicted by the instrument simulation or the IRFs
- comparing the radial profiles of a point source in data and as predicted by the IRFs

http://fermi.gsfc.nasa.gov/ssc/data/analysis/LAT_caveats.html

Overview of Fermi Science Tools

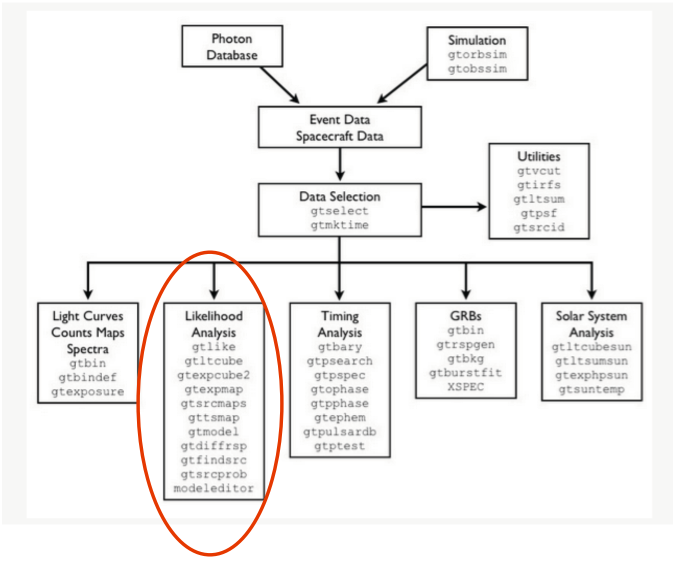

44

Maximum Likelihood Overview

45

Maximum likelihood technique

Given a set of observed data:

→ Produce a model that accurately describes the data, including parameters that we wish to estimate

→ derive the probability (density) for the data given the model (PDF)

→ treat this as a function of the model parameters (likelihood function)

→ maximize the likelihood with respect to the parameters - ML estimation.

46

Maximum likelihood ingredients

Data: $X = \{x_i\} = \{x_1, x_2, ..., x_N\}$

Model parameters: $\Theta = \{\theta_j\} = \{\theta_1, \theta_2, ..., \theta_M\}$

Likelihood: $\mathcal{L}(\Theta|X) = P(X|\Theta)$

Conditional probability rule for independent events: $P(A,B) \underset{\text{CPR}}{=} P(A)P(B|A) \underset{\text{Independence}}{=} P(A)P(B)$

For independent data:

$$P(X|\Theta) = P(\{x_i\}|\Theta) = P(x_1|\Theta)P(x_2,..,x_N|\Theta) = \cdots$$
$$= P(x_1|\Theta)P(x_2|\Theta)\cdots P(x_N|\Theta) = \prod_i P(x_i|\Theta)$$

$$\mathcal{L}(\Theta|X) = \prod_i P(x_i|\Theta)$$

$\mathcal{L}$ is the product of the probability of observing the detected counts in each bin.

47

Fermi Gamma-ray Space Telescope

Maximum likelihood estimation

Parameters can be estimated by maximizing likelihood.

→ Easier to work with log-likelihood:

$$\boxed{\ln \mathcal{L}(\Theta) = \ln \mathcal{L}(\Theta|X) = \sum_i \ln P(x_i|\Theta)}$$

Estimates of $\{\hat{\theta}_k\}$ from solving simultaneous equations: $\boxed{\left.\frac{\partial \ln \mathcal{L}}{\partial \theta_j}\right|_{\{\hat{\theta}_k\}} = 0}$

For one parameter, if we have: $\mathcal{L}(\theta) \sim e^{-\frac{(\theta-\hat{\theta})^2}{2\sigma_\theta^2}}$ **Gaussian approximation**

then: $\left.\frac{\partial^2 \ln \mathcal{L}}{\partial \theta^2}\right|_{\hat{\theta}} = -\frac{1}{\sigma_\theta^2}$

so 2nd derivative is related to "errors"

48

Fermi Gamma-ray Space Telescope

The Challenge

- Gamma-ray data is a list of counts (photons) reconstructed in the detector.
- Qualitative exploration of the data suggests the presence of sources (spatial clustering).
- Quantitative analysis requires evaluating the significance of a 'model' of our region.

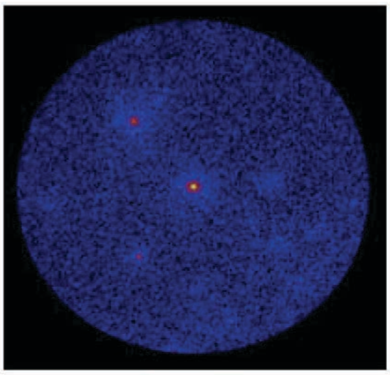

Count Map

49

20

Fermi
Gamma-ray Space Telescope

The Procedure

- Basically the initial ‘**model**’ is a guess of the various parameters of the sources in our region:
  - location
  - spectral shape
  - flux
  - etc.
- The guess can be easier if you have a starting point like the 2FGL (3FGL).
- We quantify (using the Likelihood Method) the <u>statistical significance of the model</u> and <u>vary the parameters to determine the most likely parameter values</u>.

50

Fermi
Gamma-ray Space Telescope

Why Model Fitting?

- We use the Likelihood method because the LAT data are limited by statistics, a bright diffuse background and a broad PSF.
- The model construction defines the questions we want to ask which means:
  - <u>It will not answer a question you are not asking</u> (ie. unknown parameters).
- The Likelihood will <u>not tell you if a fit is ‘good’</u>. If the model does not represent your data well, the results will also not represent reality well.

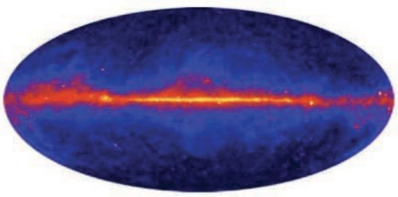

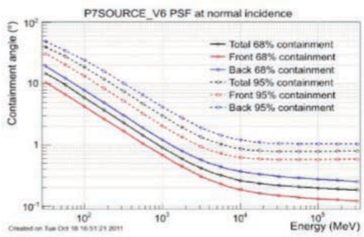

51

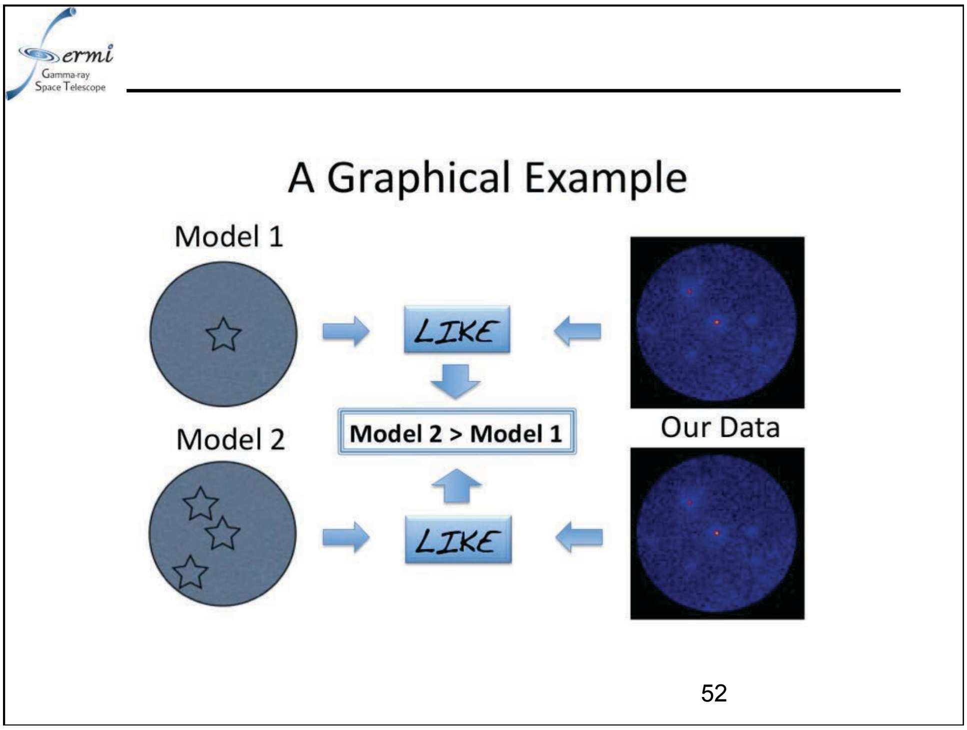
Fermi
Gamma-ray Space Telescope
A Graphical Example
Model 1
LIKE
Model 2 > Model 1
Our Data
Model 2
LIKE
52

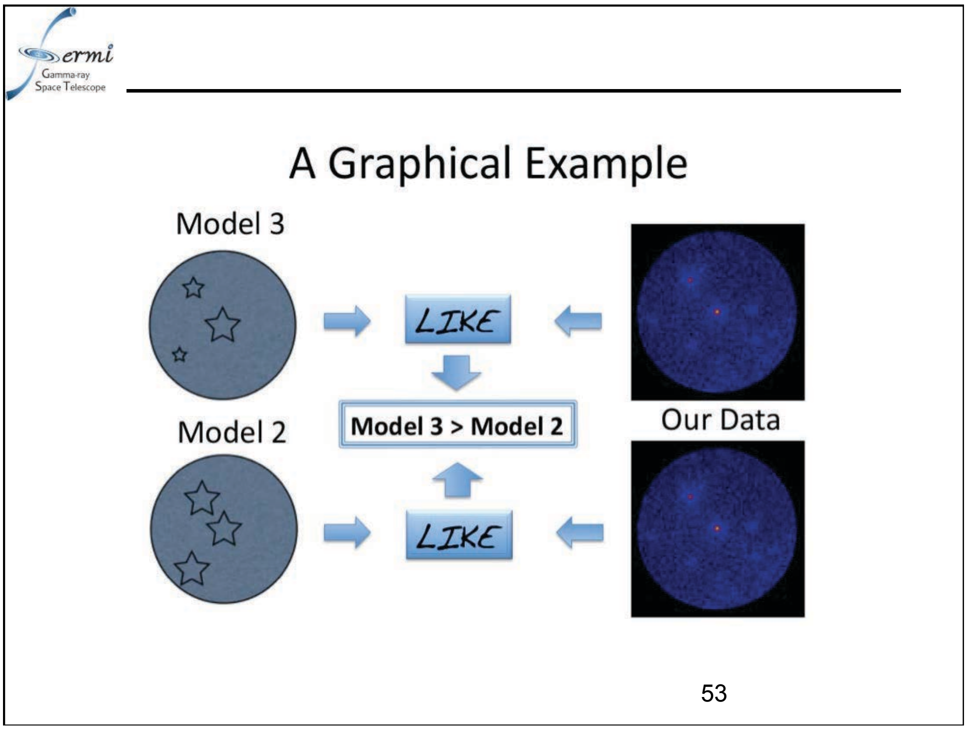
Fermi
Gamma-ray Space Telescope
A Graphical Example
Model 3
LIKE
Model 3 > Model 2
Our Data
Model 2
LIKE
53

Fermi
Gamma-ray Space Telescope

Likelihood Analysis

- The likelihood $\mathcal{L}$ is the probability of obtaining your data given an input model.
- In our case, the input model is the distribution of gamma-ray sources on the sky and includes their intensity and spectra.
- One will maximize $\mathcal{L}$ to get the best match of the model to the data. Given a set of data, one can bin them in multidimensional (energy, sky pixels, ...) bins.
- $\mathcal{L}$ is the product of the probabilities of observing the detected counts in each bin.

$$\mathcal{L} = \Pi p_k$$

54

Fermi
Gamma-ray Space Telescope

Write L as a function of the source model

- The source model is folded with the IRFs in order to obtain the predicted number of counts

- The IRFs can be decomposed into three funtions: Effective Area (proj area of the detector * efficency), Energy Dispesion, Point Spread Function

- Small number of counts in each bin --> Poisson distribuiton

- Bin size infinitesimally small

- Assume only steady source for standard analysis

The function to maximize is:

$$\log \mathcal{L} = \sum_j \log M(E'_j, \hat{p}'_j, t_j) - N_{\rm pred}$$

where the sum is performed over photons in the ROI. The predicted number of counts is $N_{\rm pred} = \int_{\rm ROI} dE' d\hat{p}' \, dt M(E', \hat{p}', t)$

55

Test Statistic

Null hypothesis max likelihood, h parameters

$$\mathrm{TS} = -2\ \log \frac{\mathcal{L}_0}{\mathcal{L}_1} \underset{N\to\infty}{\to} \chi^2_{m-h}$$

non fixed parameters

Alternative hypothesis max likelihood, m parameters

- In the limit of a large number of counts, Wilk's Theorem states that the TS for the null hypothesis is asymptotically distributed as χ_n^2 where n is the number of parameters characterizing the additional source.
- As a basic rule of thumb, the square root of the TS is approximately equal to the detection significance for a given source.

56

Summarizing

- Observed a photon from a location, at a time, with an energy.
- Assume a model: $S(E,\hat{p},t) = \sum_i \underbrace{s_i(E,t)\delta(\hat{p}-\hat{p}_i)}_{\text{Point Sources}} + \underbrace{S_G(E,\hat{p}) + S_{eg}(E,\hat{p})}_{\text{Galactic \& EG diffuse Sources}} + \underbrace{\sum_l S_l(E,\hat{p},t)}_{\text{Other Sources}}$.
- Calculate the probability of that photon being detected assuming our model: $M(E',\hat{p}',t) = \int_{SR} dE d\hat{p} R(E',\hat{p}',t;E,\hat{p})S(E,\hat{p},t)$
- Calculate the total number of predicted counts assuming our model.

$$N_{\mathrm{pred}} = \int_{\mathrm{ROI}} dE' d\hat{p}'\, dt M(E',\hat{p}',t)$$

- Adjust the model until this is maximized:

$$\log \mathcal{L} = \sum_j \log M(E'_j,\hat{p}'_j,t_j) - N_{\mathrm{pred}}$$

- Calculate the TS:

$$\mathrm{TS} = -2\ \log \frac{\mathcal{L}_0}{\mathcal{L}_1} \underset{N\to\infty}{\to} \chi^2_{m-h}$$

57

Keep in mind that ..

- Many variables may be calculated BEFORE selecting the models
- Very important to have a reliable model
- Absolute value of likelihood meaningless!
  - Likelihood function has no meaning itself, e.g., it is not a probability. Its usefulness comes from theorems such as the LRT.
- Comparison between model w/ and w/o source to reject null hypothesis = no source (TS large → reject null hypothesis)

58

Analysis Tutorial

70

Blazar one of … 3c454.3's record flares!

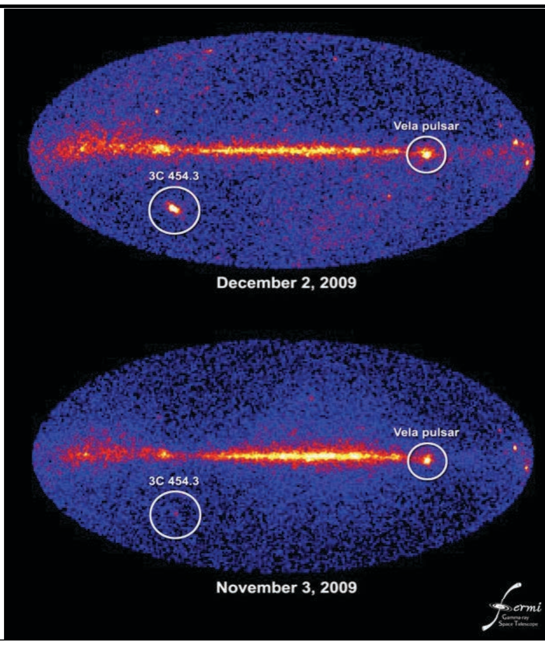

How to download data

http://fermi.gsfc.nasa.gov/cgi-bin/ssc/LAT/LATDataQuery.cgi

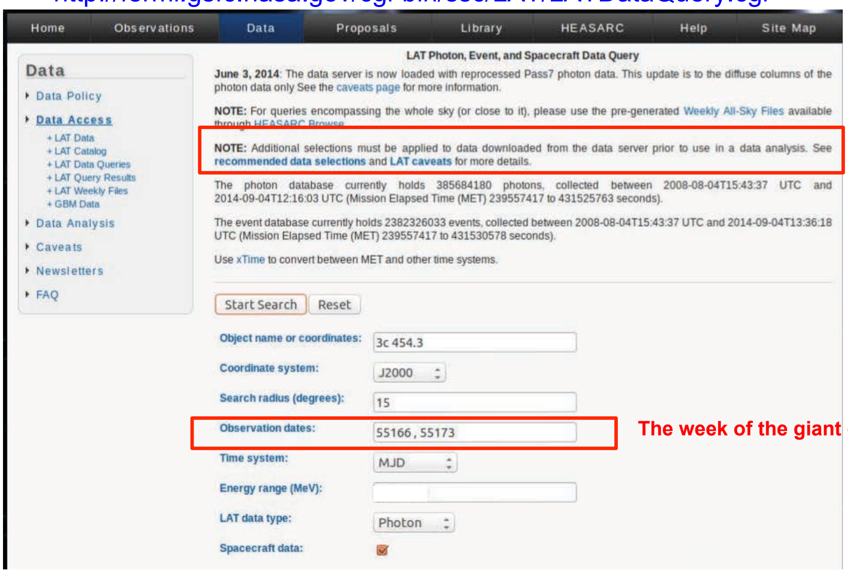

The week of the giant outburst!!

→ Download both spacecraft and photon data ←

Take note of the start and stop MET

follow the link

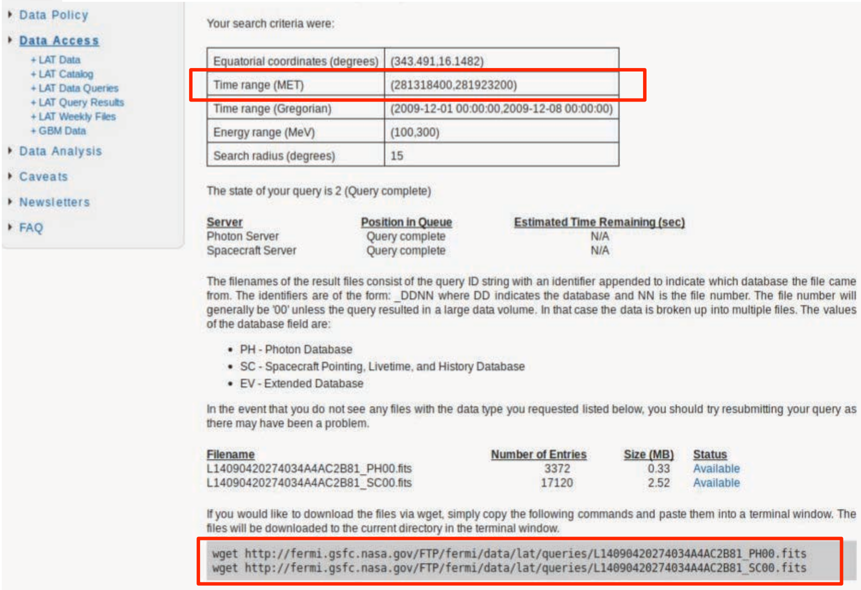

- Data Policy
- Data Access
  - + LAT Data
  - + LAT Catalog
  - + LAT Data Queries
  - + LAT Query Results
  - + LAT Weekly Files
  - + GBM Data
- Data Analysis
- Caveats
- Newsletters
- FAQ

Your search criteria were:

Equatorial coordinates (degrees)	(343.491,16.1482)
Time range (MET)	(281318400,281923200)
Time range (Gregorian)	(2009-12-01 00:00:00,2009-12-08 00:00:00)
Energy range (MeV)	(100,300)
Search radius (degrees)	15

The state of your query is 2 (Query complete)

Server	Position in Queue	Estimated Time Remaining (sec)
Photon Server	Query complete	N/A
Spacecraft Server	Query complete	N/A

The filenames of the result files consist of the query ID string with an identifier appended to indicate which database the file came from. The identifiers are of the form: _DDNN where DD indicates the database and NN is the file number. The file number will generally be '00' unless the query resulted in a large data volume. In that case the data is broken up into multiple files. The values of the database field are:

- PH - Photon Database
- SC - Spacecraft Pointing, Livetime, and History Database
- EV - Extended Database

In the event that you do not see any files with the data type you requested listed below, you should try resubmitting your query as there may have been a problem.

Filename	Number of Entries	Size (MB)	Status
L14090420274034A4AC2B81_PH00.fits	3372	0.33	Available
L14090420274034A4AC2B81_SC00.fits	17120	2.52	Available

If you would like to download the files via wget, simply copy the following commands and paste them into a terminal window. The files will be downloaded to the current directory in the terminal window.

```
wget http://fermi.gsfc.nasa.gov/FTP/fermi/data/lat/queries/L14090420274034A4AC2B81_PH00.fits
wget http://fermi.gsfc.nasa.gov/FTP/fermi/data/lat/queries/L14090420274034A4AC2B81_SC00.fits
```

gtselect (select data)

[/home/]$ gtselect evclass=128 evtype=3
Input FT1 file[ph.fits]
Output FT1 file[filtered.fits]
RA for new search center (degrees) (0:360) [343.494812]
Dec for new search center (degrees) (-90:90) [16.1495]
radius of new search region (degrees) (0:180) [15]
start time (MET in s) (0:) [281318400]
end time (MET in s) (0:) [281923200]
lower energy limit (MeV) (0:) [100]
upper energy limit (MeV) (0:) [500000]
maximum zenith angle value (degrees) (0:180) [90]

Events with a high prob. to be gammas

Setting the max ZA, filter gammas from albedo events (gamma from the Earth that can be a significant source of background)

> gtselect evclass=128 evtype=3 infile=ph.fits outfile=filtered.fits \
ra=343.49 dec=16.15 rad=15 tmin=281318400 tmax=281923200 \
emin=100 emax=500000 zmax=90

Note: all analysis steps are scriptable via explicit assign parameters on command-line. Look at the manual for details.

74

gtmktime (cut the bad time intervals)

Filter out events collected while passing in SAA and other low-quality events

[/home/]$ gtmktime
Spacecraft data file[sc.fits]
Filter expression[(DATA_QUAL>0)&&(LAT_CONFIG==1)]
Apply ROI-based zenith angle cut[no]
Event data file[filtered.fits]
Output event file name[filtered_gti.fits]

Use ZA to filter only proper GTIs

75

gtbin (Counts Map)

[/home]$ gtbin
Type of output file (CCUBE|CMAP|LC|PHA1|PHA2|HEALPIX) [CMAP]
Event data file name[filtered_gti.fits]
Output file name[CMAP.fits]
Spacecraft data file name[sc.fits]
Size of the X axis in pixels[120]
Size of the Y axis in pixels[120]
Image scale (in degrees/pixel)[0.25]
Coordinate system (CEL - celestial, GAL -galactic) (CEL|GAL) [CEL]
First coordinate of image center in degrees (RA or galactic l) [343.494812]
Second coordinate of image center in degrees (DEC or galactic b) [16.1495]
Rotation angle of image axis, in degrees[0]
Projection method e.g. AIT|ARC|CAR|GLS|MER|NCP|SIN|STG|TAN: [AIT]

76

Look at the counts map

Use DS9 to look at the counts map of your ROI and check for close-by sources
> ds9 CMAP.fits &

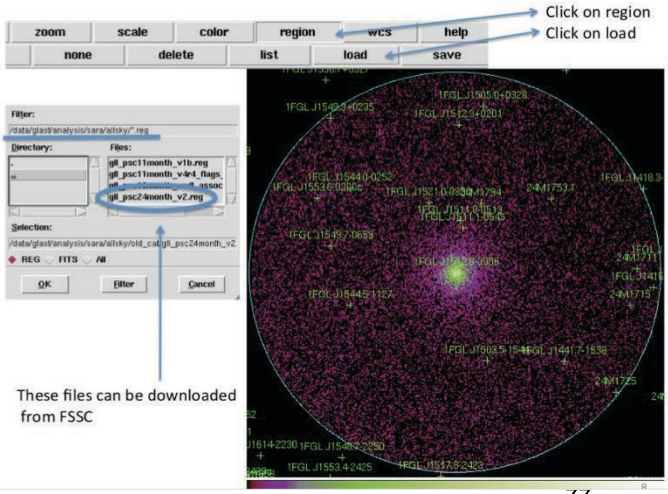

77

gtbin (Light Curve)

[/home]$ gtbin
Type of output file (CCUBE|CMAP|LC|PHA1|PHA2|HEALPIX) [LC]
Event data file name[filtered_gti_smallROI.fits] → NB selected at 1 deg
Output file name[LC.fits]
Spacecraft data file name[sc.fits]
Algorithm for defining time bins (FILE|LIN|SNR) [LIN]
Start value for first time bin in MET[281318400]
Stop value for last time bin in MET[281923200]
Width of linearly uniform time bins in seconds[86400]

Take care that just one source falls inside the gtselect'ed ROI
(and take out albedo and other low-quality gammas via gtmktime)

78

Light-curve: a quick-look

Use FitsView to look at the lightcurve:
> fv LC.fits &

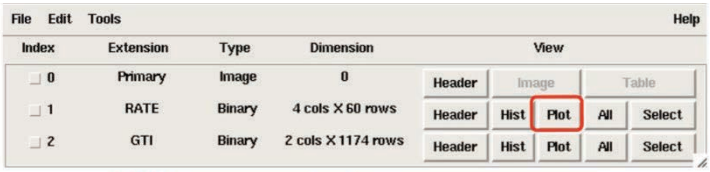

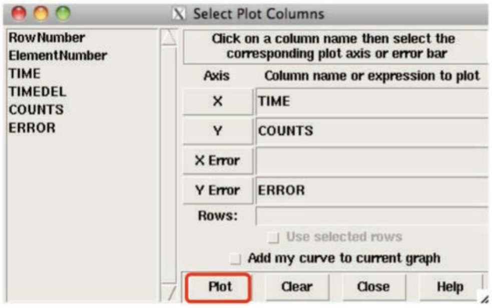

79

Light-curve: a quick-look

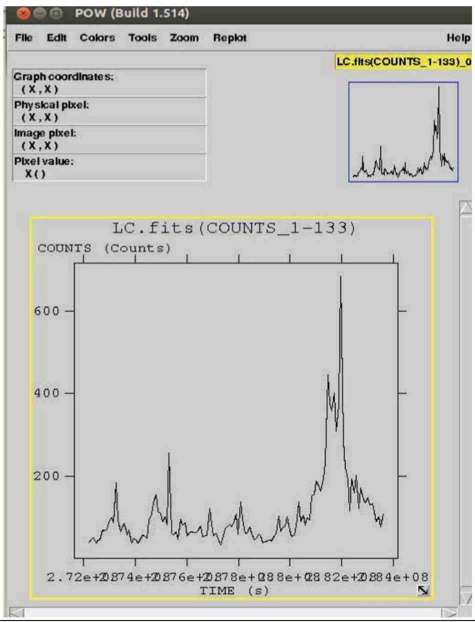

Rough estimate of light curve
(background not subtracted!)

80

gtbin – II (Light Curve)

[/home]$ gtexposure
Light curve file[] lc.fits
Spacecraft file[] sc.fits
Response functions[CALDB]
Source model XML file[none]
Photon index for spectral weighting[-2.1]

Light-curve: calculate fluxes

Use FitsView to look at the lightcurve:
> fv LC.fits &

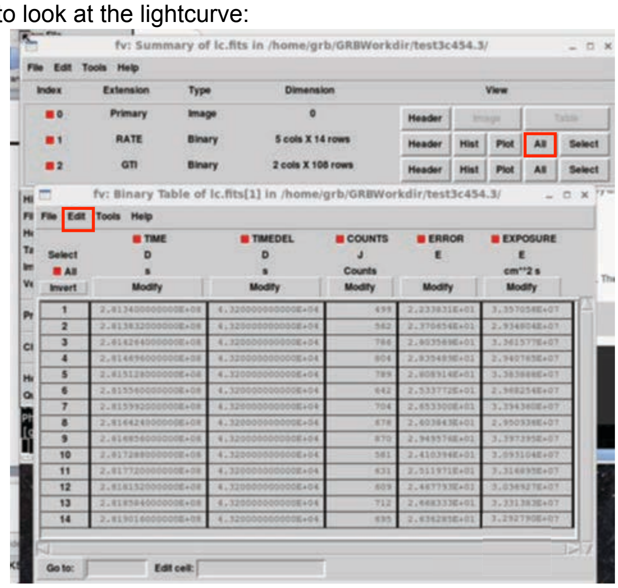

Light-curve: calculate fluxes

Insert new column
Calculate rate
Calculate rate errors

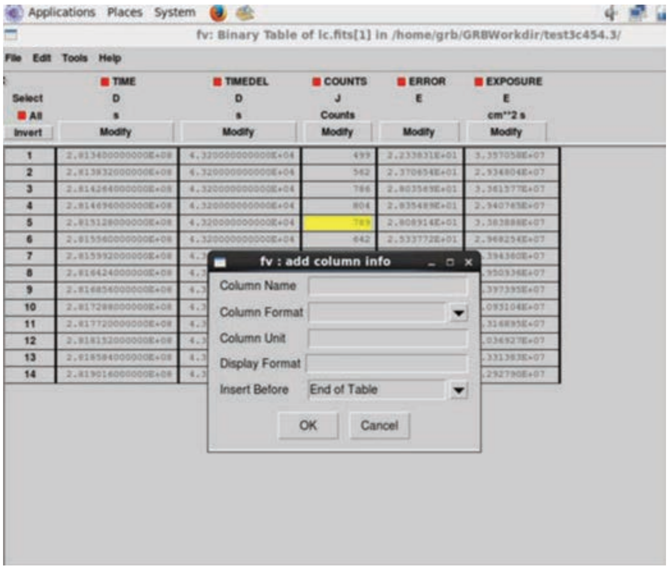

Light-curve: calculate fluxes

Insert new column
Calculate rate
Calculate rate errors

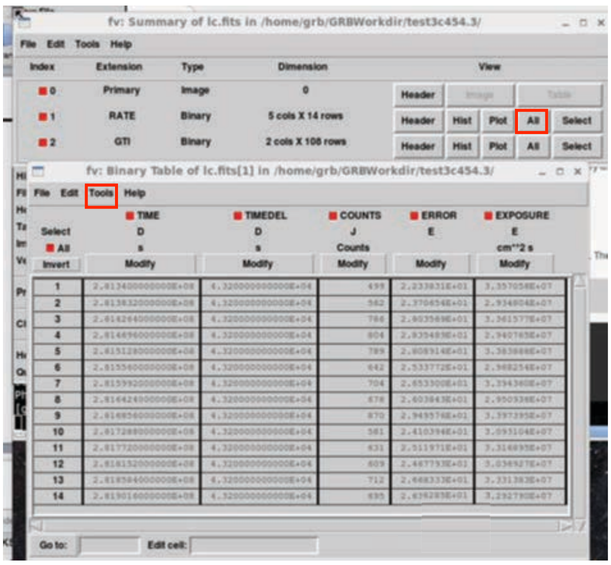

Light-curve: calculate fluxes

Insert new column
Calculate rate
Calculate rate errors

Light curve

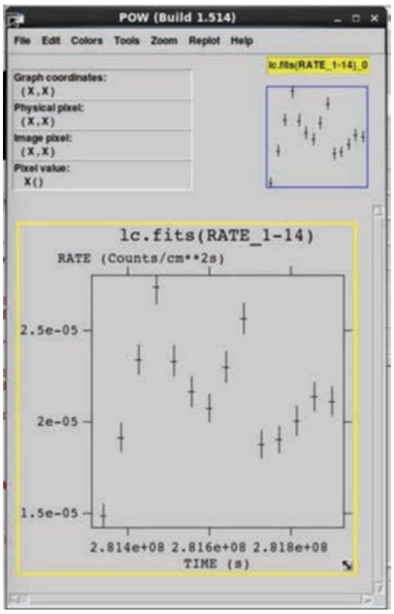

Perform the fit: the likelihood approach

In high energy gamma rays it is never possible to really isolate a source because of limited statistics and strong and structured background.
Therefore statistical techniques have to be applied.
The most used method is the likelihood analysis based on the Poisson statistics.
The method requires to assume a model for the signal detected by the telescope.

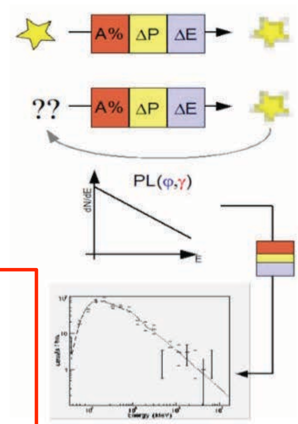

- Assume a **model**
- Model **convolved** with Instrument responce Function (IRF)
- Maximizing likelihood find the best set of parameters that reproduce the observed spectrum

87

Perform the fit: the likelihood approach

- Absolute value of likelihood meaningless!
- Comparison between model w/ and w/o source to reject H_0 = no source
- Many variables may be calculated BEFORE selecting the models
- IRFs depend on inclination angle:
  Livetime Cube: seconds in $\Delta\Omega$ with a given z,
  the time that the LAT observed a given position on the sky at a given inclination angle
  Exposure Map: integration of the effective area over the FoV weighted by the livetime over a position-energy grid, $N_{model} = \int \Phi_{model}(\Omega, E(t)) \times A_{LAT}(\Omega, E)$

88

Likelihood 1st step: gtltcube

[/home]$ gtltcube
Event data file[filtered_gti.fits]
Spacecraft data file[sc.fits]
Output file[ltCube.fits]
Step size in cos(theta) (0.:1.) [0.025]
Pixel size (degrees)[1]
……..

The "livetime cube" must be re-calculated when a new time-interval or a new ZA is selected

89

Likelihood 2nd step: gtexpmap

[/home/]$ gtexpmap
Event data file[filtered_gti.fits]
Spacecraft data file[sc.fits]
Exposure hypercube file[ltCube.fits]
output file name[expMap.fits]
Response functions[CALDB]
Radius of the source region (in degrees)[30]
Number of longitude points (2:1000) [120]
Number of latitude points (2:1000) [120]
Number of energies (2:100) [20]
Computing the ExposureMap using ltCube.fits
...

Add 15° to the ROI radius

90

gtexpmap

Quick check with DS9: fields must be homogenous

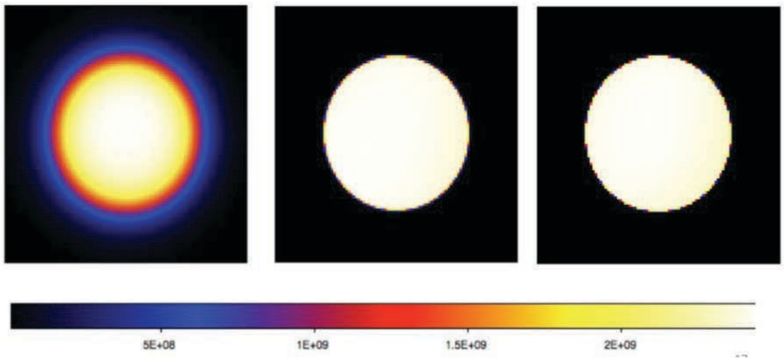

91

Likelihood 3rd step: the XML model

5. Create a source model XML file

The gtlike tool reads the source model from an XML file. The model file contains your best guess at the locations and spectral forms for the sources in your data. A source model can be created using the model editor tool, by using the user contributed tool **make3FGLxml.py** (available at the user-contributed tools page), or by editing the file directly within a text editor.

Here we cannot use the same source model that was used to analyze six months of data in the Unbinned Likelihood tutorial, as the 2-year data set contains many more significant sources and will not converge. Instead, we will use the 3FGL catalog to define our source model by running make3FGLxml.py. To run the script, you will need to download the current LAT catalog file and place it in your working directory:

```
prompt> make3FGLxml.py gll_psc_v16.fit 3C279_binned_gti.fits -o 3C279_input_model.xml
-G $FERMI_DIR/refdata/fermi/galdiffuse/gll_iem_v06.fits -g gll_iem_v06
-I $FERMI_DIR/refdata/fermi/galdiffuse/iso_P8R2_SOURCE_V6_v06.txt
-i iso_P8R2_SOURCE_V6_v06 -s 120 -p TRUE -v TRUE
This is make3FGLxml version 01r0.
The default diffuse model files and names are for pass 8
and assume you have v10r00p05 of the Fermi Science Tools or higher.
Creating file and adding sources from 3FGL
Added 312 point sources, note that any extended sources in ROI were modeled as point sources
because psForce option was set to True
prompt>
```

Note that we are using a high level of significance so that we only fit the brightest sources and we have forced the extended sources to be modeled as point sources. This only affects the lobes of Centarus A which are just outside the FOV.

It is also necessary to specify the entire path to location of the diffuse model on your system. The resulting XML model contains 312 sources. Clearly, the simple 4-source model we used for the 6-month Unbinned Likelihood analysis would have been too simplistic.

This XML file uses the spectral model from the 3FGL catalog analysis for each source. (The catalog file is available at the LAT 4-yr Catalog page.) However, that analysis used a subset of the available spectral models. A dedicated analysis of the region may indicate a different spectral model is preferred. For more details on the options available for your XML models, see:

- Descriptions of available Spectral and Spatial Models
- Examples of XML Model Definitions for Likelihood

Likelihood 3rd step

./make3FGLxml.py gll_psc_v16.fit filtered_gti.fits -o 3c454.3.xml -G /home/grb/software/GlastExt/diffuseModels/v2r0/gll_iem_v06.fits -g gll_iem_v06 -l /home/grb/software/GlastExt/diffuseModels/v2r0/iso_P8R2_SOURCE_V6_v06.txt -i iso_P8R2_SOURCE_V6_v06 -s 120 -p TRUE -v TRUE

Likelihood 3rd step: the XML model

•Backgrounds

```
<!-- Diffuse Sources -->
<source name="galactic_background"   type="DiffuseSource">
<spectrum type="PowerLaw">
<parameter free="1" max="10" min="0" name="Prefactor" scale="1" value="1"/>
<parameter free="0" max="1" min="-1" name="Index" scale="1.0" value="0"/>
<parameter free="0" max="2e2" min="5e1" name="Scale" scale="1.0" value="1e2"/>
</spectrum>
<spatialModel file=”gll_iem_v06.fits" type="MapCubeFunction">
<parameter free="0" max="1e3" min="1e-3" name="Normalization" scale="1.0" value="1.0"/>
</spatialModel>
</source>
<source name="extragalactic_background" type="DiffuseSource">
<spectrum file=”iso_P8R2_SOURCE_V6_v06.txt" type="FileFunction">
<parameter free="1" max="10" min="1e-2" name="Normalization" scale="1" value="1"/>
</spectrum>
<spatialModel type="ConstantValue">
<parameter free="0" max="10.0" min="0.0" name="Value" scale="1.0" value="1.0"/>
</spatialModel>
</source>
```

XML model

•Typical source entry for an assumed powerlaw

{<source name="......" type="PointSource">...
</source> Your sources here

```
<source name="3c454.3" type="PointSource">
<spectrum type="PowerLaw2">
<!-- Source is in ROI center -->
<parameter error="0.00" free="1" max="1000" min="1e-06" name="Integral" scale="1e-04"
value="1.000"/>
 <parameter error="0.00" free="1" max="0" min="-5" name="Index" scale="1" value="-2.000"/>
                <parameter free="0" max="3e6" min="20" name="LowerLimit" scale="1"
value="100."/>
      <parameter free="0" max="3e6" min="20" name="UpperLimit" scale="1" value="300000."/>
      </spectrum>
<spatialModel type="SkyDirFunction">
<parameter free="0" max="360.0" min="-360.0" name="RA" scale="1.0" value="343.494812"/>
<parameter free="0" max="90" min="-90" name="DEC" scale="1.0" value="16.149500"/>
</spatialModel>
</source>
```

95

XML model

Test different models... power law * HE exponential cut-off

```
<source name="3c454.3" type="PointSource">
<spectrum type="PLSuperExpCutoff">
<parameter free="1" max="1000" min="1e-05" name="Prefactor" scale="1e-07"
value="1"/>
<parameter free="1" max="0" min="-5" name="Index1" scale="1" value="-1.7"/>
<parameter free="0" max="1000" min="50" name="Scale" scale="1" value="200"/>
<parameter free="1" max="30000" min="500" name="Cutoff" scale="1" value="3000"/>
<parameter free="0" max="5" min="0" name="Index2" scale="1" value="1"/>
</spectrum>
```

•Look here for source model definition and XML model definitions:
http://fermi.gsfc.nasa.gov/ssc/data/analysis/scitools/xml_model_defs.html
http://fermi.gsfc.nasa.gov/ssc/data/analysis/scitools/source_models.html

•Useful python script to load 2FGL sources that belongs to your ROI in your XML file model (make3FGLxml.py)
http://fermi.gsfc.nasa.gov/ssc/data/analysis/user/

96

Diffuse response

[/home/]$gtdiffrspEvent data file[]filtered_gti.fits
Spacecraft data file[] sc.fits
Source model file[] 3c454.3.xml
Response functions to use[] CALDB

97

Finally... gtlike performig the actual fit

[/home/]$ gtlike plot=yes
Statistic to use (BINNED|UNBINNED) [UNBINNED]
Spacecraft file[sc.fits]
Event file[filtered_gti.fits]
Unbinned exposure map[expMap.fits]
Exposure hypercube file[ltCube.fits]
Source model file[../xml_models/_3c454.3_model_ROI15.xml]
Response functions to use[P7REP_SOURCE_V15]
Optimizer (DRMNFB|NEWMINUIT|MINUIT|DRMNGB|LBFGS) [NEWMINUIT]

Typically use DRMNGB/DRMNFB to find a rough estimate of the likelihood maxima and refine later on with **MINUIT (or NEWMINUIT)**

98

Likelihood output

{'3c454.3': {'Integral': '0.146106 +/- 0.00271733',
'Index': '-2.29973 +/- 0.017189',
'LowerLimit': '100',
'UpperLimit': '300000',
'Npred': '4171.85',
'ROI distance': '0',
'TS value': '17548.4',
'Flux': '1.46192e-05 +/- 2.7178e-07',
…
extragalactic_background': {'Normalization': '1.20197 +/- 0.23541',
'Npred': '643.953',
'Flux': '0.000170707 +/- 3.34331e-05',
},
'galactic_background': {'Prefactor': '0.739969 +/- 0.251827',
'Index': '0',
'Scale': '100',
'Npred': '357.929',
'Flux': '0.000215978 +/- 7.35023e-05',

gtlike creates two output files:
1) results.dat: fit results
2) counts_spectra.fits: the counts in a proper energy binning

99

Plot

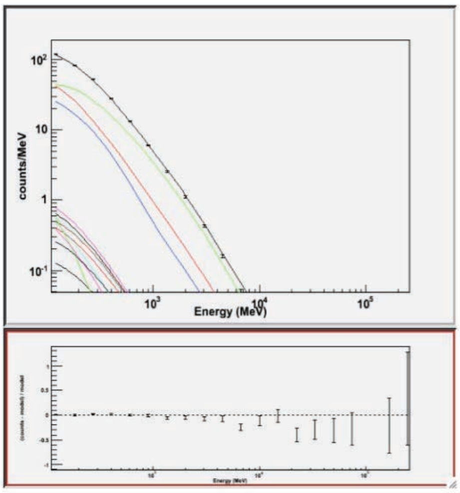

Solid lines follows the order as they are listed in the file results.dat:
black) ROI fit
red) 1st source (pks1510)
green) 2nd source (galactic)
blue) 3rd source (istropic)
Magenta) 4th source
Cyan) 5th source
...

100

Fermi Gamma-ray Space Telescope

Comparison of different models

Powerlaw * HE exp cut-off

{'3c454.3': {'Prefactor': '0.39194 +/- 0.00793161',
'Index1': '-2.12802 +/- 0.03056',
'Cutoff': '5495.55 +/- 934.857 (MeV)
'Npred': '4157.04',
'ROI distance': '0',
'TS value': '17604.2',
'Flux': '1.41693e-05 +/- 2.72878e-07'
(ph cm-2 s-1)

----> Comparing TS values for different models!

For this source, in this time interval, the model with the HE exponential cutoff is favoured with respect to the Simple Powerlaw

You can repeat analyses by yourself also following instructive and complete Tutorials on the FSSC web-site:
- Standard Likelihood: http://fermi.gsfc.nasa.gov/ssc/data/analysis/scitools/likelihood_tutorial.html
- PyLike: http://fermi.gsfc.nasa.gov/ssc/data/analysis/scitools/python_tutorial.html

101

Fermi Gamma-ray Space Telescope

SED modeling

Generate Spectral Points

To generate spectral points to plot on top of the butterfly that we just produced, you need to go back to the data selection part and use gtselect (filter in python) to divide up your data set in energy bins and run the likelihood fit on each of these individual bins. Luckily, there's a script that does this for us that we'll employ to get a final result. This script also generates the butterfly plot we just produced so you won't have to redo that again and it also does a lot of checks on the data to make sure that everything is going ok. If you've made it this far, you might be a little curious as to why we didn't jump right into using this tool but now you're in a position to play with the python tools and make them do what you want them to. The script is also much more careful in handling units and saving everything to files than we have been in this interactive session.

So download the likeSED.py user contributed tool (it's in the SED_scripts package) and load it up into python. You can find information on the usage of this tool on the same page where you downloaded it. It can be used to generate an SED plot for both binned and unbinned analyses but we're only going to work on a binned analysis here.

```
>>> from likeSED import *
This is likeSED version 12.1, modified to handle Pass 7 selections.
```

Now you need to create a likeInput object that takes our unbinnedAnalysis object, the source name and the number of bins we want as arguments. We're going to make 9 bins here like in the paper and we're also going to make custom bins and bin centers. You can have the module chose bins and bin centers for you (via the getECent function) but we're going to do it this way so we can have the double-wide bin at the end. We're also going to use the 'fit2' file (the result of our fit on the full dataset with the NewMinuit optimizer) for the fits of the individual bins but we need to edit it first to make everything fixed except for the integral value of PG 1553+113. Go ahead and do that now. We're basically assuming that the spectral index is the same for all bins and that the contributions of the other sources within the ROI are not changing with energy.

```
>>> inputs = likeInput(like,'3FGL J1555.7+1111',nbins=9)
>>> inputs.plotBins()
```

Fermi Gamma-ray Space Telescope

SED modeling

This last step will take a while (approximately 30 minutes) because it's creating an expmap and event file for each of the bins that we requested (look in your working directory for these files). Once it is done we'll tell it to do the fit of the full energy band and make sure we request that it keep the covariance matrix. Then we'll create a likeSED object from our inputs, tell it where we want our centers to be and then fit each of the bands. After this is done, we can plot it all with the Plot function.

```
>>> inputs.fullFit(CoVar=True)
Full energy range model for 3FGL J1555.7+1111:
3FGL J1555.7+1111
Spectrum: PowerLaw
32 Prefactor: 5.928e-01 2.586e-02 1.000e-04 1.000e+04 ( 1.000e-11)
33 Index: 1.621e+00 2.674e-02 0.000e+00 1.000e+01 (-1.000e+00)
34 Scale: 1.448e+03 0.000e+00 3.000e+01 5.000e+05 ( 1.000e+00) fixed

Flux 0.1-300.0 GeV 7.2e-08 +/- 4.2e-09 cm^-2 s^-1
Test Statistic 3141.46
>>> sed = likeSED(inputs)
>>> sed.getECent()
>>> sed.fitBands()
-Running Likelihood for band0-
-Running Likelihood for band1-
-Running Likelihood for band2-
-Running Likelihood for band3-
-Running Likelihood for band4-
-Running Likelihood for band5-
-Running Likelihood for band6-
-Running Likelihood for band7-
-Running Likelihood for band8-
>>> sed.Plot()
```

This produces the following three plots: a TS plot, a counts spectrum, and a butterfly plot (statistical errors only):

Fermi Gamma-ray Space Telescope

SED modeling

The TS plot shows the TS value for each bin in the spectrum produced by likeSED. Notice that the last bin is double-wide.

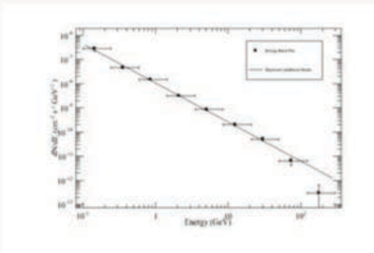

Counts spectrum produced by likeSED along with the spectral points.

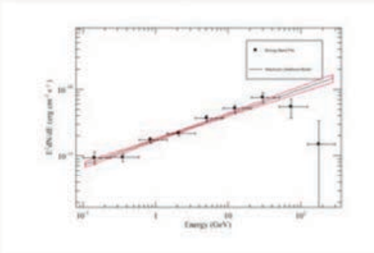

Examination of the course "Astroparticle Physics"
PhD School in Astronomy and in Physics
2016/17

Choose one of the following (a, b or c):

a) **Give a seminar of 25' (+ ~15' questions) on an article, scientific or technical.**

Some **scientific** articles you might choose for the final exam
(of course you can propose your own, and I'll answer you if it's OK for me)

1. Acceleration of petaelectronvolt protons in the Galactic Centre. By HESS Collaboration (F. Aharonian et al.). Nature 531 (2016) 476.

2. Search for Spectral Irregularities due to Photon–AxionLike-Particle Oscillations with the Fermi Large Area Telescope. By Fermi-LAT Collaboration (M. Ajello et al.). Phys. Rev. Lett. 116 (2016) no.16, 161101.

3. Detection of the Characteristic Pion-Decay Signature in Supernova Remnants. By Fermi-LAT Collaboration (M. Ackermann et al.). Science 339 (2013) 807.

4. Searches for Dark Matter annihilation signatures in the Segue 1 satellite galaxy with the MAGIC telescope. By MAGIC Collaboration (J. Aleksic et al.). JCAP 1106 (2011) 035.

5. Search for a Dark Matter annihilation signal from the Galactic Center halo with H.E.S.S. By HESS Collaboration (A. Abramowski et al.). Phys. Rev. Lett. 106 (2011) 161301.

6. Very-High-Energy Gamma Rays from a Distant Quasar: How Transparent Is the Universe? By MAGIC Collaboration (E. Aliu et al.). Science 320 (2008) 1752.

7. Evidence for a new light spin-zero boson from cosmological gamma-ray propagation? By Alessandro De Angelis, Marco Roncadelli, Oriana Mansutti. Phys. Rev. D76 (2007) 121301.

8. The energy spectrum of cosmic-ray electrons at TeV energies. By HESS Collaboration (F. Aharonian et al.). Phys. Rev. Lett. 101 (2008) 261104.

9. High Statistics Measurement of the Positron Fraction in Primary Cosmic Rays of 0.5-500 GeV with the Alpha Magnetic Spectrometer on the International Space Station. By AMS Collaboration (L. Accardo et al.). Phys. Rev. Lett. 113 (2014) 121101.

10. Probing Quantum Gravity using Photons from a flare of the active galactic nucleus Markarian 501 Observed by the MAGIC telescope. By MAGIC and Other Contributors (J. Albert et al.). Phys. Lett. B668 (2008) 253.

11. Observation of Gravitational Waves from a Binary Black Hole Merger. By LIGO and Virgo Collaborations (B. Abbott et al.). Phys. Rev. Lett. 116 (2016) 061102. [Physicists only]

Some **technical** papers/subjects you might choose
(of course you can propose your own, and I'll answer you if it's OK for me)

1. The e-ASTROGAM mission (A. De Angelis, V. Tatischeff et al.), 2017. https://arxiv.org/abs/1611.02232 . Accepted for publication in Experimental Astronomy. Take only Sections 1, 3, 4, 5, 6.
2. Describe the principle of operation of the AMS-02 detector.
3. Describe the operation principle of a system of Imaging Air Cherenkov Telescopes.
4. Describe the operation of a Silicon photomultiplier. Compare it to a CCD.

b) Analyze the data on a Fermi source that you judge interesting. Write a short report (you can copy the general structure from a Fermi paper; you'll not be accused of plagiarism). Give a seminar of 15' (+ ~15' questions) on your result.

c) Propose an original scientific article on a subject covered in the course, write it and submit it to a journal (all the classroom will help you, and it will be a "social" article. Independent of the fact that the journal will accept it or not, the professor will offer a good luck party).

Exercises

Chapter 1

1. *Number of stars in the Milky Way.* Our galaxy consists of a disk of a radius $r_d \simeq 15$ kpc about $h_d \simeq 300$ pc thick, and a spherical bulge at its center roughly 3 kpc in diameter. The distance between our Sun and our nearest neighboring stars, the Alpha Centauri system, is about 1.3 pc. Estimate the number of stars in the our galaxy.

   If we approximate the shape of the disk as a cylinder, the volume of the disk is

   $$V_d \simeq 4\pi r_d^2 h = 12.56 \times (15\,\mathrm{kpc})^2 \times (0.3\,\mathrm{kpc}) = 848\,\mathrm{kpc}^3 .$$

   We also know that the closest star to the Sun is about 1.3 pc away, and that we are in an "ordinary" part of the galactic disk. Assuming that the average distance between stars throughout the galaxy is 1.3 pc, there are a total of

   $$N_d \simeq (848\,\mathrm{kpc}^3)/(9.18 \times 10^{-9}\mathrm{kpc}^3) \simeq 9.2 \times 10^{10} stars .$$

   The volume of the bulge is 100 times smaller than the disk:

   $$V_b \simeq \frac{4}{3}\pi r_b^3 \simeq 4.18 \times (1.5\mathrm{kpc})^3 = 14.1\mathrm{kpc}^3 ,$$

   so it would contain about 1.5×10^9 stars if the density of stars in the bulge is the same as the disk - indeed we observe the density to be larger. In any case, since the volume is so smaller, we can approximate in a robust way

   $$N_s \simeq 10^{11}\, stars$$

   in the full Galaxy.

2. *Number of nucleons in the Universe.* Estimate the number of nucleons in the Universe.

   If dark matter is, as indicated by observations, not made of nucleons, then we can approximate the total mass of the observable universe by the total mass of stars (planets and clouds have negligible mass compared to stars). There are about 10^{11} galaxies in the observable universe, and about 10^{11} stars per galaxy. We assume that a typical star weights like our Sun, which has a mass $M_\odot \simeq 2 \times 10^{30}$ kg. Thus, the mass of all the stars in the observable universe is

   $$M_U \simeq 10^{11} \times 10^{11} \times (2 \times 10^{30}) \simeq 2 \times 10^{52}\mathrm{kg} ,$$

   dominated by nucleons (electrons have negligible mass). Being the nucleon mass $m \simeq m_p \simeq 1.67 \times 10^{-27}$ kg,

   $$N_{nucleons} \simeq \frac{M_U}{m_p} \simeq 1.2 \times 10^{79} .$$

   We expect most of them to be protons, due to the relatively short neutron lifetime.

3. *Galactic and extragalactic emitters of gamma rays.* In Figure 1.10, more than half of the emitters of high-energy photons lie in the Galactic plane (the equatorial line). Guess why.

   Two effects can play a role (indeed they both do, in general): (a) present detectors do not have a resolution large enough to observe the structure of galaxies out of the Milky Way, and (b) the signal from distant galaxies is attenuated – in first approximation, as $1/d^2$, where d is the distance. Notice that the size of the Milky Way is about 100 kly, while the distance of the nearest large galaxy, Andromeda, is about 2.5 Mly.

Chapter 2

1. *GZK threshold.* The Cosmic Microwave Background fills the Universe with photons with a peak energy of 0.37 meV and a density of $\rho \sim 400/\text{cm}^3$. Determine:

   (a) The minimal energy (known as the GZK threshold) that a proton should have in order that the reaction $p\gamma \to \Delta$ may occur.

   (b) The interaction length of such protons in the Universe considering a mean cross-section above the threshold of 0.6 mb.

   (a) In order that the reaction $p\,\gamma \,\to\, \Delta^+$ may occur the center-of-mass energy should be greater than the mass of the Δ particle:
$$\left(p_p + p_{\gamma CMB}\right)^2 \geq m_\Delta^2,$$
$$E_p \;\geq\; \frac{m_\Delta^2 - m_\text{p}^2}{2\,E_{\gamma CMB}\,\left(1-\beta\,cos\theta\right)}.$$
   Assuming head-on collisions,
$$E_p \;\gtrsim\; \frac{m_\Delta^2 - m_\text{p}^2}{4\,E_{\gamma CMB}} \simeq\; 3.7\;10^{20}\text{eV}.$$
   In fact the GZK is not a sharp cut-off. Taking into account the full distributions of the energy of the CMB photons (for instance the mean value of this distribution is 0.635 meV) and of the $p\;\gamma\;\to\;\pi^0\;p$ and $p\;\gamma\;\to\;\pi^+\;n$ cross sections, the effect of the GZK suppression should start to be effective for proton energies of the order of $E_p\;\sim\;6\times 10^{19}$eV.

   (b) The interaction length L_{int} is given by
$$L_{int} = \frac{1}{\sigma\,n}$$
   where σ is the total cross section and n the number density of targets (in this case the CMB photons). Replacing the given values one obtains
$$L_{int} \simeq 4\;10^{24}\;\text{cm}\;\simeq 1.3\;\text{Mpc}.$$
   In fact 0.6 mb is the peak photon-pion cross section at the Δ resonance. Taking into account all the relevant GZK energy range, a mean photon-pion cross section of around 0.1 mb should be instead considered and a more realistic value for L_{int} would be around 6 Mpc.

2. *Photon conversion.* Consider the conversion of one photon in one electron-positron pair. Determine the minimal energy that the photon must have in order that this conversion would be possible if the photon is in presence of:

   (a) one proton;

   (b) one electron;

   (c) when no charged particle is around.

In the presence of a charged particle of mass M, considered to be initially at rest, the minimal energy that the photon must have is the energy required to produce a final state where all particles are at rest in the center-of-mass frame. The total 4-momenta in the initial and final state, p^i_μ and p^f_μ, expressed respectively in the laboratory and in the center-of-mass frames are:

$$p^{i,Lab}_\mu = (E_\gamma + M, \vec{P}_\gamma) \tag{2.1}$$

$$p^{f,CM}_\mu = (M + 2m_e, \vec{0})\,. \tag{2.2}$$

Since $p^i_\mu\, p^{i,\mu}$ and $p^f_\mu\, p^{f,\mu}$ are Lorentz invariants and 4-momentum is conserved, one has:

$$\left(p^{i,\mathrm{Lab}}\right)^2 = \left(p^{i,\mathrm{CM}}\right)^2 = \left(p^{f,\mathrm{CM}}\right)^2 \tag{2.3}$$

yielding the relation:

$$(E_\gamma + M)^2 - P_\gamma^2 = (M + 2m_e)^2 \tag{2.4}$$

which leads to

$$E_\gamma^2 + M^2 + 2E_\gamma M - P_\gamma^2 = M^2 + 4m_e^2 + 4M\,m_e \tag{2.5}$$

and finally:

$$E_\gamma = 2m_e\left(1 + \frac{m_e}{M}\right)\,. \tag{2.6}$$

(a) For a spectator particle with mass $M >> m_e$ one has:

$$E_\gamma \simeq 2m_e\,. \tag{2.7}$$

In particular, for the case of the conversion in presence of a proton, the minimal energy that the photon must have is just a fraction of about 5×10^{-4} above the mass of the electron-positron pair. In fact, for a fixed momentum transferred to the spectator particle, its gain in kinetic energy decreases as the mass increases. In the limit of a very large mass, where one can assume that the velocity is small:

$$T \simeq \frac{P^2}{2M}\,, \tag{2.8}$$

the spectator recoils in order to conserve the momentum, but carries only a small fraction of the energy of the converted photon and most of the available energy is converted into the masses of the electron and of the positron. Hence, as M increases the minimal energy that the photon must have approaches the limit $2m_e$.

(b) In the case of the photon conversion in the presence of an electron, $M = m_e$, and one has:

$$E_\gamma = 4m_e\,. \tag{2.9}$$

(c) Considering now the photon conversion in vacuum, the minimum energy of the photon is obtained by letting $M \to 0$. In this case, according to equation 2.6 we have $E_\gamma \to \infty$. A photon cannot convert in an electron-positron pair in the absence of a spectator charged particle, otherwise the total momentum would not be conserved. This can be visualised by placing ourselves in the center-of-mass frame of the electron-positron. Here we would see an initial photon converting into a final state with total momentum $\vec{P} = \vec{0}$, which would violate momentum conservation.

3. π^- *decay.* Consider the decay of a flying π^- into $\mu^-\bar{\nu_\mu}$ and suppose that the μ^- was emitted along the flight line of flight of the π^-. Determine:

(a) The energy and momentum of the μ^- and of the $\bar{\nu_\mu}$ in the π^- frame.

(b) The energy and momentum of the μ^- and of the $\bar{\nu_\mu}$ in the laboratory frame, if the momentum P_π^- = 100 GeV/c).

(c) Same as the previous question but considering now that was the $\bar{\nu}_\mu$ that was emitted along the flight line of the π^- .

(a) Energy-momentum conservation in the π^- frame leads to:

$$m_\pi = E_\mu + E_\nu \tag{2.10}$$
$$\vec{0} = \vec{P_\mu} + \vec{P_\nu}\,. \tag{2.11}$$

Using the first equality and the relation between energy and momentum gives:

$$E_\mu^2 = (m_\pi - E_\nu)^2 = m_\pi^2 + E_\nu^2 - 2m_\pi E_\nu \tag{2.12}$$
$$E_\mu^2 = P_\mu^2 + m_\mu^2 \tag{2.13}$$

and, since

$$E_\nu = \left|\vec{P_\nu}\right| = \left|\vec{P_\mu}\right| \tag{2.14}$$

we get:

$$E_\nu = \frac{m_\pi^2 - m_\mu^2}{2m_\pi}\,. \tag{2.15}$$

Inserting E_ν in Eq. 2.10 we obtain:

$$E_\mu = \frac{m_\pi^2 + m_\mu^2}{2m_\pi}\,. \tag{2.16}$$

Taking the particle masses $m_\pi = 139.58\,\mathrm{MeV}$ and $m_\mu = 105.66\,\mathrm{MeV}$, gives:

$$E_\mu \simeq 109.78\,\mathrm{MeV} \quad ; \quad E_\nu \simeq 29.80\,\mathrm{MeV}\,. \tag{2.17}$$

Finally, the momenta are computed through Eq. 2.14.

(b) Defining the z axis along the direction of flight of the π^-, the momentum vectors of the final state particles in the π^- frame are:

$$\vec{P_\mu} \equiv (0, 0, P_\mu) \tag{2.18}$$
$$\vec{P_\nu} = -\vec{P_\mu} \tag{2.19}$$

and the Lorentz transformation to the laboratory frame gives

$$E_\mu^{lab} = \gamma\left(E_\mu + \beta P_\mu\right) \quad ; \quad E_\nu^{lab} = \gamma(E_\nu - \beta P_\nu) \tag{2.20}$$
$$P_\mu^{lab} = \gamma\left(\beta E_\mu + P_\mu\right) \quad ; \quad P_\nu^{lab} = \gamma(\beta E_\nu - P_\nu) \tag{2.21}$$

where γ and β are the Lorentz boost and the velocity of the π^-:

$$\gamma = \frac{E_\pi}{m_\pi} \quad ; \quad \beta = \frac{P_\pi}{E_\pi} \tag{2.22}$$

or

$$\beta\gamma = \frac{P_\pi}{m_\pi} = 719 \quad ; \quad \gamma = \sqrt{(\beta\gamma)^2 + 1} \simeq \beta\gamma. \tag{2.23}$$

Note that from the above relations one gets $\beta \sim 1$ ($\beta \simeq 0.99999902$). Using the results for the energy and momentum of the μ^- and of the $\bar{\nu}_\mu$ in the π^- frame, Eqs. 2.14, 2.15 and 2.16, their energy and momentum in the laboratory frame can be written as:

$$E_\mu^{lab} = \frac{E_\pi}{2}\left[(1+\beta) + \frac{m_\mu^2}{m_\pi^2}(1-\beta)\right] \; ; \; E_\nu^{lab} = \gamma E_\nu (1-\beta) \tag{2.24}$$

$$P_\mu^{lab} = \frac{E_\pi}{2}\left[(1+\beta) + \frac{m_\mu^2}{m_\pi^2}(\beta-1)\right] \; ; \; P_\nu^{lab} = -E_\nu^{lab}\,. \tag{2.25}$$

For $\beta \to 1$ the energy of the neutrino goes to zero and the muon energy approaches E_π. In particular this is the case for P_π^- = 100 GeV/c, see Eq. 2.23.

(c) In this case we have

$$\vec{P}_\mu \equiv (0,0,-P_\mu) \tag{2.26}$$
$$\vec{P}_\nu = -\vec{P}_\mu \tag{2.27}$$

and the Lorentz transformation to the laboratory frame yields,

$$E_\mu^{lab} = \gamma\big(E_\mu - \beta P_\mu\big) \quad ; \quad E_\nu^{lab} = \gamma(E_\nu + \beta P_\nu) \tag{2.28}$$
$$P_\mu^{lab} = \gamma\big(\beta E_\mu - P_\mu\big) \quad ; \quad P_\nu^{lab} = \gamma(\beta E_\nu + P_\nu) \tag{2.29}$$

or, using again the results from Eqs. 2.14, 2.15 and 2.16,

$$E_\mu^{lab} = \frac{E_\pi}{2}\left[(1-\beta) + \frac{m_\mu^2}{m_\pi^2}(1+\beta)\right] \; ; \; E_\nu^{lab} = \gamma E_\nu (1+\beta) \tag{2.30}$$
$$P_\mu^{lab} = \frac{E_\pi}{2}\left[(\beta-1) + \frac{m_\mu^2}{m_\pi^2}(1+\beta)\right] \; ; \; P_\nu^{lab} = E_\nu^{lab}\,. \tag{2.31}$$

Now for $\beta \to 1$ we have

$$E_\mu^{lab} \simeq E_\pi \frac{m_\mu^2}{m_\pi^2} \; ; \; E_\nu^{lab} \simeq 2\gamma E_\nu \tag{2.32}$$
$$P_\mu^{lab} \simeq E_\mu^{lab} \; ; \; P_\nu^{lab} = E_\nu^{lab}\,. \tag{2.33}$$

It should be noted that the boost due to the large momentum of the π^- results in that the μ^- reversed its direction of motion (in the π^- frame it was emitted opposite to the flight line of the π^-). Also, in this case $P_\mu^{lab} \sim E_\mu^{lab}$, i.e. the muon mass is negligible in comparison with its energy.

4. π^0 *decay.* Consider the decay of a π^0 into $\gamma\gamma$ (with pion momentum of 100 GeV/c). Determine:
   (a) The minimal and the maximal angles that the two photons may have in the laboratory frame.
   (b) The probability of having one of the photon with an energy smaller than an arbitrary value E_0 in the laboratory frame.
   (c) Same as (a) but considering now that the decay of the π^0 is into e^+e^-.
   (d) The maximum momentum that the π^0 may have in order that the maximal angle in its decay into $\gamma\gamma$ and in e^+e^- would be the same.

(a) Let us start by evaluating the decay in the CM reference frame. In this reference frame the π^0 is at rest and the two photons, that arise from the π^0 decay, have opposite directions such that the relation between their momentum is $\vec{p}_1 = -\vec{p}_2$. Since for photons, in natural units, the momentum is equal to its energy, then

$$E_{\gamma1}^* = E_{\gamma2}^* = \frac{M_{\pi^0}}{2}\,. \tag{2.34}$$

In order to obtain the energy of the photons one needs to apply the Lorentz transformations

$$\begin{pmatrix} E \\ P \end{pmatrix} = \begin{pmatrix} \gamma & \gamma\beta \\ \gamma\beta & \gamma \end{pmatrix} \begin{pmatrix} E^* \\ P^* \end{pmatrix} \tag{2.35}$$

where (E,P) are the energy and the momentum of the particle in the laboratory reference frame while (E^*,P^*) are the same quantities in the CM frame.
Using Eq. 2.35 one can now transform the energy of the photons from CM $\to$ LAB,

$$E_{\gamma1} = \gamma(E_{\gamma1}^* + \beta E_{\gamma1}^* \cos\theta^*) \tag{2.36}$$
$$E_{\gamma2} = \gamma(E_{\gamma2}^* - \beta E_{\gamma2}^* \cos\theta^*)\,. \tag{2.37}$$

The γ and β that relate reference frames can be obtained from

$$\gamma = \frac{E_\pi}{M_\pi} \quad ; \quad \beta = \frac{P_\pi}{E_\pi} \tag{2.38}$$

leading to

$$E_{\gamma 1} = \frac{E_\pi}{2}\left(1 + \frac{P_\pi}{E_\pi}\cos\theta^*\right) \tag{2.39}$$

$$E_{\gamma 2} = \frac{E_\pi}{2}\left(1 - \frac{P_\pi}{E_\pi}\cos\theta^*\right). \tag{2.40}$$

In oder to determine the minimum and maximum angle between the photons in the laboratory frame one can start by identifying two limiting situations: the photons directions are aligned with the boost direction; both photons are emitted transversely to the boost direction.

- **Maximum angle:** in the CM reference frame the angle between the photons is always $\alpha^* = 180°$. As the boost cannot reverse the momentum of the photon travelling against the boost direction, the angle that the photons will do in the LAB frame will continue to be $\alpha = 180°$.
  Furthermore, for $\theta^* = 0°$,

$$E_{\gamma 1} = \frac{E_\pi}{2} + \frac{P_\pi}{2} \tag{2.41}$$

$$E_{\gamma 2} = \frac{E_\pi}{2} - \frac{P_\pi}{2}. \tag{2.42}$$

- **Minimum angle:** this occurs when both photons are emitted transversely to the boost direction, i.e., $\cos\theta^* = 0$. To evaluate the minimum angle let us start by noting that the Lorentz transformation only alter physical quantities that have a non-zero projection along the boost axis. Therefore, the transverse momentum of γ_1 in the LAB is equal to its transverse momentum in the CM frame, leading to $P^T_{\gamma 1} = E^*_{\gamma 1}$. The longitudinal momentum (in the boost direction) can be obtained through the Lorentz transformations (Eq. 2.35),

$$P^{\parallel}_{\gamma 1} = \gamma\beta E^*_{\gamma 1} + \underbrace{\gamma P^*_{\gamma 1}\cos\theta^*}_{=0} \tag{2.43}$$

  Therefore, the minimum angle between the two photons is given by

$$\alpha = 2\arctan\left(\frac{E_{\gamma 1}}{\gamma\beta E_{\gamma 1}}\right) \simeq 2\frac{M_\pi}{P_\pi} \tag{2.44}$$

  where the approximation for small angles $\tan\theta \sim \theta$ was used; the factor of 2 comes from the symmetry of the system, i.e., both photons will have the same angle with the boost direction.

(b) As seen in the previous problem

$$E_{\gamma 1} \in \left[\frac{E_\pi}{2}; \frac{E_\pi}{2} + \frac{P_\pi}{2}\right] \tag{2.45}$$

$$E_{\gamma 2} \in \left[\frac{E_\pi}{2} - \frac{P_\pi}{2}; \frac{E_\pi}{2}\right]. \tag{2.46}$$

Therefore, the photon that fulfils the problem condition is the one moving in the opposite direction to the boost, i.e., photon 2.
The photon energy in the LAB has to be smaller than E_0, and so

$$E_{\gamma 2} = \frac{E_\pi}{2}\left(1 - \frac{P_\pi}{E_\pi}\cos\theta^*\right) \leq E_0 \tag{2.47}$$

leading to the condition

$$\delta \equiv \cos\theta^* \geq \frac{E_\pi}{P_\pi} - \frac{2E_0}{P_\pi}. \tag{2.48}$$

The emission of the photons in the CM frame is isotropic. Thus, the probability of finding a photon with a given solid angle is uniform. As a consequence, we can write

$$\text{Prob} = \int_{\delta}^{1} d\cos\theta^* = 1 - \delta\,. \tag{2.49}$$

Notice that the cosine of an angle is bounded between -1 and +1, which justifies the upper bound of the integral.
Substituting Eq. 2.48 in Eq. 2.49 and noticing that $E_\pi/P_\pi \simeq 1$ we finally obtain

$$\text{Prob} = \frac{2E_0}{P_\pi}\,. \tag{2.50}$$

(c) In this problem we are in a situation similar to π^0 decay but now photons 1 and 2 are substituted by the e^- and the e^+, respectively (this is an arbitrary choice). Like before we have two limiting situations when $\cos\theta^* = \pm 1$ and $\cos\theta^* = 0$. However, as now the particles produced during the decay are massive, their momentum might be reversed by the boost, even if they are produced backwards.
The condition for the particle to be emitted in the LAB frame, always in the direction of the boost, even if the particle is emitted in the opposite direction of the boost ($\cos\theta^* = 180^\circ$), can be easily obtained from the Lorentz transformation

$$P_e = \gamma\beta E_e^* - \gamma P_e^* > 0 \tag{2.51}$$

This means that if the particle is always emitted forward in the LAB frame then the following condition has to be fulfilled:

$$\frac{P_e^*}{E_e^*} = \beta_e < \beta_\pi = \frac{P_\pi}{E_\pi}\,. \tag{2.52}$$

As the electron and the positron have the same mass, then in the CM reference frame, they will share the same amount of energy coming from the decay of the pion and so

$$E_e^* \equiv E_{e^-}^* = E_{e^+}^* = \frac{M_\pi}{2}\,. \tag{2.53}$$

Hence, using the relation $P = \sqrt{E^2 - m^2}$, it is possible evaluate numerically Eq. 2.52,

$$0.999973 < 0.99999(9)\,. \tag{2.54}$$

The above result confirms that, in the LAB frame, all particles will be produced in the direction of the boost, independent of their production angle. Thus, in the LAB, the **minimum angle** is zero and will occur when $\cos\theta^* = \pm 1$.
Naturally, the **maximum angle** between the electron and the positron, α, will be in the opposite limiting situation, i.e. $\cos\theta^* = 0$. The procedure to compute this angle is the same used to evaluate the minimum angle in (a),

$$\alpha = 2\arctan\left(\frac{P_e^T}{P_e^{\|}}\right) \simeq 2\frac{\sqrt{(E_e^*)^2 - m_e^2}}{\gamma\beta E_e^*} \tag{2.55}$$

where the approximation $\tan\theta \sim \theta$ was used for small angles.
By neglecting the electron mass with respect to the pion mass, one gets finally for the minimum angle

$$\alpha \simeq \frac{1}{\beta\gamma} \tag{2.56}$$

with $\beta = P_\pi/E_\pi$ and $\gamma = E_\pi/m_\pi$.

(d) The maximum angle between the two photons is $\alpha = 180^\circ$, independent of the pion momentum. For the electron and positron to make an angle of 180° in the LAB frame, the particle must be aligned with the boost direction and the condition in Eq. 2.52 must not be fulfilled (otherwise the momentum of the particle emitted backwards would be reversed). Therefore, the condition is

$$\beta_e^* > \beta_{CM} \tag{2.57}$$

and thus

$$P_\pi < \sqrt{\frac{m_\pi^2\left(\frac{P_\pi^2}{P_\pi^2+m_\pi^2}\right)^2}{1-\left(\frac{P_\pi^2}{P_\pi^2+m_\pi^2}\right)^2}} \simeq 19\,\text{GeV}/c\,. \tag{2.58}$$

Chapter 3

1. *The measurement by Hess.* Discuss why radioactivity decreases with elevation up to some 1000 m, and then increases. Can you make a model? This was the subject of the thesis by Schrödinger in Wien in the beginning of XX century.

   Ionizing radiation must carry more than 10 eV in energy in order to be able to ionize atoms and molecules. The level of radioactivity decreases with elevation up to about 1000 m because in these altitudes the sources of ionising radiation are mostly on ground. This can be modelled as $e^{-h/\lambda}$. There is an inflection on the profile density of ionising particles in the atmosphere, when radiation from the soil attains a minimum. After this height, radiation begins to increase with altitude because of the contribution of cosmic rays to ionisation. Therefore, the particle flux can be written as

   $$F = Ae^{-h/\lambda} + Bh + c$$

   where h is the height measured from ground level, λ a parameter related to atmospheric attenuation, the other terms being model constants.

2. *Antimatter.* The total number of nucleons minus the total number of antinucleons is believed to be constant in a reaction – you can create nucleon-antinucleon pairs. What is the minimum energy of a proton hitting a proton at rest to generate an antiproton?

   The reaction involving the minimal number of new particles while assuring charge and baryon number conservation is:

   $$pp \to ppp\bar{p}\,.$$

   The minimum energy is obtained when the antiproton and the three protons are produced at rest in the center mass frame, i.e.:

   $$\sqrt{s} = 4m_p, \;\; s = 16m_p^2$$

   (proton and antiproton have the same mass). In the laboratory frame, the value of s before the reaction is

   $$s = (p_1 + p_2)^2 = 2m_p^2 + 2E_p m_p\,.$$

   As s is conserved in the reaction and it is also Lorentz-invariant, we can equate the two expressions, obtaining:

   $$16m_p^2 = 2m_p^2 + 2E_p m_p\,;$$

   $$E_p = 7m_p \simeq 6.57\,\mathrm{GeV}\,.$$

3. *Fermi maximum accelerator.* According to Enrico Fermi, the ultimate human accelerator, the "Globatron", would be built around 1994 encircling the entire Earth and attaining energy of around 5000 TeV (with an estimated cost of 170 million US1954 dollars...). Discuss the parameters of such an accelerator.

   For the sake of reference, the circumference of the LHC is 27 km, using 8.3 T magnets. The corresponding proton-proton center of mass energy achieved is 14 TeV.

   The CM energy that a proton-proton collider can achieve is related to its perimeter and the magnetic field strength of its bending magnets. Fermi assumed a magnetic field of 2 T, which would allow obtaining a maximum energy of 5 PeV, comparable to that of CR at the "knee" of the spectrum. This "Globatron", going around Earth's equator would be some 40.000 km long. Using the same magnetic field as in the LHC, the Globatron would achieve energies of about 20 PeV.

4. *Cosmic pions and muons.* Pions and muons are produced in the high atmosphere, at a height of some 10 km above sea level, as a result of hadronic interactions from the collisions of cosmic rays with atmospheric nuclei. Compute the energy at which charged pions and muons respectively must be produced to reach in average the Earth's surface.

   You can find the masses of the lifetimes of pions and muons in your Particle Data Booklet.

   An unstable particle produced in the high atmosphere can only reach the Earth's surface if the time of flight, t, is smaller than the average lifetime in the Earth reference frame, τ. This condition imposes that

$$\frac{L}{c} = \beta\,\tau = \beta\,\gamma\,\tau_0 \tag{3.1}$$

   with τ_0 the average lifetime in the rest frame. Given that

$$\beta\,\gamma = \sqrt{\gamma^2 - 1}\,, \tag{3.2}$$

   one has

$$\gamma = \sqrt{\left(\frac{L}{c\,\tau_0}\right)^2 + 1}\,. \tag{3.3}$$

   Taking

$$m_\pi \quad = 139.57\,\mathrm{MeV}/c^2 \qquad c\,\tau_\pi \quad = 7.8\,\mathrm{m} \tag{3.4}$$

$$m_\mu \quad = 105.66\,\mathrm{MeV}/c^2 \qquad c\,\tau_\mu \quad = 658.6\,\mathrm{m} \tag{3.5}$$

   the minimum energy at which charged pions and muons must be produced at a height of 10 km above sea level to reach in average the Earth's surface is:

$$E_\pi \quad \simeq 180\,\mathrm{GeV} \tag{3.6}$$

$$E_\mu \quad \simeq 1.6\,\mathrm{GeV}\,. \tag{3.7}$$

   Given that the pion and muon masses are of the same order, they have identical boost for the same production energy. Hence, in this case it is the difference in the lifetimes that dictates the distance they can travel before decaying. In fact the minimum energies computed above differ by a factor of $\sim$ 100, which is approximately the factor between the pion and muon lifetimes.

5. *Very-high-energy cosmic rays.* Justify the sentence "About once per minute, a single subatomic particle enters the Earth's atmosphere with an energy larger than 10 J" in Chapter 1.

   The differential CR spectrum can be written as $dF/dE = AE^{-\alpha}$, so that the flux above a certain energy E_1 is given by:

$$F(E > E_1) = \int_{E_1}^{E_{\mathrm{inf}}} (dF/dE)dE = 1/2A/E_1^2\,, \tag{3.8}$$

   for $\alpha = -3$. Here we use $A = 3.375 \times 10^{22}$ eV^{2}m^{-2}s^{-1}sr^{-1}, derived from the fact that, at $E \simeq 1.5 \times 10^9$ eV, the differential flux is of $\simeq 1 \times 10^{-5}$ eV^{2}m^{-2}s^{-1}sr^{-1}. So, $F(E > E_1) = 4.33 \times 10^{-18}$ m^{-2}s^{-1}sr^{-1}, and finally, the number of particles reaching the Earth per minute is, $N = 2\pi AF(E > E_1)$, where A is the surface area of the Earth and 2π [sr] counts the entire solid angle of arrival of particles. From which we obtain the value of one sub atomic particle per minute.

6. *Very-high-energy neutrinos.* The IceCube experiment in the South pole can detect neutrinos crossing the Earth from the North pole. If the cross section for neutrino interaction on a nucleon is $(6.7 \times 10^{-39}E)$ cm^2 with E

expressed in GeV (note the linear increase with the neutrino energy E), what is the energy at which half of the neutrinos interact before reaching the detector? Comment the result.

The mean free path of the neutrino can be calculated from the cross section:

$$\lambda \simeq \frac{1}{\mathscr{N}\rho\sigma}$$

where ρ is the density of the material, and $\mathscr{N}$ is Avogadro's number.

One has thus the equation

$$e^{-2R/\lambda} = \frac{1}{2},$$

where R is the radius of the Earth.

Solving for σ one has

$$2R\mathscr{N}\rho\sigma = \ln 2 \Longrightarrow \sigma = \frac{\ln 2}{2R\mathscr{N}\rho}$$

and assuming an average density $\rho \simeq 5.51$g/cm^3, a diameter $2R \simeq 12.7 \times 10^8$cm, and the Avogadro's number 6.02 $\times 10^{23}$, one has

$$\sigma \simeq 1.64 \times 10^{-34}\,\text{cm}^2\,.$$

In the approximation of the problem, one has thus

$$E \sim 25\,\text{TeV}\,.$$

7. If a π^0 from a cosmic shower has an energy of 2 GeV:

   (a) Assuming the two $\gamma-$rays coming from its decay are emitted in the direction of the pion's velocity, how much energy does each have?

   (b) What are their wavelengths and frequencies?

   (c) How far will the average neutral pion travel, in the laboratory frame, from its creation to its decay? Comment on the difficulty to measure the pion lifetime.

Chapter 4

1. *Compton scattering.* A photon of wavelength λ is scattered off a free electron initially at rest. Let λ' be the wavelength of the photon scattered in the direction θ. Compute: (a) λ' as a function of λ, θ and universal parameters; (b) the kinetic energy of the recoiling electron.

We will apply to this scattering problem the conservation of four-momentum in the frame in which the electron is initially at rest: we will choose the x-asis along the line containing the photon and the electron before the scattering. As in the text, we will indicate with primes the quantities after the scattering, e.g. λ', and without primes those before the scattering, e.g. λ. We will call the four momenta (before and after the scattering) with q_μ and q'_μ for the photon, and with p_μ and p'_μ for the electron. In the chosen frame we have

$$q_\mu = (h\nu/c, h\nu/c, 0, 0) \qquad q'_\mu = (h\nu'/c, h\nu'\cos\theta/c, h\nu'\sin\theta/c, 0),$$
$$p_\mu = (m_e c, \vec{0}) \qquad p'_\mu = (\gamma' m_e c, \vec{p}\,'),$$

where $\gamma' = (1 - v'^2/c^2)^{-1/2}$. From the time component of energy momentum conservation,

$$q_\mu + p_\mu = q'_\mu + p'_\mu,$$

we obtain

$$\frac{h\nu}{c} + m_e c = \frac{h\nu'}{c} + m_e \gamma' c \quad \Rightarrow \quad h\nu - h\nu' + m_e c^2 = m_e \gamma' c. \tag{4.1}$$

Conservation of three-momentum can be expressed using the angle θ between the incident and scattered photon. Since from the spatial part of momentum conservation the total three momentum before the scattering (and only related to the photon in the chosen frame) must equal the sum of the three momenta after scattering, the three momenta $\vec{q}$, $\vec{q}\,'$ and $\vec{p}\,'$ form a triangle, with an angle θ at the vertex formed by $\vec{q}$ and $\vec{q}\,'$. Using Carnot rule on this triangle, we get

$$m_e^2 \gamma'^2 v'^2 = \frac{h^2\nu'^2}{c^2} + \frac{h^2\nu'^2}{c^2} - 2\frac{h^2\nu\nu'}{c^2}\cos\theta. \tag{4.2}$$

Equation (4.1) can be first rewritten as

$$(h\nu - h\nu' + m_e c^2)^2 = m_e^2 \gamma'^2 c^2, \tag{4.3}$$

and, solving for v'^2 by remembering that $\gamma'^2 c^2 = c^2 - v'^2$, results in

$$v'^2 = c^2 - \frac{m_e^2 c^6}{(h\nu - h\nu' + m_e c^2)^2}.$$

From the above and (4.3), with a little algebra, we then obtain

$$m_e^2 \gamma'^2 v'^2 = \frac{(h\nu - h\nu' + m_e c^2)^2}{c^2} - m_e^2 c^2,$$

and, by comparison with (4.2),

$$\frac{(h\nu - h\nu' + m_e c^2)^2}{c^2} - m_e^2 c^2 = \frac{h^2\nu^2}{c^2} + \frac{h^2\nu'^2}{c^2} - 2\frac{h^2\nu\nu'}{c^2}\cos\theta.$$

The above result can be now simplified into

$$-\frac{2h^2\nu\nu'}{c^2}+2hm_{\rm e}(\nu-\nu')=-\frac{2h^2\nu\nu'}{c^2}\cos\theta \quad\Rightarrow\quad \frac{h}{m_{\rm e}c^2}(1-\cos\theta)=\frac{1}{\nu'}-\frac{1}{\nu}.$$

The sane expression in terms of the photon wavelength before and after the scattering, $\lambda=c/\nu$ and $\lambda'=c/\nu'$, respectively, is

$$\lambda'-\lambda=\frac{h}{m_{\rm e}c}(1-\cos\theta),$$

and gives us the relationship between λ, λ', the photon scattering angle θ, and the universal parameters c, h, and $m_{\rm e}$. The kinetic energy of the scattered electron, $T'_{\rm e}$, can then be calculated as

$$\begin{aligned}
T'_{\rm e} &= m_{\rm e}\gamma' c^2-m_{\rm e}c^2\\
&= \frac{hc}{\lambda}-\frac{hc}{\lambda'}\\
&= \frac{hc}{\lambda}\left(1-\frac{1}{1+h(1-\cos\theta)/(\lambda m_{\rm e}c)}\right)\\
&= \frac{hc}{\lambda}\left(\frac{(1-\cos\theta)}{\lambda m_{\rm e}c/h+(1-\cos\theta)}\right),
\end{aligned}\tag{4.4}$$

again in terms of c, h, $m_{\rm e}$, λ, and the scattering angle of the photon θ.

2. *Cherenkov radiation.* A proton with momentum 1.0 GeV/c passes through a gas at high pressure. The index of refraction of the gas can be changed by changing the pressure. Compute: (a) the minimum index of refraction at which the proton will emit Cherenkov radiation; (b) the Cherenkov radiation emission angle when the index of refraction of the gas is 1.6.

(a) The boost can be obtained using

$$\gamma=\frac{E}{m}=\frac{\sqrt{p^2+m^2}}{m}=1.46\tag{4.5}$$

where m is the mass of the proton and p its momentum. The velocity, β, can obtained inverting the boost formula:

$$\gamma=\frac{1}{\sqrt{1-\beta^2}}.\tag{4.6}$$

The condition for Cherenkov light emission is

$$\cos\theta=\frac{1}{n\beta}\leq 1\tag{4.7}$$

where n is the medium refraction index.

Hence, using Eq. 4.7 and Eq. 4.6, one finds that the refraction index necessary to produce Cherenkov light is

$$n\geq\frac{1}{\sqrt{1-\frac{1}{\gamma^2}}}\simeq 1.37.\tag{4.8}$$

(b) Again, using Eq. 4.7, and taking now $n=1.6$, and β from Eq. 4.6, one gets

$$\cos\theta=\frac{1}{n\beta}=\frac{1}{1.6\times 0.729}\simeq 0.86\tag{4.9}$$

which means that $\theta\simeq 31^\circ$.

3. *Nuclear reactions.* The mean free path of fast neutrons in lead is of the order of 5 cm. What is the total fast neutron cross section in lead?

Using equation 2.25 in the textbook, we have:

$$\sigma_t=\frac{\omega_A}{LN_{\rm int}}=6\times 10^{-24}\ {\rm cm}^2.\tag{4.10}$$

4. *Photodetectors.* What gain would be required from a photomultiplier in order to resolve the signal produced by 3 photoelectrons from that due to 2 or 4 photoelectrons? Assume the fluctuations in the signal are described by Poisson statistics, and consider that two peaks can be resolved when their centers are separated by more than the sum of their standard deviations.

The number of electrons, N, produced by $N^{(pe)}$ photoelectrons is

$$N = GN^{(pe)} \tag{4.11}$$

where G is the PMT gain.

From the problem one has that the condition to have resolved peaks is

$$\mu_1 - \mu_2 \geq \sigma_1 + \sigma_2 \tag{4.12}$$

where μ is the distribution mean and σ its standard deviation. If the distributions follow Poisson statistics then

$$\mu_i = N_i \quad \text{and} \quad \sigma_i = \sqrt{N_i}\,. \tag{4.13}$$

Therefore, Eq. 4.12 becomes

$$N_{i+1} - N_i \geq \sqrt{N_{i+1}} + \sqrt{N_i}\,. \tag{4.14}$$

Using Eq. 4.11 the above equation provides

$$G(N_{i+1}^{(pe)} - N_i^{(pe)}) \geq \sqrt{G}\left(\sqrt{N_{i+1}^{(pe)}} + \sqrt{N_i^{(pe)}}\right) \tag{4.15}$$

and so the gain must be

$$G \geq \left(\frac{\sqrt{N_{i+1}^{(pe)}} + \sqrt{N_i^{(pe)}}}{N_{i+1}^{(pe)} + N_i^{(pe)}}\right)^2 \tag{4.16}$$

From the above condition one has that for $N_i^{(pe)} = 2$ and $N_{i+1}^{(pe)} = 3$

$$G \geq 9.9 \simeq 10 \tag{4.17}$$

and for $N_i^{(pe)} = 3$ and $N_{i+1}^{(pe)} = 4$,

$$G \geq 13.93 \simeq 14\,. \tag{4.18}$$

5. *Cherenkov counters.* Estimate the minimum length of a gas Cherenkov counter used in the threshold mode to be able to distinguish between pions and kaons with momentum 20 GeV. Assume that 200 photons need to be radiated to ensure a high probability of detection and that radiation covers the whole visible spectrum (neglect the variation with wavelength of the refractive index of the gas).

The number of Cherenkov photons emitted per unit of track length and per unit of the photon energy interval is:

$$\frac{d^2N_\gamma}{dE\,dx} \simeq 370 \sin^2\theta_c\,\mathrm{eV}^{-1}\,\mathrm{cm}^{-1}\,. \tag{4.19}$$

In the whole visible spectrum ($\lambda \in [300, 700]$ nm) the Cherenkov light yield in a length L (in cm) is:

$$N_\gamma = \int_0^L \int_{E(700\,\mathrm{nm})}^{E(300\,\mathrm{nm})} \frac{d^2N_\gamma}{dEdx} dE\,dx \simeq 875 \sin^2\theta_c\,L \tag{4.20}$$

where

$$\sin^2\theta_c = 1 - \cos^2\theta_c = 1 - \frac{1}{n^2\beta^2} \tag{4.21}$$

and the variation with wavelength of the refractive index was neglected.

From these relations it is clear that for a fixed number of radiated photons, the length of the Cherenkov counter can be minimised by increasing the refractive index of the gas. However, in order to be able to distinguish between pions and kaons, by operating the detector in threshold mode, the maximum n that can be used is the value matching the kaon threshold velocity, $\beta = 1/n$. Writing the kaon threshold velocity in terms of its momentum, p_K, gives for the refractive index,

$$n^2 = \frac{1}{\beta^2} = \frac{m_K^2 + p_K^2}{p_K^2} \simeq 1 + 6 \times 10^{-4} \tag{4.22}$$

and, inserting this relation in Eq. 4.21, the angle of the Cherenkov photons emitted by the pion is then

$$\sin^2\theta_c = 1 - \frac{1}{n^2\beta_\pi^2} = 1 - \frac{m_\pi^2 + p_\pi^2}{m_K^2 + p_K^2} = \frac{m_K^2 - m_\pi^2}{m_K^2 + p_K^2} \tag{4.23}$$

where use was made of the assumption $p_K = p_\pi$. From Eqs. 4.20 and 4.23, the length of the Cherenkov counter is then

$$L = \frac{N_\gamma}{875}\frac{m_K^2 + p_K^2}{m_K^2 - m_\pi^2}\,\text{cm} = \frac{N_\gamma}{875}\frac{1+\left(\frac{p_K}{m_K}\right)^2}{1-\left(\frac{m_\pi}{m_K}\right)^2}\,\text{cm} \simeq \frac{N_\gamma}{875}\left(\frac{p_K}{m_K}\right)^2\,\text{cm}, \tag{4.24}$$

using the approximations $p_K^2 >> m_K^2$ and $m_\pi^2 << m_K^2$.

Taking $N_\gamma = 200$, $m_\pi = 139.58\,\text{MeV}$ and $m_K = 493.68\,\text{MeV}$ the minimum length of the gas Cherenkov counter is

$$L \simeq 3.6\,\text{m}. \tag{4.25}$$

6. *Electromagnetic calorimeters.* Electromagnetic calorimeters have usually 20 radiation lengths of material. Calculate the thickness (in cm) for a calorimeters made of of BGO, $PbWO_4$ (as in the CMS experiment at LHC), uranium, iron, tungsten and lead. Take the radiation lengths from Appendix B or from the Particle Data Book.

Let us compute the thickness, and compare it to the weight per unit area per radiation length:

$$\begin{aligned}
\mathrm{L_{BGO}} &= 22.3\,\text{cm}\,; \quad \rho X_0 = 7.97\,\text{g/cm}^2 \\
\mathrm{L_{PBWO_4}} &= 17.8\,\text{cm}\,; \quad \rho X_0 = 7.39\,\text{g/cm}^2 \\
\mathrm{L_{U}} &= 6.4\,\text{cm}\,; \quad \rho X_0 = 6.00\,\text{g/cm}^2 \\
\mathrm{L_{Fe}} &= 35.2\,\text{cm}\,; \quad \rho X_0 = 13.84\,\text{g/cm}^2 \\
\mathrm{L_{W}} &= 7.0\,\text{cm}\,; \quad \rho X_0 = 6.76\,\text{g/cm}^2 \\
\mathrm{L_{Pb}} &= 11.2\,\text{cm}\,; \quad \rho X_0 = 6.37\,\text{g/cm}^2\,.
\end{aligned}$$

Besides uranium, a material quite expensive and complicated to treat, if your main problem is space a good material to build a converter for an electromagnetic calorimeter is lead, or, even better, tungsten – but tungsten will be a bit heavier and quite more expensive. Iron is cheap and performs reasonably well. BGO and lead tungstate ($PbWO_4$) occupy a space a larger than Pb or W, but they are active materials, and thus you can use them for a very performant homogeneous calorimeter (you do not need to add a sensitive detector).

7. *Cherenkov telescopes.* Suppose you have a Cherenkov telescope with 7 m diameter, and your camera can detect a signal only when you collect 100 photons from a source. Assuming a global efficiency of 0.1 for the acquisition system (including reflectivity of the surface and quantum efficiency of the PMT), what is the minimum energy (neglecting the background) that such a system can detect at a height of 2 km a.s.l.?

Considering a global efficiency of 0.1, the minimum number of Cherenkov photons that must be collected by the telescope in order to detect a signal is $N_\gamma = 1000$. Since the area of the telescope is $38.5\,\text{m}^2$, this corresponds to a minimum density of about 26 photons/m^2 in the Cherenkov "light pool" of the shower. The mean density of Cherenkov photons at a height of 2 km a.s.l. is about 10 photons/m^2, for a primary of 100 GeV, and about 150 photons/m^2 for a primary of 1 TeV (see Chapter 4 of the textbook). Taking the conservative number of 100 photons/m^2 per 1 TeV of primary energy, the minimum energy of the primary yielding the required density of photons is thus of about 260 GeV.

8. *Cherenkov telescopes.* If a shower is generated by a gamma-ray of E= 1 TeV penetrating the atmosphere vertically, considering that the radiation length X_0 of air is approximately 37 g/cm^2 and its critical energy E_c is about 88 MeV, calculate the height h_M of the maximum of the shower in the Heitler model and in the Rossi approximation B.

See the answer to question a. in Problem 10.8.

9. *Cherenkov telescopes.* Show that the image of the Cherenkov emission from a muon in the focal plane of a parabolic IACT is a conical section (approximate the Cherenkov angle as a constant).

---

10. *Energy loss.* In the Pierre Auger Observatory the surface detectors are composed by water Cherenkov tanks 1.2 m high, each containing 12 tons of water. These detectors are able to measure the light produced by charged particles crossing them. Consider one tank crossed by a single vertical muon with an energy of 5 GeV. The refraction index of water is $n \simeq 1.33$ and can be in good approximation considered constant for all the relevant photons wavelengths. Determine the energy lost by ionization and compare it with the energy lost by Cherenkov emission. Consider that the mean energy loss rate for water is somewhere between the helium gas and carbon.

Let us start by evaluating the energy lost by ionisation. Using the dE/dX plot in the Particle Data Group booklet (PDG) one gets that a 5 GeV muon in a material with characteristic between carbon and helium gas loses about

$$\frac{dE}{dX} \simeq 2.1\,\mathrm{MeV\,cm^2\,g^{-1}} \tag{4.26}$$

The amount of matter traversed by the muon is

$$X = l\,\rho_{water} \simeq 120\,\mathrm{g\,cm^{-2}} \tag{4.27}$$

where $l = 120$ cm is the height of the tank and ρ_{water} the water density.
Thus, the muon energy lost by ionisation is

$$E_{loss}^{ionisation} = X\,\frac{dE}{dX} \simeq 252\,\mathrm{MeV}\,. \tag{4.28}$$

Let us now compute the energy lost due to Cherenkov radiation. Assuming that in average each photon carried about 3.5 eV, then

$$E_{loss}^{Cherenkov} = \langle E \rangle_\gamma\, N_\gamma \tag{4.29}$$

with N_γ being the number of produced Cherenkov photons. This last quantity can be obtained through

$$\frac{d^2N}{dE\,dx} = 370\sin^2(\theta_c)\,\mathrm{photons\;eV^{-1}\,cm^{-1}}\,. \tag{4.30}$$

Knowing that $E_\mu = 5\,\mathrm{GeV}$ and that the boost is $\gamma = E_\mu/m_\mu$ one gets that the velocity of the particle is

$$\beta = \sqrt{1-\frac{1}{\gamma^2}} = \sqrt{1-\left(\frac{m_\mu}{E_\mu}\right)^2} \simeq 0.9998 \tag{4.31}$$

and the Cherenkov emission angle is

$$\theta_c = \arccos\left(\frac{1}{\beta\,n}\right) = 41.25^\circ\,. \tag{4.32}$$

We can now obtain the number of produced Cherenkov photons by integrating equation 4.30 in energy and path:

$$N_\gamma \simeq 370\,\sin^2(\theta_c)\,\Delta E\,\Delta X = 19302 \text{ photons} \tag{4.33}$$

where it was assumed that $n(E)$ is constant.

Finally, the ratio between the energy lost by ionisation and the one lost by Cherenkov emission is

$$\frac{E_{loss}^{ionisation}}{E_{loss}^{Cherenkov}} \simeq 3730 \tag{4.34}$$

which means that the energy lost by Cherenkov emission can be neglected for practical purposes.

11. *Bremsstrahlung radiation.* Consider a circular synchrotron of radius R_0 which is capable of accelerating charged particles up to an energy of E_0. Compare the Bremsstrahlung radiation emitted by a proton and an electron and discuss the difficulties to accelerate these particles with this technology.

The electrons lose energy due to Bremsstrahlung at a rate $\sim 10^{13}$ times higher than the protons, the reason being that the radiative power scales with $1/m^4$, where m is the mass of the charged particle. Furthermore, radiation losses in the presence of magnetic field also scale with B^2. Therefore, a circular collider, which needs to apply all the way intense magnetic fields to bend and confine the particle's trajectories, cannot be used to accelerate electrons efficiently at very-high energies due to prohibitive, intense radiative losses, a factor which is less critical for protons.

12. *Muon energy loss.* A muon of 100 GeV crosses a layer of 1 m of iron. Determine the energy loss and the expected scattering angle.

Chapter 6

1. *Grey disk model in proton-proton interactions.* Determine, in the framework of the grey disk model, the mean radius and the opacity of the proton as a function of the center-of-mass energy (you can use Figure 6.70 to extract the total and the elastic proton-proton cross-sections).

Chapter 8

1. *Cosmological principle and Hubble law.* Show that the Hubble law does not contradict the Cosmological principle (all points in space and time are equivalent).

The cosmological principle principle expresses the fact that, on large enough scales, the matter distribution in the universe is homogeneous and isotropic. The fact that the Hubble law does not contradict this statement can be shown by proving that, given a homogeneous and isotropic distribution of matter, the Hubble law results as a consequence.

If we consider a spacetime with homogeneous and isotropic spatial sections, in comoving coordinates the metric has the form

$$ds^2 = dt^2 - a^2(t)\left\{d\chi^2 + \Sigma^2(\chi)(d\theta^2 + \sin^2\theta d\phi^2)\right\},$$

where $\Sigma^2(\chi) = \sin^2\chi$ (resp. χ^2, $\sinh^2\chi$), depending on the closed (respectively flat, open) character of the spatial sections. If we call D the distance between an observer in the origin of the above reference system and another point, we measure $D = D(t)$ along a surface of constant time t; by also choosing to consider the radial distance (i.e., constant θ and ϕ), we end up with the three conditions $dt = d\theta = d\phi = 0$, so that $D(t) = a(t)\chi$. For the observed velocity $V(t)$ of a body at a constant value of the coordinate χ we then obtain

$$V(t) = \frac{dD(t)}{dt} = \dot{a}(t)\chi = \frac{\dot{a}(t)}{a(t)}D(t).$$

In the above relation $\dot{a}(t)/a(t) = H(t)$ is the Hubble constant, so that the above relation gives the Hubble law $V(t) = H(t)D(t)$. This shows that the Hubble law is consistent with a homogeneous and isotropic cosmological model that respects the cosmological principle.

2. *Asymptotically matter-dominated Universe.* Consider a Universe composed only by matter and radiation. Show that whatever would have been the initial proportion between the matter and the radiation energy densities this Universe will be asymptotically matter dominated.

Let us imagine a two components universe, filled by matter and radiation. Let us assume that these two components are not interacting. This last hypothesis allows us to write two independent energy conservation laws for matter and radiation. If ρ_{r} is the radiation density, and ρ_{m} is the matter density, the corresponding conservation laws imply

$$\rho_{\mathrm{r}} \propto a^{-4} \quad \text{and} \quad \rho_{\mathrm{r}} \propto a^{-3}, \tag{8.1}$$

where a is the scale factor of the Friedmann metric. In the two component universe the Friedmann equation reads

$$\frac{\dot{a}^2}{a^2} = \frac{8\pi G}{3}(\rho_{\mathrm{r}} + \rho_{\mathrm{m}}).$$

Let us now consider a universe that is initially radiation dominated. In this case we can neglect ρ_{m} with respect to ρ_{r}, and we can write with good approximation

$$\frac{\dot{a}^2}{a^2} = \frac{8\pi G}{3}\rho_{\mathrm{r}} \propto a^{-4}$$

for the Friedmann equation above. Then, $a \propto t^{1/2}$, and, using (8.1) this shows that, in this epoch, the radiation density behaves as $\rho_{\mathrm{r}} \propto t^{-2}$, while the matter density evolves as $\rho_{\mathrm{m}} \propto t^{-3/2}$. Thus the radiation content dilutes faster as the universe expands in the radiation dominated epoch. Eventually the radiation will dilute so much that the radiation domination condition will not be satisfied anymore. After enough time, the matter content will become dominant. In this other epoch, the universe evolution will be governed by the Friedmann equation

$$\frac{\dot{a}^2}{a^2} = \frac{8\pi G}{3}\rho_{\rm m} \propto a^{-3},$$

in which we are now neglecting $\rho_{\rm r}$ with respect to $\rho_{\rm m}$. Accordingly, the scale factor now evolves as $a \propto t^{2/3}$, and the radiation and matter densities scale as $\rho_{\rm r} \propto t^{-2-2/3}$ and $\rho_{\rm m} \propto t^{-2}$, respectively.

As we could anticipate from the conservation laws, radiation will continue to become less and less important for the evolution of the universe, so that the universe is eventually matter dominated. Of course, the same conclusion would have been reached if we would have started with a matter dominated universe, as we would have been from the beginning in the second regime. In presence of matter and radiation, the universe will then become, eventually, matter dominated.

3. *WIMP "miracle"*. Show that a possible Weak Interacting Massive Particle (WIMP) with a mass of the order of m_χ 100 GeV would have the relic density needed to be the cosmic dark matter (this is the so called WIMP "miracle").

As we are talking about cold Dark Matter, the appropriate asymptotic form for the equilibrium number density of particles χ with mass $m_\chi \simeq 100\,\text{GeV}$ is the nonrelativistic limit:

$$n \sim (m_\chi T)^{3/2} \exp\left(-m_\chi/T\right)\right) . \tag{8.2}$$

Decoupling happens when $\Gamma \sim n\sigma \sim H$, where H is the Hubble constant, which, using the Friedmann equations, can be rewritten as $H \sim T^2/M_{\rm pl}$ with $M_{\rm pl} = (8\pi G)^{-1/2}$. Using this information we can recast the freeze-out condition as:

$$x^{-1/2}e^{-x} \sim \frac{1}{M_{\rm pl}\,\sigma\, m_\chi} , \tag{8.3}$$

where $x = m_\chi/T$. Numerical values can be now inserted noting that for a weak interacting particle $\sigma \simeq G_F^2 m_\chi^2 \simeq 10^{-8}\,\text{GeV}^{-2}$. Solving numerically the previous equation in the range $10^{-10} - 10^{-20}$, one finds x in the range $20-50$. Now, we know that:

$$\Omega_\chi = \frac{\rho_\chi}{\rho_c} = \frac{m_\chi n}{\rho_c} = \frac{m_\chi}{\rho_c}\frac{n}{T_0^3}T_0^3 , \tag{8.4}$$

with $T_0 = 2.75$ K $\simeq 10^{-4}$ eV. After decoupling annihilations cease and the density of dark matter particles will just decrease with a^{-3}, exactly like temperature does, so the ratio n/T^3 remains constant and we can take its value at freeze-out. In particular, using $n\sigma \sim H$, we can write $n \simeq T^2/M_{\rm pl}\sigma$ and finally:

$$\Omega_\chi = \left(\frac{T_0^3}{\rho_c M_{\rm pl}}\right)\frac{x}{\sigma} \simeq \frac{x}{40}\left(\frac{10^{-8}\,\text{GeV}^{-2}}{\sigma}\right) , \tag{8.5}$$

which gives the right relic density for dark matter $\Omega_\chi \simeq 0.2$, given that $\sigma \simeq 10^{-8}\,\text{GeV}^{-2}$ and $x \simeq 20$.

4. *Classical black hole.* Compute the relation between the radius and the mass of a black hole in classical physics.

---

5. *Virial theorem.* A cluster of galaxies, called Abell 2715 (at a redshift $\simeq 0.114$), contains about 200 galaxies, each the mass of the Milky Way. The average distance of the galaxies from the center of the cluster is 1 Mpc. If Abell 2715 is a virialized system, what is the approximate average velocity of the galaxies with respect to the center? The Milky Way galaxy has a mass of about 2.0×10^{42} kg.

If Abell 2715 is a virialized system, then its potential energy E_p will be twice its entire kinetic energy E_k. If it has 200 galaxies, each of mass 2×10^{42} kg, then the mass of the entire cluster is $200 \times 2 \times 10^{42} = 4 \times 10^{44}$ kg. So on average, each galaxy will have potential and kinetic energies

$$< E_p >= \frac{GMm}{r} = \frac{(6.67 \times 10^{-11}) \times (4 \times 10^{44}) \times (2 \times 10^{42})}{1\text{Mpc} \times (3.1 \times 10^{22}\text{m/kpc})}$$

$$< E_k >= \frac{mv^2}{2} = \frac{2 \times 10^{42}}{2} v^2$$

where v is the average velocity of the galaxies in this cluster.

For the entire cluster, we can use the virial theorem to solve for v.

$$[200 < E_p >] = 2 \times [200 \times < E_k >$$

$$200 \times 1.7 \times 10^{52} = 2 \times 200 \times (10^{42} \times v^2)$$

$$v = \sqrt{0.85 \times 10^{10}} = 9.2 \times 10^5 \mathrm{m/s} = 920 \mathrm{km/s}.$$

6. *M/L.* At r = 10^5 light-years from the center of a galaxy the measurement yields $v_{meas} = 225$ km/s while the expected velocity calculated from the luminous mass is of v_{calc} = 15 km/s. Calculate the visible and the true galaxy mass, and the ratio M/L between the total and the luminous masses. How high is the average dark matter mass density?

---

7. *The WIMP annihilation prefers the production of heavy fermions.* Demonstrate that, in the reaction $\chi\chi \to f\bar{f}$,

$$\left(1 - \frac{|p|}{E + m_f}\right) = \frac{m_f}{2m_\chi + m_f},$$

where χ is a generic WIMP and E, p are respectively the energy and the momentum of the fermion produced in the decay. Use the above relation to compute, for a WIMP of mass $m_\chi = 30 GeV$, the ratios of the branching fractions into $\tau^+\tau^-$ and into $b\bar{b}$, in the hypothesis that

(a) the WIMP has spin 0;

(b) the WIMP has spin 1/2 (note: in this case, use the Clebsch-Gordan coefficients to compute the relative probabilities of the singlet and of the triplet state).

Chapter 9

1. *Neutrino interaction cross section.* Explain the peak in the cross section in the (anti)neutrino interaction cross section for an (anti)neutrino energy around 10^{16} eV (Fig. 9.1).

The s-channel excitation of a W^- boson on-shell, commonly known as the Glashow resonance, can be initiated by the electron antineutrino hitting an electron at a laboratory energy around 6.3 PeV.

If we call x the direction of motion of the (anti)neutrino, the energy-momentum 4-vector of the system constituted by the (anti)neutrino and by an electron at rest can be written, neglecting the neutrino mass, as

$$(E_\nu^2 + m_e, E_\nu^2, 0, 0)$$

(we omitted the bar over the antineutrino symbol). The square of the invariant mass of the system is thus

$$m_{inv}^2 = (E_\nu^2 + m_e)^2 - E_\nu^2 \simeq 2E_\nu m_e \,.$$

The energy at which one can produce a W boson on shell is

$$E_\nu \simeq \frac{m_W^2}{2m_e} \simeq 6.3\,\mathrm{PeV}\,,$$

and this corresponds to a peak on the cross section.

2. *Neutrino from Supernova 1987A.* In 1987, a supernova explosion was observed in the Large Magellanic Cloud, and neutrinos were measured in three different detectors. The neutrinos, with energies between 10 and 50 MeV, arrived with a time span of 10 s, after a travel distance of about $c(5 \times 10^{12}\mathrm{s})$, and three hours before photons at any wavelength.

   (a) Can this information be used to determine a neutrino mass? Discuss the quantitative mass limits that could be derived from the SN1987A.

   (b) This was the only SN observed in neutrinos, up to now, but the same reasoning can be used in pulsed accelerator beams. Derive the needed time and position precision to measure masses $\sim$1 eV, given a beam energy $E \sim 1$ GeV and a distance L.

   (a) It is noted that the neutrinos arrive before light; if we would assume that they leave the source at the same time, this would mean that neutrinos are faster than light,

$$\beta = \frac{v}{c} = \frac{p}{E} > 1\,,$$

   which implies $E^2 - m^2 > E^2$ and $m^2 < 0$. In fact, this is not the correct interpretation, but that the light itself is delayed by interaction on the source (more than neutrinos).

   Likewise, some neutrinos can be emitted earlier than others, and that explains the time span. However, if they are emitted at the same time but have a large mass, then the most energetic should arrive earlier, which is not reported by the experiments. From the observed time and energy span, an upper limit can still be derived for the mass.

For both calculations we use

$$\Delta\beta = \Delta(\frac{v}{c}) = \frac{\Delta T}{L}\,.$$

$\Delta\beta \simeq -2\times10^{-8}$, between the neutrinos and the light, $\Delta\beta \simeq 2\times10^{-12}$, between the neutrinos themselves. On the other hand,

$$\beta = \frac{p}{E} = \sqrt{1-\frac{m^2}{E^2}} \simeq -\frac{1}{2}\frac{m^2}{E^2}$$

$$\Delta\beta \simeq \frac{m^2}{2}\frac{E_1^2-E_2^2}{E_1^2E_2^2}$$

$$m = \sqrt{2\Delta\beta\frac{E_1^2E_2^2}{E_1^2-E_2^2}}\,.$$

The comparison between neutrinos and gammas would give an imaginary mass, m = 10 i keV, while the comparison between neutrinos would give an upper limit of 20 eV.

(b) Accelerator beams are in general pulsed, and thus we have the time of emission of the neutrino (known within this pulse), and the length until they are detected, as well as their energy. To measure a mass $m\sim1$ eV with $E\sim1$ GeV, we need a precision $m/E\sim10^{-9}$. The error on $(\Delta\beta/\beta)$ is about $\sqrt{(\Delta L/L)^2+(\Delta T/T)^2}$, since the relative uncertainties are summed in quadrature, and thus both the distance and timing precision must be of this order of magnitude or better. Present experiments have accuracies of $L\sim1$ cm and $T\sim1$ ns.

Chapter 10

1. *Neutrinos from SN1987A.* Neutrinos from SN1987A, at an energy of about 50 MeV, arrived in a bunch lasting 13 s from a distance of 50 kpc, 3 hours before the optical detection of the supernova. What can you say on the neutrino mass? What can you say about the neutrino speed (be careful...)?

This exercise is very similar to 9.2, and we refer to that for the first question. About the second question, no relevant conclusions can really be drawn unless a hypothesis is done on the relative time of emission of neutrinos compared to the time of emission of photons. If you would assume that the delay between the photon bunch and the neutrino bunch is due to a superluminal speed c_ν of neutrinos, you would obtain

$$\frac{c_\nu}{c} \simeq 1 + 2 \times 10^{-9}..$$

Notice they the OPERA experiment had claimed that neutrinos were traveling from CERN to Gran Sasso (a distance of 730 lm) 60 ns before photons; this would imply $c_\nu/c \simeq 1 + 2 \times 10^{-5}$.

2. *Time lag in light propagation.* Suppose that the speed c of light depends on its energy E in such a way that

$$c(E) \simeq c_0 \left(1 + \xi \frac{E^2}{E_P^2}\right),$$

where E_P is the Planck energy (second-order Lorentz Invariance Violation). Compute the time lag between two VHE photons as a function of the energy difference and of the redshift z.

---

3. *Photon spectrum in hadronic cascades.* Demonstrate that in a decay $\pi^0 \to \gamma\gamma$, once boosted for the energy of the emitting π^0, the probability to emit a photon of energy E_γ is constant over the range of kinematically allowed energies.

---

4. *Extensive electromagnetic air showers.* The main characteristic of an electromagnetic shower (say, initiated by a photon) can be obtained using a simple Heitler model. Let E_0 be the energy of the primary particle and consider that the electrons, positrons and photons in the cascade always interact after travelling a certain atmospheric depth $d = X_0$, and that the energy is always equally shared between the two particles. With this assumptions, we can schematically represent the cascade as in Figure 4.10.

   (a) Write the analytical expressions for the number of particles and for the energy of each particle at depth X as a function of d, n and E_0.

   (b) The multiplication of the cascade stops when the particles reach a critical energy, E_c (when the decay probability surpasses the interaction probability). Using the expressions obtained in the previous question, write as a function of E_0, E_c and $\lambda = d/\ln(2)$, the expressions, at the shower maximum, for:

      i. the average energy of the particles,
      ii. the number of particles, N_{max},
      iii. the atmospheric depth X_{max}.

(a) At the n-th generation,

$$X = n \times d \tag{10.1}$$

and the number of produced particles is simply

$$N = 2^n \,. \tag{10.2}$$

As the energies of the particles are the same at the end of each generation, the energy of each particle is equal is the primary energy divided by the number of particles at this level, i.e.,

$$E_i = \frac{E_0}{2^n} \,. \tag{10.3}$$

(b) i. By construction:

$$E = E_c \tag{10.4}$$

ii.

$$N_{max} = \frac{E_0}{E_c} \,. \tag{10.5}$$

iii. Using Eq. (10.2),

$$N_{max} = 2^{n_{max}} \Leftrightarrow n_{max} = \frac{\ln(N_{max})}{\ln(2)} \tag{10.6}$$

where n_{max} is the maximum number of levels.
Since $d = \lambda \ln(2)$ the maximum atmospheric depth can be written as

$$X_{max} = n_{max} \times d = \frac{\ln(N_{max})}{\ln(2)} d = \lambda \ln\left(\frac{E_0}{E_c}\right) \tag{10.7}$$

where Eq. (10.6) and Eq. (10.5) were used to evaluate n_{max} and N_{max}, respectively.

5. *Extensive hadronic air showers.* Consider a shower initiated by a proton of energy E_0. We will describe it with a simple Heitler-like model: after each depth d an equal number of pions, n_π, and each of the 3 types is produced: π^0, π^+, π^-. Neutral pions decay through $\pi^0 \to \gamma\gamma$ and their energy is transferred to the electromagnetic cascade. Only the charged pions will feed the hadronic cascade. We consider that the cascade ends when these particles decay as they reach a given decay energy E_{dec}, after n interactions, originating a muon (plus an undetected neutrino).

   (a) How many generations are needed to have more that 90% of the primary energy, E_0 in the electromagnetic component?

   (b) Assuming the validity of the superposition principle, according to which a nucleus of mass number A and energy E_0 behaves like A nucleons of energy E_0/A, derive expressions for:

      i. the depth where this maximum is reached, X_{max},
      ii. the number of particles at the shower maximum,
      iii. the number of muons produced in the shower, N_μ.

In this case:

$$N_{tot} = n_\pi^n \; ; \; N_{ch} = \left(\frac{2}{3} n_\pi\right)^n \; ; \; E_i = \frac{E_0}{n_\pi^n} \tag{10.8}$$

where N_{ch} is the number of charged particles at the level n and n_π the number of pions produced at each interaction.

(a) At each interaction $1/3$ of the energy goes into the electromagnetic channel through the π^0 decay. Therefore the energy that remains for the charged particles is

$$E_{ch} = \left(\frac{2}{3}\right)^n E_0. \tag{10.9}$$

Thus the fraction of electromagnetic energy rises as $E_{em} = E_0 - E_{ch}$. Hence

$$\frac{E_{em}}{E_0} = 1 - \left(\frac{2}{3}\right)^n . \tag{10.10}$$

Taking $E_{em}/E_0 = 0.9$ and inverting Eq. (10.10) to obtain the number of generations (levels), one gets

$$n = \frac{\ln(0.1)}{\ln(2/3)} \simeq 5.7\,\text{generations}. \tag{10.11}$$

(b) i. Let us start by evaluating X_{max} for protons. In this case from Eq. (10.8), and recalling that the shower development stops when the energy of the particles reaches E_{dec}, one obtains

$$X_{max} = d \times n_{dec}. \tag{10.12}$$

The maximum number of generations is $E_{max} = E_0/n_\pi^{n_{dec}}$. Inverting this last expression one gets

$$n_{dec} = \frac{\ln(E_0/E_{dec})}{\ln(n_\pi)}, \tag{10.13}$$

which leads, using Eq. (10.12), to

$$X_{max} = d\frac{\ln(E_0/E_{dec})}{\ln(n_\pi)} . \tag{10.14}$$

For iron we have 56 nucleons (i.e. the atomic number A = 26 protons + 30 neutrons). Using the superposition principle each nucleon carries $E_0/56$ of the primary energy. Substituting in Eq. (10.14),

$$X_{max} = d\frac{\ln\left(\frac{E_0}{AE_{dec}}\right)}{\ln(n_\pi)} = \frac{d}{\ln(n_\pi)}\left(\ln\left(\frac{E_0}{E_{dec}}\right) - \ln(A)\right) . \tag{10.15}$$

Notice that the X_{max} evolution with energy is the same for proton and iron and the curves are separated by a constant term: $\ln(A)$.

ii. Again starting with protons we have for the number of particles at the shower maximum

$$N_{max} = n_\pi^{n_{dec}} = \frac{E_0}{E_{dec}} . \tag{10.16}$$

For iron primaries,

$$N_{max} = An_\pi^{n_{dec}} . \tag{10.17}$$

Using the superposition principle and the result of Eq. (10.13) it is easy to see that

$$N_{max} = An_\pi^{\frac{\ln\left(\frac{E_0}{AE_{dec}}\right)}{\ln(n_\pi)}} = A\frac{E_0}{AE_{dec}} = \frac{E_0}{E_{dec}} \tag{10.18}$$

which means that the number of particles at the shower maximum does not depend on the primary mass composition.

iii. The number of muons in the shower, for this simplified model, is given by

$$N_\mu = N_{ch}|_{X=X_{max}} = \left(\frac{2}{3}n_\pi\right)^{n_{dec}} . \tag{10.19}$$

Therefore for proton primaries, using Eq. (10.13),

$$N_\mu = \left(\frac{2}{3}n_\pi\right)^{\frac{\ln(E_0/E_{dec})}{\ln(n_\pi)}} = \left[\left(\frac{2}{3}n_\pi\right)^{\log_{\frac{2}{3}n_\pi}(E_0/E_{dec})}\right]^{\frac{\ln\left(\frac{2}{3}n_\pi\right)}{\ln(n_\pi)}} = \left(\frac{E_0}{E_{dec}}\right)^{\frac{\ln\left(\frac{2}{3}n_\pi\right)}{\ln(n_\pi)}} = \left(\frac{E_0}{E_{dec}}\right)^\beta \tag{10.20}$$

where β is a parameter related with the multi-particle production in the hadronic interactions, in particular, the ratio between the hadronic and the electromagnetic component of the interaction.
For iron, using again the superposition principle and the final result of Eq. (10.20), one gets

$$N_\mu = A\left(\frac{E_0/A}{E_{dec}}\right)^\beta = A^{1-\beta}\left(\frac{E_0}{E_{dec}}\right)^\beta . \tag{10.21}$$

6. *Propagation.* The transparency of the Universe to a given particle depends critically on its nature and energy. In fact, whenever it is possible to open an inelastic channel of the interaction between the *travelling* particle and the Cosmic Microwave Background, its mean free path diminishes drastically. Assuming that the only relevant phenomena that rules the mean free path of the *travelling* particle is the CMB (CνB), estimate the order of magnitude energies at which the transparency of the Universe changes significantly, for:

   (a) Photons;

   (b) Protons;

   (c) Neutrinos.

   Assume $\langle E_{\gamma_{CMB}} \rangle \simeq 0.24$ meV; $\langle E_{\nu_{C\nu B}} \rangle \simeq 0.17$ meV.

(a) For photons the dominant process is the interaction with the photons of the cosmic microwave background, γ_{CMB}, through pair creation:

$$\gamma + \gamma_{CMB} \rightarrow e^+ + e^- \,. \tag{10.22}$$

To determine the minimum energy at which this process can occur it is useful to compute the inner product of the four-momentum vector. This quantity is a Lorentz invariant and thus we can easily relate quantities in the laboratory frame with the ones in the center-of-mass frame. For convenience, the calculations for the photons (before the interaction) will be considered in the laboratory while the products of such interaction will be considered in the center-of-mass. Therefore,

$$P_\mu^{LAB} = (E_\gamma + E_b, \vec{P}_b + \vec{P}_\gamma) \tag{10.23}$$

$$P_\mu^{CM} = (2m_e, \vec{0}) \,. \tag{10.24}$$

where it was assumed that $E_b \equiv E_{\gamma_{CMB}}$. Using

$$s = (P_\mu P^\mu)_{LAB} = (P_\mu P^\mu)_{CM} \tag{10.25}$$

$$P_\mu P^\mu = E^2 - \vec{P} \cdot \vec{P} \tag{10.26}$$

one obtains the following equation:

$$4m_e^2 = (E_b + E_\gamma)^2 - (P_b^2 + P_\gamma^2 + 2\vec{P}_b \cdot \vec{P}_\gamma) \,. \tag{10.27}$$

Taking into account that for photons $E = |\vec{P}|$ and that $\vec{P}_1 \cdot \vec{P}_2 = |P_1||P_2| \cos\theta$, one gets that the energy of the incoming photon is given by

$$E_\gamma = \frac{2m_e^2}{E_b(1 - \cos\theta)} \,. \tag{10.28}$$

Notice that we are looking for the minimal energy that allows for this process to happens, so $\cos\theta = -1$. Inputing the values given in the problem one gets

$$E_\gamma = \frac{m_e^2}{E_b} \simeq 10^{14}\,\text{eV} \,. \tag{10.29}$$

(b) For protons the dominant inelastic channel is via

$$\begin{aligned} p + \gamma_{CMB} &\rightarrow (\Delta^+) \rightarrow p + \pi^0 \\ p + \gamma_{CMB} &\rightarrow (\Delta^+) \rightarrow n + \pi^+ \,. \end{aligned} \tag{10.30}$$

As in the previous problem, we want to find the minimum energy of the proton for which the process is possible. Moreover, we will use the Lorentz invariant s and consider once again that the proton and the gamma are in the Lab frame and the products of the interaction in the center-of-mass frame. Let us then start by defining our kinematics:

$$P_\mu^{LAB} = (E_p + E_b, \vec{P}_p + \vec{P}_b) \tag{10.31}$$

$$P_\mu^{CM} = (m_p + m_\pi, \vec{0}) \,. \tag{10.32}$$

Therefore, using Eq. (10.26), one can write:

$$(E_b+E_p)^2-P_b^2-P_p^2-2\vec{P}_b.\vec{P}_p=(m_p+m_\pi)^2\,. \tag{10.33}$$

Solving the above equation for E_p and recalling that $P_p=\sqrt{E_p^2+m_p^2}$ one gets:

$$2E_bE_p-2E_b\sqrt{E_p^2+m_p^2}\cos(\theta)=m_\pi^2+2m_pm_\pi\,. \tag{10.34}$$

Since $E_p \gg m_p$ the proton momentum can be approximated by its energy ($P_p \simeq E_p$). Therefore,

$$E_p=\frac{m_\pi^2+2m_pm_\pi}{4E_b}\simeq 6\times 10^{19}\,\mathrm{eV}\,. \tag{10.35}$$

where $\cos\theta$ was taken to be -1, i.e., the proton and the photon have opposite directions.

(c) The Universe becomes opaque to the neutrinos when they the following inelastic interaction channel opens:

$$\nu+\nu_{C\nu B}\to Z\,. \tag{10.36}$$

Again considering that the interaction occurs in the laboratory frame and noticing that the interaction occurs if there is enough energy to produce a Z at rest, one can write

$$P_\mu^{LAB}=(E_\nu+E_b,\vec{P}_\nu+\vec{P}_b) \tag{10.37}$$

$$P_\mu^{CM}=(m_Z,\vec{0})\,. \tag{10.38}$$

and similarly as before one can write the following expression:

$$(E_b+E_\nu)^2-P_b^2-P_\nu-2\vec{P}_b\cdot\vec{P}_\nu=m_Z^2 \tag{10.39}$$

$$E_\nu=\frac{m_Z^2}{2E_b(1-\cos\theta))}\,. \tag{10.40}$$

Therefore, the minimum energy of the neutrino that allows the process in Eq. (10.36) is

$$E_\nu=\frac{m_Z^2}{4E_b}\simeq 10^{24}\,\mathrm{eV}\,. \tag{10.41}$$

7. *Fermi acceleration mechanisms.* Calculate, for first and second order Fermi acceleration mechanism, how many times has the particle to cross the cloud (shock) to gain a factor 10 on its initial energy. Assume $\beta=10^{-4}$ for the magnetic cloud and $\beta=10^{-2}$ for the shock wave. Repeat the previous exercise assuming $\beta=10^{-4}$ for both acceleration mechanisms.

(a) At each passage through the cloud or shock wave the particle gains some energy that is proportional to its energy. Therefore for n crossings the energy of the particle relatively to its initial energy, E_0 is given by

$$E=E_0(1+\varepsilon)^n\,. \tag{10.42}$$

where ε is the gain and it is proportional to β for the acceleration in a shock wave (Fermi first order acceleration mechanism) and proportional to β^2 for the *collision* with the magnetic cloud (Fermi second order acceleration mechanism). β is the velocity of the astrophysical object (shock wave or cloud).

Inverting Eq. (10.42) one can obtain the number of times that a particle should cross in order to increase its energy from E_0 to E,

$$n=\frac{\ln\left(\frac{E}{E_0}\right)}{\ln(1+\varepsilon)}\,. \tag{10.43}$$

In this problem we want to know how many times a particle should cross a cloud or a shock wave to increase its energy by a factor of 10, so $E/E_0=10$. Finally, using Eq. (10.43), we have

$$n(\varepsilon\propto\beta;\beta=10^{-2}) \simeq 2.3\times 10^2\,\mathrm{cycles} \tag{10.44}$$

$$n(\varepsilon\propto\beta^2;\beta=10^{-4}) \simeq 2.3\times 10^8\,\mathrm{cycles}\,. \tag{10.45}$$

Therefore, in realistic astrophysical conditions the particle needs to cross only 230 times the shock wave to gain a factor of 10 on its energy while it should cross a cloud 2.3×10^8 times to gain the same energy.

(b) Here we assume that both the shock wave and the magnetic cloud have the same velocity $\beta = 10^{-4}$.

$$n(\varepsilon \propto \beta; \beta = 10^{-4}) \simeq 2.3 \times 10^{4}\,\text{cycles} \tag{10.46}$$

$$n(\varepsilon \propto \beta^2; \beta = 10^{-4}) \simeq 2.3 \times 10^{8}\,\text{cycles}\,. \tag{10.47}$$

Even considering the same velocity for the two astrophysical phenomena the Fermi first order acceleration needs 10000 times less cycles than the Fermi second order mechanism.

8. *Imaging Array Cherenkov Telescopes.* In the isothermal approximation, the depth x of the atmosphere at a height h (i.e., the amount of atmosphere above h) can be approximated as

$$x \simeq X e^{-h/7\,\mathrm{km}}\,,$$

with $X \simeq 1030$ g/cm^2. If a shower is generated by a gamma ray of E= 1 TeV penetrating the atmosphere vertically, considering that the radiation length X_0 of air is approximately 36.6 g/cm^2 (440 m) and its critical energy E_c is about 88 MeV and using Rossi approximation B:

	Incident electron	Incident photon
Peak of shower t_{max}	$1.0 \times (\ln y - 1)$	$1.0 \times (\ln y - 0.5)$
center of gravity t_{med}	$t_{max} + 1.4$	$t_{max} + 1.7$
Number of e^+ and e^- at peak	$0.3y/\sqrt{\ln y - 0.37}$	$0.3y/\sqrt{\ln y - 0.31}$
Total track length	y	y

(a) Calculate the height h_M of the maximum of the shower in the Heitler model and in the Rossi approximation B.

(b) If 2000 useful Cherenkov photons per radiation length are emitted by charged particles in the visible and near UV, compute the total number N_γ of Cherenkov photons generated by the shower (note: the critical energy is larger than the Cherenkov threshold).

(c) Supposing that the Cherenkov photons are all emitted at the center of gravity of the shower - that in the Heitler approximation is just the maximum of the shower minus one radiation length, compute how many photons per square meter arrive to a detector at a height h_d of 2000 m, supposing that the average attenuation length of photons in air is 3 km, and that the light pool can be derived by a opening of $\sim 1.3^\circ$ from the shower maximum (1.3° is the Cherenkov angle and 0.5° comes from the intrinsic shower spread). Comment on the size of a Cherenkov telescope, considering an average reflectivity of the mirrors (including absorption in transmission) of 70%, and a photodetection efficiency (including all the chains of acquisition) of 20%.

(d) Re-do the calculations for $E = 50$ GeV, and comment.

(a) Let us start by computing the depth of the shower maximum, X_{max}, for the two models and afterwards convert it into an altitude using the atmosphere model provided in the problem

$$X_{max} \simeq X e^{-\frac{h}{7\mathrm{km}}} \tag{10.48}$$

In the Heitler model,

$$X_{max} = X_0 \left(1 + \frac{\ln(E/E_c)}{\ln(2)}\right) \simeq 530\,\mathrm{g\,cm^{-2}} \tag{10.49}$$

where $E = 1$ TeV, $E_c = 88$ MeV and $X_0 = 36.6\,\mathrm{g\,cm^{-2}}$.
In the Rossi approximation B model,

$$X_{max} = X_0 \left[\ln\left(\frac{E}{E_c}\right) - 0.5\right] \simeq 325\,\mathrm{g\,cm^{-2}}\,. \tag{10.50}$$

Inverting Eq. (10.48) to obtain the height of X_{max} one gets

$$h_M = -7\mathrm{km}\,\ln\left(\frac{X_{max}}{X}\right)\,. \tag{10.51}$$

Hence,

- Heitler: $h_M \simeq 4.9\,\text{km}$
- Rossi: $h_M \simeq 8.6\,\text{km}$
- MC: $h_M \simeq 9.5\,\text{km}$

where MC is the value for a full Monte Carlo EAS simulation.

(b) The total number of Cherenkov photons generated by the shower is

$$N_\gamma^{total} = \left(\frac{E}{E_c}\right) N_\gamma^{Ch} \simeq 2.27 \times 10^7\,\text{photons} \tag{10.52}$$

where N_γ^{Ch} is the number of Cherenkov photons per radiation length and (E/E_c) the total track length in units of radiation length.

(c) In this problem we will use the Rossi approximation B model to evaluate the shower main characteristics for a 1 TeV photon induced shower. It shall be assumed that all the photons are coming from the center of gravity of the shower, t_{med}. This quantity can be computed using

$$t_{med} = t_{max} + 1.7 = \ln\left(\frac{E}{E_c}\right) - 0.5 + 1.7 \simeq 10.5 \tag{10.53}$$

or, in traversed matter units,

$$X_{med} = t_{med}\, X_0 \simeq 385.7\,\text{g}\,\text{cm}^2\,. \tag{10.54}$$

Using the *isothermal* approximation as atmosphere model one obtains for the altitude

$$h_{med} = -7\ln\left(\frac{X_{med}}{X}\right) \simeq 6.88\,\text{km}\,. \tag{10.55}$$

Using this altitude as emission point and knowing that the light pool can be derived from an opening angle of $\simeq 1.3°$, one gets for r_p

$$r_p = (h_{med} - h_d)\tan\theta \simeq 110.6\,\text{m}. \tag{10.56}$$

Therefore the number of photons at ground is

$$n_\gamma = \frac{N_\gamma\big|_{ground}}{A} = \frac{N_\gamma\, e^{-(h_{med}-h_d)/3}}{\pi\, r_p^2} = 116\,\text{photons m}^{-2}\,. \tag{10.57}$$

where A is the area of the light pool at ground and $N_\gamma\big|_{ground}$ is the number of Cherenkov photons that reach the ground. N_γ is the total number of photons produced by the shower, calculated in the previous problem, while the exponential term represents the attenuation of these photons while travelling through the atmosphere.

IACTs telescopes of VERITAS and HESS have areas, A_{det} of $\simeq 100\,\text{m}^2$. Thus, the number of detected photons is

$$n_\gamma^{det} = n_\gamma A_{det}\, \varepsilon_{ref}\, \varepsilon_{acq} \simeq 1629\,\text{photons} \tag{10.58}$$

where ε_{ref} and ε_{act} are the reflective and acquisition efficiencies, respectively.

(d) This problem is solved in the same way by taking into account that the primary energy is now of 50 GeV. We summarize the results in the following table.

E [GeV]	t_{med}	X_{med} (g/cm^2)	h_{med} [km]	r_p [m]	N_γ	n_γ (ph/m^2)	N_γ^{det}
50	7.5	276.0	9.22	163.7	1.1×10^6	1	17
1000	10.5	385.7	6.88	110.6	2.2×10^7	116	1629

For showers induced by photons with $E = 50$ GeV the number of detected Cherenkov photons is extremely low (of the order of the background fluctuations). Therefore these kind of IACT are not suited to measure gamma-ray induced showers below 50 GeV.

9. *Flux of cosmic rays.* Translate Eq. 10.1 in the textbook into TeV.

10. *Flux of photons from Crab.* Consider Eq. 10.1 in the text and let us assume that the flux of cosmic rays between 0.05 TeV and 2 PeV follows this expression.

    The flux from the most luminous steady (or almost steady) source of gamma rays, the Crab Nebula, follows, according to the measurements from MAGIC, a law

$$N_\gamma(E) \simeq 3.23 \times 10^{-11} \left(\frac{E}{\mathrm{TeV}}\right)^{-2.47-0.24\left(\frac{E}{\mathrm{TeV}}\right)} \mathrm{TeV}^{-1}\mathrm{s}^{-1}\mathrm{m}^{-2}. \tag{10.59}$$

    Compute the number of photons from Crab hitting every second a surface of 10 000 m^2 above a threshold of 50 GeV, 100 GeV, 200 GeV, 1 TeV, up to 500 TeV. Compare this number to the background from the flux of cosmic rays in a cone of 1 degree of radius.

---

11. If the average magnetic field in the Milky Way is 1 μG, what is the minimum energy of a proton coming from Crab Nebula (at a distance of 2 kpc from the Earth) we can detect as “pointing” to the source?

---

12. $\gamma\gamma \to e^+e^-$. Compute the energy threshold for the process as a function of the energy of the target photon, and compare it to the energy for which the absorption of extragalactic gamma-rays is maximal.

---

13. *Mixing photons with paraphotons.* The existence of a neutral particle of tiny mass μ, the paraphoton, coupled to the photon, has been suggested to explain possible anomalies in the CMB spectrum and in photon propagation (the mechanism is similar to the one discussed to the photon-axion mixing, but there are no complications related to spin here). Calling ϕ the mixing angle between the photon and the paraphoton, express the probability of oscillation of a photon to a paraphoton as a function of time (note: the formalism is the same as for neutrino oscillations). Supposing that the paraphoton is sterile, compute a reasonable range of values for ϕ and μ that could explain an enhancement by a factor of 2 for the signal detected at 500 GeV from the AGN 3C279 at $z \simeq 0.54$.

---

14. *Standard model of particle physics cannot provide dark matter.* Name all particles which are described by the SM and write down through which force(s) they can interact. Why can we rule out that a dark matter particle does interact through the electromagnetic force? Why can we rule out that a dark matter particle does interact through the strong force? Now mark all particles which pass the above requirements and could account for dark matter, and comment.

---

15. *Tremaine-Gunn bound.* Assume that neutrinos have a mass, large enough that they are non-relativistic today. This neutrino gas would not be homogeneous, but clustered around galaxies. Assume that they dominate the mass of these galaxies (ignore other matter). We know the mass M(r) within a given radius r in a galaxy from the velocity v(r) of stars rotating around it. The mass could be due to a few species of heavy neutrinos or more species of lighter neutrinos. But the available phase space limits the number of neutrinos with velocities below the escape velocity from the galaxy. This gives a lower limit for the mass of neutrinos. Assume for simplicity that all neutrinos have the same mass. Find a rough estimate for the minimum mass required for neutrinos to dominate the mass of a galaxy. Assume spherical symmetry and that the escape velocity within radius r is the same as at radius r.

    Compare this value to the results $m < 0.2$ eV, from cosmology. What do you conclude?
